12-1-2001

Colorimetric tolerances of various digital image displays

Jason Gibson

Colorimetric Tolerances of Various Digital Image Displays

Jason Gibson

B.S. Imaging Science
Rochester Institute of Technology (1994)

A thesis submitted in partial fulfillment of the requirements for the degree of Master of Science in Color Science in the Center for Imaging Science in the College of Science of the Rochester Institute of Technology

December, 2001

_____

Signature of Author
Jason E. Gibson

_____

Accepted by Coordinator,
M.S. Degree Program

Chester F. Carlson Center for Imaging Science
College of Science
Rochester Institute of Technology
Rochester, New York

Certificate of Approval

M.S. Degree Thesis

The M.S. Degree Thesis of Jason E. Gibson has been examined and approved by two members of the color science faculty as satisfactory for the thesis requirement for the Master of Science degree.

_____

Dr. Mark Fairchild,
Thesis Advisor

_____

Dr. Ethan Montag

Thesis Release Permission Form

Chester F. Carlson Center for Imaging Science
College of Science
Rochester Institute of Technology
Rochester, New York

Colorimetric Tolerances of Various Digital Image Displays

I, Jason E. Gibson, hereby grant permission to the Wallace Memorial Library of R.I.T. to reproduce my thesis in whole or in part. Any reproduction will not be for commercial use or profit.

Dated 12/24/01

Colorimetric Tolerances of Various Digital Image Displays

Jason E. Gibson

Submitted to the

Chester F. Carlson Center for Imaging Science College of Science
Rochester Institute of Technology
Rochester, New York

In partial fulfillment of the requirements for the degree of
Master of Science in Color Science.

Abstract

Visual experiments on four displays (two LCD, one CRT and hardcopy) were conducted to determine colorimetric tolerances of images systematically altered via three different transfer curves. The curves used were: Sigmoidal compression in L*, linear reduction in C*, and additive rotations in h_{ab}. More than 30 observers judged the detectability of these alterations on three pictorial images for each display. Standard probit analysis was then used to determine the detection thresholds for the alterations. It was found that the detection thresholds on LCD's were similar or lower than for the CRT's in this type of experiment. Summarizing pixel-by-pixel image differences using the 90th percentile color difference in $\Delta E'_{ab}$ was shown to be more consistent than similar measures in ΔE_{94} and a prototype ΔE_{2000}. It was also shown that using the 90th percentile difference was more consistent than the average pixel wise difference. Furthermore, S-CIELAB pre-filtering was shown to have little to no effect on the results of this experiment since only global color-changes were applied and no spatial alterations were used.

Acknowledgements

The author wishes to thank all those who helped make this thesis a reality:

My many patient observers without whom, none of this would be possible.

Dr. Mark Fairchild for his expertise and encouragement.

Mitch Rosen for his advice, support and encouragement, even when things looked dim.

Sharron, Sergio, Arturo, Lawrence, Scott and Sun Ju–my fellow students for the many interesting questions, discussions and otherwise friendly banter during the past two years.

My family for putting up with me for another two years... sorry I had to leave so soon.

My extraordinary wife Sarah who's love and encouragement have brightened my life more than she'll ever know.

A Special thanks to the IBM T.J. Watson Research Center for their kind support and funding of this research project.

Come to the edge.
"It's too high"
Come to the edge!
So I did
And you pushed
And I Flew...
-anonymous

Contents

Appendices

List of Figures

List of Tables

List of Equations

Copyright and Trademark Notice

During the course of writing this thesis, a good-faith effort was made to ensure that proper copyrights, trademarks, and rights-reserved marks have been applied in accordance with current standards.

The author has taken great care in the preparation of this thesis, but makes no express, implied or statutory warranty of any kind and assumes no responsibility for errors or omissions. No liability is assumed for incidental or consequential damages in connection with or arising out of the use of the information contained in this document or derivative works.

Within this document:

© Indicates that the brand or product denoted is copyrighted by the respective company.

™ Indicates that the brand or product denoted is a trademark of the respective company.

® Indicates that the brand or product denoted is a registered trademark of the respective company.

1 Introduction

1.1. The Color Image Tolerance Problem

The development of methods to specify and measure visual tolerances is of great importance to many industries. For example, to economically manufacture products, the producer needs to know how far from the standard color a particular product can be and still be deemed identical, or at least acceptably close, in color. In some cases, quality control of such processes can be performed by human observers who individually check each product off the line versus a visual standard. Obviously, this process will not work in high-volume applications unless hundreds of inspectors are employed. In addition to the logistical constraints, human observers are also subject to fatigue, aging, and inattentiveness to task, all of which can introduce errors into the process.

To provide a more consistent and objective measure of color, an appropriate color-measurement device can be substituted for the human observer. This device can then measure samples from the production line and compare them mathematically to a standard set of values via any one of a number of color difference formulas. If the computed difference between the sample and the standard is too large, the sample (or lot) can be rejected.

Much of the early development of color-difference formulas was dominated by "traditional" color industries such as textiles, paint and plastics which were primarily interested in large uniform areas of color in direct edge contact. The current CIE94 color difference formula, ΔE_{94}, specifies reference conditions which "...describe a set of experimental and material variables that are typical of the conditions used in developing object colour visual colour-difference data sets." [CIE 1995]. The conditions specified clearly require uniform color samples:

> *Background field:* uniform, neutral grey with L'=50.
> *Sample separation*: minimum sample separation achieved by placing the sample pair in direct edge contact.
> *Sample structure*: homogeneous colour without visually apparent pattern of nonuniformity.

With the advent of computer imaging systems and displays capable of rendering high quality pictorial images in full color, the need for formulas and methods to deal with the added complexity of images are now being investigated [Stokes 1991, Uroz 1999, CIE 1999]. Figure 1.1-1 shows an example of the issue at hand.

Uniform areas of color can be easily and reliably compared using standard CIE color difference formulas or by way of custom formulas developed for specific industrial needs. The patches shown in Figure 1.1-1(a) meet the reference requirements for applying the CIE94 color difference equation. They are in direct edge contact, have a uniform gray surround, and exhibit no visible texture as shown in the magnified area of the right hand sample. The CIE94 color difference formula prediction would correlate quite well to careful visual scaling of these samples.

Digital images, which are a spatially organized collection of thousands, or even millions of small uniform areas of color called pixels, are a far more complex. As the magnified section of Figure 1.1-1(b) shows, the individual pixels within an image have complex surrounds. If the image was halftoned for printing, the individual dots made by the printer would then constitute the uniform areas and would be in an even more complex arrangement. Since images are viewed in whole, not as individual dots, there is a complex relationship between the individual pixels, and the image which they comprise [Pointer 1994, Tremeau 1995, Wandell 1994, Zhang 1996].

Figure 1.1-1 Comparing Uniform Patches vs. Images

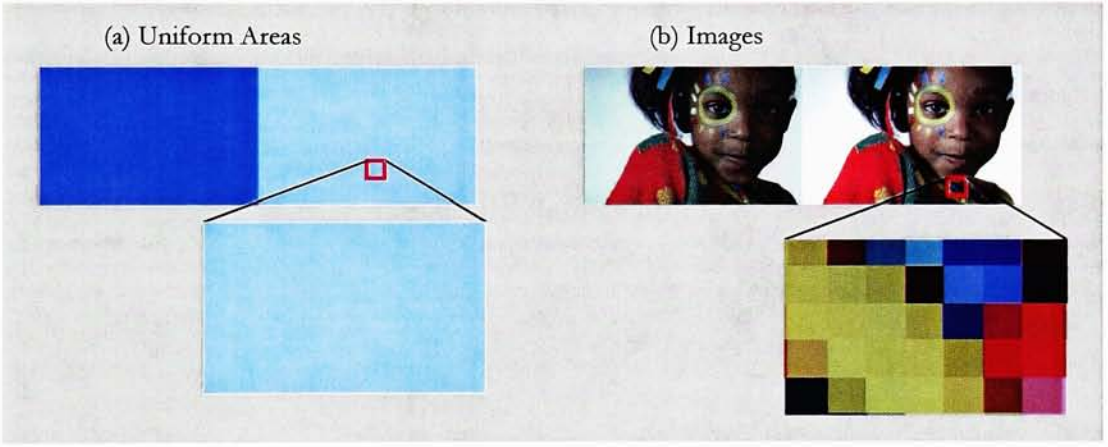

Despite this complexity, the simple average pixel-wise color difference between two images has been found to work quite well in many cases [Farnand 1996, Stokes 1991]. Other statistics such as the 99th percentile of differences between two sets of pallet colors processed along with the images have also been used with some success [Uroz 1999]. For purposes of this experiment, the arithmetic mean and 90th percentile of the pixel-wise differences will be used.

Both Stokes [1991] and Uroz [1999] have produced notable works in the area of color differences in images. Stokes work established visual thresholds for 10 systematic color-altering transforms using images displayed on a CRT. Uroz examined two systematic transforms and one random transform simulating system noise using large format prints.

This research project continues Stokes' and Uroz's work in four ways. First, by expanding the available data on difference thresholds for global color changes started by Stokes. Secondly, by examining two summary statistics (average and 90th percentile difference) to describe the overall color difference between the images as was done by Uroz. Thirdly, by examining the qualitatively impact of display properties such as resolution, contrast, and luminance on the difference thresholds for systematic global color changes. And finally by examining the effects of S-CIELAB pre-filtering of the images before calculating the summary statistics to account for the spatial properties of the human visual system.

1.2. Project Overview

During the course of the project, tolerances for systematic changes in luminance contrast, overall system gain, and color cast were developed for images displayed on two LCD displays (the IBM Roentgen prototype [Schleupen 1998], and a SGI® 1600SW™), a flat-screen CRT display (a Sony GDM-F500 FD Trinitron™), and continuous tone hardcopy output (Fujix® Pictrography® 3000). Details of each of the project's components can be found in subsequent chapters as described below.

Chapter one introduces the problem of image tolerance and describes the goal of the project.

Chapter two describes the background and prior art motivating this thesis. A brief review of color tolerances for uniform areas of colors such as used in the textile, paint and plastics industries is given. Image related industries such as photography, graphic arts, television, and computer graphics are also described. A review of prior-art concludes the chapter.

Chapter three describe the four display devices used in the experiments as well as the various measurement devices used in characterizing them.

The fourth chapter describes the characterization results of the four displays including a detailed analysis and comparison of the three monitors used.

Chapter five presents the methodologies used in conducting this experiment. This chapter covers how the images were selected and manipulated, how the psychophysical data were collected and processed and the various color difference equations used.

The sixth chapter presents the thresholds of the four displays in terms of the magnitude of the free parameter in each of the three transforms used. Though these comparisons are dependent on the transforms used, they provided a reasonable way to compare the relative sensitivity of the observers to the changes in each of the tested display.

Chapter seven presents these same thresholds translated into terms of pixel-by-pixel color-differences using several color difference formulas. While this methods ignores the possibility of complex interactions of adjoining pixels in an image, it does have intuitive appeal and has been used with some success in the past.

Chapter eight presents the results of using S-CIELAB pre-filtering, which attempts to account for some of the spatial properties of the human visual system, before taking pixel-by-pixel color differences.

Section nine presents some concluding remarks and comments regarding this work, as well as some suggestions for future research areas.

Section ten contains an extensive bibliography of works consulted. Various informative appendices are also included.

The enclosed CD (ISO 9660 Level 2 Mode 1 Joliet) contains electronic forms of this document, as well as the raw data, images, and much of the code used during this work. Consult the ReadMe.txt file on the disc for an overview of its contents.

2 Background and Prior Art

The measurement and use of visual color tolerances are well established in the field of color science. Their development is closely related to the development of basic colorimetry and its associated color difference formulae which began in the early 1930's with the CIE's adoption of the 2° standard observer. By the early 1970's, dozens of color difference formulas were in active use, each developed by a specific company or industry to solve their particular needs [CIE 1995]. In an effort to standardize these formulae, the CIE adopted the CIELAB and CIELUV color difference formulas as international standards in 1976 [CIE 1986]. Despite its known deficiencies in dealing with critical color differences and simplistic chromatic adaptation models, ΔE^*_{ab} greatly simplified the choice of color difference formulas for many industries. Ongoing research into this area has lead to improved standards such as the CIE ΔE_{94} [CIE 1995] color difference equation, and the pending CIE ΔE_{2000} [Fairchild 2000].

The development of these formulas was largely driven by the needs of two major industrial groups. The oldest, and most developed, are those which deal primarily with large uniform areas of color such as textiles, paints and plastics. A somewhat newer group consists of industries which deal with color as part of complex images such as photography, graphic arts, television, and more recently digital color imaging and computer peripherals. These two industries will be discussed in the following two sections. The final sections of this chapter review the work of Stokes [1991] and Uroz [1999].

2.1. Textiles, Paints and Plastics–Uniform Color Areas

Much of the theoretical foundation for deriving colorimetric tolerances in images has been developed in the textile, paint, and plastics industries to deal with uniform color areas. Often, techniques used for such areas are applied to images on a pixel-by pixel basis for deriving tolerances with varying degrees of success. While this approach has intuitive appeal, it ignores the complex interactions neighboring image pixels may have on an observers overall perception of the image.

The development of these formulas is still an active area of interest. New formulae such as JPC79 [McDonald 1980], CMC [Clarke 1984, McDonald 1988] have been introduced to correct these deficiencies. In 1995, the CIE introduced the CIE94 color-difference equation (ΔE_{94}) as a replacement for the CIELAB ΔE^*_{ab} formula [CIE 1995]. The CIE TC 1-47 'Hue & Lightness Dependent Correction to Industrial Colour Difference Evaluation' is now is the process of creating another CIELAB based color difference formula to be known as ΔE_{2000}. See section 5.3 for more details on these equations. Many of these formulas have also been extended to account for chromatic adaptation and environmental effects such as surround and illumination levels. Currently, Hunt [1987, 1991, 1994], Nayatani [1993a, 1993b], Fairchild [1991, 1995, 1996 1998a, 1998b], and the CIE [1998] have published extensive research in this area.

2.2. Photography, Graphic Arts, Television and Computer Graphics–Image Related

Until recently, these industries have not had the computational resources necessary to manipulate images on a pixel-by-pixel basis. Therefore, much of the development in these fields has involved innovative solutions to the problems of color reproduction and setting tolerances.

2.2.1. Photography

The study of color tolerances in images is perhaps best developed in the field of photography. As early as the 1920's, Jones [1921] quantified tone reproduction tolerances for black and white images using psychophysical experimentation. However, due to the long standing use of densitometry in this field, colorimetry has only recently been applied. When colorimetry has been applied, it has tended to be simple pixel by pixel implementation of the formulas found in the textile, paints and plastics industries.

Of particular note in the field of photography is the extensive research into the tolerances of memory colors for skin tones, blue sky, and green grass [Bartleson 1959, 1962, Hunt 1974]. These studies were often hybrid experiments, deriving tolerances of uniform fields within a static background image. The tolerances derived were used as test points for complex imaging systems. If the test points did not fall within a specified range, the entire system was deemed unacceptable. While this work provided tolerances for a few important colors, it did not provide overall tolerances for color images. Furthermore, these tolerances are dependent on the particular colors chosen in designing the target, therefore much care has to be taken in properly selecting the colors and colorants used. The 24 patches of the Macbeth ColorChecker® chart represent one such well designed target [McCamy 1976].

2.2.2. Graphic Arts

The developments in the field of graphic arts and printing are similar to those in photography. The fundamental equations for color half-tone printing were laid out by Neugebauer [1937] and later modified by Yule and Nielsen [1951]. An excellent review of the development of these and other models is given by Wyble [2000]. However, none of these models has proven to make adequate colorimetric predictions although progress is being made [Viggiano 1990, Balasubramanian 1999]. Until a more accurate model can be developed, it will remain difficult to deal with issues external to the media such as viewing conditions.

Liquid crystal displays such as the SGI 1600SW and the IBM Roentgen typically have much high luminance levels than CRT's such as the SONY GDM-F500. This can be especially important for graphic arts prepress work as is made clear by this passage from a working draft of ISO 3664 *Viewing conditions - for Graphic Technology and Photography* [ISO 1997b]:

> Colour monitors are increasingly being used to display and view digital images in graphic technology and photography. In order to ensure consistency of assessment in this situation it is important that the viewing conditions in which the monitors are placed are reasonably well specified. However, it should be noted that adherence to these specifications does not ensure that the monitor will match the hardcopy without provision of a defined colour transformation to the displayed image, or use of proper colour management. ... In practice, even with high quality colour management, an accurate match is difficult to achieve because the luminance levels generally differ significantly between hardcopy (prints or transparency) and softcopy (monitor).

For reference, luminance levels for typical print viewing conditions are listed below.

Table 2.2-1 Luminance Levels for Typical Print Viewing Environments

Class Room	100–180 cd/m^2
Bright Room	200 – 300 cd/m^2
Graphic Arts Light booth	350–375 cd/m^2
MCSL Print Viewing Room	1150 cd/m^2

Work regarding cross-media color reproduction and viewing include [Berns 1991a, Braun 1996, Fairchild 1999, Hseue 1998, Lo 1996].

Along with the color discrimination aspects of a computer display, the contrast and text quality are also important aspects to consider. A principal determinant in the legibility of text is the luminance contrast ratio, which should be a minimum of 3:1 and preferably at least 10:1 [MacDonald 1999]. A second factor is the ability to properly control the kerning of text for better readability. It is expected that a production version of a high density display like Roentgen will exceed in this aspect.

2.2.3. Television

The entire color television industry was established using the principles of colorimetry available at the time [Bingley 1953, 1954a, 1954b; Hunt 1995; NTSC 1954]. The original NTSC camera sensitivities were linear transforms of the CIE standard observer. Television has also adopted the use of the CIELUV color difference equations, which along with a set of uniform color bars, are used to establish color tolerances [CIE 1974]. Results of these tests are very dependent on the chosen samples. Furthermore, there appears to be little consensus on which set of colors should be used [Breneman 1957, McCamy 1976]. Common practice is to include a series of neutrals, critical colors, and saturated colors. The neutrals help maintain the systems gray-scale. By over sampling important colors such as skin tones, grass, and sky, the accuracy of these colors is maintained. The saturated colors are used to establish the overall gamut of the system.

2.2.4. Computer Graphics

The field of computer generated graphics has not used the principles of color science until recently. Previous work in this field has primarily focused on simplistic, easy to program, models of color such as RGB and HSV, rather than more robust methods [Foley 1990, Hall 1989] though recent work is seeking to correct this [Johnson 1999, Pattanaik 1998]. Until the development and implementation of robust, standardized color management methods, the large differences in set-up between displays typically renders complex color models useless. That is, if sending the same signal to two different monitors produces widely different colors, then there is little use in developing sophisticated color-models to generate them, or for that matter to compare them.

2.3. Prior Art – Stokes 1991

This research is in part a continuation of the work by Stokes in 1991. The following sections outline the experiments he performed, and a summary of his results.

2.3.1. Experimental Method

For his research, Stokes used a set of six transforms to manipulate the sample images. Since symmetry of thresholds was not assumed, each transform was divided into high and low or positive and negative parameter levels. The final 10 combinations used are shown in Table 2.3-1 below. The formula of each transfer function is listed in Table 2.3-2.

Table 2.3-1 Transfer Functions Implemented by Stokes

CIELAB Dimension	Transfer Function	Parameter Values	Abbreviation
Lightness	Multiplicative Factor	≤ 1.0	LMF
	Power	≥ 1.0	LPH
		< 1.0	LPL
	Sigmoidal	≥ 1.0	LSH
		< 1.0	LSL
Chroma	Multiplicative Factor	≤ 1.0	CMF
	Power	≥ 1.0	CPH
		< 1.0	CPL
Hue Angle	Additive Offset	≥ 0.0	HOH
		< 0.0	HOL

Table 2.3-2 Transfer Function Formulas

Function	Formula
Additive Offset	$Output = Input + k$
Multiplicative Factor	$Output = k(Input)$
Power	$Output = Input^{k}$
Sigmoidal	$Out = \begin{cases} \dfrac{(Input*2)^{k}}{2} & Input < 0.5 \\ \dfrac{\left[((Input*2)-1.0)^{1/k}\right]+1.0}{2} & Input \geq 0.5 \end{cases}$

To test for scene dependence [Jones 1941], six different pictorial images were used which included manufactured objects, nature scenes, and people. Images were also chosen to represent a variety of perceived object distances [Corey 1983], and overall chroma levels [Bartleson 1958].

During the experiment, the observer viewed a neutral gray field between each set of images while they were being loaded into memory (~5 seconds). When loaded, the reference images were displayed. Three keys allowed the observer to switch between the known reference image, a manipulated image, and a standard image which was identical to the reference image. To preserve the observers state of adaptation, the gray adapting field was displayed for 0.2 seconds when alternating between images. The observer was instructed to toggle between the images and stop on the one which was different from the known reference image. They were then asked to judge if that was an acceptable reproduction for an expensive book of photographic reproductions. After both judgments were made, the next set of images were displayed. A total of 852 judgments (using 426 images) per observer were made in three one-hour long sessions

A standard probit analysis was then performed on the data to determine the median tolerance (T50) after correcting for the 50% natural chance rate of the experiment. Along with the T50 point, fiducial limits were calculate which express the probability that, within a certain percentage, the estimated T50 point will fall with in a particular range.

2.3.2. Perceptibility Tolerances

Table 2.3-3 below lists the overall perceptibility tolerances on the k values and the average image ΔE^*_{ab} and MCSL (a precursor to ΔE_{94}) color difference along with 95% confidence limits found by Stokes. The tight fiducial limits on the tolerances allow the results to be useful as tolerances. The symmetry of the results has been used in subsequent studies to limit the number of transfer functions studied, allowing instead for either shorter observational time, or for more images to be judged. The large 5° hue angle shift was surprising because previous work had indicated that observers are extremely sensitive to hue angle shifts using uniform patches. Apparently, the complexity of images substantially lowers the observers sensitivity to such changes. From these results, a rough color tolerance was devised using a CIELAB color difference of 2.01 (with a 95% CI of 1.11–4.06).

Table 2.3-3 Perceptibility Tolerances as Measured by Stokes

	Transfer Function Constant (K)			Average $\Delta E'_{ab}$			Average MCSL		
Function	T50	Lower	Upper	T50	Lower	Upper	T50	Lower	Upper
LMF	0.93	0.92	0.95	2.56	1.70	3.32	2.56	1.72	3.07
LPH	1.11	1.10	1.13	3.32	1.57	4.06	3.32	1.94	4.02
LPL	0.90	0.89	0.92	3.07	2.10	3.99	3.07	2.10	3.99
LSH	1.17	1.16	1.19	2.38	1.61	2.85	2.38	1.61	2.85
LSL	0.88	0.87	0.89	1.94	1.14	2.44	1.94	1.14	2.44
CMF	0.91	0.90	0.92	2.19	1.23	3.41	0.94	0.48	1.26
CPH	1.13	1.11	1.14	2.39	1.50	3.00	1.15	0.72	1.45
CPL	0.89	0.88	0.9	2.49	1.45	3.64	1.24	0.73	1.80
HOH	5.9	5.2	6.5	2.52	2.01	3.47	1.80	1.28	2.16
HOL	-4.9	-5.6	-4.1	2.01	1.11	2.66	1.43	0.85	1.77
			Average	2.49	1.54	3.29	1.98	1.26	2.48
			Stdev.	0.43	0.34	0.54	0.82	0.57	0.99

2.3.3. Acceptability Tolerances

During the experiment, acceptability tolerances were also collected. These are summarized in the table below. As with the perceptibility tolerances, the major findings for this section of the experiment were the tolerances themselves, the tightness of the fiducial limits, and the apparent symmetry for all of the dual sided functions. A CIELAB color difference of 6.6 was found to give a rough indication of acceptable differences though no raw data were shown to support this. This result agrees well with previous research by Stamm [1981].

Table 2.3-4 Acceptability Tolerances as Measured By Stokes

	Transfer Function Constant (K)		
Function	T50	Lower	Upper
LMF	0.91	0.90	0.91
LPH	1.19	1.18	1.20
LPL	0.87	0.85	0.88
LSH	1.35	1.32	1.38
LSL	0.84	0.82	0.85
CMF	0.85	0.83	0.87
CPH	1.18	1.17	1.18
CPL	0.08	0.77	0.82
HOH	9.2	8.2	10.3
HOL	-8.9	-11.1	-6.3

2.4. Prior Art – Uroz 1999

For his MSc in Colour Imaging from the University of Derby in England, Joan Uroz performed an image color tolerance experiment using large format ink-jet prints from a Hewlett-Packard DesignJet 2500 CP thermal inkjet printer.

2.4.1. Experimental Method

Using Stokes finding of general symmetry in tolerances, Uroz selected three compressive transforms of interest to the printing industry. A compressive power transform in L* was used to simulate loss of contrast. A multiplicative reduction in chroma to mimic changes in gain. And a random pixel by pixel transform in L*, a* and b* was used to simulate noise in the overall system. The functional forms of the two systematic transforms are shown in Table 2.4-1 below. The random changes were produced using a pairs of randomly chosen radial and azimuth angles from a normal distribution with a mean of L*=50, a*=b*=0 and a standard deviation of 15° Thus 99.857% of the points were within a ±45° cone of the original pointing towards the center of the CIELAB space.

Table 2.4-1 – Systematic Transforms used by Uroz

Dimension	Formula
Lightness (L*)	$L^*_T = L^*_K + \left(L^*_W - L^*_K\right)\left[\frac{L^*_{in} - L^*_K}{L^*_W - L^*_K}\right]^a$
Chroma (C^*_{ab})	$C^*_{ab,out} = b \cdot C^*_{ab,in}$

Where:
L^*_{in} is the input L* value
L^*_K is the L* value of the printer black (3 in the case of Uroz)
L^*_W is the L* value of the paper white (93 in the case of Uroz)
L^*_T is the transformed L* value
a>1, b < 1 to produce compressive transforms

Along with each of the four images used, Uroz created a 128 color pallet of the predominant color in the image using Adobe Photoshop's Adaptive Palette Indexing algorithm. This palette was processed and printed along with the images to allow quantitative measurements of its colors after transformation and printing.

Ten sets of pairs for both L* and C^*_{ab} adjusted images were chosen based on the results of a pilot experiment. Eighty pairs were formed (10 levels, 2 transforms, 4 images) from the possible combination. Five color normal observers, experienced with making color difference evaluations, were asked whether or not they perceived a difference between the pairs, and if so, to mark where on the image they perceived the differences. Observations were conducted in a D50 viewing booth with a 45/0 geometry.

A similar experiment was then conducted using two of the four images from above at 7 levels each of random CIELAB variation (14 pairs). For this section nine color normal observers were used to maintain a similar statistical significance in the results. The first five observers had also participated in the previous experiment with the systematically changed images. The additional four observers were less experienced in evaluating color differences.

2.4.2. Perceptibility Tolerances

Using the palettes printed with each transformed image, Uroz compared two different stimulus metrics. The first metric assumed that an observer would respond to the average color difference in the image and was the arithmetic average of the pixel-wise ΔE^*_{ab}'s. The second metric assumed that the observers segmented the image into recognizable features (face, shirt, sky etc...) and made their judgment on first pair that could be perceived as different. To model this process, the 99th percentile ΔE^*_{ab} was used. Upon further analysis, it was found that the average color difference would not provided adequate normality for use in Probit analysis and the 99th percentile was chosen.

Uroz then compared threshold results using 99th percentile differences in both ΔE^*_{ab} and ΔE_{94}. Overall threshold results along with 95% confidence limits are shown in the tables below for the three transforms used.

Table 2.4-2 Threshold Values for Systematic Changes in L and C*ab*

Color Difference Metric	Dimension	Threshold	Lower	Upper
ΔE^*_{ab}	C^*_{ab}	4.48	3.62	5.13
	L^*	4.30	3.61	4.87
Overall Systematic Changes		4.39	3.87	4.83
ΔE_{94}	C^*_{ab}	1.85	1.44	2.09
	L^*	3.58	2.95	4.08

Table 2.4-3 Threshold Values for Random CIELAB Changes

Image	Threshold	Lower	Upper
Fruit	2.63	0.99	3.55
Musicians	1.07	N/A	2.17
Overall	1.94	N/A	2.59

When expressed in terms of ΔE^*_{ab}, tolerances for both lightness and chroma were statistically similar, which was not the case when expressed in ΔE_{94}. Stokes reported an overall threshold for systematic changes of approximately 2 ΔE^*_{ab} using the average pixel-wise difference between the images. Uroz reports that the average value that corresponds approximately to the pallet-99%-precentile is 2.3 ΔE^*_{ab} which is in very close agreement despite the different metrics and procedures.

2.5. Current Standards Activities

In October 1998, CIE division 8: Imaging Technology approved the creation of TC 8-02 "Colour Difference Evaluation in Images" This committee, chaired (as of this writing) by Prof. Ronnier Luo, is seeking to study, develop, and standardize methods to derive colour differences for images. It is expected that this research project will tie in with their efforts as much as possible. More information regarding this committee, along with their current technical reports can be found on the on the CIE Division 8 web site: www.colour.org [CIE 2000].

3 Equipment – Displays and Devices

This section details the various displays and measurement devices used during this project.

3.1. Sony GDM-F500 CRT Display

During this analysis this display was driven by an Apple Macintosh® G3 computer at a resolution of 1280x1024 @80Hz. The white point was set at 6500K using the monitor's built-in controls and all forms of color management were either turned off or set to nominal conditions. Because most CRTs are sensitive to magnetic field variations, all measurements were taken without moving the display. The onboard degaussing feature was used several times before beginning measurements. Apple's ColorSync® software was set in a generic RGB mode during all phases of testing.

3.1.1. Product Features

The GDM-F500 is Sony's flagship model display for CAD and graphic professionals. This virtually flat 21" CRT uses the FD Trinitron tube. Other enhancements include:

- HiDensity™ Electron Gun which allows for a tight 0.22 mm aperture grille pitch.
- Enhanced Elliptical Correction System™ technology which uses additional focusing elements to correct for the elliptical beam shape distortions near the edges of the screen.
- GeoLock Plus™ circuitry which automatically senses and neutralizes electromagnetic fields thereby reducing image color distortion commonly noticeable on large CRTs.

3.1.2. Further Information

More information about this display can be found on Sony's web site: http://www.ita.sel.sony.com/products/displays/fseries/gdmf500.html.

White papers containing more details on the various technologies used in this, and other Sony displays can be found at: http://www.ita.sel.sony.com/products/displays/displaytech.html.

3.2. SGI® 1600SW™ LCD Panel

The all digital 1600SW display was driven by a Silicon Graphics Visual Workstation® 320 running Microsoft® Windows NT®. The SGI ColorLock™ sensor and software was used to calibrate the display to the sRGB setting (D65 white point, gamma of 2.2) prior to making measurements.

3.2.1. Product Features

The 1600SW is an active matrix digital LCD, flat panel display with a SXGA-wide (1600 x 1024) format. Product features include:

- Adjustable white balance via software and dynamic backlight adjustment. Accurate to within 25K.
- ColorLock™ system which uses factory characterization data stored within the onboard memory of each monitor and a specially designed photopic sensor to self-correct the panel.

3.2.2. Display Defects

Current manufacturing methods are not capable of producing 100 percent defect-free active matrix LCD's at reasonable cost. Therefore, to increase yield, manufacturers allow some level of defects to be shipped [Evanicky 1999] . The most common defects are weak pixels and ones that are stuck in one state which appear as unchanging bright or dark spots depending on the display mode (normal bright vs. normal dark).

Silicon Graphics specifications allows no more that 5 green defects per monitor, with no more than a total of 8 bright defects of all colors combined. On the particular display used in this study (SN 92000350N), there are two noticeable "on" red pixels near the edges of the screen.

3.2.3. Viewing Angle

One of the major issues facing the designers of LCD displays is viewing angle. The pixels of an LCD display do not emit light (as in a CRT) but rather obtain it from a backlight source and transmit it along their molecular axes. Since the twisted-nematic liquid crystals exhibit birefringence, changes in viewing angle lead to changes in appearance.

SGI defines the viewing angle of their displays to be the range of angles giving acceptable contrast ratios and linear gray scales. This display claims a viewing angle of 120° horizontal, +45°/-55° vertical. From casual observation of the display, these values seems to be correct.

3.2.4. Further Information

More information can be found on SGI's web site at: www.sgi.com/peripherals/flatpanel. A well written introduction to LCD display technologies, as well as the specific advances made in the SGI display can be found at: http://www.sgi.com/flatpanel/pdf/lcdisplays.pdf.

3.3. IBM Roentgen LCD Prototype

The IBM Roentgen display is a prototype 200ppi digital active matrix TFTLCD display in a QSXGA (2560 x 2048) format [Bassak 1998, Schleupen 1998]. To avoid the need for a special high-end adapter, the screen is divided into four columns each controlled by it's own SXGA display adapters inside an IBM IntelliStation® Z Pro running Windows NT.

3.3.1. Display Defects

As with the SGI display, several defects are present in the IBM display. Being a prototype defects are more widespread and varied. Although every effort was taken to minimize their impact, many were unavoidable in the measurement area. Such defects as described below would not be present in a final product.

Shot Boundaries – Ten regularly spaced vertical bands appear across the width of this unit, each one corresponds to a single exposure in the photolithography process used in manufacturing the panel. Slight miss-alignment of the edges cause a mach banding effect, emphasizing their appearance, especially on light backgrounds. These can be eliminated using better alignment control.

White Blobs – Several small white blobs are visible on the screen which are caused by a disruption in the cell block creating interference. These can be eliminated or screened out in manufacturing.

Black Blobs – A noticeable black blob caused by contamination on the back polarizer is also present.

Line Defects – Since LCD displays are essentially accessed in a row/column format, any missed connection in the 1.6 miles of specially formulated thin-film copper wire can cause an entire row or column of pixels to be unaddressable. A white line also appears in several locations due to weak gate lines. IBM has developed technologies to minimize these defects in the prototype unit.

Horizontal Smudges – One area on the display has a smudged appearance on the front glass due to residual chemicals left from hand buffing the polyamide layer which aligns the liquid crystals.

Uneven Illumination – For the prototype, an off-the-shelf back light system was used since increased resolution was the primary focus. A customized back light unit would improve both the intensity and uniformity of the back light in production units.

3.3.2. Viewing Angle

The viewing angle of the prototype display is very limited, even small shifts in position alter its appearance. A commercial version of the display would be better optimized in this area.

3.3.3. Further Information

Additional information can be found at www.research.ibm.com/news/detail/factsheet200.html.

3.4. Fujix® Pictrography® 3000 Printer

The Fujix Pictrography is an 8 bit per channel CMY printer using a laser-exposed thermal development transfer marking method. The Fujix was driven by an Apple Macintosh computer running Adobe® Photoshop® 5.5. To ensure consistent performance, all known forms of color management in the Macintosh OS and in Photoshop were either turned off or set to generic values. All images were printed on Fuji's high quality photo-thickness paper stock.

3.4.1. Further Information

More information regarding this printer can be found on Fuji Film's web site at: http://home.fujifilm.com/products/digital/pictro/p3000/spec.html.

3.5. Summary Comparison of Displays

The table below lists some key features of each display used in this thesis for comparison.

Table 3.5-1 Summary Comparison of Display Physical Characteristics

	Sony GDM-F500	SGI 1600SW	IBM Roentgen prototype	Fujix Pictrography 3000
Viewing Size	19.8" Diagonal	17.3" Diagonal	16.3" Diagonal	291 x 204 mm
Resolution	~72 ppi	110 ppi	200 ppi	400dpi
Pixel Pitch	0.22 mm	0.231 mm	0.126 mm	1/400 inch
Total Pixels	1280H x 1024V@80Hz	1600H x 1024V	2560H x 2048V	3800 x 2759
Bits per channel	8	8	6	8
Luminance	56 cd/m²	161 cd/m²	153 cd/m²	836 cd/m²
Contrast	427:1	276:1	205:1	30:1

Please note the following points:

- In this comparison, viewing size is defined as the diagonal size of the viewable area of the display.
- Luminance measurements of monitor white were made on a central 3.5" square of maximum white surrounded by mid gray.
- Luminance measurements of paper white was made on unprinted media placed in the viewing booth in the same position used for the test samples during the observer sessions.

3.6. Measurement Devices

3.6.1. LMT C1200 Colorimeter (S/N 038899)

The LMT C1200, a high end tristimulus colorimeter was used for making all tristimulus measurements during this experiment. Readings were taken using a custom MATLAB®/C software controller via a GP-IB interface card on a Macintosh G3 computer.

The C1200 uses four specially selected silicon detectors (two for $\bar{x}$, and one each for $\bar{y}$ and $\bar{z}$) in combination with 17 hand-cut glass filters to achieve a very high level of absolute accuracy. In addition, the sensors and filters are thermostaticly stabilized such that variations in the surrounding temperature between 0 and 35°C do not effect the accuracy of the measurements. The photocurrent amplifiers are also stabilized to reduce offset-drift [LMT 1984].

In a study by Berns, Gorzynski and Motta, this C1200 was compared to a Minolta CS-100 colorimeter, a Minolta TV-2160 color analyzer and a Photo Research PR703A tele-spectroradiometer and found to be the most accurate. The LMT had an RMS error of 0.25 ΔE^*_{ab} compared to 0.88 for the PR703A, 5.58 for the TV2160 and 4.28 for the CS-100 [Berns 1993b].

3.6.2. LMT L1009 Photometer (S/N 118605-05)

The L1009 is a high precision instrument for luminance measurements meeting class A requirements of DIN 5032 part 7 and CIE publication number 69 [CIE 1987]. The measuring range of the L1009 is from 0.0001 cd/m² to 19,990,000 cd/m². The L1009 incorporates angular fields of 3°, 1°, 20' and 6'. The L1009 was used in checking the luminance additivity of the three monitors and in measuring the print viewing environment.

3.6.3. Photo Research® PR® -704 Tele-Spectroradiometer (S/N 1008)

The PR704 tele-spectroradiometer measures spectral radiance ($^{W}/_{m^2 \cdot sr}$) from 380–780nm at 2nm increments. While the PR-704 could have been used in characterizing the three monitors used in this study, it is susceptible to viewing-angle dependency errors on the two LCD panels unlike the LMTC1200 [Berns 1993b]. The PR-704 was thus used only to compare the spectral properties of the three monitors and to measure the room illumination for the print experiment.

3.6.4. GretagMacbeth™ Spectrolino™ Spectrophotometer (S/N 3.257-10323)

The automated SpectroScan™ x/y measurement stage made reading the 1000 patches used in characterizing the printer convenient.

A recent student project at RIT examined the precision and repeatability of the Spectrolino used in this study [Henley 1999]. Readings in the tables below are an average of 12 measurements over the time frame specified. Short term accuracy was measured with replacement versus the given calibration values provided by BCRA [Billmeyer 1981].

Table 3.6-1 GretagMacbeth Spectrolino Precision

	Short Term		Medium Term	Long Term
ΔE^*_{ab}	No Replacement	With Replacement	(4 hour period)	(2 weeks)
Light Gray	0.01	0.32	0.02	0.14
Dark Blue	0.04	0.11	0.13	0.16
Pink	0.08	0.14	0.06	0.13
Medium Blue	0.01	0.31	0.02	0.17
Yellow	0.08	0.14	0.07	0.07
MCDM	0.04	0.17	0.05	0.11

Table 3.6-2 GretagMacbeth Spectrolino Accuracy – Short Term With Replacement

Tile	ΔE^*_{ab}
Light Grey	0.85
Medium Grey	0.66
Dark Grey	0.42
Pink	0.82
Maroon	0.31
Yellow	0.90
Brown	0.46
Light Green	1.18
Dark Green	0.70
Green Blue	0.58
Medium Blue	0.95
Dark Blue	0.47
Average	0.64

4 Display Characterization

In order to understand the properties of each of the four displays used, a careful characterization of each was conducted. The details of this process and the resulting findings are presented below.

For the three emissive displays, an extensive characterization was performed. Characteristics such as the spectral power distribution of the primaries, peak luminance and contrast were measured for comparison. Spatial independence and chromatic constancy of primaries were also tested.

To model each of the three monitors, neutral ramps (dr=dg=db), primary ramps, internal flare (dr=dg=db=0), display white (dr=dg=db=0) and the maximum primaries were measured. From these data, each monitors electro-optical transfer curve was established using the GOG model [Berns 1996] relating digital counts to linear tristimulus scalars (RGB). These scalars, along with the peak chromaticities of the primaries allow for transformations between input digital counts and tristimulus values and from tristimulus values to the digital counts required to achieve them on the display.

For the Fujix hardcopy output, a direct 3D CLUT was used. Measurements from a 10^3 regular sampling of RGB were used to interpolate a 60^3 bounding box sampling of LCh space. Results from this process are included in the appropriate sections below.

In this experiment, the forward transform (dc to XYZ) of the Sony monitor was used to create the original LCh images. The reverse transforms (XYZ to dc) for each individual display was used to create the images presented to the observer.

4.1. Measurement Conditions

4.1.1. Emissive Displays

Colorimetric measurements of the three emissive displays were made using an LMT C1200 Colorimeter which gives readings in arbitrary tristimulus units. Luminance measurements in cd/m^2 were made using an LMT L1009 Photometer with a 1° aperture. Spectral Radiance measurements and additional luminance and spectral measurements were made using a Photo Research PR704 spectroradiometer. All colorimetric coordinates were determined using the CIE 1931 Standard Colorimetric Observer (2°). Colorimetric errors are evaluated in terms of ΔE_{94} color differences with the standard parametric factors. There was no ambient illumination in the room during measurements.

Unless otherwise noted, all measurements were performed on a central 3.5" uniform square patch with the remainder of the display filled with a medium gray background represented by RGB digital counts of (128,128,128). This was done to simulate the load placed on the display during normal usage.

As with all LCD displays, the appearance of both the SGI and IBM displays is angular dependent. To ensure a consistent evaluation of each display, all measurements were made at a 0° incident angle.

4.1.2. Hard Copy Output

Colorimetric measurements of the printed Fujix output were made using the GretagMacbeth Spectrolino. To minimize measurement noise, temporal correlation and improve precision, the 10 target pages were measured in random order, three times each and the results averaged. The black backing of the SpectroScan stage was used in all cases.

Before beginning this experiment, the Pictrography was carefully cleaned and a new set of consumables was installed. All printing was done with this single set to minimize variation in consumables. The de-ionized water used in the transfer process was changed prior to each printing session to minimize contamination build up in the system.

4.2. Spectral Properties

To successfully characterize a display it needs to have stable primaries. To examine the spectral stability of the display's primaries, a series of four logarithmically spaced patches {35,81,145,255} was displayed for each primary and measured with the PR704. A five step ramp, including black, was also measured. If the primaries were spectrally stable, the normalized plots of each ramp shown in the figures below would appear as a single curve.

During the measurement process, every effort was made to keep the PR704 perpendicular to the display to minimize angular effects. At the distances used for measurement, the 0.5° circular aperture spanned approximately 20 pixels on the display.

While the PR704 provided data from 380–780nm at 2nm intervals, only the range from 400-700nm was evaluated in this section. If the tristimulus values used in subsequent stages were to be calculated from these data it is suggested that the range be extended to at least 720nm to capture the red phosphor emission near 710nm [Berns 1993b]. Issues such as the tradeoff between bandpass and sampling increment must also be addressed. Since a very accurate colorimeter, the LMT C1200, was available which gives tristimulus values directly, these spectral measurements were made for illustrative purposes only.

4.2.1. Sony CRT Display

The spectral radiance characteristics of the Sony display are shown in the figures below. Figure 4.2–1 shows the spectral radiance distribution of the white. Figure 4.2-2 shows the corresponding plot for the displays black. Plots of the neutral and primary ramps are shown in Figure 4.2-3 – Figure 4.2-6 below. In these figures the solid line represents the full on primary {level 255}, and the broken lines the intermediate levels. The curves are normalized to their respective maximum radiance level.

Figure 4.2-1 White Radiance-Sony CRT

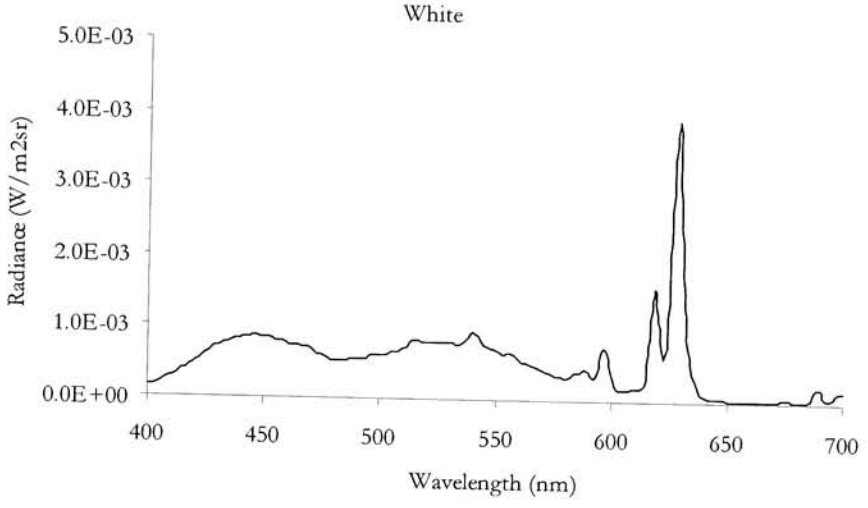

Figure 4.2-2 Black Radiance-Sony CRT

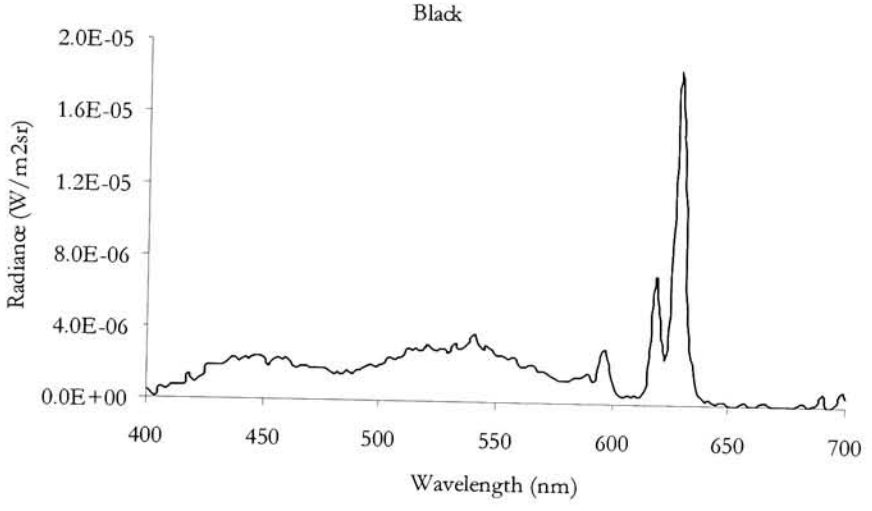

Figure 4.2-3 Normalized Gray Ramp-Sony CRT

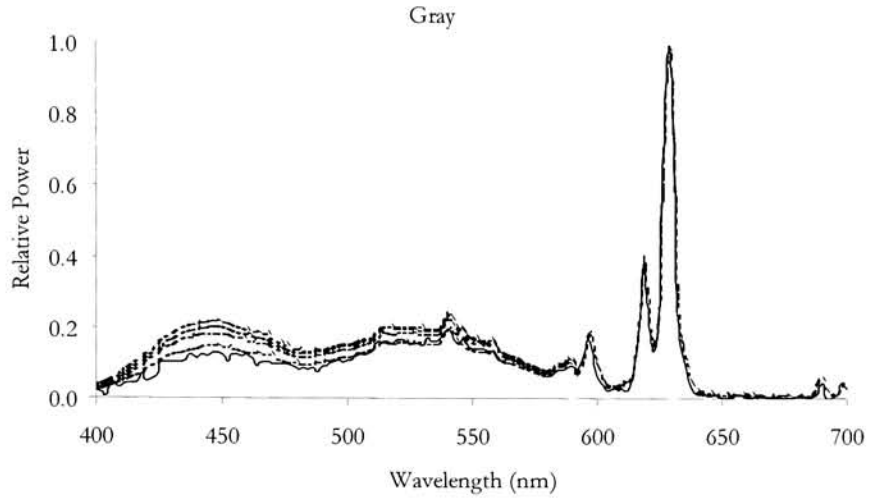

Figure 4.2-4 Normalized Red Ramp-Sony CRT

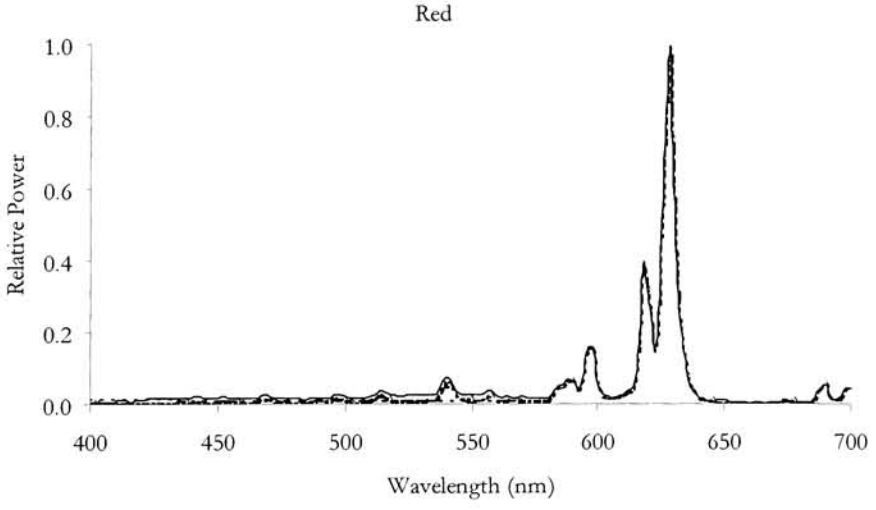

Figure 4.2-5 Normalized Green Ramp-Sony CRT

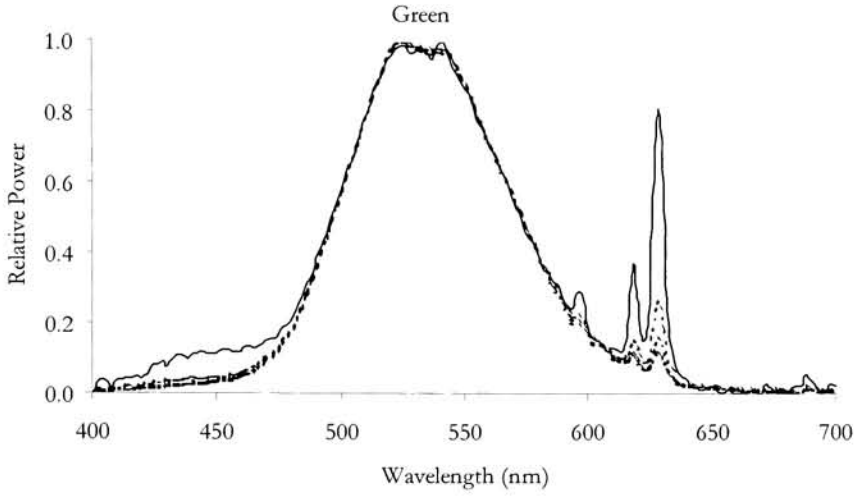

Figure 4.2-6 Normalized Blue Ramp-Sony CRT

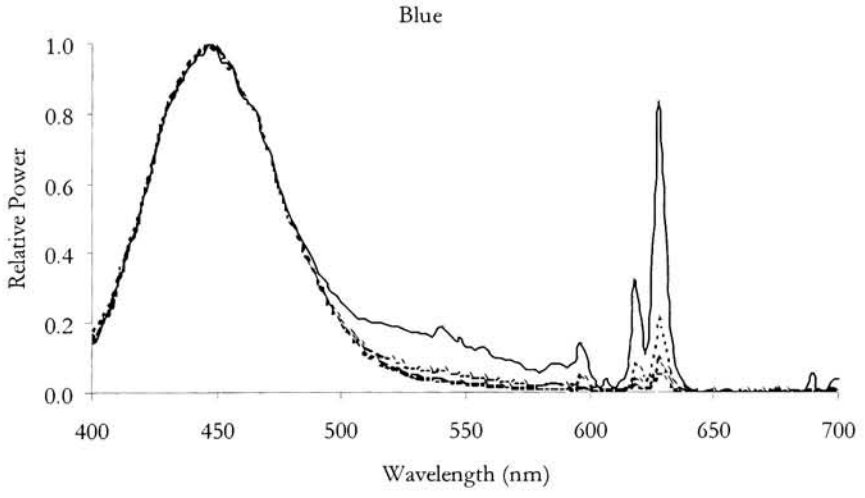

Based on the figures above, it would appear that the Sony display exhibits reasonable spectral stability as to be expected from a good quality CRT. From spectral measurements such as these, the purity of each channel can be readily evaluated. For example, the strong peak near 630nm from the rare-earth elements used in the red phosphor is visible in both the green and blue channels.

4.2.2. SGI LCD Panel

The corresponding measurements for the SGI display are given below. The white, shown in Figure 4.2-7, is characteristic of the fluorescent backlight utilized in this display. The non-zero radiance for the black state, Figure 4.2-8 (compare to Figure 4.2-2), is common for LCD displays as the polarizers are unable to fully extinguish the backlight and a small amount leaks through.

Figure 4.2-7 White Radiance-SGI LCD

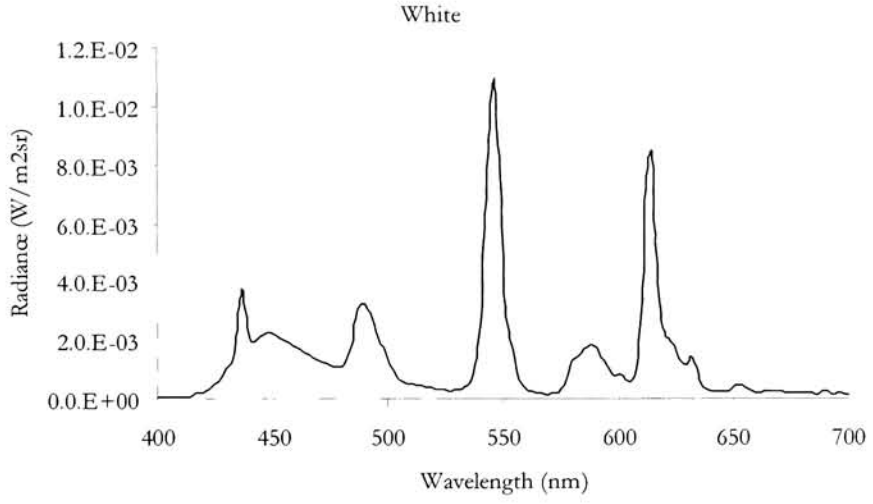

Figure 4.2-8 Black Radiance-SGI LCD

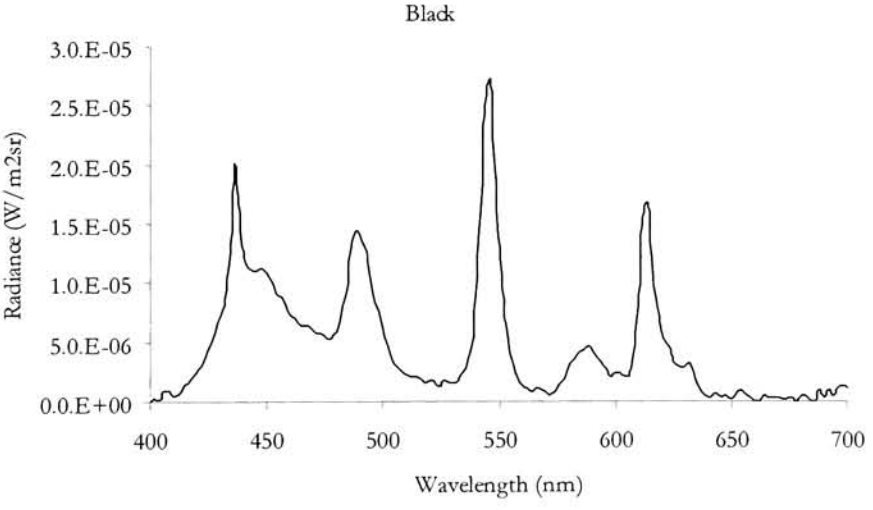

Figure 4.2-9 Normalized Gray Ramp-SGI LCD

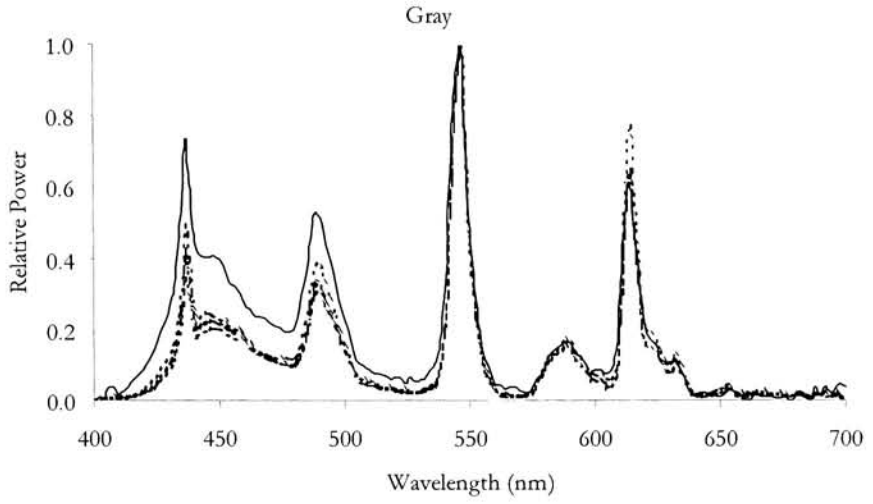

Figure 4.2-10 Normalized Red Ramp-SGI LCD

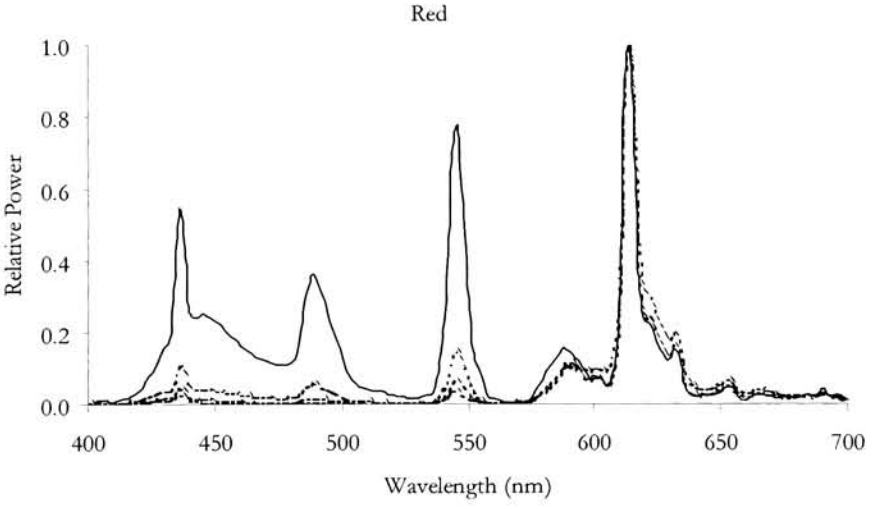

Figure 4.2-11 Normalized Green Ramp-SGI LCD

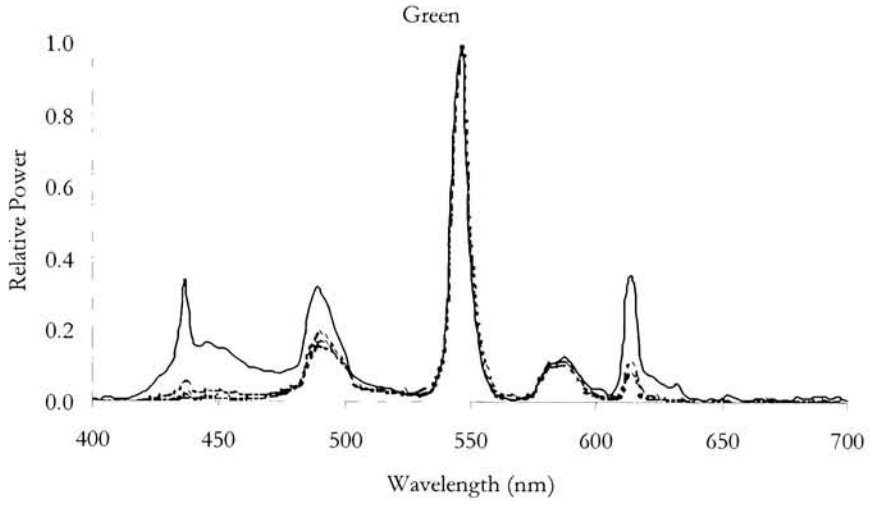

Figure 4.2-12 Normalized Blue Ramp-SGI LCD

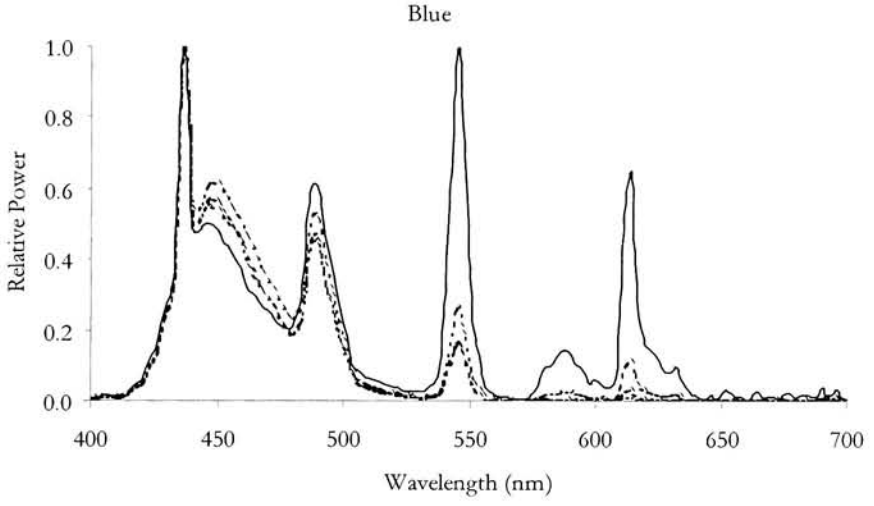

The maximum radiance normalized plots of each channel appear to have greater variability than was seen in the Sony monitor, especially in the blue. Furthermore, the characteristics of the fluorescent backlight are visible in all three channels.

4.2.3. IBM LCD Prototype

Measurements on the IBM display follow. Again, the characteristics of the fluorescent backlight are clearly visible from the white shown in Figure 4.2-13.

Figure 4.2-13 White Radiance-IBM LCD

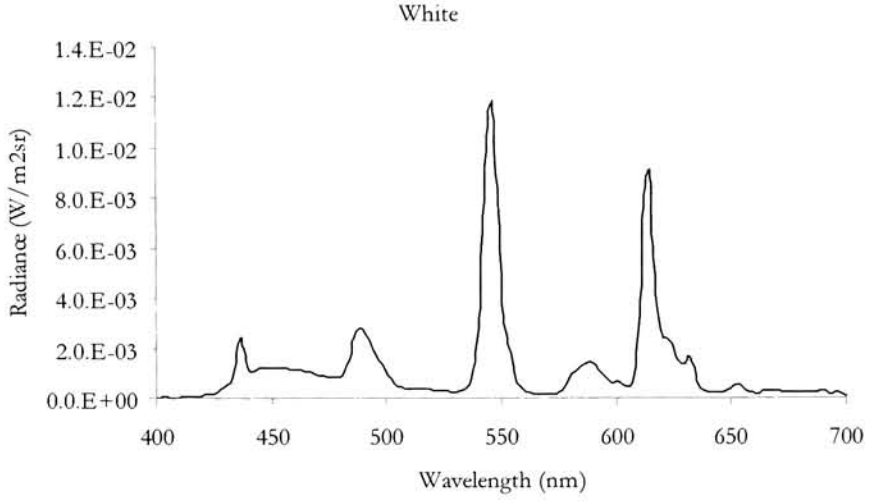

Figure 4.2-14 Black Radiance-IBM LCD

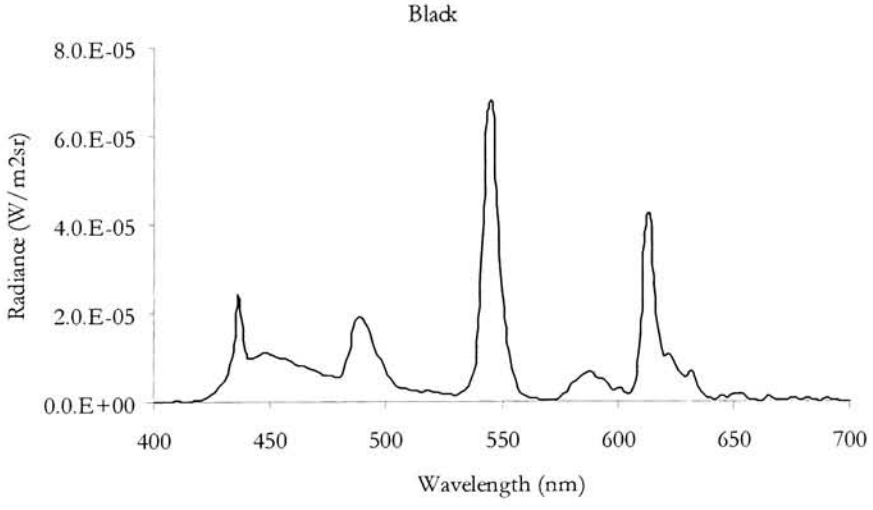

Figure 4.2-15 Normalized Gray Ramp-IBM LCD

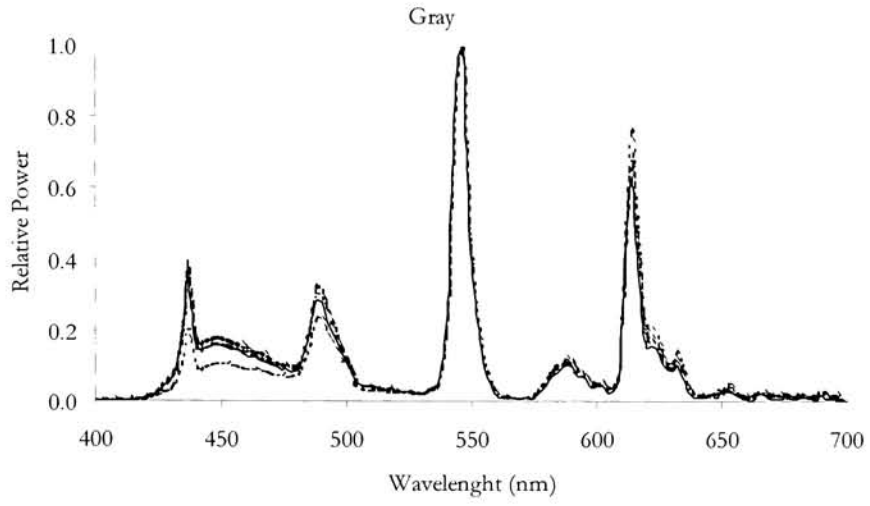

Figure 4.2-16 Normalized Red Ramp-IBM LCD

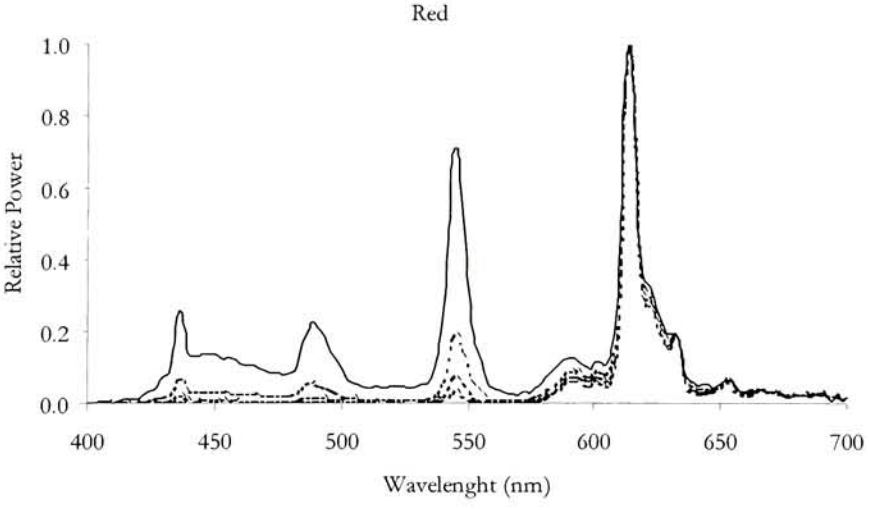

Figure 4.2-17 Normalized Green Ramp-IBM LCD

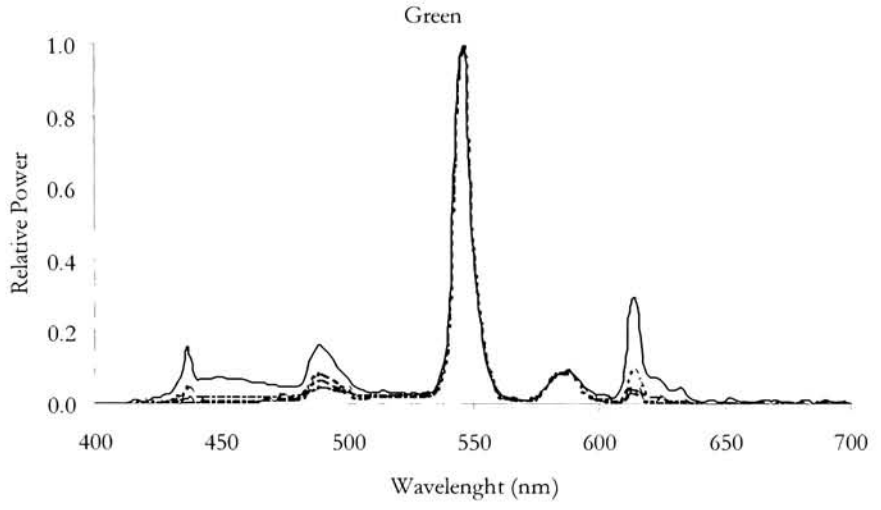

Figure 4.2-18 Normalized Blue Ramp-IBM LCD

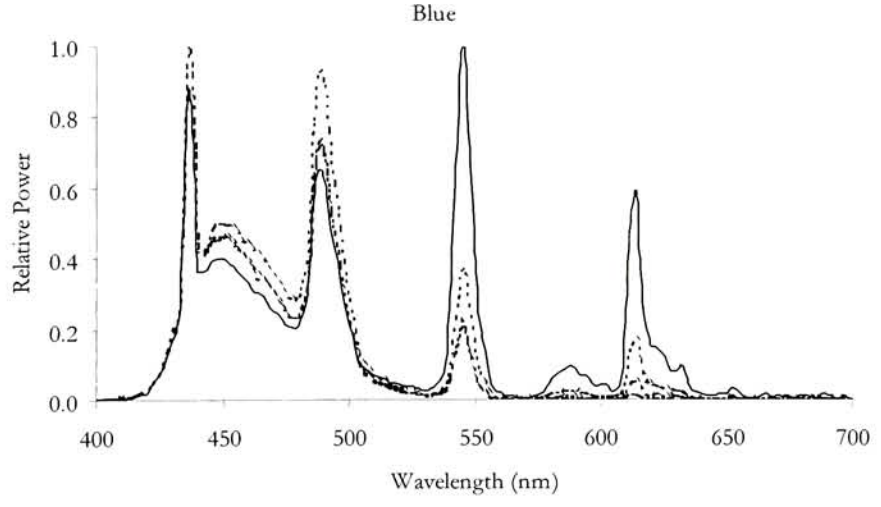

4.2.4. Fujix Pictrography Prints

Figure 4.2-19 below is the spectral power distribution of the room illumination used for viewing the Fujix prints. The data were measured using the PR 704 off a white Halon reference target.

Figure 4.2-19 Print Viewing Room Illumination

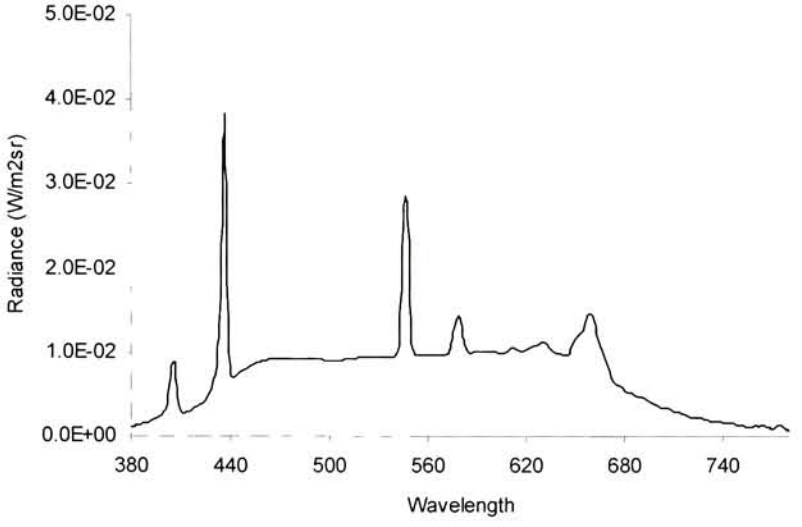

4.2.5. Comparison of Peak Spectral Radiance

Table 4.2-1 compares the peak spectral radiance output of each display for white, black, and the primaries. The two LCD displays have higher peak radiance in all three channels than the conventional display, due in part to the use of a narrow-band fluorescent backlight.

Table 4.2-1 Peak Spectral Radiance Values for Each Display

Peak Radiance (W/m^2sr)E-03	Sony	SGI	IBM
White Point	3.94	10.9	12.0
Black	0.02	0.03	0.07
Red	3.83	5.5	8.2
Green	0.75	8.8	11.0
Blue	0.83	3.4	2.4

4.2.6. Comparison of Spectral Variability.

To summarize the observed deviations from stability, coefficients of variation ($CV = \sigma/\mu$) were computed. That is, at each wavelength (400–700nm, 2nm), the standard deviation and average of all four (or five) normalized measurements at that wavelength was computed and the ratio taken. The average of all 151 CVs for each ramp is shown in Table 4.2-2. By normalizing the standard deviation with the mean, CVs are directly comparable across changes of magnitude.

Table 4.2-2 Spectral Variability-Average CV Over Wavelength

	Sony CRT	SGI LCD	IBM LCD
Gray	0.20	0.34	0.19
Red	0.35	0.81	0.84
Green	0.32	0.72	0.69
Blue	0.57	0.72	0.63

These results show that the Sony display was overall more spectrally stable than the two LCD displays. The SGI had the most spectral variability.

4.2.7. LCD Backlight Comparison

Examining Figure 4.2-20, it appears that the SGI and IBM display use a similar fluorescent back light, with the SGI display having slightly more output in the blue end of the spectrum. Since the IBM display is a prototype unit designed for testing the new LCD, a standard back light was used. With some optimization of the backlight and filters used that the IBM display could be improved.

Figure 4.2-20 Backlight Comparison of IBM and SGI Panels

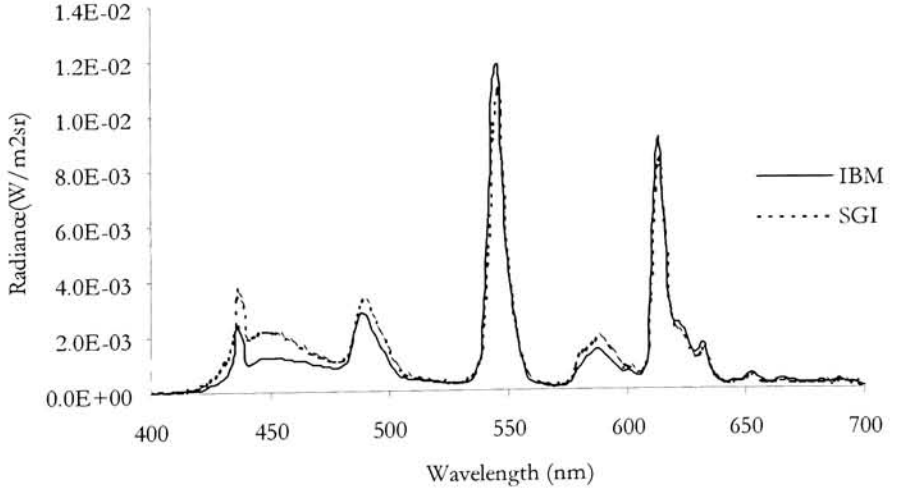

4.3. Temporal Stability

Both CRT and LCD displays require time to reach a steady state from a cold start. For CRT's, the electron beams and high voltage circuits place a great deal of heat and stress on the internals components, the effects of which take time to reach equilibrium. A similar process, with out the high voltages, also occurs for LCD's, the transmission characteristics of the LCD filters change as a function of temperature and thus require time to stabilize.

Experience with displays similar to the ones used in this experiment, show that several hours may be required to reach stability. Berns [1993b] states that CRT's can take from 15 minutes to more than 3 hours to reach stability after initial power up. A Sony PVM1942Q monitor used in their study was found to take 1 hour to reach steady state conditions. Fairchild's [1998] analysis of the Apple Studio Display LCD found that the white point of the display stabilized after 45 minutes but the gray state continued to change even after 4 hours. Despite such instabilities, Fairchild was able to develop an adequate model of the display after allowing sufficient warm up time.

While no specific warm-up tests were run for the displays evaluated in this report, a four hour warm up was allowed for each display based on the above mentioned data. To check the adequacy of this assumption, a post hoc evaluation of the temporal stability of each monitor was performed.

During the characterization process, several repeat measurements of each primary were made over the course of several hours, Table 4.3-1 below shows the ΔE_{94} mean color difference from the mean (MCDM) for each primary after a four hour warm up. The time span for these measurements is over three and a half hours for each display.

Table 4.3-1 Temporal Stability of Each Display

	Sony	SGI	IBM
Red	0.13	0.06	0.05
Green	0.14	0.05	0.04
Blue	0.08	0.04	0.03

The results indicate that the two LCD panels were very stable over the time of measurement and therefore the four hours warm-up time was adequate. The slightly larger variability seen on the CRT is not surprising and is small enough to be of little concern. Based on this analysis, a minimum of four hours warm-up was allowed for each display before beginning an observer session.

4.4. Spatial Independence

Spatial independence refers to the impact that a color displayed on one area of the monitor has on a color in another area. Characterizing a display that does not exhibit this property is difficult if not impossible. To test the spatial independence of each display, a series of nine color stimuli were measured on nine different background made up of the same nine colors for a total of 81 colorimetric measurements [Fairchild 1998]. The CIELAB coordinates of each stimulus were then computed using the average value of white on gray as the CIELAB reference white. The data are summarized in Table 4.4-1 for each display using mean color-difference from the mean (MCDM) metrics in terms of CIE94 color differences. The MCDMs were calculated both across background (i.e. how did the nine different backgrounds affect each of the foreground colors), and across stimuli (i.e. how much did the nine different foreground colors change on a given background). The data in this section were not flare corrected since only changes are compared.

Table 4.4-1 ΔE_{94} MCDMs for Spatial Independence Measurements

	Sony		SGI		IBM	
Color	Background	Stimuli	Background	Stimuli	Background	Stimuli
Black {0}	0.76	1.67	0.10	0.03	0.15	0.13
Gray{128}	0.18	0.53	0.07	0.26	0.15	0.48
White {255}	1.68	0.44	0.14	0.07	0.17	0.25
Red {128}	0.42	0.64	0.08	0.05	0.23	0.23
Red {255}	0.52	0.32	0.06	0.04	0.22	0.13
Green {128}	0.53	0.32	0.09	0.12	0.19	0.31
Green {255}	0.44	0.26	0.05	0.03	0.28	0.12
Blue {128}	0.63	0.92	0.08	0.07	0.19	0.14
Blue {255}	0.38	0.43	0.06	0.05	0.27	0.06

The overall MCDM for the SGI display was 0.08, 0.21 for the IBM, and 0.62 for the Sony display. Given that each pixel in an active-matrix TFT-LCD is physically distinct from it's neighbors, good spatial independence was expected as demonstrated above. The two LCD's tested above were on par with other LCD's such as the Apple Studio Display which has an overall MCDM of 0.20 [Fairchild 1999]. In a conventional CRT, a single scanning electron beam is used to address each pixel of a given color and lower quality displays can often suffer from poor spatial independence.

4.5. Luminance and Contrast

Using the LMT L1009 photometer, the luminance of the three primaries, black and white of each monitor was measured. The contrast of the display calculated as the ratio of white to black. Results are summarized in the tables bellow. The targets were displayed as both full-screen colors, Table 4.5-1, and as 3.5" squares with gray surround, Table 4.5-2, for comparison. The large difference in values point to the need for carefully defining the measurement conditions before stating results.

Table 4.5-1 Measured Luminance and Contrast–Full Screen

Color	Sony (cd/m^2)	SGI (cd/m^2)	IBM (cd/m^2)
Red	15.47	44.5	38.3
Green	36.0	110.3	93.9
Blue	3.51	13.81	11.92
White	55.8	167.8	150.7
Black	0.004	0.541	0.665
Contrast (W/K)	13950:1	310:1	227:1

Table 4.5-2 Measured Luminance and Contrast–3.5" Square with Gray Surround

Color	Sony (cd/m^2)	SGI (cd/m^2)	IBM (cd/m^2)
Red	15.70	42.9	38.4
Green	39.3	106.4	94.5
Blue	3.96	13.34	12.19
White	55.9	161.5	152.7
Black	0.131	0.584	0.745
Contrast (W/K)	427:1	276:1	205:1

Comparing the two tables above, it can be seen that the two LCD panels maintained their black level, and therefore contrast, as the target size was reduced. Given the nature of the LCD display, it is expected that this trend would continue to hold even for very small targets. In comparison, the CRT had an extremely large contrast with a full screen measurement, and a more moderate contrast when the target was reduced in size. Reducing the target size further would cause still more reduction in contrast

Sony The full screen luminance of the Sony monitor is more than a factor of two lower than either of the two LCD displays tested but is typical of most good quality CRT displays. The full screen contrast ratio is typical for CRT's since, when properly setup, little to no light is emitted from the black state on a CRT.

SGI The SGI monitor has the highest luminance output of the thee monitors tested in this report. While not as high luminance as the Apple Studio display measured by Fairchild [1998] which measured 188 cd/m^2, the SGI's contrast ratio was considerably higher (310:1 vs. 250:1) indicating a darker black level. The measured contrast ratio is on par with the manufactures claim of 350:1. To achieve this SGI uses two techniques. First, a negative birefringence compensation film is placed after the liquid crystal cell to compensate for the positive birefringence introduced by the liquid crystal giving a greater extinction level. Second, thick color filters are used to maintain high saturation levels in the primary color sub-pixels thus minimizing the impact of any stray leakage from adjacent pixels.

IBM The weaker performance of the IBM display is most likely due to it's prototype nature and would be improved upon in a commercial version.

4.6. Chromaticity Constancy of Primaries

The gain-offset-gamma (GOG) model for characterizing displays uses a two stage process. First, three 1D-LUT's are used to transform the incoming digital counts into linear scalars. Second, the linear scalars are multiplied by a 3x3 primary mixing-matrix. Thus the estimated signal is a scaled version of the full strength primaries. For this process to work, the chromaticity coordinates of each level must remain constant. To test this assumption, a series of 16 logarithmically spaced steps in red, green, blue were measured along with a 17 log-step gray ramp. As in Fairchild [1998], the black level flare has been removed from each measurement before computing the chromaticities. Results for each display are given below.

4.6.1. Sony CRT

Figure 4.6-1 Chromaticity of Red, Green, Blue Primaries and Neutrals-Sony CRT

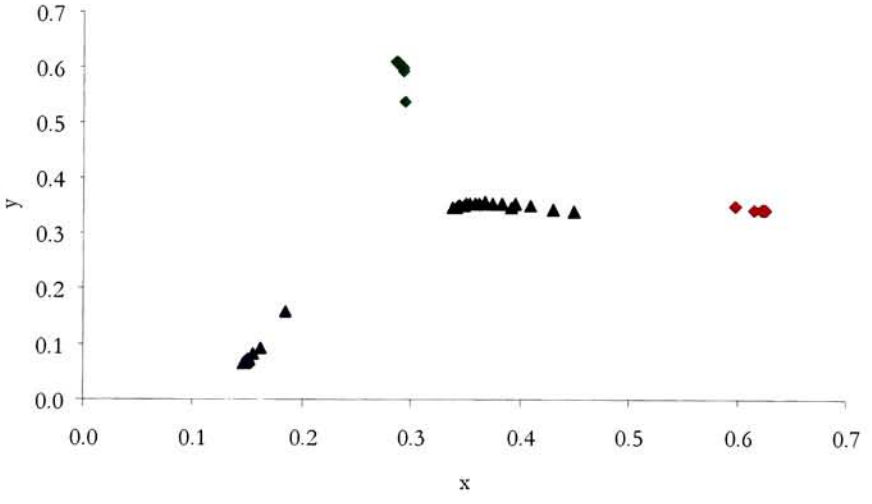

The primary constancy of the Sony display appears adequate, as is expected of a high quality CRT. The tendency of each primary towards the white point may indicate that some residual flare was not accounted for. The large variation in the gray levels is due primarily to the undefined nature of chromaticity coordinates at very low tristimulus values, and is of little concern in modeling the displays colorimetry.

4.6.2. SGI LCD

Figure 4.6-2 Chromaticity of Red, Green, Blue Primaries and Neutrals-SGI LCD

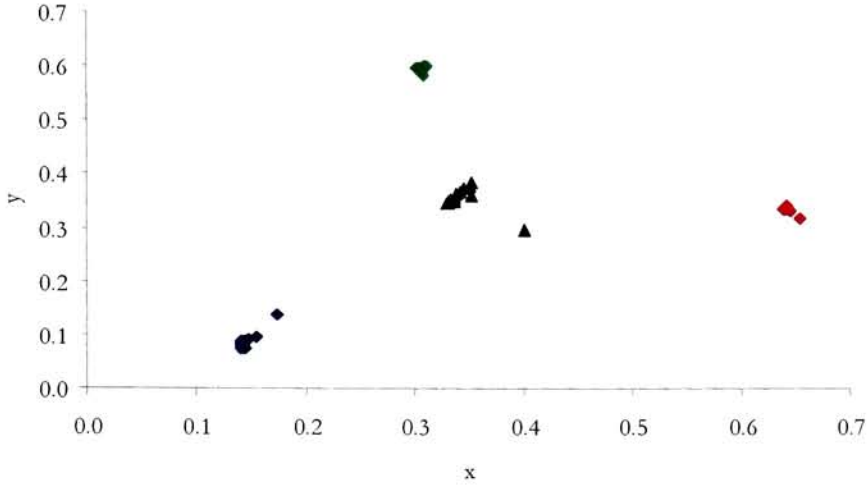

The SGI display appears to exhibit good consistency in the primaries and has a stable gray scale. The one outlying point in the gray ramp is the black. The tristimulus values of the black patch, after subtracting the average flare value, were slightly non zero {-0.001, -0.0008, -0.0007} and therefore produced an outlying point in chromaticity space. Had these values been hard clipped to 0, they would have produced an undefined value and caused an error in the code used to compute them. In practice, such small deviations from zero are insignificant and would be removed, their inclusion here is simply to serve as an illustrative warning.

4.6.3. IBM LCD

Figure 4.6-3 Chromaticity of Red, Green, Blue Primaries and Neutrals-IBM LCD

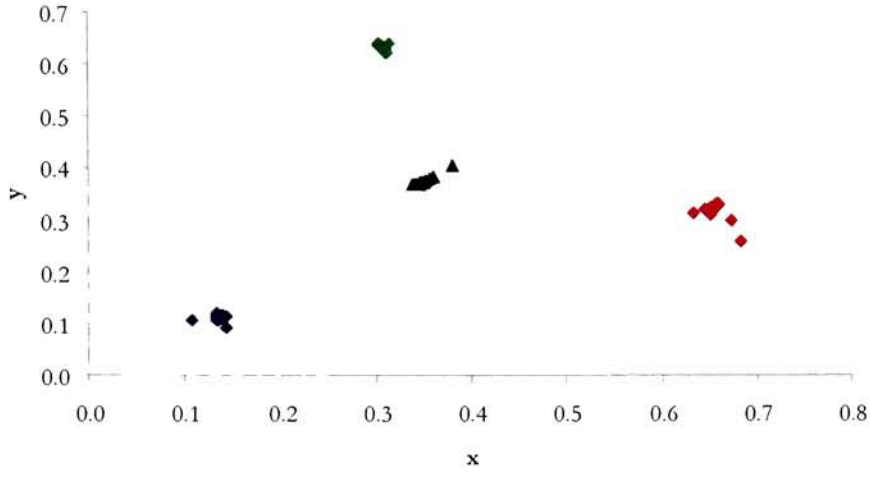

As with the other two monitors measured, the IBM display appears to exhibit good consistency in the primaries and has a stable gray scale.

4.6.4. Summary Comparison of Chromaticity Constancy

To summarize the variability of each displays primaries, Table 4.6-1 lists the coefficient of variation in both the x and y dimensions for each primary.

Table 4.6-1 Chromaticity Variability

Color	Sony		SGI		IBM	
	x	y	x	Y	X	Y
Red	0.01	0.00	0.01	0.01	0.01	0.02
Green	0.01	0.03	0.01	0.01	0.02	0.01
Blue	0.06	0.31	0.01	0.15	0.08	0.07
Gray	0.09	0.01	0.02	0.01	0.03	0.02

4.7. Additivity

The additivity of each display was evaluated in both luminance, Table 4.7-1, and tristimulus space, Table 4.7-2. Luminance values were measured with the LMT L1009 photometer at a distance such that its 1° spot size spanned approximately 20 pixels on the display. The LMT C1200 colorimeter used for tristimulus measurements has a 3" diameter aperture and is set 2.25" back from the front surface of the device by means of a matte black tube. All tristimulus values in this section were flare corrected by subtracting the average tristimulus values of the black squares measured (8 in all) from the corresponding values of each sample. Results for each display are discussed in the various sub-sections below.

Table 4.7-1 Luminance Additivity

Color	Sony (cd/m^2)	SGI (cd/m^2)	IBM (cd/m^2)
R+G+B	54.98	168.61	144.12
White	55.8	167.8	150.7
Difference	1.5%	-0.5%	4.5%

Table 4.7-2 Tristimulus Additivity

	Sony			SGI			IBM		
Value	White	R+G+B	% Diff.	White	R+G+B	% Diff.	White	R+G+B	% Diff.
X	35.78	35.53	0.70%	84.83	84.82	0.01%	75.92	70.14	7.61%
Y	36.94	36.70	0.63%	87.40	87.33	0.08%	81.32	75.21	7.51%
Z	33.26	32.77	1.46%	69.02	68.96	0.09%	41.46	40.22	2.98%

The values for Luminance additivity and the Y tristimulus value do not match in part because different instruments were used. The L1009 displays readings directly in cd/m^2 whereas the units for the C1200 are only linearly related to cd/m^2. No correction transform was used since only relative values were required. Furthermore, the L1009's design required that it be placed several feet from the display to allow the user to focus on the display thus making it more susceptible to stray light than the C1200 which was placed in direct contact with the display surface.

Sony The small failure of additivity for this display might well be due to a small increase in flare at the high luminance levels which is not present when estimating the flare from black alone. On many CRT's there is circuitry on board the display which increases the power sent to the electron guns to compensate for their increased load. The degree of additivity is sufficient to justify the use of a 3x3 primary matrix transform.

SGI The additivity on this display was excellent, exceeding many other displays tested at the MCSL. Given the high resolution of this display and the discrete nature of each pixel, it is not surprising that the additivity was good. The use of the 3x3 primary matrix transform is well justified.

IBM The large differences between white and R+G+B are disturbing. A possible cause may be the strong angular dependency of this display. The LMT colorimeter was used with a very large acceptance cone and may therefore be subject to color shift errors. However, a substantial failure of additivity was also observed using various aperture sizes both with the LMT photometer and the colorimeter as shown in the table below.

Table 4.7-3 Additivity vs. Aperture Size – LMT Colorimeter

	3" Aperture			1" Aperture			0.5" Aperture		
Color	X	Y	Z	X	Y	Z	X	Y	Z
Red	37.84	19.279	0.263	3.764	1.916	0.027	0.749	0.381	0.005
Green	21.34	45.069	3.403	2.121	4.494	0.34	0.421	0.892	0.066
Blue	5.988	5.439	33.62	0.61	0.543	3.417	0.121	0.108	0.675
R+G+B	65.16	69.787	37.29	6.495	6.953	3.784	1.291	1.381	0.746
White	70.6	75.509	38.55	7.004	7.482	3.862	1.385	1.483	0.76
% Difference	7.7%	7.6%	3.3%	7.3%	7.1%	2.0%	6.8%	6.9%	1.8%

Table 4.7-4 Additivity vs. Aperture Size – LMT Photometer

	Aperture Size			
Color	6'	20'	1deg	3deg
Red	36.5	36.6	36.6	36.4
Green	88.8	89.0	88.8	88.2
Blue	11.6	11.60	11.58	11.54
R+G+B	136.9	137.2	136.98	136.14
White	143.3	143.5	143.3	142.4
%Difference	4.5%	4.4%	4.4%	4.4%

4.8 Electro-Optical Transfer Function

4.8.1 Sony CRT Display

The basic procedure for characterizing a color CRT display using the gain-offset-gamma (GOG) model is given in [Berns 1996, Berns 93a, 93b]. In the basic implementation a fitted nonlinear function is first used to convert normalized digital counts $\{d_r, d_g, d_b\}$ into linear scalars {R,G,B}. These scalars are then linearly combined via a 3x3 matrix and the internal flare added in. In some cases three 1D LUTs can be substituted for the nonlinear transfer functions.

Being a conventional CRT display, the GOG model described above was used to characterize the Sony display. From a 17 step, logarithmically spaced gray ramp, target RGB scalars were estimated using the inverse 3x3 mixing matrix. Then, using a simplex nonlinear estimation, a constrained GOG model was fitted using Equation 4.8-1. The estimated parameters are given in Table 4.8-1, and the resulting curves are plotted in Figure 4.8-1 – Figure 4.8-3.

Equation 4.8-1 GOG Model Constrained to Gain+Offset=1.0

$$\bullet = \left(Gain \times \left(\frac{d_c}{255} \right) + (1 - Gain) \right)^{Gamma}$$

Where: • refers to the red, green, or blue scalar (RGB).

Table 4.8-1 Estimated GOG Parameters for Sony Monitor

Channel	Gain	Gamma
Red	1.0025	1.6553
Green	1.0200	1.7052
Blue	1.0200	1.7581

As a quick test of the models fit, the modeling data were estimated and the ΔE_{94} difference computed. Average error was 0.61, with a maximum of 1.13. A more robust test of the fit using independent data is given in section 4.9.

Figure 4.8-1 Measured Data and Fitted GOG model for the Red-channel

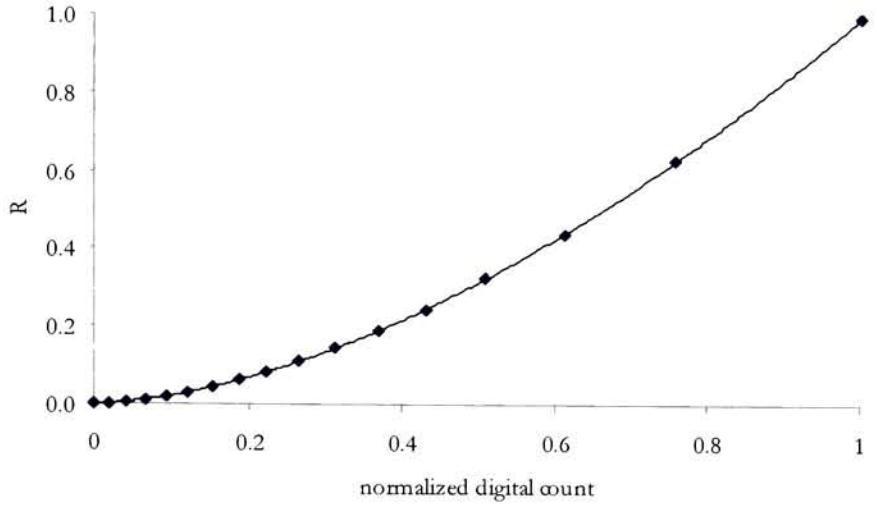

Figure 4.8-2 Measured Data and Fitted GOG model for the Green-channel

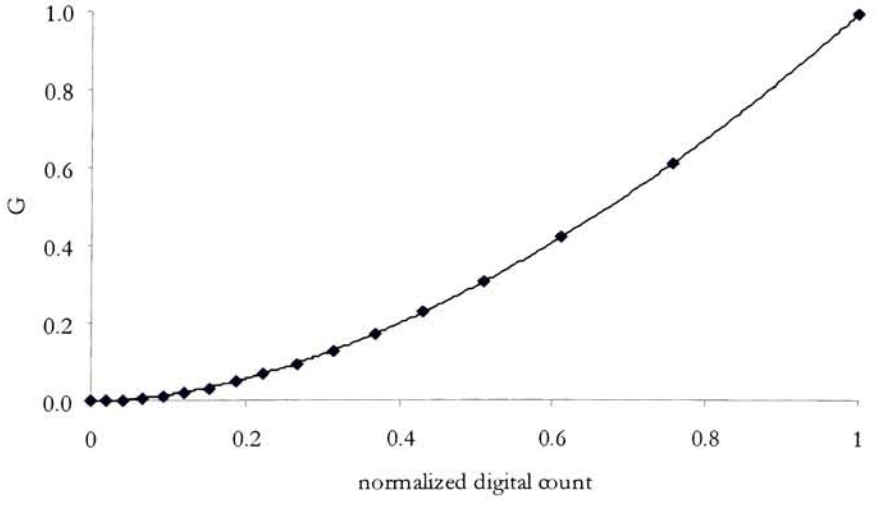

Figure 4.8-3 Measured Data and Fitted GOG model for the Blue-channel

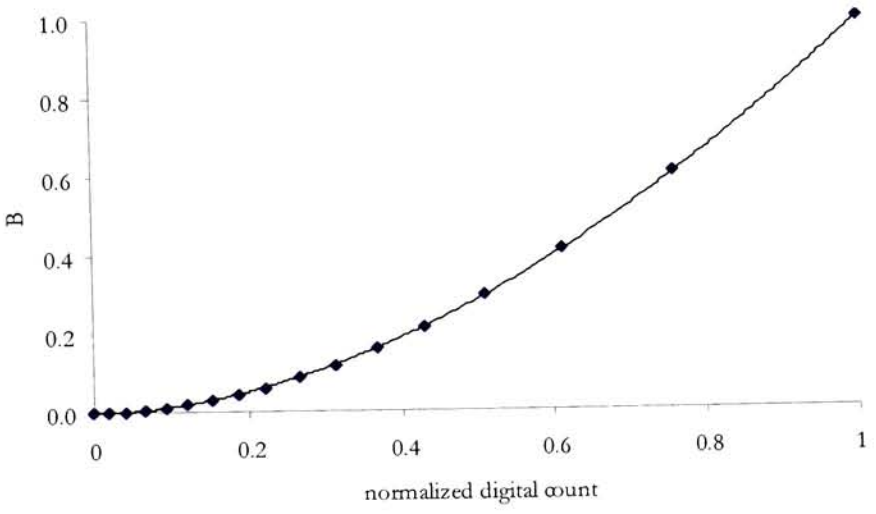

4.8.2 SGI LCD Panel

Both a conventional GOG model using a 17 step neutral ramp, and a cubic spline interpolation of three 52 step ramps (red, green, blue) were used in modeling the SGI display. The estimated parameters of the GOG model are shown in the table and graphs below.

Table 4.8-2 Estimated GOG Parameters for SGI Display

Channel	Gain	Gamma
Red	0.6706	4.4622
Green	0.8000	3.2559
Blue	0.9507	2.2841

The low estimated gain terms indicate a poor dark state. Preferably, the gain terms should all be slightly greater than 1.0 which creates negative offsets (offset = 1.0 - gain) and ensures that no light is being emitted at the black level.

As with the Sony display, the fit of each model was initially evaluated by re-estimating the data used to create the model. Results for the two models tested for the SGI are shown in Table 4.8-3. An independent data set is evaluated in section 4.9.

Table 4.8-3 Redistribution Errors for SGI Models

Model	Average ΔE_{94}	Maximum ΔE_{94}	Number of Points measured
GOG	2.94	6.72	17 logarithmically spaced gray patches
LUT	0.97	2.2	52 steps each for RGB, 156 total

Figure 4.8-4 Measured Data and Fitted GOG model for the Red-channel

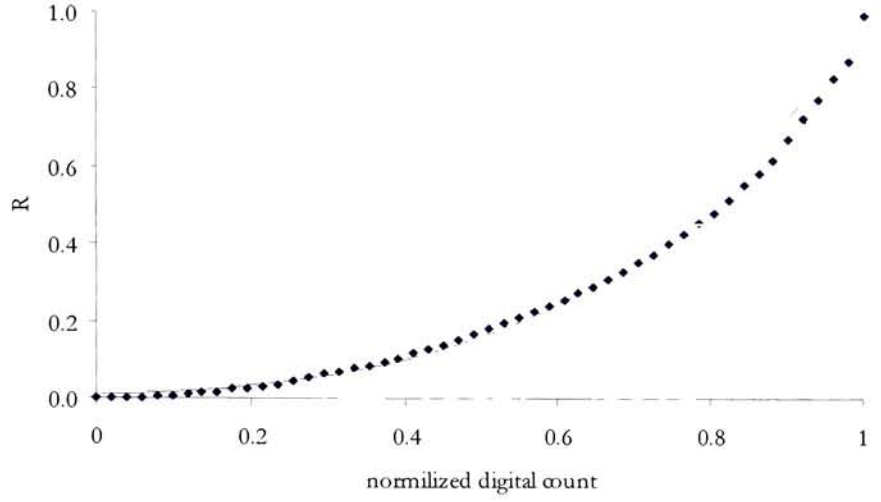

Figure 4.8-5 Measured Data and Fitted GOG model for the Green-channel

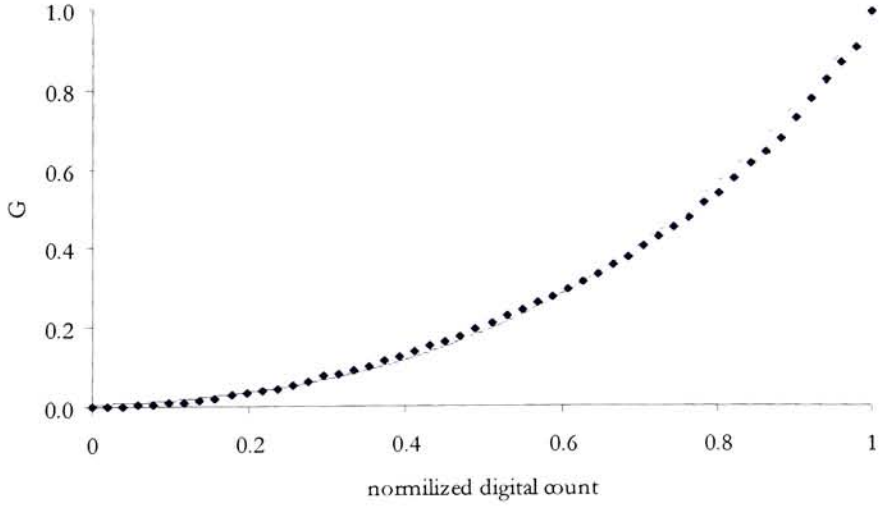

Figure 4.8-6 Measured Data and Fitted GOG model for the Blue-channel

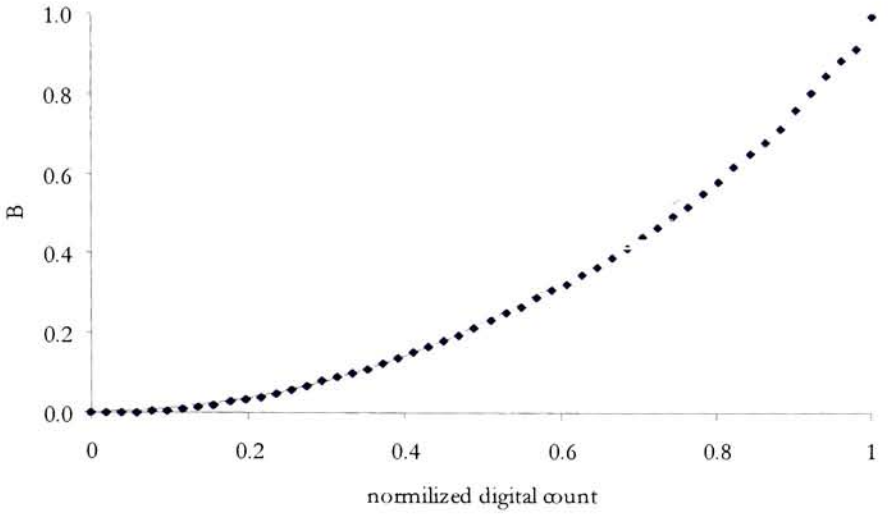

Although the GOG model fit the low end of each channel reasonably well, the systematic trend to overestimate the at the high end of the scale indicates that this model might not perform well overall. Therefore, a set of three 1D LUTs were created from the 52 step primary ramps using cubic-spline interpolation between the nodes. The resulting transfer curves are shown below.

Figure 4.8-7 Measured Data and LUT for the Red-channel

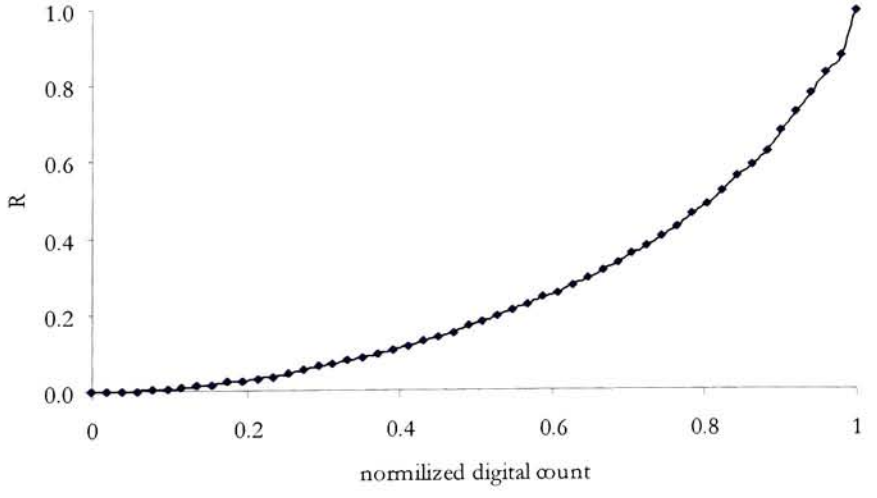

Figure 4.8-8 Measured Data and LUT for the Green-channel

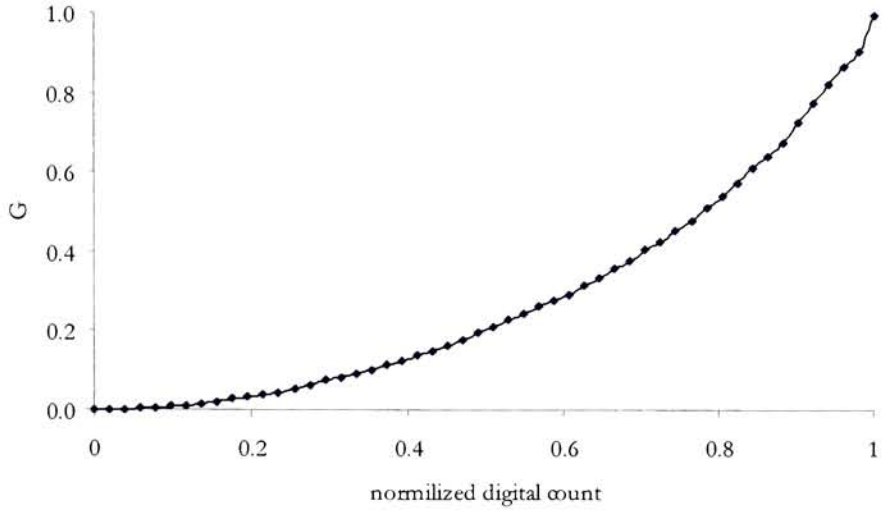

Figure 4.8-9 Measured Data and LUT for the Blue-channel

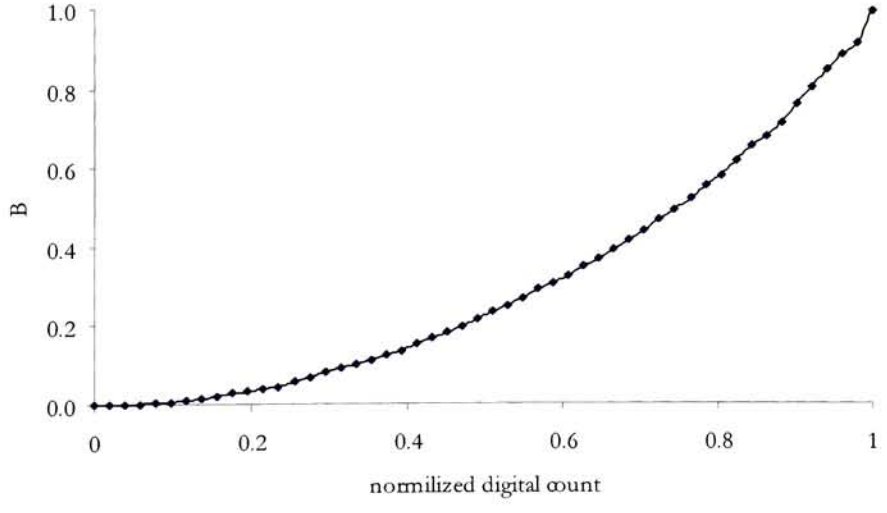

While the cubic spline function gives a much better fit to the measured data, such fits need to be used with some caution. Since the measurements nodes are always fit by the spline, any noise in those points will result in an unstable model.

Measurements	High Quality Display	Low Quality Display
High Quality	Best Option, many methods available.	1D LUTs with interpolation. Physical models questionable.
Low Quality	OK with physical models. Be sure to average several points to reduce noise.	Do not attempt this combination

4.8.3 *IBM LCD Prototype*

Being a 6 bit/channel device, a direct LUT was easily built by measuring all 64 levels for each primary. Since no interpolation was needed, the lines in the figures below are for clarity only, the 64 discrete points were all that was required.

Figure 4.8-10 Measured Data for the Red-channel

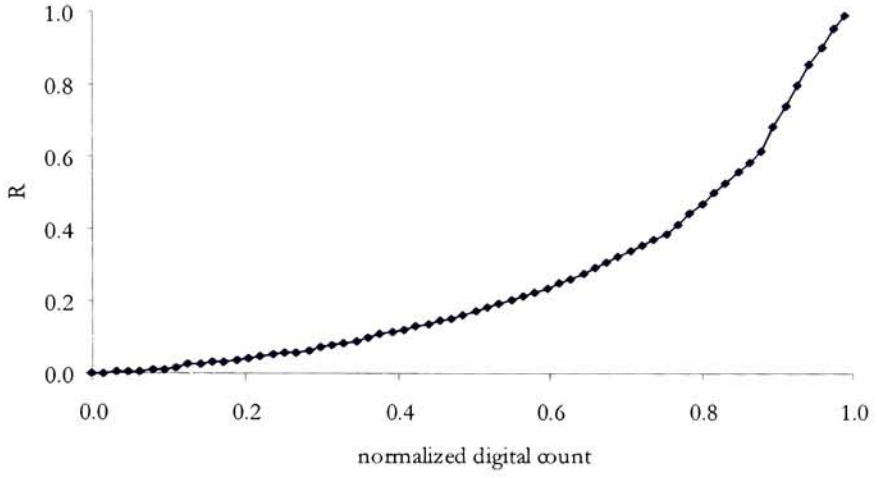

The rather jagged shape of this transfer curve, and the two below for green and blue, clearly suggest that the GOG model is inappropriate for this display.

Figure 4.8-11 Measured Data for the Green-channel

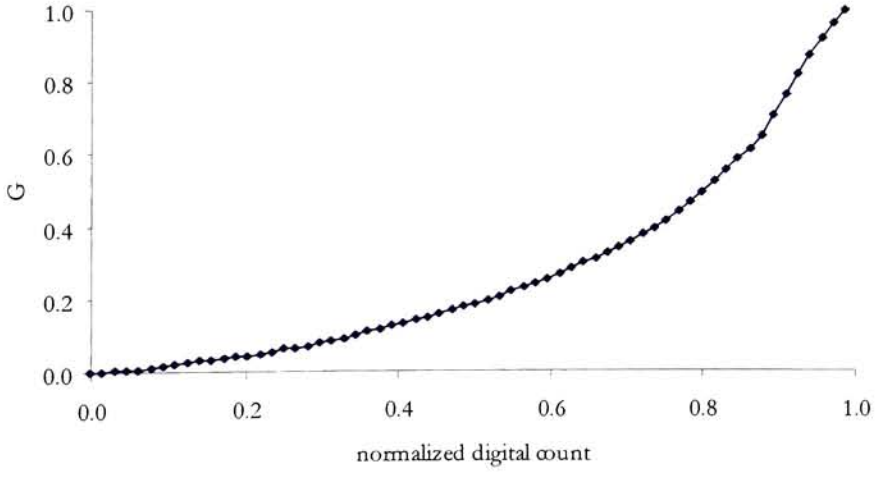

Figure 4.8-12 Measured Data for the Blue-channel

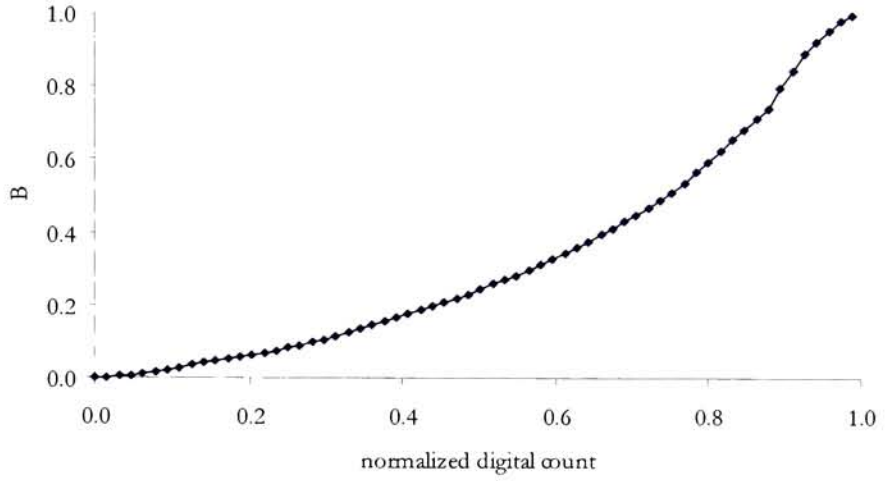

For reasons to be discussed in the following section, two additional models were evaluated for this display. Their relevant characteristics are described below. The redistribution performance of all three models is given in Table 4.8-4.

Peak Model In this model the 3x3 primary mixture matrix is made from the tristimulus values of the peak red, green, and blue primaries. The LUT was then built by multiplying the RGB ramps with the inverse of this matrix to obtain target scalar values.

Scaled Model To account for the lack of additivity, the columns of the above 3x3 were scaled such that the row sums were equal to the white point. The LUT was then built using the ramp data such that: $R=X/X_{max}$ of the red ramp, $G=Y/Y_{max}$ from the green ramp, and $B=Z/Z_{max}$ from the blue.

Fit Model The 3x3 mixture matrix for this model was derived from a least squares fit to 283 points. The Scaled Model LUT was used.

Table 4.8-4 Redistribution Errors for IBM Display Models

Model	Average ΔE_{94}	Maximum ΔE_{94}	# of Points in Model
Peak	0.58	1.74	192 step RGB ramp
Scaled	1.36	2.60	192 step RGB ramp
Fit	1.20	6.55	283 various

The poor performance of the Scaled model on the ramp data is to be expected since it was not specifically created to fit that data set. The Fit model performed poorly on this test but was built on a more representative data set including: the full 192 step RGB ramp, two repeat measures of a smaller RGB ramp, two repeat measurements of a 17 step gray scale, and the 9 patches from the spatial independence test which were presented on gray backgrounds.

4.9 Model Performance and Evaluation

The performance of the emissive display models derived above was tested by measuring a 3x3x3 target and an additional 15 pre-selected random colors for a total of 42 patches. A 3x3x3 target refers to a sampling design in which three levels are chosen, {44, 128, 212} in this instance, and each of the red, green, and blue channels are varied in all 27 combinations of these levels. That is, the first patch displayed would have a RGB triplet of {44,44,44}, the next patches are then {44,44,128}, {44,44,212},... ,{212,212,212}. The 15 pre-selected random colors were included to increase the sample size and to counter any systematic effects caused by the 3x3x3 sampling design. The results, in terms of ΔE_{94} between measured and predicted values are summarized in Table 4.9-1. The three methods listed for the IBM display refer to different models used and will be explained in section 4.9.3.

Table 4.9-1 ΔE_{94} Colorimetric Errors for 3x3x3 Independent Data Set

	Quartile				
Display	25%	50%	75%	Average	Maximum
Sony	0.23	0.33	0.41	0.36	1.10
SGI (GOG)	1.63	1.89	2.07	1.98	5.57
SGI (LUT)	0.83	1.05	1.23	1.01	1.81
IBM (Peak)	3.77	5.28	6.442	4.91	7.92
IBM (Scaled)	2.49	3.68	4.87	3.73	7.63
IBM (Fit)	2.81	4.40	5.26	4.06	7.34

In building the SGI-LUT and IBM models, a 17 step gray scale was measured twice as a check on repeatability. The average of these two sets forms a second independent data set on which to test these four models as shown in Table 4.9-2 below. In the case of the Fit model, the two gray scales were included in the modeling set, so its inclusion in the table below is for comparison only.

Table 4.9-2 ΔE_{94} Colorimetric Errors for 17 Step Gray Scale Data Set

Model	Average	Maximum
SGI (LUT)	0.78	1.62
IBM (Peak)	2.71	8.09
IBM (Scaled)	2.07	6.23
IBM (Fit)	2.15	6.49

The model for the Fujix printer was verified using 100 independent patches, results are shown below.

Table 4.9-3 ΔE_{94} Colorimetric Errors for 100 Independent Points–Fujix Pictrography

Measure	ΔE_{94}		
25th percentile	3.18		
50th Percentile	3.94	Average	3.97
75th percentile	4.74	Maximum	6.54

4.9.1 Sony CRT Display

Overall, the model for the Sony display fit quite well as is typical of a properly set up high quality CRT. The performance of both the redistribution test and the independent data set suggest that the model is robust and should perform well in subsequent testing.

4.9.2 SGI LCD Panel

As expected based on the systematic errors observed in the GOG model fits, the LUT based method performed better on the SGI display. The LUT model should be adequate for most purposes and is on par to the results found by Fairchild [1998] for an Apple Studio display (average of 1.02, maximum of 2.88 on 100 independent samples). The LUT model performance on the gray-scale data were adequate.

4.9.3 IBM LCD Prototype

Overall the IBM models performed less than satisfactory. However, given the time constraints on this project, the errors had to be tolerated.

One possible solution in cases where physical models fail is to use a 3D look-up-table. A reasonable sampling of the RGB cube could be made (say 10x10x10 or 13x13x13) and up-sampled to the full space using the physical model. This method was not explored due to the lack of automated measurement equipment for the PC running the IBM display. A 13^3 sampling would have taken over 18 hours to do manually.

Another possible solution would be to measure several hundred more patches and add them to the data set used in the Fit model. This would require fewer measurements and may have provide better results.

A third solution, had time and resources allowed, would have been to do a ground-up physical model of the display starting with the optical properties of its individual components. This procedure was used with great success in Sliverstein [1993].

The relative merits and weaknesses of each model tested are discussed below.

Peak Model This model had the best redistribution performance of the three models tested. The average ΔE_{94} was 0.58 compared to 1.36 for the Scaled model and 1.19 for the Fit model. However, the performance on the 3x3x3 independent data set, and the gray scale data set was worse than the other two models as shown in Table 4.9-1 and Table 4.9-2.

Scaled Model This model had the poorest redistribution performance of the three tested, though not totally unacceptable. The performance on the 3x3x3 independent data set, and the gray scale data set was better than either of the other two models but still higher than desired.

Fit Model This model is interesting in that, while it was never the best model for any of the data sets tested, it was also never the worst. This is typical of statistical fits as they tend to evenly distribute the error. The fit on the 3x3x3 independent data set is rather high. A possible improvement to this model may be to use an appropriately weighted regression (i.e. using the Neugebauer quality factor weights [Neugebauer 1956]) since minimizing errors in XYZ does not directly minimize errors in CIELAB.

A table comparing the rankings of the three methods is given below for comparison, the average error as well as the maximum error is given in parentheses next to each model. It would appear from the overall results that the Scaled model would be the best choice to work with in further analysis.

Table 4.9-4 Rankings of IBM Models for Three Data Sets

Rank	Redistribution	3x3x3 + Random	17 step Gray Scale
1st	Peak (0.56, 1.74)	Scaled (3.73, 7.64)	Scaled (2.07, 6.23)
2nd	Fit (1.20, 6.55)	Fit (4.06, 7.34)	Fit (2.15, 6.55)
3rd	Scaled (1.36, 2.60)	Peak (4.91, 7.93)	Peak (2.71, 8.15)

5 Methods and Processes

5.1. Experimental Methods

5.1.1. Image Selection and Processing

In any experiment using pictorial images, careful image selection is important. Common concerns are scene content dependence [Jones 1941, Farnand 1996], perceived object distance [Corey 1983], and overall chroma [Bartleson 1958]. The presence of memory colors can also effect tolerances [Farnand 1996].

In an experiment similar to the present one, Stokes [1991] found little evidence of scene content dependency. Using large-format ink-jet prints Uroz found no evidence of image dependency for systematic changes in lightness. However, Uroz found threshold values for linear reduction in chroma to be image dependent. Not surprisingly, Uroz found threshold values for random changes in L^*, C^*_{ab}, and h_{ab} to be highly scene dependent [Uroz 1999].

Selection of appropriate test images for this experiment was limited by several factors. First, very high resolution images were needed from good quality scans. To make a 4"x6" image on the 400dpi Fujix printer requires a 1600x2400 pixel image. Secondly, images with fine details were desired to preserve any resolution effects and avoid quantization artifacts on the 6-bit IBM display. Finally, images with varied scene content and colors were desired to reduce image dependency in the results. After weighing these concerns versus available images, the three shown in the figures below were selected. The images shown here are reduced 25% from their original 4x6" size and have been sub-sampled for printing. Furthermore, no color-management has been applied, the images are therefore only representational in nature.

Figure 5.1-1 Girl Image

The "Girl" image is a commonly used test image from a *Kodak Photo CD*™ sample disk. The girl's bright red sweater and hair offer a good deal of texture. The multi colored paint around her eye and the ribbons in her hair are prominent features of the image.

Figure 5.1-2 Flower Image

The "Flower" image is a close up of five purple-blue flowers with yellow-orange pistils and stamens. Prominent features of this image included several deep shadows in the grassy background and a fine vein structure in the petals.

Figure 5.1-3 Currency Image

The "Currency" image is a close-up of currency from many different countries. It is different from the other images in several regards. Unlike the other two images, this image has few high chroma features. Furthermore, this image consists mostly of fine details and has relatively few uniform areas.

Each source images was sub-sampled or cropped to 2400x1600 pixels to create three base images. To avoid potential gamut boundary issues, the first and last 25 digital counts of these images were linearly compressed, limiting the images to the range [25, 235]. Each of these gamut-reduced images was then sub-sampled to 432x288 pixels for the Sony display, 660x440 pixels for the SGI, and 1200x800 pixels for the IBM display. The prints were made as the full 2400x1600 resolution. Once appropriately sized, the images were then converted to CIELAB L^*, C^*_{ab}, h_{ab} space using the GOG model developed for the Sony display. The reverse model for each display was then used to create the original and transformed images used during the experiment.

5.1.2. Transfer Functions and Dimensions

In his thesis, Stokes [1991] describes twelve transforms using four mathematical operators (multiplicative gain, additive offset, power, and sigmoid) and the three CIELAB dimensions of lightness, hue and chroma. Several of these, such as additive offsets in chroma, can be eliminated as having no physical correlate. Of the remaining combinations, three transforms were selected for this experiment as being representative of common processes in imaging. Changes in contrast were modeled using a sigmoidal transform in CIELAB lightness (L*). Changes in system gain were simulated using multiplicative transforms in CIELAB chroma (C^*_{ab}). Overall color casts were modeled using additive offsets in CIELAB hue (h_{ab}). The mathematical form of each of these transforms is given in the table below and are identical to those used by Stokes [1992] as shown in Table 2.3-2.

Table 5.1-1 Transfer Functions Used

Function	Formula
Additive Offset (Model for Color Cast)	$Output = Input + k$
Multiplicative Factor (Model for gain control)	$Output = k(Input)$
Sigmoidal (Model for contrast changes)	$Out = \begin{cases} \dfrac{(Input*2)^k}{2} & Input < 0.5 \\ \dfrac{\left[((Input*2)-1.0)^{1/k}\right]+1.0}{2} & Input \geq 0.5 \end{cases}$

Based on the results of Stokes [1991], tolerances were assumed to be symmetric about the starting point to reduce the number of images required by half. To avoid gamut boundary issues, compressive transforms were used in both chroma and lightness. In each of the four visual experiments, the threshold values of k in the above equations were determined. These thresholds will be referred to as 'parametric thresholds' since they are directly related to the free parameter manipulated in the transform equations.

5.2. Psychophysical Methods

When measuring visual tolerances, three general classes of methods can be employed: the method of adjustment, the methods of limits and the method of constant stimuli.

For the method of adjustment (MOA) the observer is asked to control the magnitude of some stimuli until it is just perceptible or just perceptibly different from some starting point. The threshold is then estimated by from the average setting after a sufficiently large number of trials. In the first instance an absolute threshold is found, in the latter, a difference threshold is measured.

In a method of limits (MOL) experiment, the observer is presented with a series of stimuli at predefined levels in an ascending or descending series. The observer is asked to signal when a change from visible to not visible (descending, or vice versa for ascending series) occurs. After some fixed number of trials, the process is stopped and the threshold is estimated from the series of transitions formed.

The method of constant stimuli (MOCS) involves presenting the observer a number of stimuli chosen to be clustered just above and below threshold. Each of these stimuli are then presented a large number of times and the frequency of detection for each is recorded. A variation of this method known as two alternative forced choice (2AFC) was used for the three monitor experiments. The print experiment used a variation of a rank order method typically used in scaling experiments.

More details of these and other psychophysical techniques are given in [Bartleson 1984, Fairchild 1998, Engeldrum 2000]. A useful guide for designing and conducting visual experiment is given by ASTM E1808-96 [1996].

5.2.1. Two Alternative Forced Choice with Anchor – Monitor Experiments

For the three experiments conducted on monitors (The Sony, SGI, and IBM displays) a two alternative forced choice with anchor methods was used. During a session, observers were shown a total of 75 image triplets. For each triplet, the known original (anchor) was presented first. Then, using one of three keys, the observer was able to select between two alternative images (denoted A and B) or bring up the know original (denoted O). A brief flash of mid-gray ($d_r=d_g=d_b=128$) between images was used to preserve adaptation and prevent the observer from observing the lack of re-draw when the unknown original was displayed. The image being displayed was indicated by a letter A, B, or O in the upper left of the display. When the observer felt they had the image which was different than the known original, a fourth key was used to register their response and bring up the next triplet. Between triplets, a mid-gray screen was presented for approximately one second to maintain a more uniform state of adaptation.

The observers' progress was marked by a beep or text message every 19 images. Candy treats were provided during the session to help motivate the observer.

Three practice trials using obvious changes were presented at the start of each session. This allowed the observer to become aquatinted with the controls, ensure they understood the directions, and give them a few moments to adapt to the environment. If an incorrect answer was given during the trials, the observer was reminded that they were to select the different image. All observers were verbally reminded to select the different image before beginning the actual experiment.

Each display was masked off to be 11.5" x 7.5" to eliminate differences in aspect ratio between monitors. For the Sony display, observers were allowed to view the images at any distance, but were encouraged to maintain an average of 20-21". For the SGI and IBM LCD displays, observers viewed the images through a 0.5" tall x3.0" wide slit in a black foam-core mask 20" from the display. Although somewhat uncomfortable for the observers, it was found that even small changes in seating position could lead to large perceptual changes in the images with these displays. If these changes occurred between viewing the original and one of the trial images, an incorrect judgment might have been made. Care was taken to ensure that the observers chair was properly adjusted before beginning the experiment to ensure their comfort.

5.2.2. Rank Confusion Scaling– Print Experiment

The 'Two Alternative Forced Choice with Anchor' method used for the three monitors experiments is not easily transferable to hardcopy output. One difficulty is that multiple copies of each original image would be needed, one for the anchor and one or more to be included with the test pairs.

Producing multiple originals is prohibitive since printed output can vary print to print, day to day and, in the case of the Fujix Pictrography, between sets of consumables. This variability affects the test samples as well, but for convenience it is assumed that the intended changes are greater than the random ones and thus the relative order of the differences are preserved. If only two copies of the original were made to minimize this variability, the subjects might become aware of differences in ware between the test samples which are used once per observer session , and the unknown original which is used in every presentation of a given image.

One solution to these challenges is to instruct the observer to make a 'same/different' judgment of each test sample versus a single standard sample [Uroz 1999]. While experimentally convenient, this method relies on the consistent judgment of the observer even at very small levels of difference. When samples near threshold are presented, some observers may simply reply 'different' in an effort to appear more sensitive.

After much consideration, a novel approach was selected and dubbed "Rank Confusion Scaling" This approach is similar to the procedure used in the Farnsworth-Munsell 100 Hue test in which observers are asked to arrange a set of chips to form a smooth progression of hue between two fixed end points. The 100 hue test is scored by assigning points based on the distance of chip reversals, the farther the reversal.

In this study, observers were asked to rank order test samples in terms of difference from an un-altered anchor. This ordering was then compared to the order based on the amount of transformation applied. It is hypothesized that pairs of samples whose mutual difference in the amount of transformation applied is below threshold will be confused more often than pairings whose difference are well above threshold. The frequency of confusion for all possible parings is then computed and analyzed using standard probit analysis. With careful selection of samples, this method can provided data at more levels than a 2AFC design (N choose 2 versus N).

5.2.3. Observer Selection

The observer selection and training process was guided by ASTM E1499-92 [1992]. Due to the laboratory's location, observers were primarily selected from the faculty, staff, and students of the Chester F. Carlson Center for Imaging Science. The observers experience was assessed by the experimenter based on discussions with the observer before each session. While attempts were made to balance for gender and age, the inherent bias in the population towards young to middle age males made this task difficult. Research has shown that memory matching, as was used in the display experiments, is loosely age and gender dependent [Perez-Carpinell et al. 1998, 1998b]. However, the delay times used in this study were much shorter than those used by Perez-Carpinell who examined times of 15 seconds, 15 minutes and 24 hours.

5.2.4. Statistical Analysis

The observers' responses to each level of a particular transform constitutes a binary data set. For the three monitor experiments, the observer either correctly identified the different image, or chose the duplicate original. For the print experiment, the relative order of placement was used to construct the binary data set, with the assumption that the process of rank ordering a set of samples involves a similar process to making ${}_nC_2$ pair-wise comparisons. In practice the observer would rarely bother to directly compare the extremes which would have led to unanimous decisions in a paired-comparison paradigm.

Given the design of the experiment, an observer randomly guessing at each trial would be likely to get 50% correct. In this situation it is common to select the thresholds as being the point at which 75% of the observers correctly identified the original. That is, the point at which the observers do half again as good as the chance rate of 50%. Other points could also be selected depending on the particular situation.

It is unlikely that a particular pre-determined level of transformation will precisely generate the desired probability of correct identification. Furthermore, due to observer variability, noise exists in the data. A regression model can be used to address both of these issues.†

Further details of this and similar methods can be found in [Finney 1971, SAS 1989, Hosmer 1989].

Equation 5.2-1 General Linear Probability Model

$$P_{ij} = \mathrm{F}(\alpha_s + \beta_s x_{js})$$

Where

P_{ij} is the probability that a sample (j) is judged greater than the standard (s)
F is a cumulative distribution function describing the psychometric curve (aka. linking function)
x_{js} is the sample's scale value relative to the standard
α,β are the parameters of the cdf (F) to be estimated

† Adaptive methods which drive the stimulus to a predetermined probability of detection can also be used. However, they require (semi-)continuous stimuli and more complex program controls. See for example [Treutwein 1995].

In this experiment, the Gaussian model shown in Equation 5.2-2 was used to describe the basic form of the psychometric curve. The solution to this equation, known as the probit or z-value, is shown in Equation 5.2-3. No closed-form inverse exists for this model, thus numerical methods such as weighted least squares, minimum chi-square, maximum likelihood and various other nonlinear regression techniques are employed [Aldrich 1984, Bock 1968, Engeldrum 2000, Liao 1994]. For purposes of this experiment, the maximum likelihood method implemented in SAS/STAT® was used.

Equation 5.2-2 Gaussian Model

$$P_{js} = \mathrm{F}\left(\alpha_s + \beta_s x_{js}\right) = \frac{1}{\sqrt{2\pi}} \int_{-(\alpha_s + \beta_s x_{js})}^{\infty} e^{-\frac{u^2}{2}} du = \Phi\left(\alpha_s + \beta_s x_{js}\right)$$

Equation 5.2-3 Inverse Gaussian Model

$$\Phi^{-1}\left(P_{js}\right) = \alpha_s + \beta_s x_{js} = z$$

As was shown in the background section, there exists a large number of color-difference formulas to choose from. To allow the results of this study to be generally applicable, two standard CIE formulas, ΔE^*_{ab} and ΔE_{94} were selected. A proposed version of CIE TC 1-47, to be known as ΔE_{2000} was also included as an early trial of this formulas capabilities.

5.3. Color Difference Equations

5.3.1. ΔE^*_{ab}

Along with the 1976 CIELAB color space, the CIE created a simple color difference formula to express the difference between two stimuli using the euclidean distance between the two points. This formula superceded the 1964 Uniform space color-difference formula [CIE 1986]. This formula is incorporated into most spectrophotometers and color matching software.

Equation 5.3-1 Formula for Computing ΔE^*_{ab}

$$\Delta E^*_{ab} = \sqrt{(\Delta L^*)^2 + (\Delta a^*)^2 + (\Delta b^*)^2}$$

5.3.2. ΔE_{94}

When the CIE introduced the CIELAB color space and its associated color difference formula, they recognized the importance of color-difference formula to industry and that "None of the existing colour-difference formulae, including those recommended by the CIE, is entirely satisfactory and more experimental work is required to arrive at and accurate method of calculating colour-differences [CIE 1986]." Recommendation was made to continue investigating this very important issue.

Since then further research into color-difference formulas led to the formation of several major new experimental data sets [e.g. Berns 1991c, Luo 1986, Witt 1983 and Witt 1987] which together suggested that a colour-difference model with performance superior to the 1976 recommendations could be created.

The new data was primarily taken form experiment on object colors with color differences from threshold through the range of color differences observed in the manufacture of colored materials. The CIE also defined a set of reference conditions representing common levels of the experimental variables used in developing these object color visual colour-difference data sets. These are:

Table 5.3-1 CIE94 Reference Conditions

Illumination	Source simulating the spectral relative irradiance of CIE Standard Illuminant D_{65}.
Illuminance	1000 lx.
Observer	Normal color vision.
Background Field	Uniform, neutral grey with L*=50.
Viewing Mode	Object.
Sample Size	Greater than 4 degrees subtended visual angle.
Sample Separation	Minimum sample separation achieved by placing the sample pair in direct edge contact.
Sample Color-Difference Magnitude	0 to 5 CIELAB units.
Sample Structure	Homogeneous color without visually apparent pattern of nonuniformity.

With this new information the CIE Technical Committee TC1-29, Industrial Color-Difference Evaluation, developed an extension to the CIE 1976 CIELAB color-difference model. Their model, known as CIE94 ΔE_{94} contains corrections for systematic chroma-dependent variation in color-difference perception (the $S_\bullet$ terms†) and factors which can be used to correct for the parametric effects of various conditions of use (the $k_\bullet$ terms). The details of this formula and its development are given in [CIE 1995].

Equation 5.3-2 Formula for Computing ΔE_{94}

$$\Delta E_{94} = \sqrt{\left(\frac{\Delta L^*}{k_L S_L}\right)^2 + \left(\frac{\Delta C^*_{ab}}{k_C S_C}\right)^2 + \left(\frac{\Delta H^*_{ab}}{k_H S_H}\right)^2}$$

Where

$$k_L = k_C = k_H = 1$$

$$S_L = 1$$

$$S_C = 1 + 0.045\left(C^*_{ab,1} \cdot C^*_{ab,2}\right)^2$$

$$S_H = 1 + 0.015\left(C^*_{ab,1} \cdot C^*_{ab,2}\right)^2$$

The performance of this formula will be effected by deviation from the reference conditions, which necessitates the parametric factor terms $k_\bullet$. Common deviations included:

- Changes in viewing and illuminating conditions which affect the validity of CIELAB as a color space.
- Changes in the source correlated color temperature from 6500 K which affect the accuracy of the chromatic adaptation transform embedded in CILALB.
- Illuminance levels significantly lower than 1000 lx which result in reduced discrimination and the possibility of rod intrusion which may cause significantly reduced correlation between colorimetry and the perceived colors of metameric stimuli.

† The subscripted '•' symbol represents either the L, C or H term as appropriate.

5.3.3. Delta E_{2000} Draft Equation

Continued research into the creation of effective color-difference formulae has led the CIE to create yet another generation of improvement on the original 1976 ΔE^*_{ab} formula. While not officially released as of this writing, the currently proposed form of this new equation, to be known as ΔE_{2000}, is given in Equation 5.3-3 below [Fairchild 2000]. The final version will be published by CIE TC1-47.

Equation 5.3-3 Proposed form of ΔE_{2000}

$$\Delta E_{2000} = \sqrt{\left(\frac{\Delta L^*}{K_L S_L}\right)^2 + \left(\frac{\Delta C'}{K_C S_C}\right)^2 + \left(\frac{\Delta H'}{K_H S_H}\right)^2 + R_T\left(\frac{\Delta C' \Delta H'}{S_C S_H}\right)^2}$$

Where

$$\Delta L^* = L^*_1 - L^*_2$$

$$\Delta C' = C'_1 - C'_2$$

$$\Delta H' = 2\sqrt{C'_1 C'_2}\sin\left(\frac{\Delta h'}{2}\right)$$

$$S_L = 1 + \frac{0.015\left(\bar{L}^* - 50\right)^2}{\sqrt{20 + \left(\bar{L}^* - 50\right)^2}}$$

$$S_C = 1 + 0.045 \cdot \bar{C}'$$

$$S_H = 1 + 0.015 \cdot \bar{C}' T$$

$$T = 1 - 0.04\cos(\bar{h}' - 20) + 0.1\cos\left(2\bar{h}' + 3\right) + 0.1\cos\left(3\bar{h}' - 14\right) - 0.08\cos\left(4\bar{h}' - 28\right)$$

$$R_T = -\sin(2\Delta\theta)R_C$$

$$\Delta\theta = 30\exp\left\{-\left[\frac{h' - 275^\circ}{25}\right]^2\right\}$$

$$R_C = 2\sqrt{\frac{\bar{C}'^7}{\bar{C}'^7 + 27^7}}$$

$$C' = \sqrt{a'^2 + b^{*2}}$$

$$a' = (1 + G)a^*$$

$$G = 0.5\left(1 - \sqrt{\frac{\bar{C}^{*7}}{\bar{C}^{*7} + 25^7}}\right)$$

$$h' = \tan^{-1}\left(b^* / a'\right)$$

The over-bar symbol ' $-$ ' indicates the arithmetic mean of the values for a pair of samples.

This formula is similar in form the CIE94 equation with several important differences. First, a non-unity S_L term has been incorporated to account for some newly discovered dependencies in L*. Second, C' and h' term have been introduced which are dependent on a revised a* denoted as a'. Third, a rotational chroma/hue interaction term is introduced which servers to properly tilt the tolerance ellipsoids especially in the blue region where such changes have been know to occur for some time now [Ebner 1998, Hung 1995]. As of this writing, the most likely changes to the formula before final publication will be in computing the T factor and a slight modification to the a' term. Before implementing this formula, please check with the CIE for the latest version.

Within the CIE it is generally felt that this will be the last CIELAB based color difference formula to be developed. In future formulations it is likely that some of the more prominent systematic errors in CIELAB accounted for by the $S_\bullet$ terms will simply be incorporated in a new, more uniform color space. This new space will be more computationally complex, but will lead to much simpler color differences formulas [Berns 2000].

5.3.4. Optimizing l:c Ratios

One of the features of color difference formulas such as CMC, and more recently ΔE_{94} and ΔE_{2000} is that they include parametric correction factors (l:c in CMC, k_L, k_C, k_H in CIE94 and CIE2000) to account for variation in experimental conditions from the defined reference conditions. In practice, the hue term is typically set to unity, and the lightness and chroma parameters are adjusted to better fit the perception data.

Since the data collected in this experiment varied uni-dimensionally in lightness, chroma or hue, optimizing the l:c ratio was very straightforward. The k_L term was set equal to the ratio of the threshold for lightness only changes to the threshold for chroma only changes. The k_C and k_h terms were then set to unity.

In most cases, the data collected will not or can not be considered to be uni-dimensional. In these cases, a regression approach can be used as described in Berns [1996].

5.4. S-CIELAB

S-CIELAB was developed by Brian Wandell, X. Zhang et al. at Stanford University to measure color reproduction errors of digital images. Where as ΔE^*_{ab}, and its various derivatives, can be used quite successfully to predict color differences between large uniform color patches, it is not well suited for predicting color differences between areas exhibiting patterns such as halftones. Performing a point-by-point comparison between a continuous tone image and its halftoned counter part, CIELAB would predict very large errors at most points. By adding an appropriately designed low-pass filter simulating the eye's integration of the halftone pattern, these errors can be greatly reduced.

S-CIELAB is a spatial extension to CIELAB, developed for measuring color reproduction errors of digital images. It is implemented in a three stage process. First, the input image is transformed into an opponent color space consisting of one luminance and two chrominance channels. Second, each component image is convolved with a low-pass filter representing the spatial sensitivity of the human eye for that color component. Third, the three filtered images are re-combined to form a single XYZ image from which the CIELAB coordinates can be computed and an appropriate ΔE computed.

Chapter 8 describes the results of applying S-CIELAB filtering to several of the images used during the course of this study. Further information on this method can be found in [Zhang 1996,]. As of this writing, code for a MATLAB implementation of this procedure can be found on the web at: white.stanford.edu/html/xmei/scielab/introduction.html.

5.5. Calculation of Overall Threshold

In the next several chapters, the results for the three individual images will be summarized by an overall measure of the threshold. The point estimate of this term is the average of the three individual image-wise thresholds. Error bars for this estimate were calculated as described below.

Since the error-bars from the individual images were calculated using normal distribution statistics, the sample standard deviation, s, can be calculate and then pooled as shown below. This pooled standard deviation can then be used to calculate confidence intervals based on the student-t distribution.

Equation 5.5-1 Overall Confidence Interval Estimation

$$s^2_{pool} = \frac{\sum_{all\ i}(n_i - 1)s_i^2}{\sum_{all\ i}(n_i - 1)} \quad \text{where: } s_i = \frac{s_{iA} + s_{iB}}{2}, \quad s_{iA} = \frac{CI_{upper,i}\sqrt{n_i}}{z_{\frac{\alpha}{2}}} \ \& \ s_{iB} = \frac{CI_{lower,i}\sqrt{n_i}}{z_{\frac{\alpha}{2}}} \quad \text{(a)}$$

$$CI = \pm t_{\frac{\alpha}{2}}\, s_{pool} \sqrt{1 \Big/ \sum_{all\ i} n_i} \quad \text{(b)}$$

where:
$CI_{upper/lower,i}$ = the upper or lower confidence interval for the i^{th} image.
n_i = the number of samples for the i^{th} image.
$\alpha = 0.05$

6 Parametric Threshold Results and Discussion

The thresholds presented in this chapter will be referred to as parametric thresholds since they represent the value of the free parameter, k, in the transform equations (Table 5.1-1) that would result in half the observers correctly identifying the transformed image. Though theses comparisons are dependent on the transforms used, they provided a direct comparison of the observer's relative sensitivity for each display tested. The first four sections present the results from each display individually; the fifth section will present summarized results for all four displays. The final section of this chapter compares the parametric thresholds versus various physical parameters of the display such as resolution and contrast to examine qualitative trends between the parametric thresholds and various physical parameters.

6.1. Sony GDM-F500 CRT Display

The Sony GDM-F500 display was selected as being representative of a commonly available high-end CRT displays. It provides a baseline comparison for the two LCD panels and the prints. It also provides a point of commonality with Stokes [1991] who used a similar Sony display for his thesis. The raw SAS analysis output for this display is presented in Appendix A.1.

6.1.1. Observer Statistics

A total of 34 color normal observers participated in this experiment. Details about the observer population are shown in Table 6.1-1.

Table 6.1-1 Observer Statistics–Sony CRT

Average Age	29	# Experienced	28
Age Range	21–54	# Inexperienced	6
# Male	25	Average Time	0:31 min
# Female	9	Time Range	0:15-1:01

*6.1.2. Parametric Results for Sigmoidal Compression in L**

Results for the sigmoidal compression in L are given in Table 6.1-2 and*

Figure 6.1-1 below. In this, and subsequent tables, the data in the column labeled "Mean" are the estimated mean threshold. The "Lower" and "Upper" columns are the 95% fiducial limits of the mean threshold. An asterisk (*) in the "LOF" column indicates a lack of fit at the α=0.1 level.

The overall results in the lightness dimension correspond quite well with those found by Stokes in 1991. Results by image show some variability, with the Currency image standing out as having a somewhat lower sensitivity than the others.

Table 6.1-2 Parametric Thresholds for Lightness Compression–Sony CRT

	Mean	Lower	Upper	LOF
Stokes 1991	0.88	0.87	0.89	
Overall	0.86	0.81	0.91	
Currency	0.83	0.77	0.86	
Flower	0.88	0.86	0.91	
Girl	0.87	0.86	0.89	

Figure 6.1-1 Parametric Sensitivity for Lightness Compression–Sony CRT

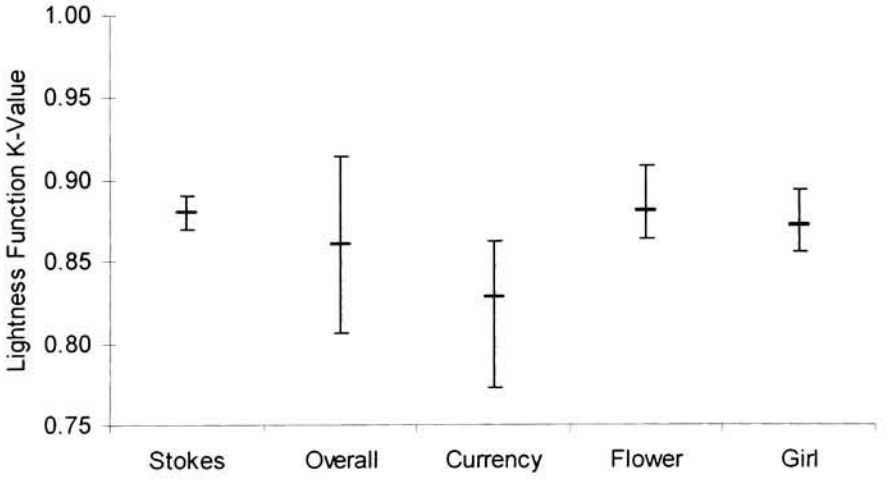

6.1.3. Parametric Results for Linear Reduction in C^*_{ab}

As with the results with the lightness transform, the chroma reduction thresholds on the Sony display match well with the findings of Stokes. In this dimension, the Girl image has a slightly higher sensitivity than the other two images, perhaps due to its high chroma content.

Table 6.1-3 Parametric Thresholds for Chroma Reduction–Sony CRT

	Mean	Lower	Upper	LOF
Stokes 1991	0.91	0.90	0.92	
Overall	0.90	0.85	0.95	
Currency	0.89	0.87	0.92	
Flower	0.87	0.85	0.90	
Girl	0.94	0.92	0.99	

Figure 6.1-2 Parametric Sensitivity for Chroma Reduction–Sony CRT

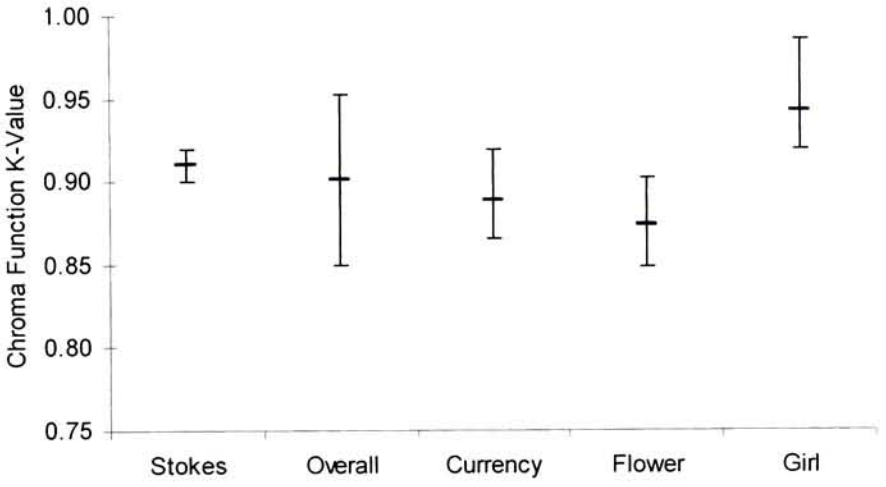

6.1.4. *Parametric Results for Additive Rotations in h_{ab}*

As with the other two dimensions, the results for hue rotation match well with those of Stokes [1991]. In the chroma dimension, the Girl image appears to be slightly more sensitive than the other two images. Note that the y-axis of Figure 6.2-3 has been reversed such that the null transform (k=0) is on top. In this way higher sensitivity is indicated by higher dashes on the graph, as was done in the previous two figures.

Table 6.1-4 Parametric Thresholds for Hue Rotation–Sony CRT

	Mean	Lower	Upper	LOF
Stokes 1991	5.9	5.2	6.5	
Overall	6.3	3.1	9.4	
Currency	6.8	5.3	8.2	
Flower	7.2	4.9	9.3	
Girl	4.7	2.6	6.0	

Figure 6.1-3 Parametric Sensitivity for Hue Rotation–Sony CRT

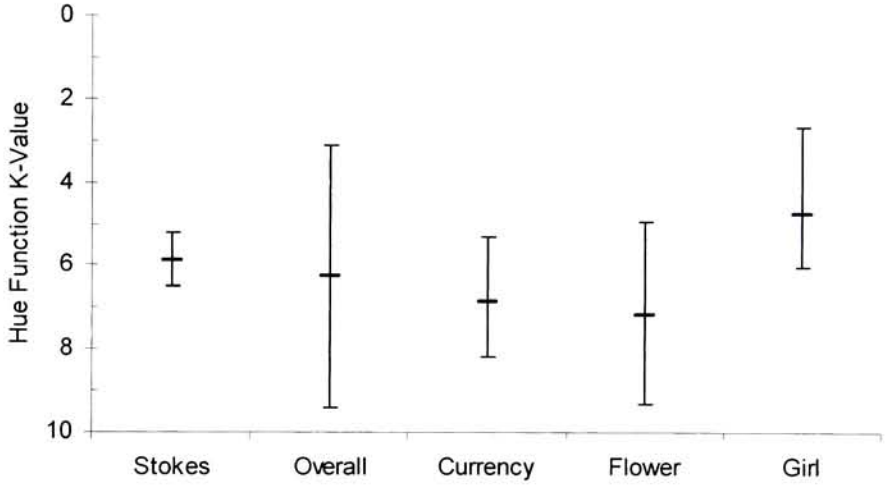

6.1.5. *Observer Comments*

At the end of each session, an informal interview of the observer was conducted in an effort to determine the methods by which they were making their decisions. For the Sony CRT display, the majority of observers felt they guessed on every presentation of the Currency image, regardless of the transform or level. Most observers used the large red bill located near the middle on the left side of the picture as their only reference. This impression was not born out in the data since the estimated threshold for this image was in line with the other two. Observers commented on focusing on the red sweater in the Girl image, and the yellow-orange pistils in the Flower image. Some observers commented on being able to see contrast changes in the girl's hair.

6.2. SGI® 1600SW™ Panel

The SGI 1600SW LCD was chosen as representative of a commercially available high quality LCD panel. At 100ppi, it is the highest resolution flat-panel display currently available. The inclusion of this display allows the prototype IBM TFTLCD to be compared to an actual commercial LCD display. The raw SAS analysis output for this display is presented in Appendix A.2.

6.2.1. Observer Statistics

A total of 32 color normal people participated in this experiment, 25 of which also participated in the CRT experiment. The make up of the observer population is shown in Table 6.2-1.

Table 6.2-1 Observer Statistics–SGI LCD

Average Age	30	# Experienced	25
Age Range	22 – 41	# Inexperienced	7
# Males	24	Average Time	0:24 min
# Females	8	Time Range	0:14 – 0:43

*6.2.2. Parametric Results for Sigmoidal Compression in L**

Results for the sigmoidal compression in lightness are given in Table 6.2-2 and Figure 6.2-1 below. The overall lightness results are similar to those found by Stokes. Results by image show a bit more variability than seen with the Sony CRT. The Currency image had a higher sensitivity than the overall results. Whereas the Flower image had a lower tolerance than the overall results.

Table 6.2-2 Parametric Threshold for Lightness Compression–SGI LCD

	Mean	Lower	Upper	LOF
Stokes 1991	0.88	0.87	0.89	
Overall	0.86	0.81	0.92	
Currency	0.81	0.75	0.84	
Flower	0.91	0.88	0.94	
Girl	0.87	0.85	0.89	

Figure 6.2-1 Parametric Sensitivity for Lightness Compression–SGI LCD

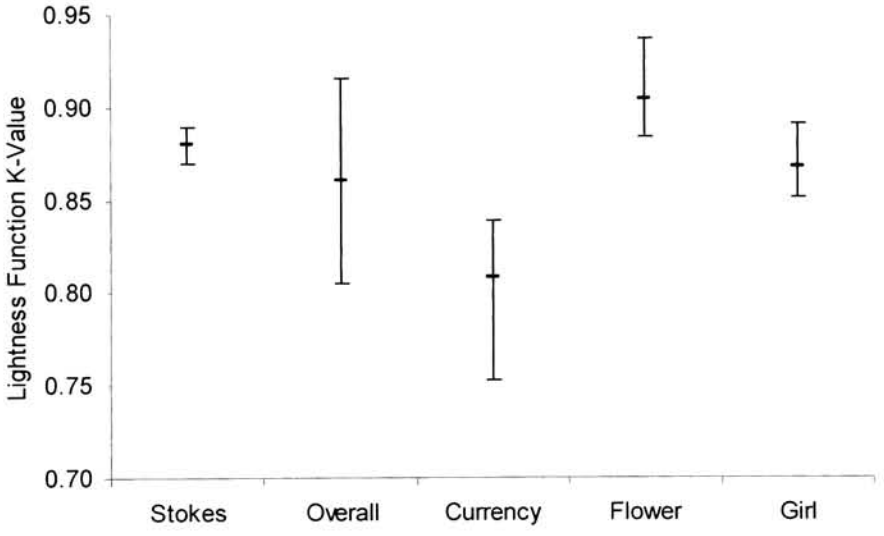

6.2.3. Parametric Results for Linear Reduction in C^*_{ab}

Estimated thresholds for linear compression in chroma are shown in the table and figure below. The overall results match those found by Stokes [1991]. The Flower image was slightly less sensitive than the overall results.

Table 6.2-3 Parametric Threshold for Chroma Reduction–SGI LCD

	Mean	Lower	Upper	LOF
Stokes 1991	0.91	0.90	0.92	
Overall	0.91	0.86	0.96	
Currency	0.93	0.90	0.97	
Flower	0.86	0.84	0.89	
Girl	0.94	0.92	0.97	

Figure 6.2-2 Parametric Sensitivity for Chroma Reduction–SGI LCD

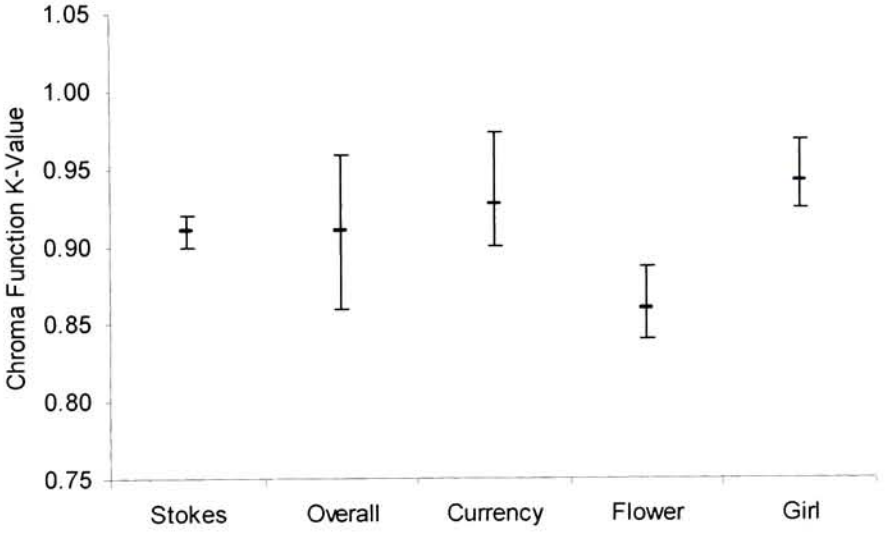

6.2.4. Parametric Results for Additive Rotations in h_{ab}

The overall sensitivity for hue rotation was found to be significantly higher than found on the CRT or by Stokes. As with the Sony display, the Girl image was found to have a significantly higher sensitivity than the other two images. The Flower image had a slightly lower sensitivity than the others.

Table 6.2-4 Parametric Thresholds for Hue Rotation–SGI LCD

	Mean	Lower	Upper	LOF
Stokes 1991	5.9	5.2	6.5	
Overall	4.19	0.66	7.72	
Currency	4.4	2.3	5.8	
Flower	6.0	3.1	7.9	
Girl	2.2	-0.2	3.5	

Figure 6.2-3 Parametric Sensitivity for Hue Rotation–SGI LCD

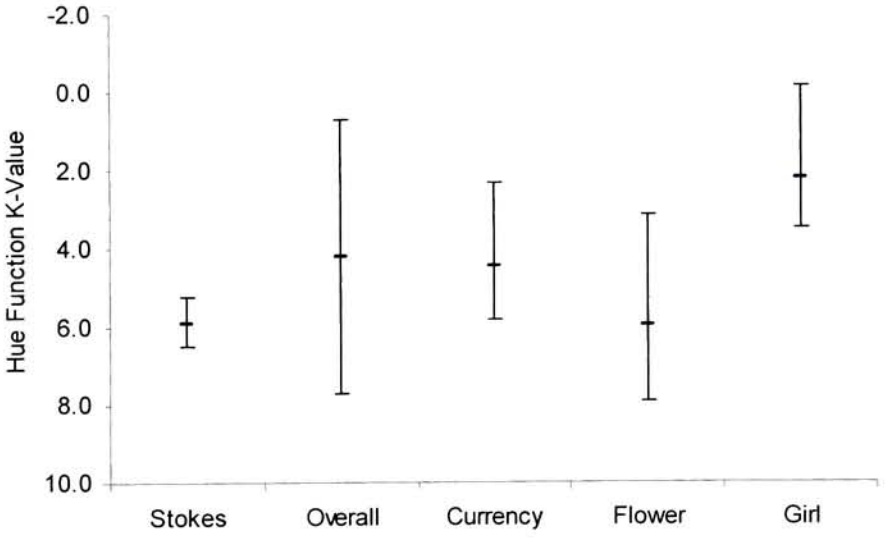

6.2.5. Observer Comments

For the SGI display, the majority of observers who had also participated in the Sony experiment, commented that this one was much easier. Observers felt generally confident of their answers, even on the Currency image. In general, observers appeared to focus on the same regions of the images as before. An observer with an extensive pre-press background used the girl's skin as his primary reference for that image. A few observers commented on seeing differences in the yellow areas in the Currency image not seen in the previous experiment.

6.3. IBM Roentgen LCD Prototype

This project was sponsored by IBM T.J. Watson Research Center to help them understand how their 200ppi Roentgen prototype compared to commercially available products.. This panel represents a possible future trend in flat-panel display technology. It is also a prototype device built to test the feasibility of actually producing such a high-resolution LCD panel. As such, many defects were present that would not be included in a final product of this type. The results from this display must be interpreted with this in mind. The raw SAS analysis output for this display is presented in Appendix A.3.

6.3.1. Observer Statistics

A total of 37 observers participated in this part of the experiment, 21 of which had participated in the previous two. The composition of the observer population is shown in Table 6.3-1.

Table 6.3-1 Observer Statistics–IBM LCD

Average Age	29	# Experienced	25
Age Range	19–53	# Inexperienced	12
# Male	29	Average Time	0:27 min
# Female	8	Time Range	0:14 – 1:02

*6.3.2. Parametric Results for Sigmoidal Compression in L**

Results for the sigmoidal compression in lightness are given in Table 6.3-2 and Figure 6.3-1. The overall results correspond quite well with those found by Stokes in 1991. Results by image show some variability, with the flower image standing out as having a higher sensitivity than the other two images. Note the lack of fit and the subsequently large error bars for the Girl image.

Table 6.3-2 Parametric Thresholds for Lightness Compression–IBM LCD

	Mean	Lower	Upper	LOF
Stokes 1991	0.88	0.87	0.89	
Overall	0.87	0.63	1.11	
Currency	0.87	0.85	0.90	
Flower	0.84	0.79	0.89	
Girl	0.91	0.86	1.3	*

Figure 6.3-1 Parametric Sensitivity for Lightness Compression–IBM LCD

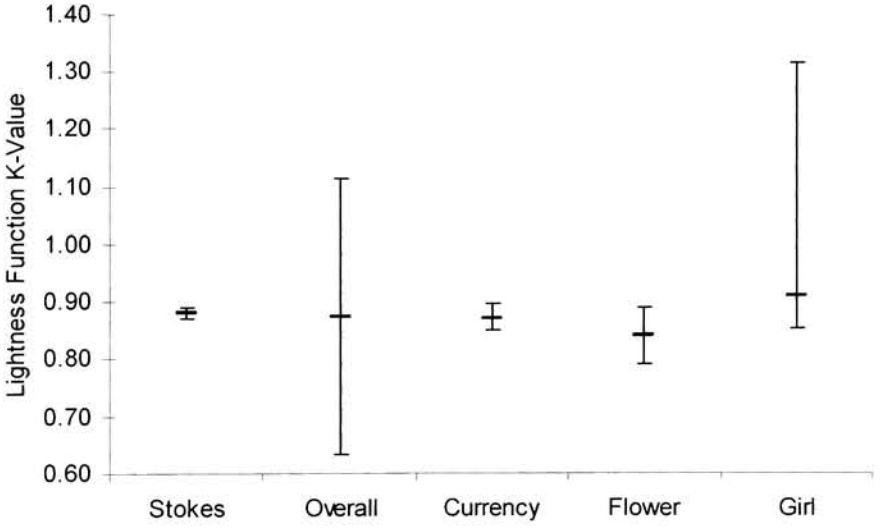

6.3.3. Parametric Results for Linear Reduction in C^*_{ab}

The estimated overall threshold for linear compression in CIELAB chroma matches with previous findings. In this dimension, the flower image has a slightly lower sensitivity than the other two images.

Table 6.3-3 Parametric Thresholds for Chroma Reduction–IBM LCD

	Mean	Lower	Upper	LOF
Stokes 1991	0.91	0.90	0.92	
Overall	0.90	0.82	0.98	
Currency	0.93	0.89	1.01	
Flower	0.86	0.83	0.90	
Girl	0.92	0.89	0.97	

Figure 6.3-2 Parametric Sensitivity for Chroma Reduction–IBM LCD

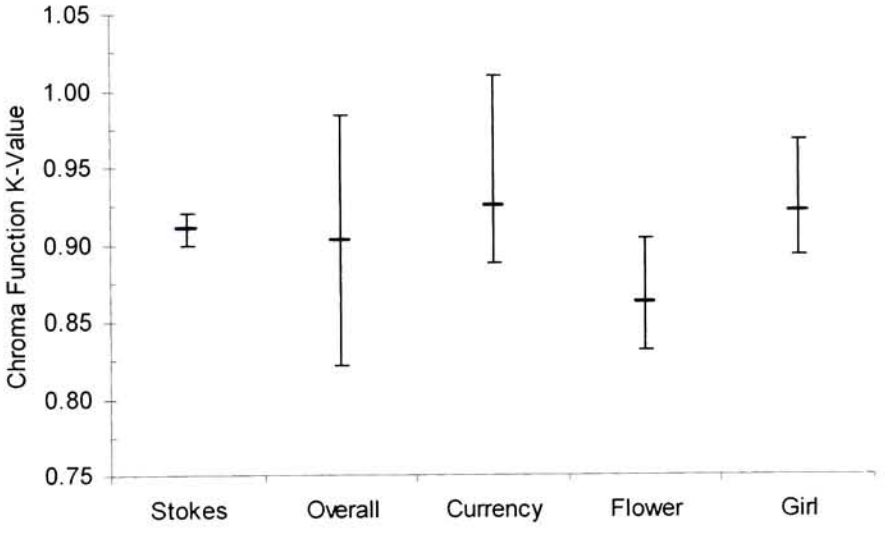

6.3.4. Parametric Results for Additive Rotations in h_{ab}

As with the other two dimensions, the overall results for hue rotation match well with those of Stokes [1991]. As in the chroma dimension, the mean sensitivity for the flower image is lower than the overall results. The lack of fit for the overall results is likely due to the poor fits to both the flower and girl images as well as the difference in performance of the flower image relative to the other two.

Table 6.3-4 Parametric Thresholds for Hue Rotation–IBM LCD

	Mean	Lower	Upper	LOF
Stokes 1991	5.9	5.2	6.5	
Overall	5.8	-0.79	12.43	
Currency	4.8	-0.2	7.3	
Flower	7.9	2.8	11.4	*
Girl	4.7	0.6	6.9	*

Figure 6.3-3 Parametric Sensitivities for Hue Rotation–IBM LCD

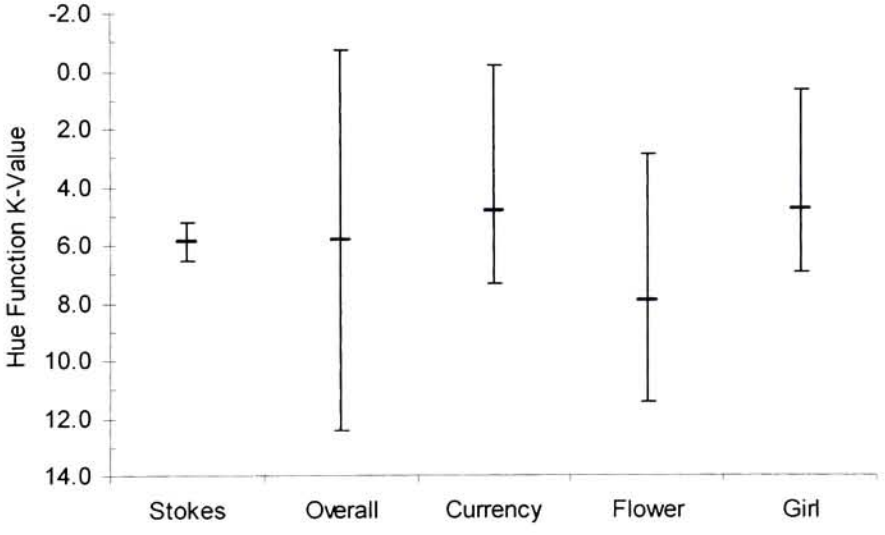

6.3.5. Observer Comments

Observers who had participated in the three previous experiments tended to comment that this display was somewhat easier than the other three. Most observers also noted being troubled by the many defects on the screen but did not feel they affected their judgments.

6.4. Fujix® Pictrography® 3000 Printer

The Pictrography prints were included in the experiment to provide a high-end anchor to compare against the three monitors. The raw SAS output for this experiment is shown in appendix A.4.

6.4.1. Observer Statistics

A total of 35 observers participated in this part of the experiment, 21 had also participated in the previous three. The composition of the observer population is shown in Table 6.3-1.

Table 6.4-1 Observer Statistics–Fujix Print

Average Age	28	# Experienced	28
Age Range	19 – 42	# Inexperienced	7
# Male	25	Average Time	0:47
# Female	10	Time Range	0:21 – 1:40

*6.4.2. Parametric Results for Sigmoidal Compression in L**

The full scale error bars associated with the Currency image is the dominating feature of Figure 6.4-3. During the ranking experiments, observers assigned entirely random orders to the lightness manipulated Currency images. Each of the nine images appeared in each of the nine spots with nearly equal probability. The change between the original and the most highly manipulated image in the stack was below threshold for this image. Due to time constraints, a second set of images exploring a larger range of transformations was not created or explored. Furthermore, it was found that compressing the images much beyond what had already been used tended to create noticeable artifacts in the images due in part to the weakness of the $L^*C^*_{ab}h_{ab}$ to RGB transform created for the printer.

Table 6.4-2 Parametric Thresholds for Lightness Compression–Fujix Print

	Mean	Lower	Upper	LOF
Stokes 1991	0.88	0.87	0.89	
Overall	0.75	0.24	1.26	
Currency	0.57	0.00	1.0	*
Flower	0.84	0.81	0.90	
Girl	0.83	0.81	0.87	

Figure 6.4-1 Parametric Sensitivity for Lightness Compression-Fujix Print

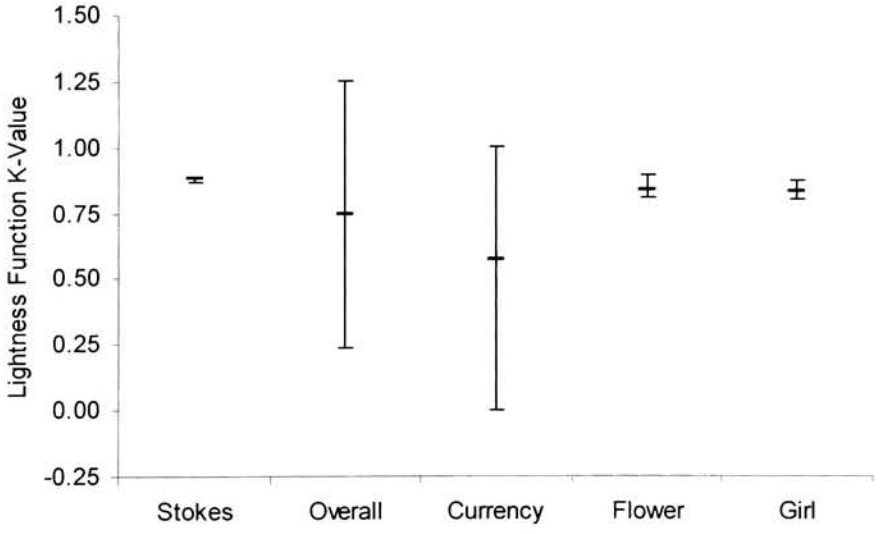

6.4.3. Parametric Results for Linear Reduction in C^*_{ab}

While each of the three individual images produced good fits to the model, the overall combination of all three did not. This is due in part to the flower image being estimated to have a threshold substantially different than the other two images.

Table 6.4-3 Parametric Thresholds for Chroma Reduction–Fujix Print

	Mean	Lower	Upper	LOF
Stokes 1991	0.91	0.90	0.92	
Overall	0.97	0.94	1.0	
Currency	0.98	0.96	0.99	
Flower	0.95	0.93	0.97	
Girl	0.99	0.97	1.01	

Figure 6.4-2 Parametric Sensitivities for Chroma Reduction–Fujix Print

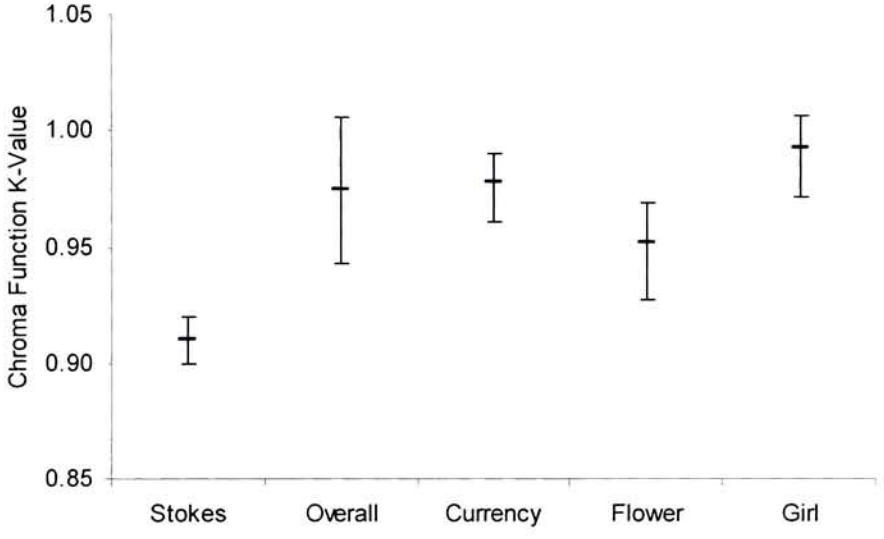

6.4.4. *Parametric Results for Additive Rotations in h_{ab}*

The negative estimates for the Girl image and Overall threshold are due to two factors. First, the samples presented were very close to threshold so there was insufficient range to create a robust estimate of the threshold. Secondly, the probit analysis was not constrained to be all positive.

Table 6.4-4 Parametric Thresholds for Hue Rotations–Fujix Print

	Mean	Lower	Upper	LOF
Stokes 1991	5.9	5.2	6.5	
Overall	0.3	-2.9	3.4	
Currency	0.8	-2.4	2.0	*
Flower	-1.8	0.3	1.6	
Girl	-2.0	-0.3	0.7	

Figure 6.4-3 Parametric Sensitivity for Hue Rotations–Fujix Print

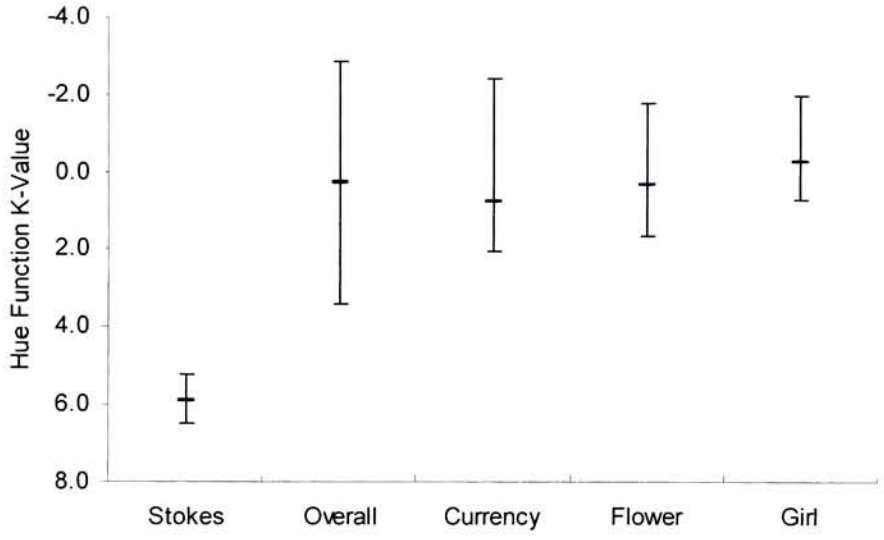

6.4.5. *Observer Comments*

The majority of observers commented that this task was much harder than the 2AFC used on the emissive displays. Most observers also stated that they felt that they were simply guessing and had little to no confidence in their answer. When asked to explain the increased difficulty, they suggested that for the other displays, they were able to focus on a single point in the image and toggle between the three choices looking for the one that appeared different even with the slight delay between images. With the prints, they found it hard to do such a direct comparison. Other comments suggested that they non-uniform lighting caused shadows that made differences appear to be position dependent. To obtain high luminance levels, the prints were placed close to 5 banks of fluorescent lights, placing them further away would have increased the uniformity of lighting but reduced the intensity.

6.5. Summary Comparison of Parametric Thresholds

The data presented in Tables 3–6 are to be interpreted as follows. The boldface numbers represent the mean threshold for the display in that row for the transform in that column. The plain type numbers to the right of the threshold are the upper and lower 95% fiducial limits. An asterisk indicates a lack of fit at α=0.1. For example, the estimated threshold for chroma on the SGI display was 0.91 with a range of [0.93,0.91].

Table 6.5-1 Overall Comparison of Parametric Thresholds

	Lightness		Chroma		Hue	
Stokes CRT	**0.88**	0.89 0.87	**0.91**	0.92 0.90	**5.9**	6.5 5.2
Sony CRT	**0.86**	0.91 0.81	**0.90**	0.95 0.85	**6.3**	9.4 3.1
SGI LCD	**0.86**	0.92 0.81	**0.91**	0.96 0.86	**4.2**	7.7 0.7
IBM LCD	**0.87**	1.11 0.63	**0.90**	0.98 0.82	**5.8**	12.43 -0.79
Fujix Print	**0.75**	1.26 0.24	**0.97**	1.01 0.94	**0.3**	3.4 -2.9

Figure 6.5-1 Overall Parametric Sensitivities for Lightness Compression

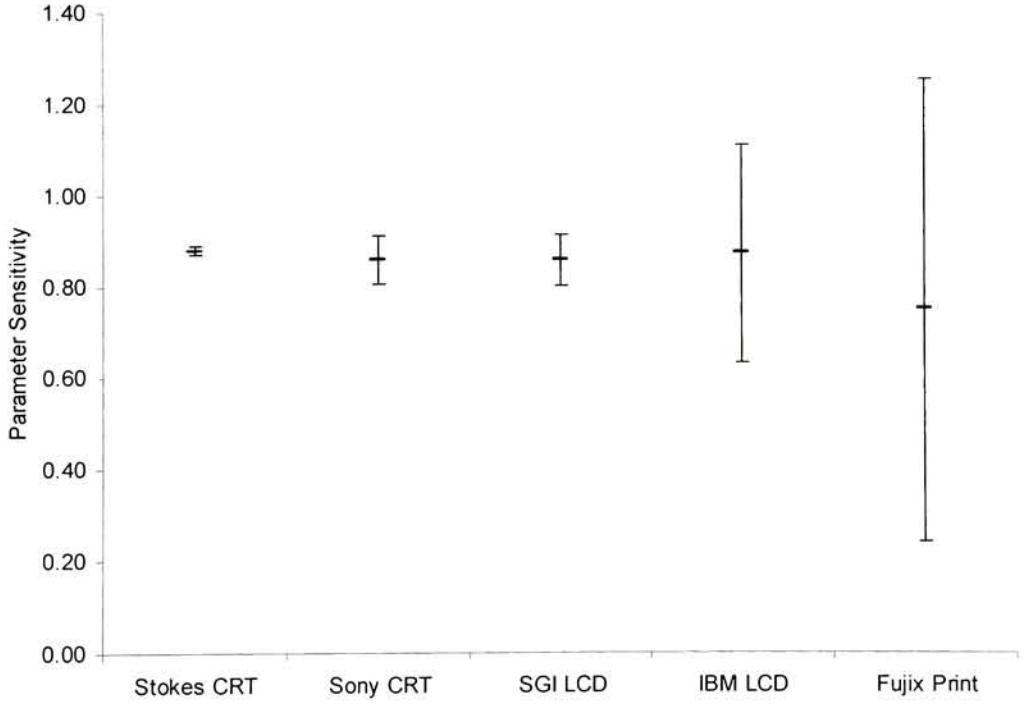

Figure 6.5-2 Overall Parametric Sensitivities for Linear Chroma Reduction

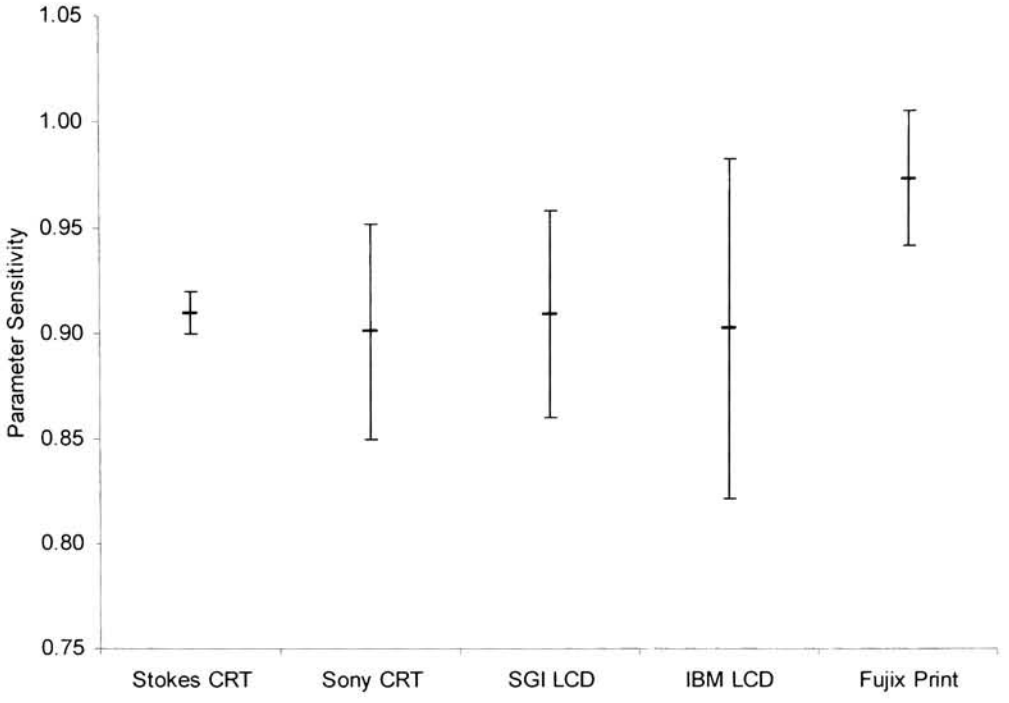

Figure 6.5-3 Overall Parametric Sensitivities for Hue Rotation

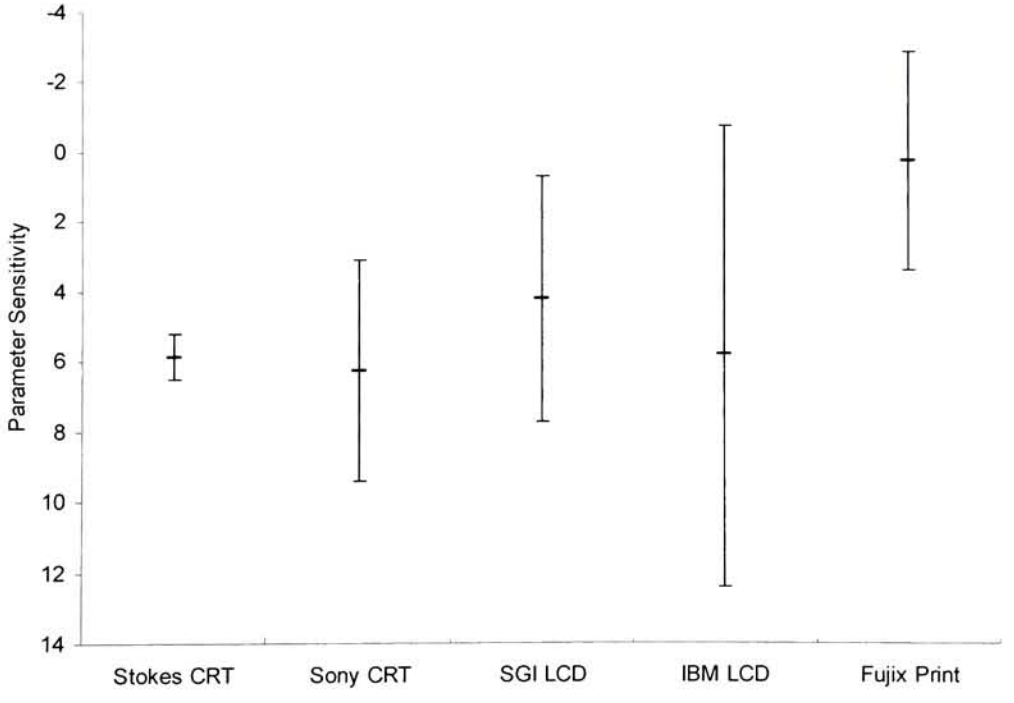

6.6. Parametric Results Versus Parameters

One of the goals of this project was to look for any possible trends between various display parameters and the resulting color difference tolerances in images. While more an observational study, rather than an experiment that predicted an outcome, the following three sets of figures were produced to look for the presence of any qualitative trends. The figures below plot the overall parametric thresholds (k-values) from each display as a function of white point luminance, contrast ratio and resolution. Data from Stokes' experiment are included for comparison.

Figure 6.6-1 Sensitivity versus White Point Luminance

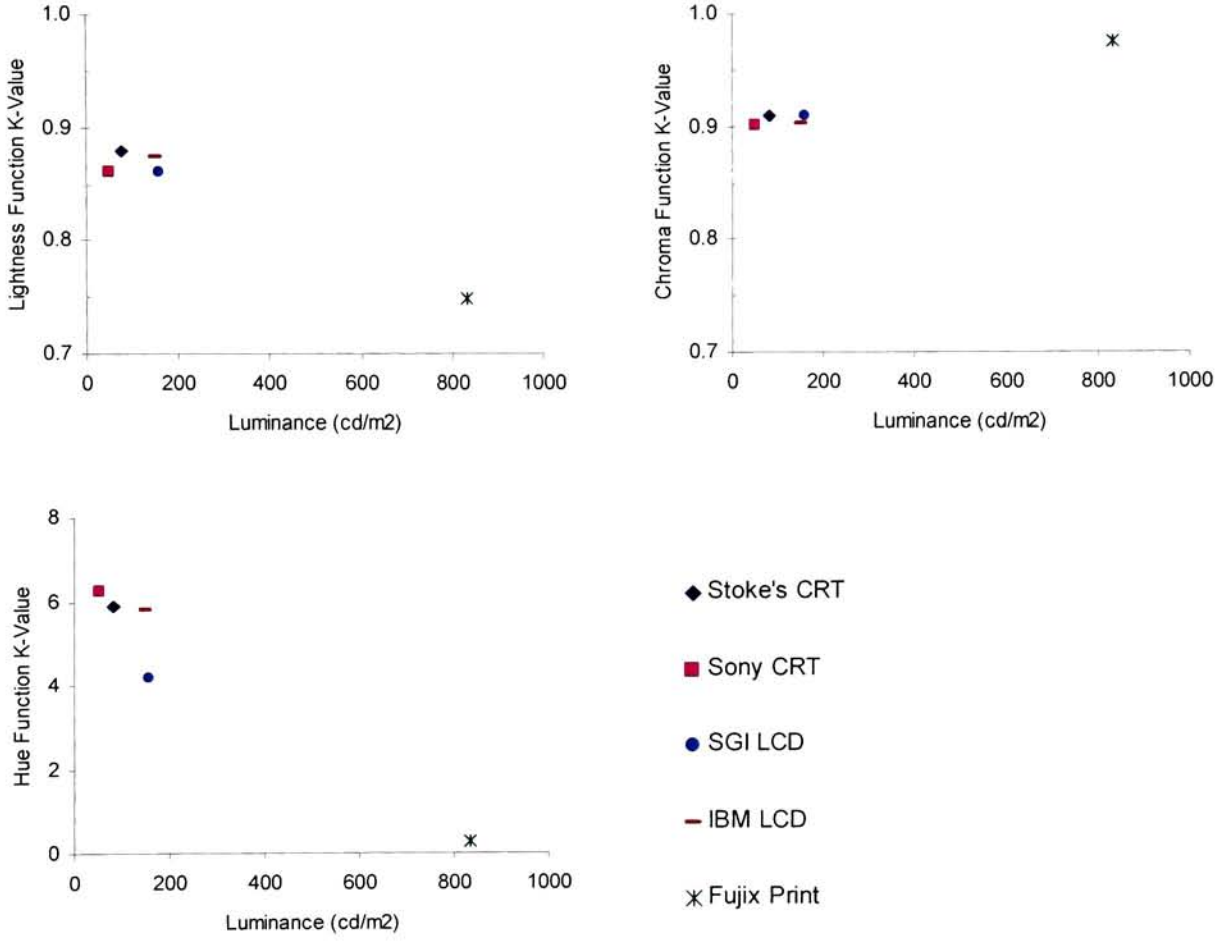

In the above figures, the four monitors tend to cluster together with similar luminance levels and sensitivities. The Fujix prints stand out as having both a very high luminance level and very high overall sensitivity in all three dimensions.

Figure 6.6-2 Sensitivity versus Contrast Ratio

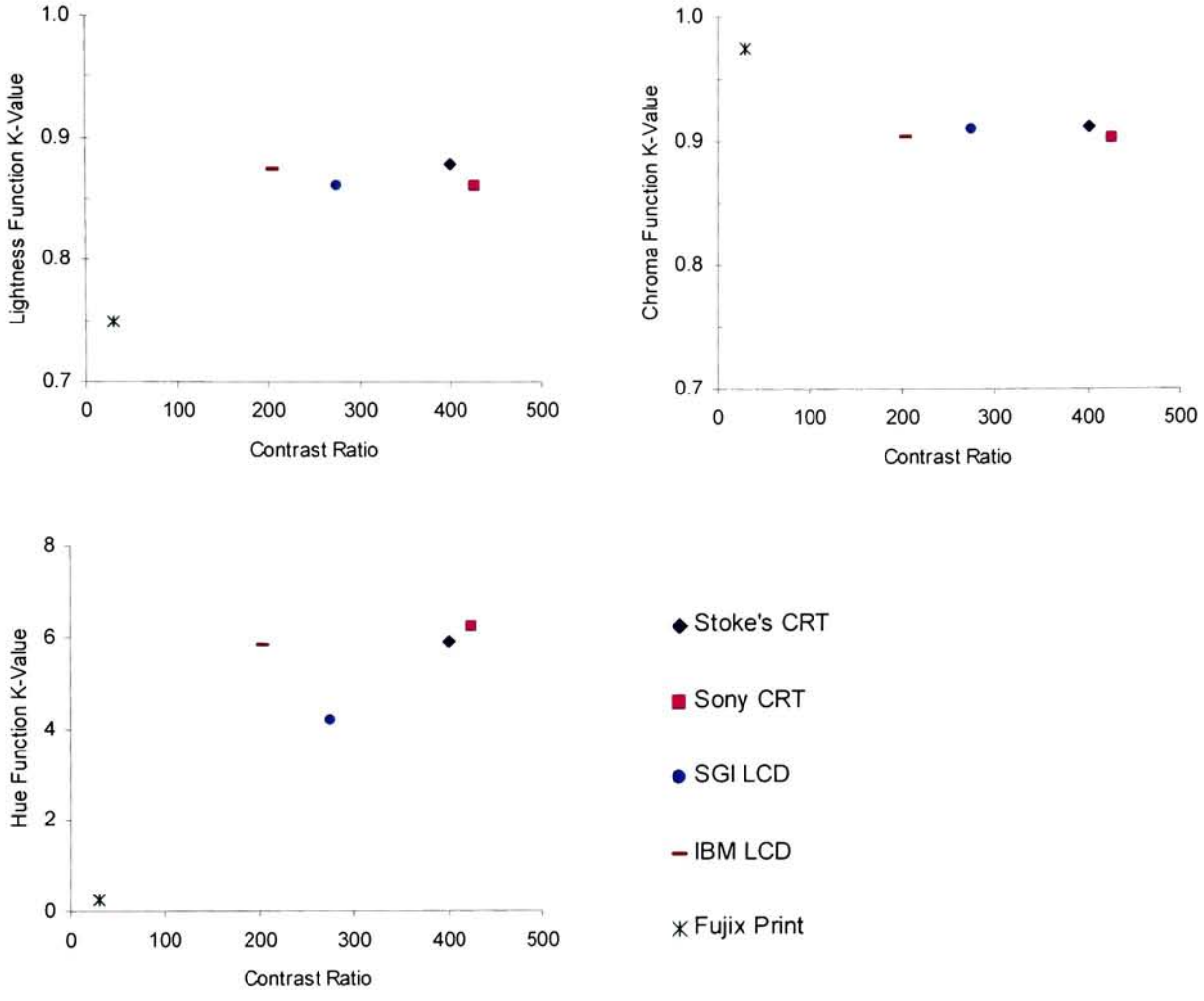

A slight trend towards increased detection threshold with increased contrast ratio is seen for both the lightness and hue functions.

Figure 6.6-3 Sensitivity versus Addressable Resolution

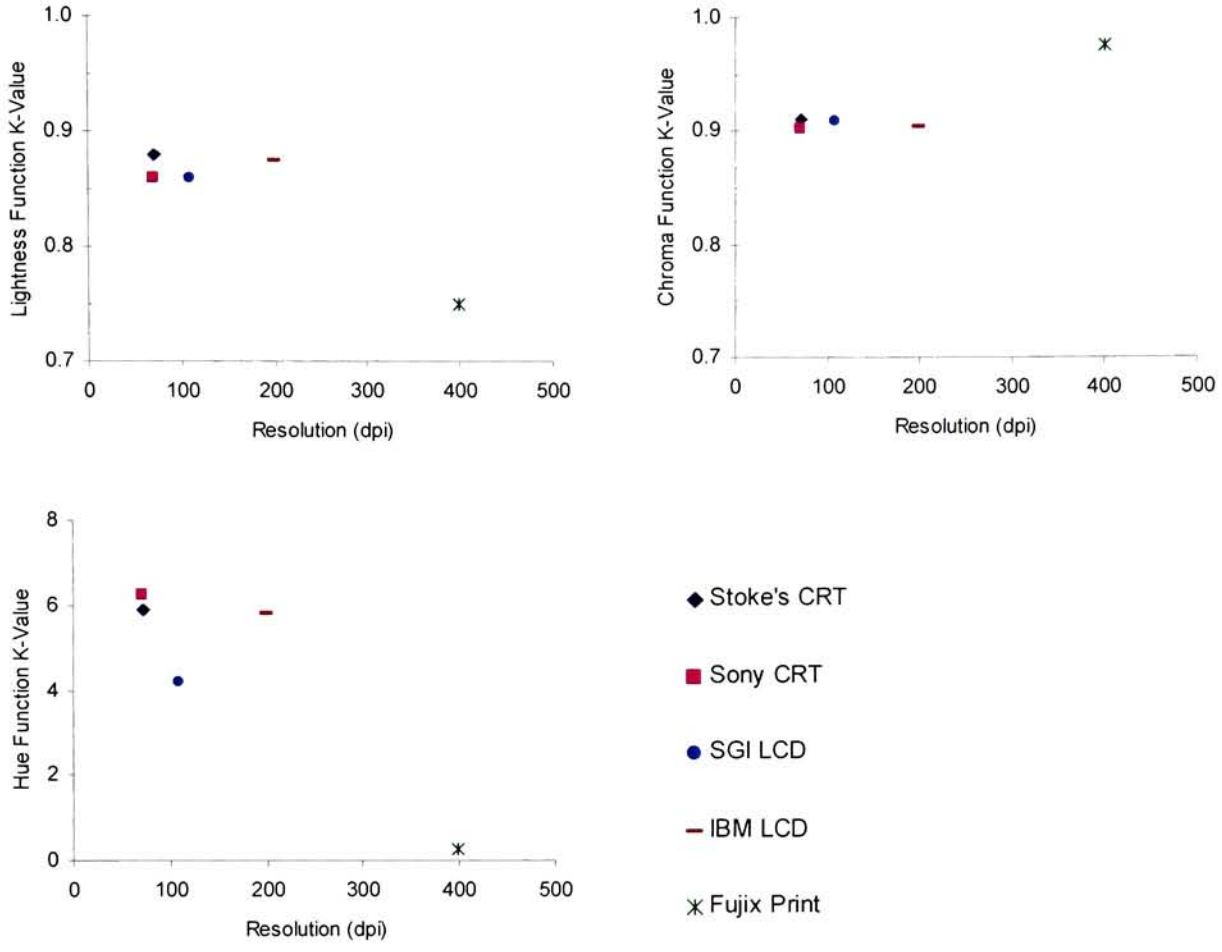

Sensitivity to lightness and chroma changes tended to be constant with increasing resolution except for the printed samples at 400ppi. Given the overall poor fitting of the print data, these results may be a bit misleading. For hue, there is a slight trend towards increasing sensitivity with increasing resolution.

7 Colorimetric Threshold Results – Pixel-by-Pixel Differencing

The parametric thresholds presented in the previous chapter are interpretable only in the context of the specific transforms used. To make these thresholds more universally interpretable, this chapter presents the thresholds expressed in terms of color difference from the original.

7.1. Analysis Process

7.1.1. Difference Calculations

To calculate the color difference between the original and threshold image, both images were treated as a collection of patches. The point-by-point color difference between the two images was calculated. For the print samples, the raster images that were sent to the printer were used. Both the printing process and monitor models were assumed to introduce only uniform bias errors. Because of this, only relative comparisons can be made since the actual colorimetry presented to the observer is unknown.

As discussed in previous chapters, there are many color difference formulas from which to choose. For this project, three CIE color differences formulas were selected as being representative of current industrial practice, ΔE^*_{ab}, ΔE_{94} and ΔE_{2000}. To show the flexibility of the ΔE_{94} and ΔE_{2000} formulas, differences were also computed with their k_L, k_C and k_H terms adjusted to minimize the variance between dimensions. These formulas are discussed in chapter 5. The $k_\bullet$ values used are tabulated and discussed in section 7.7.

7.1.2. Selection of Summary Measure

Computing the pixel-wise color difference for each image pair results in a very large data set (3,840,000 individual differences in the case of the Fujix Pictrography prints) for each image. The data set must be summarized before interpreting the results. The latest report from CIE TC8-02 [CIE 2000] recommends reporting:

- Mean, standard deviation and coefficient of skewness of ΔE.
- Selected percentiles of the ΔE distribution.
- Mean and standard deviations of, and correlations between ΔL^*, Δa^* and Δb^*

For purposes of this thesis, the mean and standard deviation of the ΔE's were recorded along with the quartiles and deciles of the distribution. Since the data is treated as varying uni-dimensionally, the correlations between individual dimensions were not needed.

In this experiment, the estimated thresholds represent just-noticeable differences (JNDs) in color for a given transform/image pair. It is logical that a good summary statistic should give equal values to each threshold since each represents a 1 JND change and to be widely applicable the JND's should be image and transform independent.

Two possible summary statistics were chosen for analysis: the arithmetic average (as used by Stokes) and the 90th percentile ΔE's (as used by Uroz) of the pixel-wise differences. These two statistics were collected for each image, transform and display for all five difference metrics. Results from transform/image pairs that did not achieve an α=0.10 fit to the probit were removed to avoid skewing the data. For the remaining 31 pairs, the average and coefficient of variation (CV= σ/μ) was then computed. The CV was chosen to measure the dispersion of the data rather than the standard deviation (σ) since it is independent of the mean value. The results of this analysis are shown in Table 7.1-1 below. As expected, the Average and 90th percentile measures are highly correlated (R^2 = 0.92), but based on this analysis, the 90th percentile ΔE^*_{ab} metric is the most consistent (i.e. has the lowest CV). This result agrees well with the findings of both Stokes [1991] and Uroz [1999].

Table 7.1-1 Metric Performance

Formula	Metric	Measure	
		μ	CV
ΔE^*_{ab}	Average ΔE*	1.46	0.56
	90th% ΔE*	2.42	**0.45**
ΔE_{94}	Average ΔE*	1.15	0.69
	90th% ΔE*	1.71	0.61
$\Delta E_{94\ (l:c)}$	Average ΔE*	0.93	0.65
	90th% ΔE*	1.37	0.62
ΔE_{2000}	Average ΔE*	1.34	0.70
	90th% ΔE*	1.99	0.73
$\Delta E_{2000\ (l:c)}$	Average ΔE*	1.13	1.49
	90th% ΔE*	0.61	0.58

Stokes [1991] found that the average ΔE^*_{ab} was a more consistent measure than ΔE^*_{MCSL}, a predecessor to ΔE_{94}. This can be seen in the above table that the CV for the Average ΔE^*_{ab} of 0.45 is lower than the CV for the average of the other four formulas tested.

Uroz [1999], using a slightly different method, also arrived at a similar conclusion. He computed the Pearson's χ^2 goodness of fit to a normal distribution for the images when distributed against both the average and 99th percentile ΔE^*_{ab} between pairs of pallet colors. The null hypothesis that the data is distributed normally failed to be rejected for the 99th percentile color differences and was rejected in favor of the alternate for the average color difference.

He then compared the 99th percentile results for both ΔE^*_{ab} and ΔE_{94} and noted that "The thresholds tend to be less image dependent and less colour dimension dependent when expressed in terms of ΔE^*_{ab} than when described in ΔE_{94} units."

ΔE^*_{ab} vs. $\Delta E_{94/2000}$ A possible reason for why ΔE^*_{ab} works better than ΔE_{94} for images may be due to the fact that the CIE94 and proposed CIE2000 formulas were optimized to describe smaller color differences [CIE 1995, CIE 2000, Uroz 1999]. That any of them provide a good measure is interesting in its own right since both were designed for uniform patches.

90th percentile vs. Average Based on the difference maps and comments made by the observers during testing, Uroz hypothesized that the observers responses should be well correlated to high percentile color differences. He theorizes that observers were somehow segmenting the images into recognizable features (face, shirt, sky...) and comparing them one by one until they found the first feature that could be perceived as different.

7.1.3. Data to be Presented

The next four sections (7.2–5) of this chapter will present the colorimetric threshold results for each display. For completeness, data will be shown for all five color difference metrics (ΔE^*_{ab}, ΔE_{94}, $\Delta E_{94(l:c)}$, ΔE_{2000} and $\Delta E_{2000(l:c)}$) using both summary statistics (Average and 90th percentile). As in chapter 6, data that was ill-fit by the probit (α=0.10) will be marked with an asterisk (*).

Section 7.6 will present an overall summary comparison of the ΔE thresholds for both the average and 90th percentile metrics. As in chapter 6, the final section examines the qualitative relationship between the metrics and the physical parameters of the displays.

7.2. Sony GDM-F500 CRT Display

This, and the following three section present the pixel-by-pixel colorimetric difference data as follows: for each of the three color space manipulations graphs showing the average and 90th percentile color differences will be shown. A brief description of the results will follow. The chapter concludes with overall observations for the display in question.

Unlike Chapter 6, the raw data for each of the measures will not be included directly in the text. See the companion CD for details.

*7.2.1. Colorimetric Results for Sigmoidal Compression in L**

The graphs below show the threshold results for sigmoidal compression in L* on the Sony CRT display. Figure 7.2-1 (a) shows the overall average ΔE at threshold along with the results for each image individually. Results from Stokes are included for reference. Figure 7.2-1 (b) shows the results when the 90th percentile ΔE is used. The error-bars in each case represent 95% fiducials as were used in Chapter 6. In cases where the error-bars extend beyond the range of the graph, the description will indicate it's upper limit. Reading left to right for each image, the columns represent: ΔE^*_{ab} , ΔE_{94} , $\Delta E_{94\ (l:c)}$, ΔE_{2000} , $\Delta E_{2000\ (l:c)}$.

Figure 7.2-1 Lightness Thresholds – Sony CRT

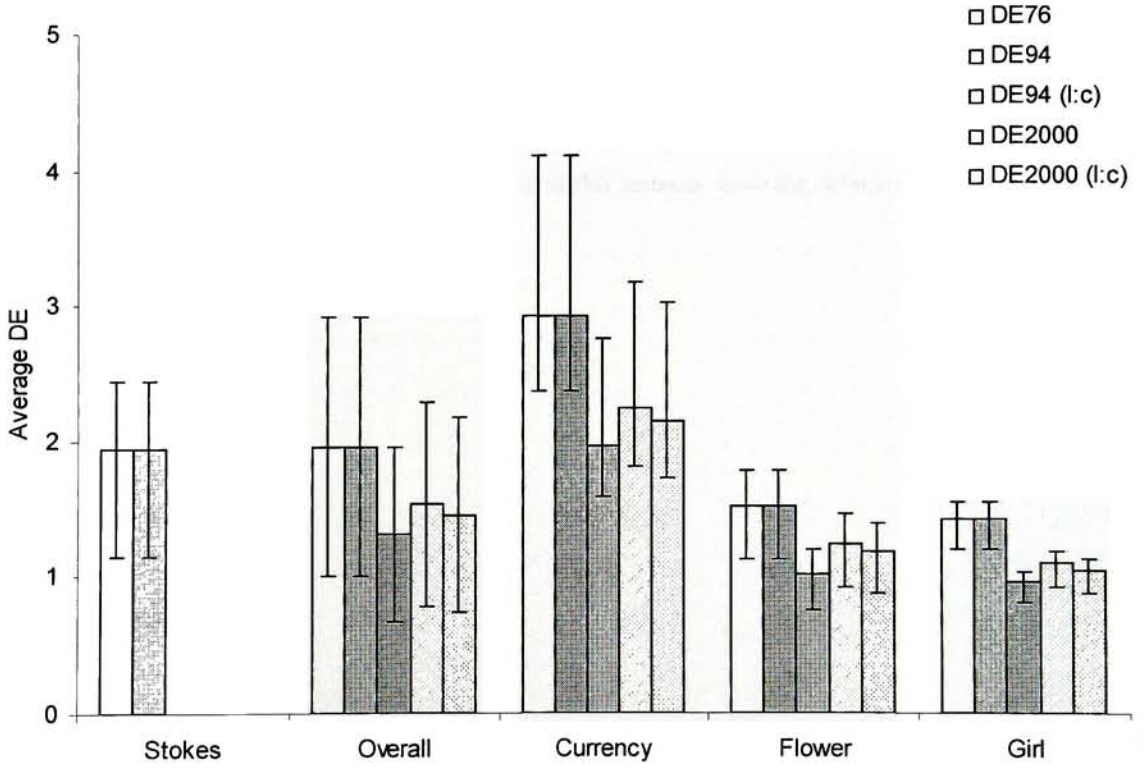

(a)

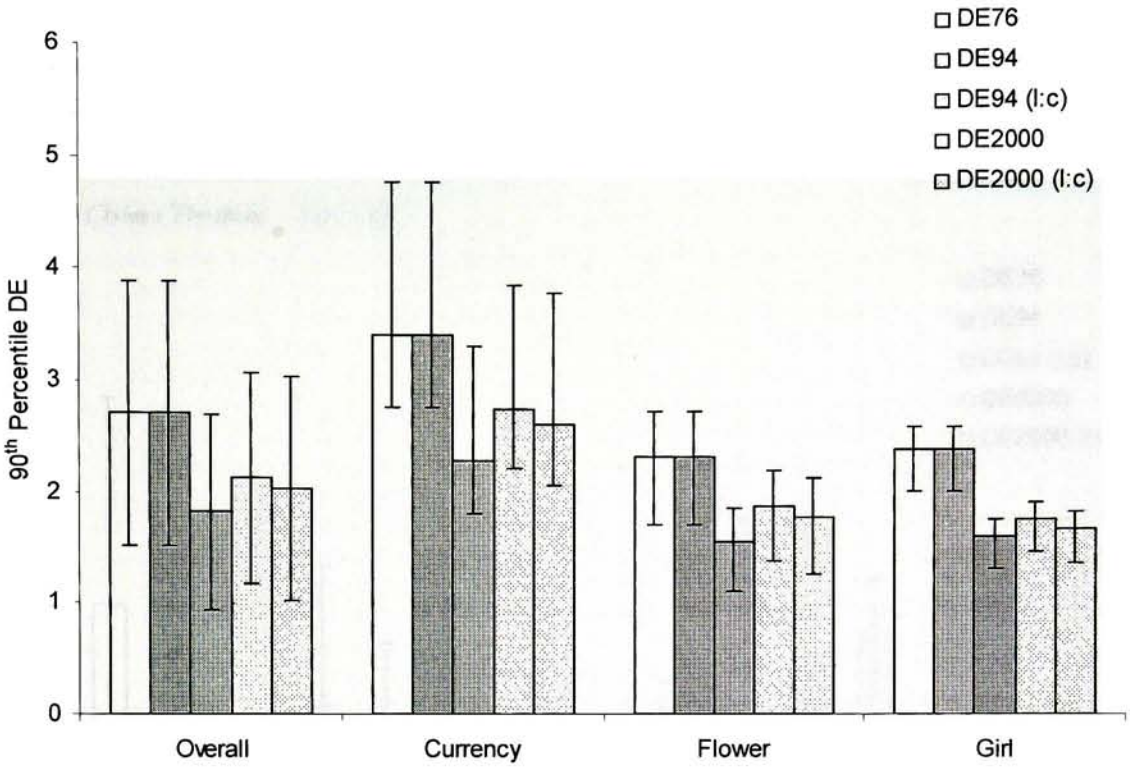

(b)

Comparing figure (a) and (b) above, the more consistent nature of the 90th percentile metric is readily seen. It is also important to note that the relative relationships between the five color difference formulas is maintained. Note that the values for ΔE^*_{ab} and ΔE_{94} are identical in this instance since the default of $k_L = 1.0$ was used for ΔE_{94} and the images varied only in L^*.

*7.2.2. Colorimetric Results for Linear Reduction in C**

The figures below plot the threshold results for linear reduction in C* on the Sony CRT display. The graphs follow the same formatting as used in the above section.

Figure 7.2-2 Chroma Thresholds – Sony CRT

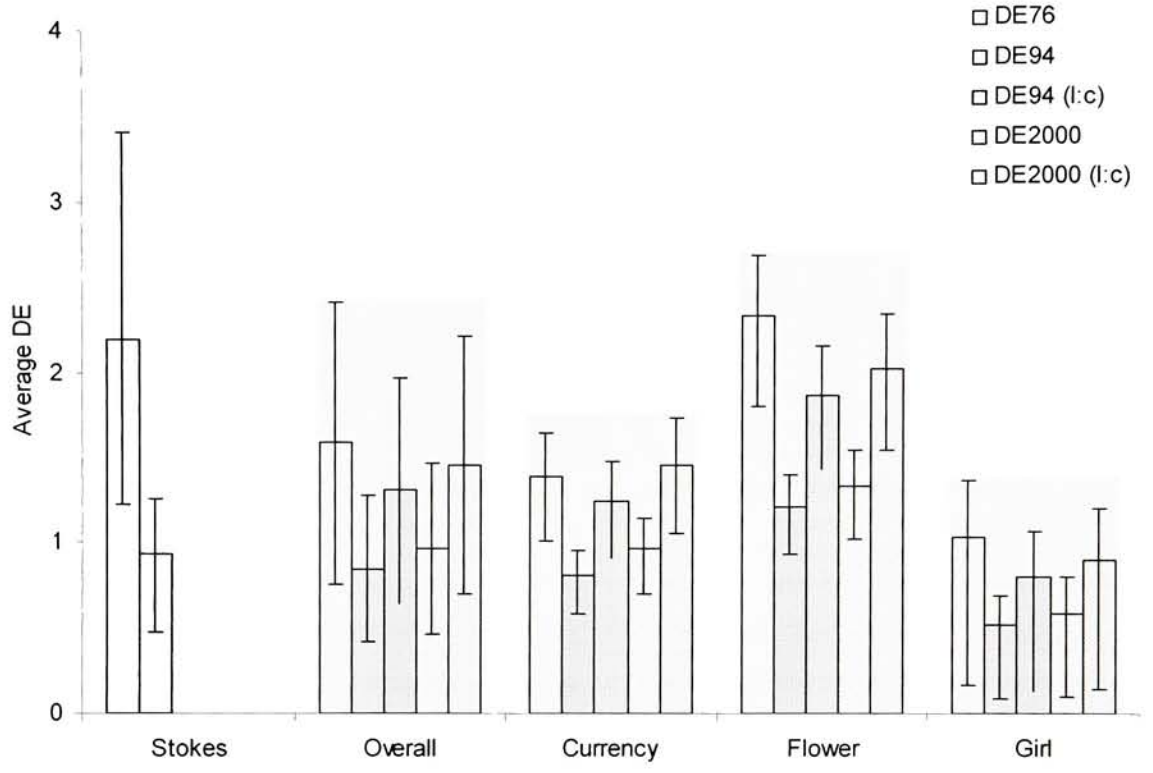

(a)

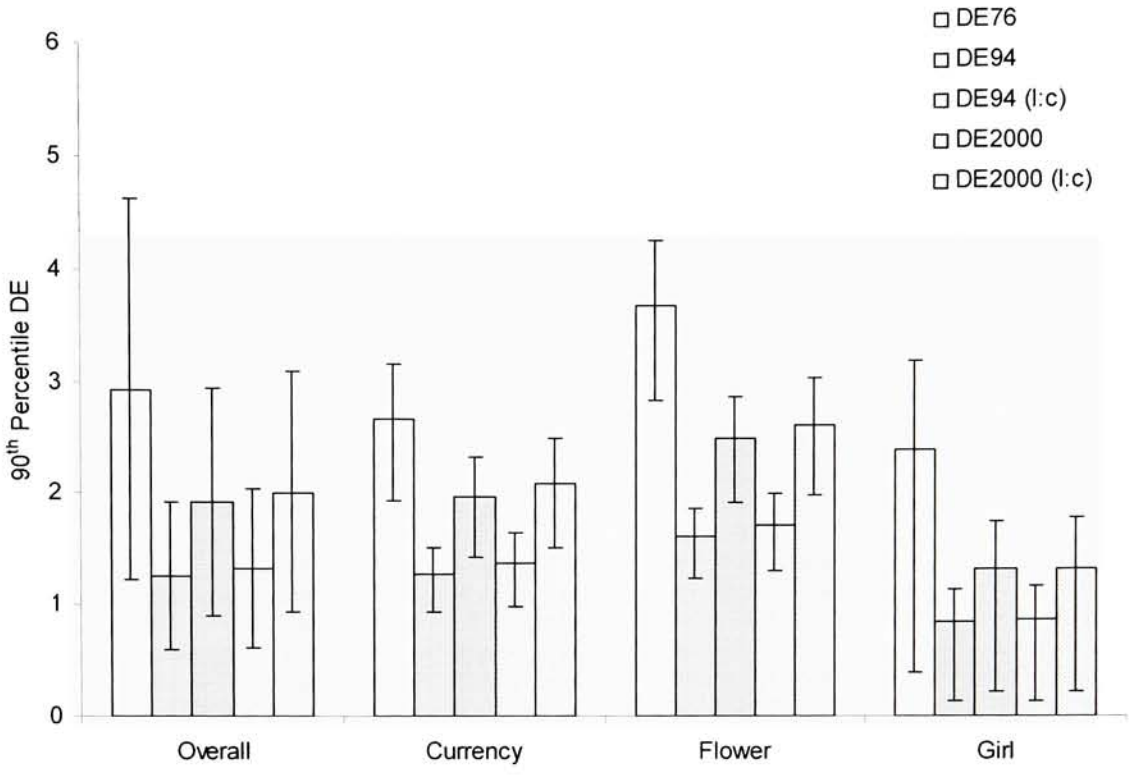

(b)

As in the previous sub-section, the relative stability of the 90th percentile metric is seen comparing (a) and (b) above. The relative ranking between images is consistent with that of the parametric thresholds, as is expected. For instance, the Girl image on the Sony CRT was shown to have higher sensitivity to chroma than the Currency and Flower images (Figure 6.1-2). Here it is seen that the ΔE at threshold for the Girl image was lower (more sensitive) than for the other two images.

7.2.3. Colorimetric Results for Additive Rotations in h_{ab}

Figure 7.2-3 Hue Thresholds – Sony CRT

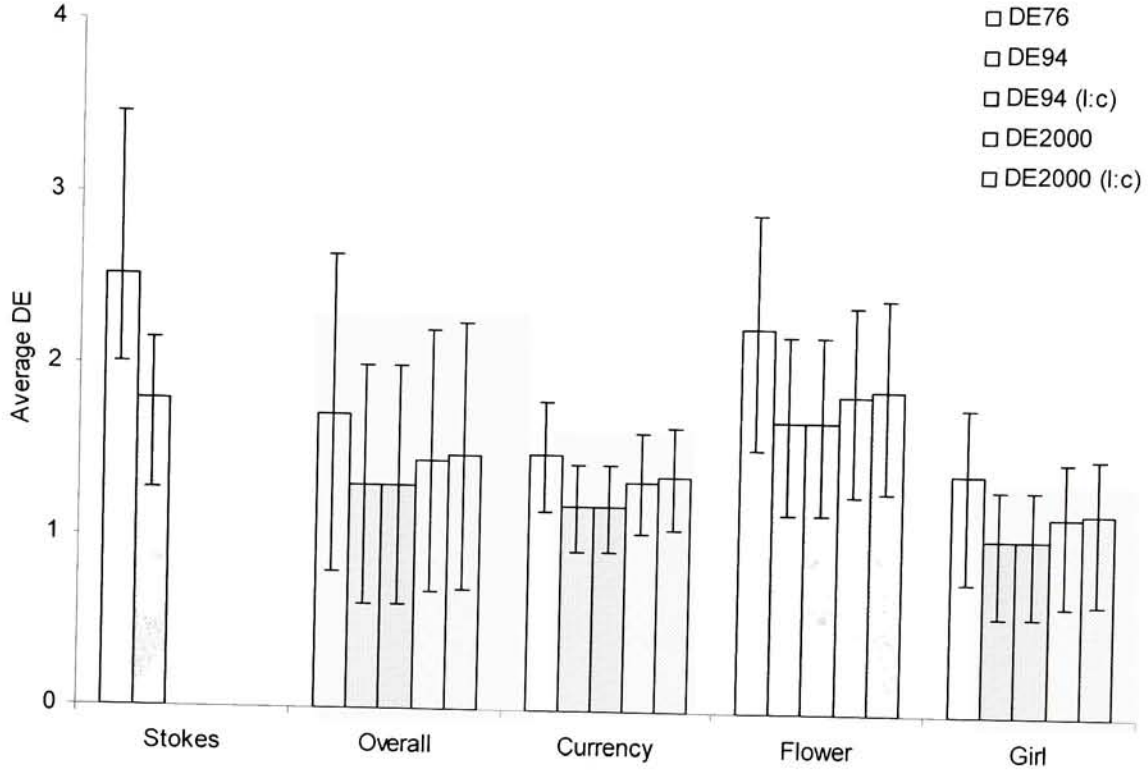

(a)

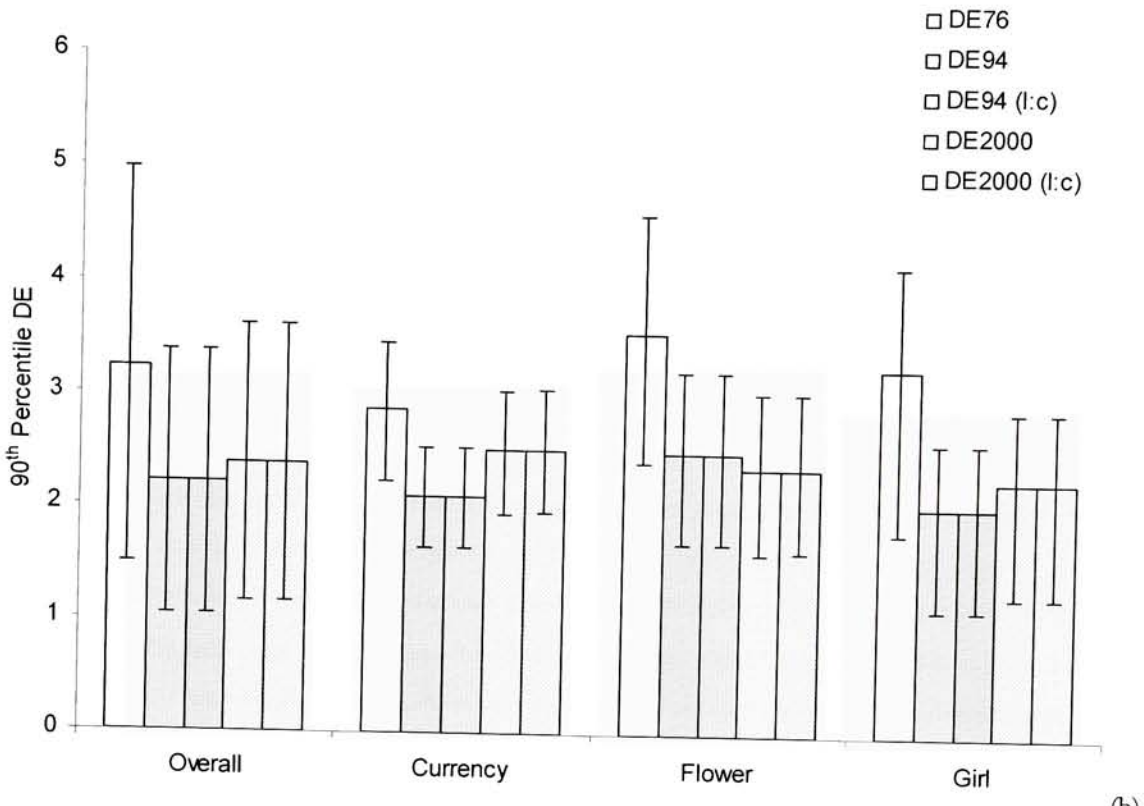
DE76
DE94
DE94 (l:c)
DE2000
DE2000 (l:c)
90th Percentile DE
0
1
2
3
4
5
6
Overall
Currency
Flower
Girl

(b)

7.2.4. Overall Remarks – Sony CRT

From the above graphs several features can be seen. First, as expected the ΔE_{94} values are smaller (~½) than the ΔE^*_{ab} thresholds, except in the L* dimension where they are equal. Results for ΔE_{2000} are generally slightly larger than ΔE_{94}.

Secondly, the poor prediction job of the average ΔE summary statistic can be seen by examining the variably in thresholds determined for a single image, as well as in the overall case versus the 90th percentile ΔE. To be useful, a difference metric should yield equal values for equal perceptual steps in all directions. If this were the case, then moving a threshold amount in lightness, chroma, or hue should all result in the same difference being reported.

There are at least two explanations for this second point. First of all, CIELAB space is known to be only pseudo-isotropic which may be responsible for some of the observed variations. More importantly, not all averages are created equally. For example consider the results of the following two processes on an image with uniform L* distribution. Process A moves each pixel with an L* less than 50 by 2.0 ΔE. Process B adds 1.0 ΔE to each pixel. The average ΔE difference between both images and the original is 1.0 but they would not appear the same. Thus simple summary statistics such as the overall average error are not appropriate.

Looking at the image-wise results, it can be seen that the Currency image stands out in the lightness dimension as having much larger ΔE's than the others possibly due to its low chroma content and lack of contrast. In the chroma and hue dimensions, the Flower image stands out as having higher ΔE's than the other two. This image had large amounts of high frequency content which may have masked the chroma changes. Detection of hue changes may have been hampered by the fact that the image was dominated by the purple flower petals and green grass giving few reference points from which to detect changes.

7.3. SGI® 1600SW™ LCD Panel

The following sections contain the pixel-by-pixel colorimetric difference data for the SGI 1600SW LCD panel display. Results from both the average ΔE and 90th percentile ΔE summery statistics are shown for comparison.

*7.3.1. Colorimetric Results for Sigmoidal Compression in L**

Figure 7.3-1 Lightness Thresholds– SGI LCD

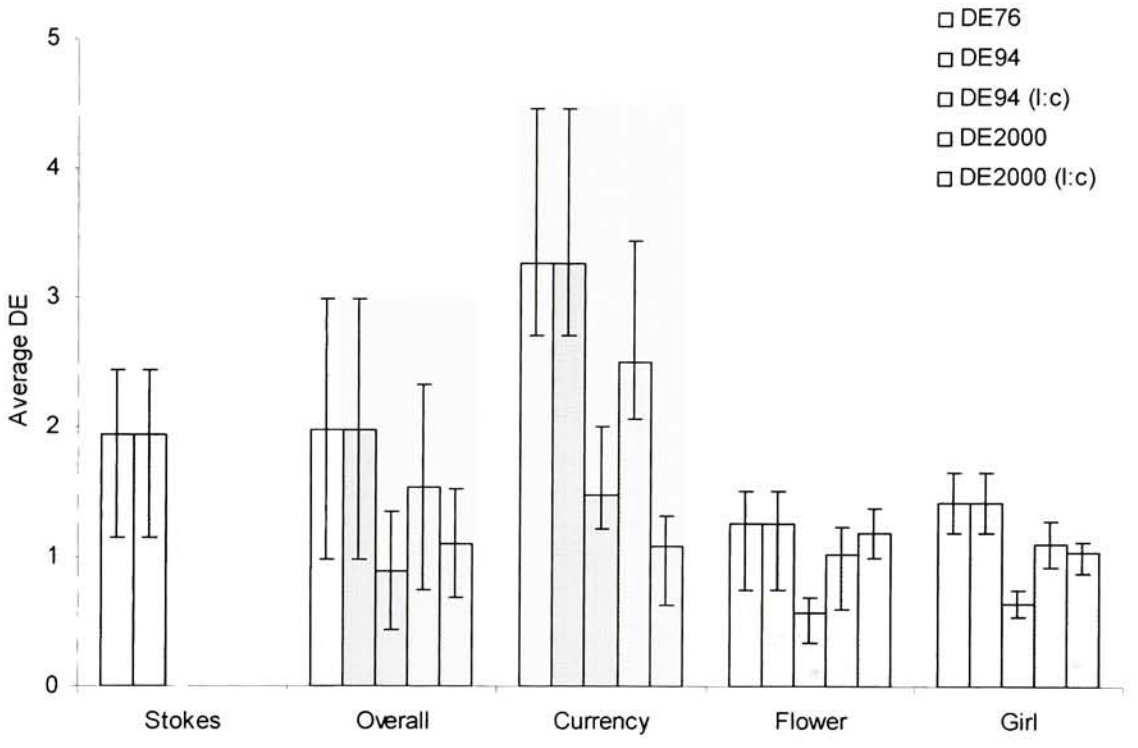

(a)

As noted before, the ΔE^*_{ab} and ΔE_{94} values are identical since the variation was in L* only.

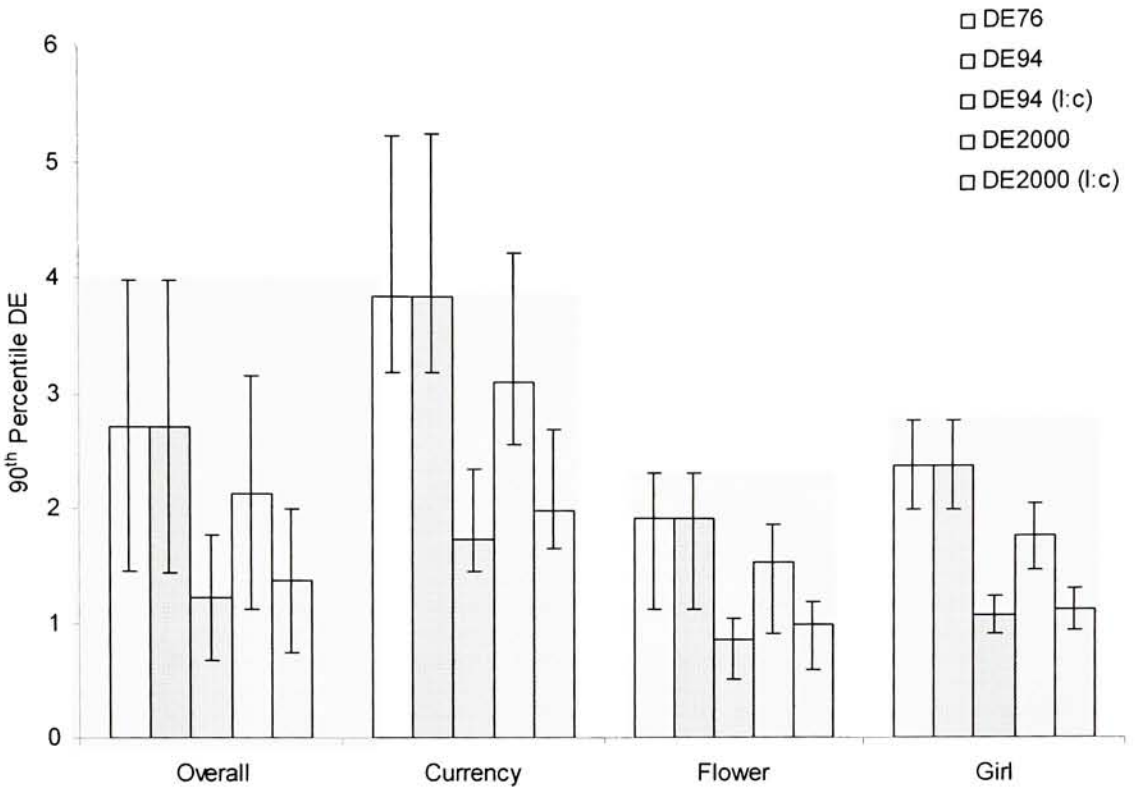

(b)

As with the Sony CRT display, the Currency image stands out possibly due to its low chroma content and lack of contrast.

*7.3.2. Colorimetric Results for Linear Reduction in C**

Figure 7.3-2 Chroma Thresholds– SGI LCD

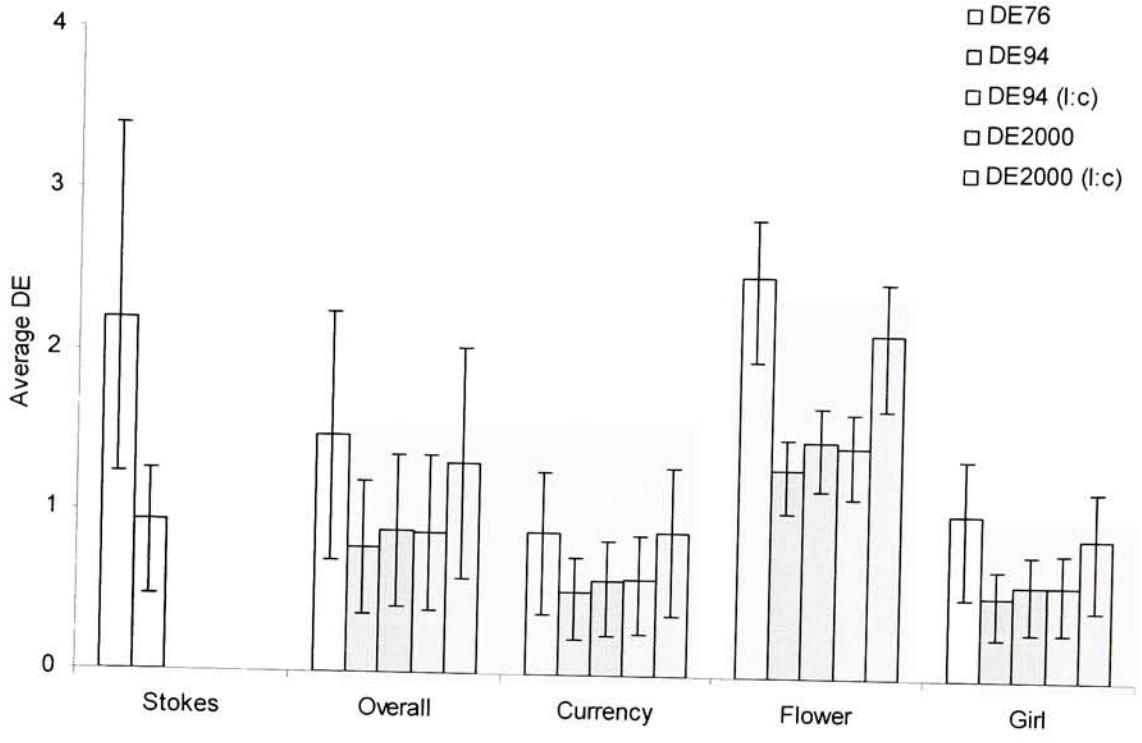

(a)

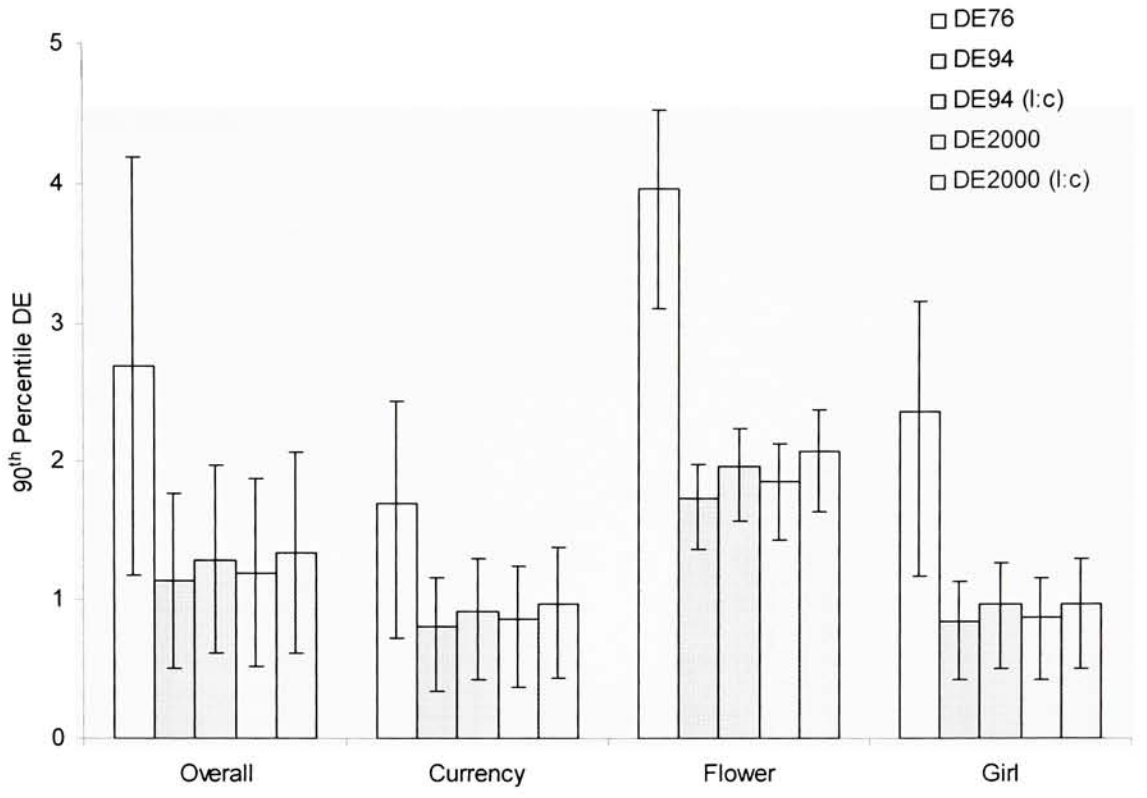

(b)

The Flower image here stands out as having a higher tolerance to changes in chroma. Because this image was dominated by high chroma greens, the content may have masked the smaller changes.

Figure 7.3-3 Hue Thresholds– SGI LCD

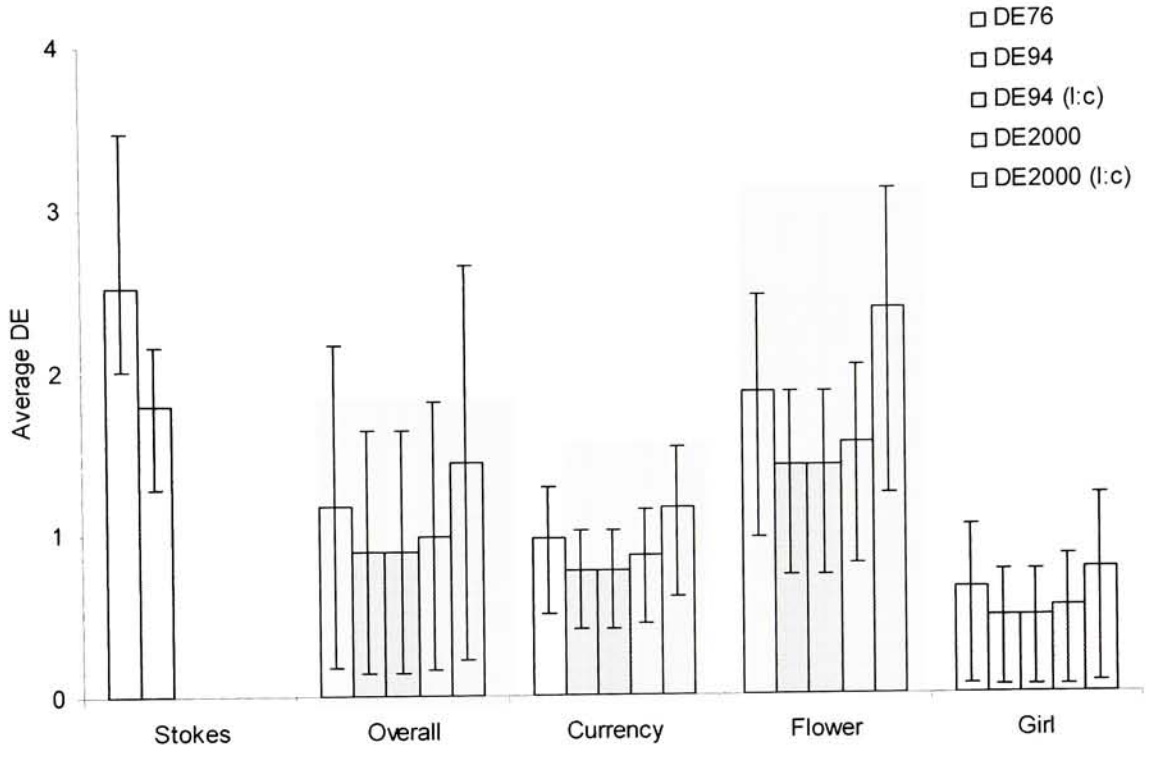

(a)

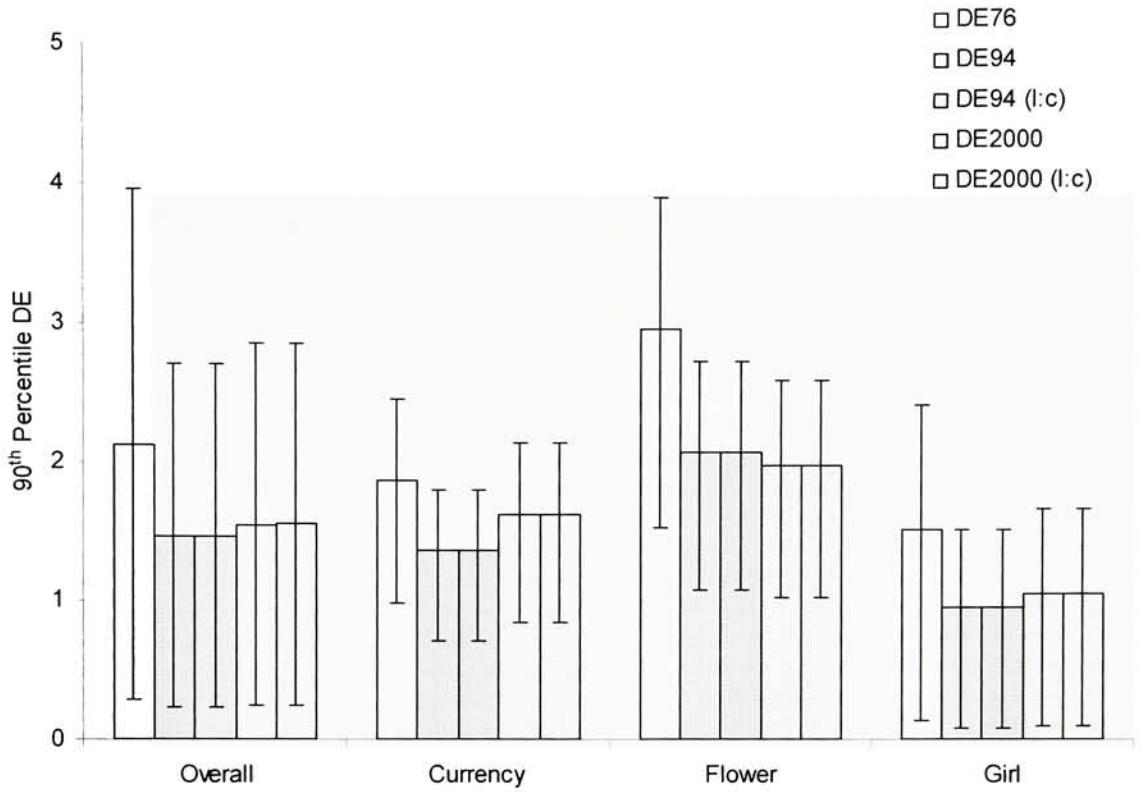

(b)

Here, as in Figure 6.2-3 the higher tolerance of the Flower image versus the Girl image is evident.

7.3.4. Overall Remarks – SGI LCD

As with the Sony CRT, the relative stability of the 90th percentile metric versus the average can be seen. It is also interesting to note that both monitors showed very similar ΔE versus percentile trends. The major difference being in the magnitude of the differences.

7.4. IBM Roentgen LCD prototype

Pixel-wise colorimetric results for the prototype IBM LCD panel are show below. Results from both the average ΔE and 90th percentile ΔE summery statistics are show for comparison.

*7.4.1. Colorimetric Results for Sigmoidal Compression in L**

Figure 7.4-1 Lightness Thresholds– IBM LCD

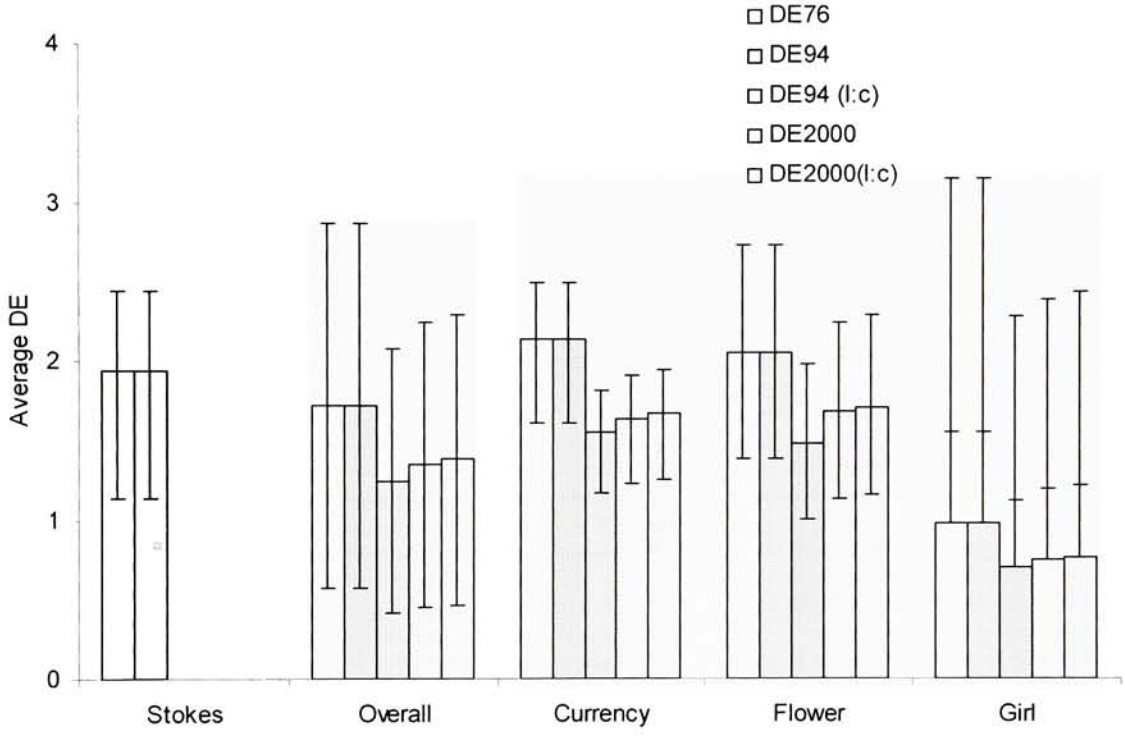

(a)

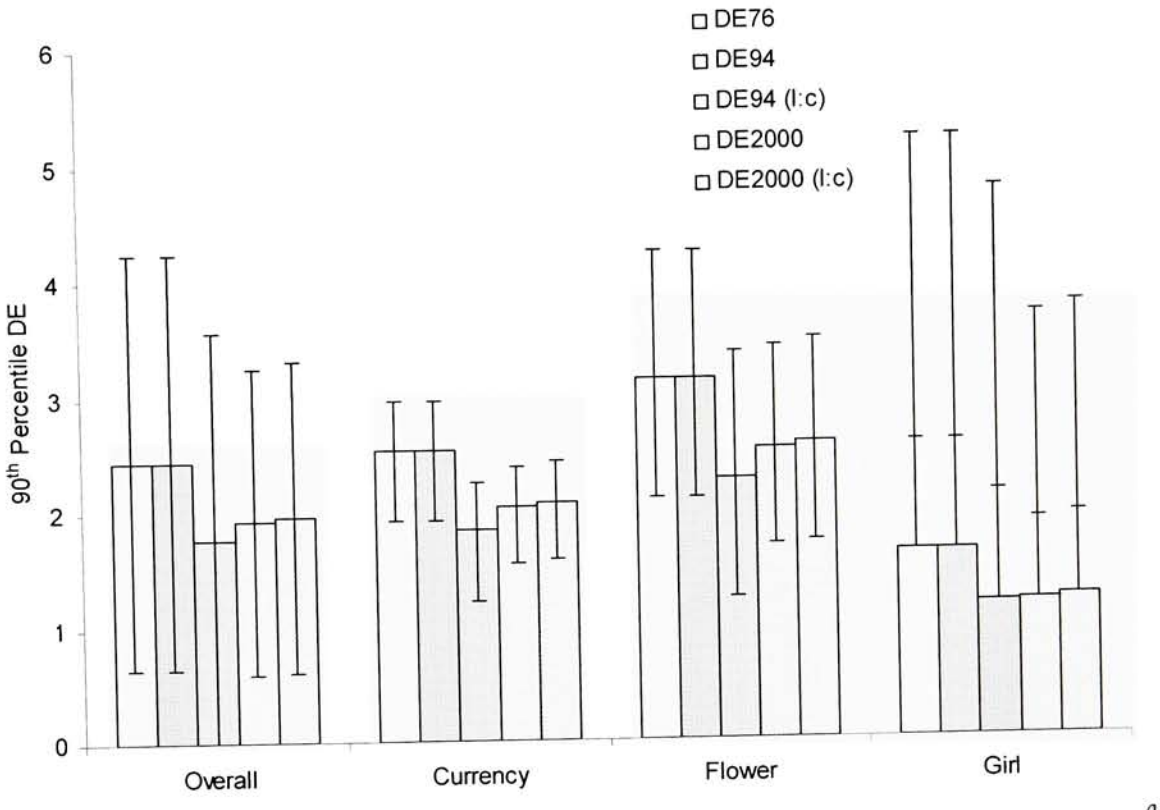
DE76
DE94
DE94 (I:c)
DE2000
DE2000 (I:c)
90th Percentile DE
0
1
2
3
4
5
6
Overall
Currency
Flower
Girl

(b)

*7.4.2. Colorimetric Results for Linear Reduction in C**

Figure 7.4-2 Chroma Thresholds– IBM LCD

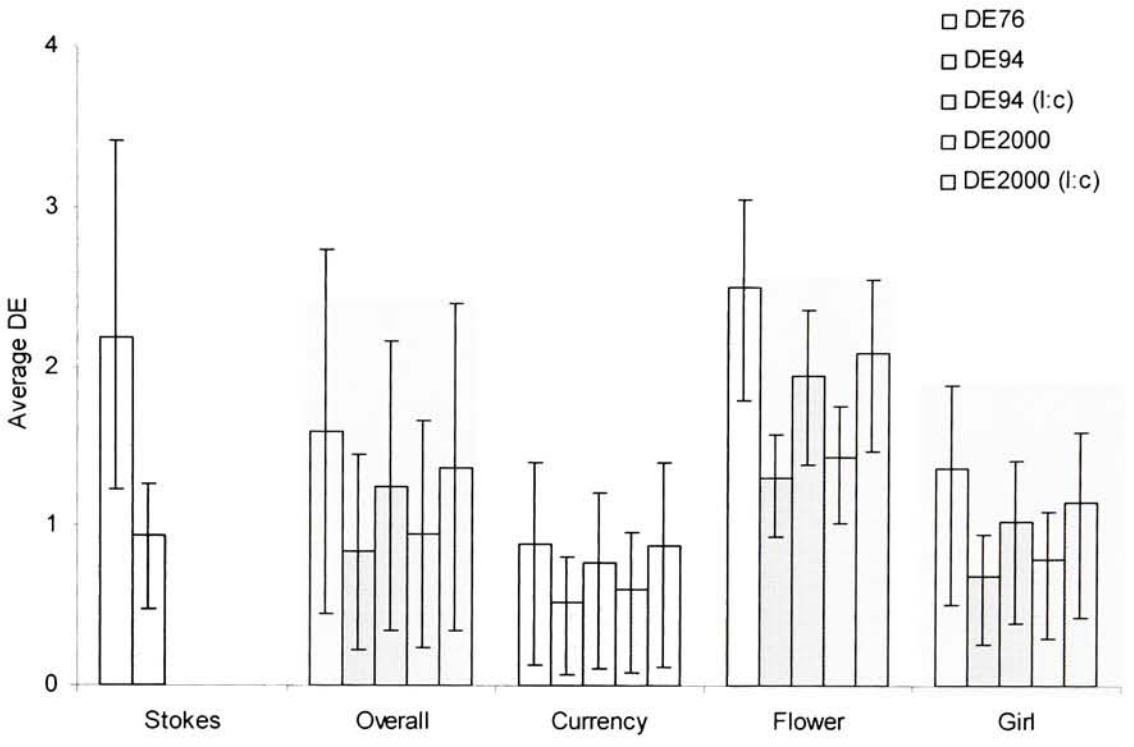

(a)

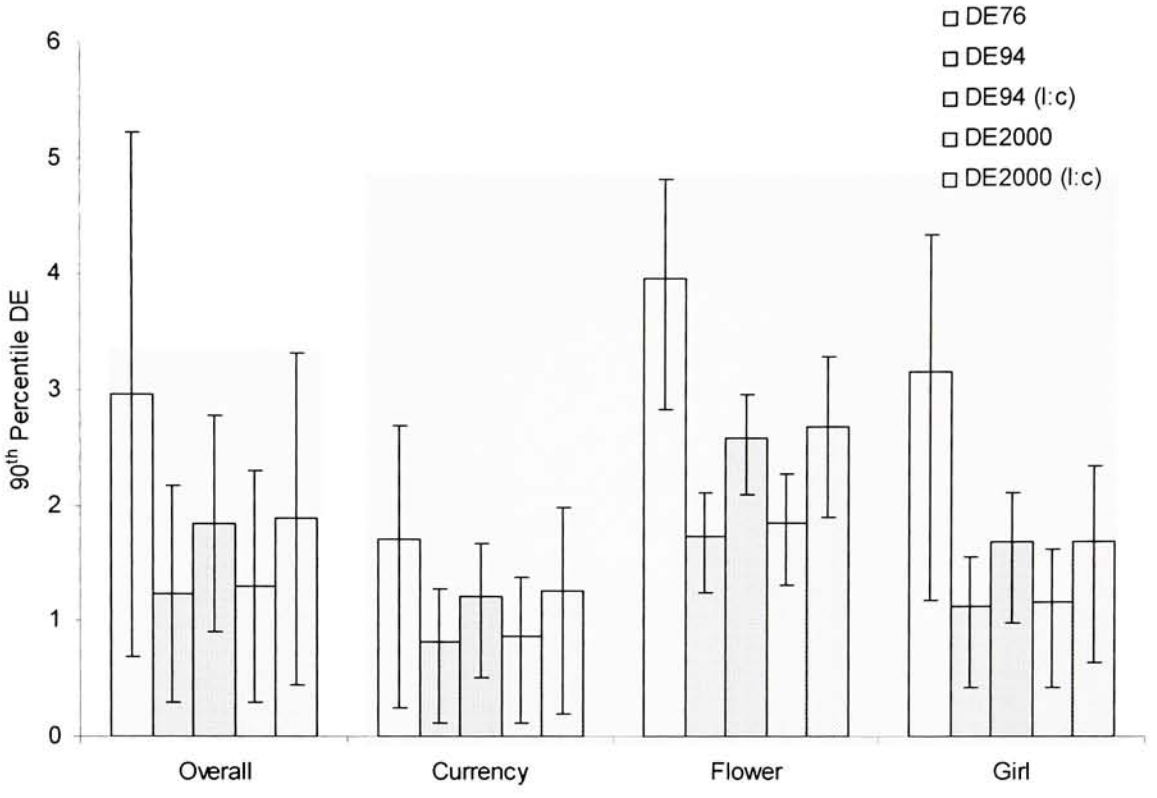
DE76
DE94
DE94 (l:c)
DE2000
DE2000 (l:c)
90th Percentile DE
0
1
2
3
4
5
6
Overall
Currency
Flower
Girl

(b)

7.4.3. Colorimetric Results for Additive Rotations in h_{ab}

Figure 7.4-3 Hue Thresholds– IBM LCD

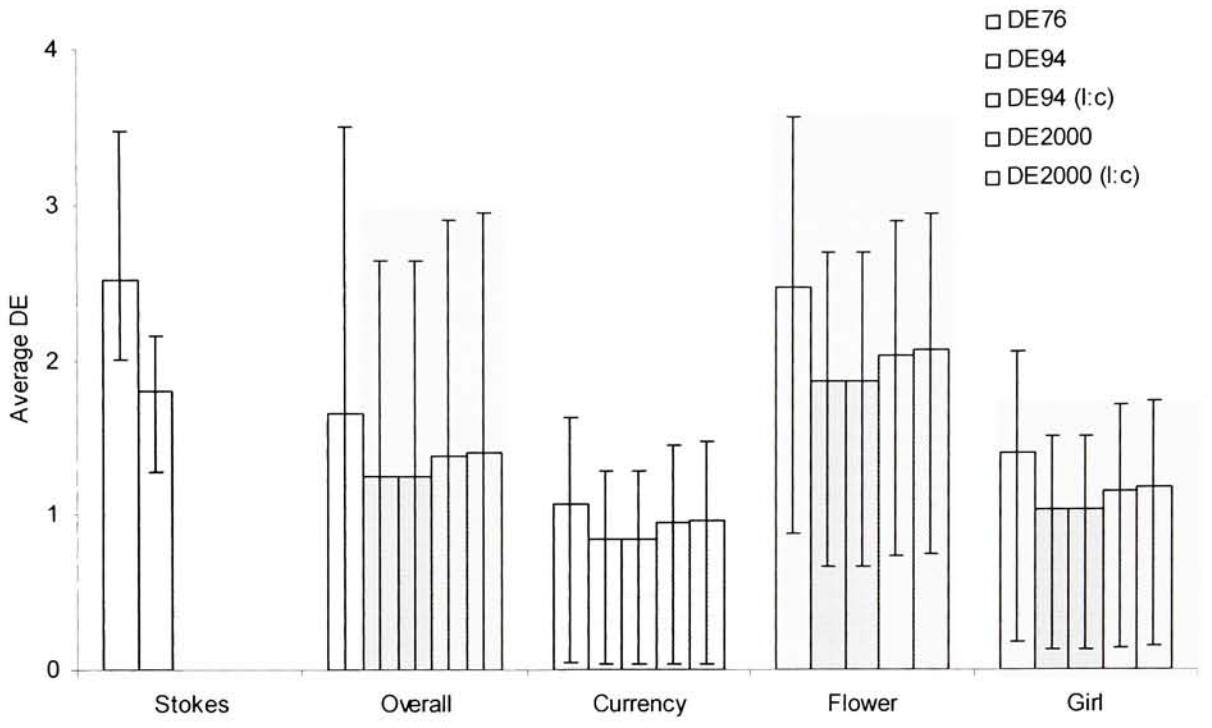

(a)

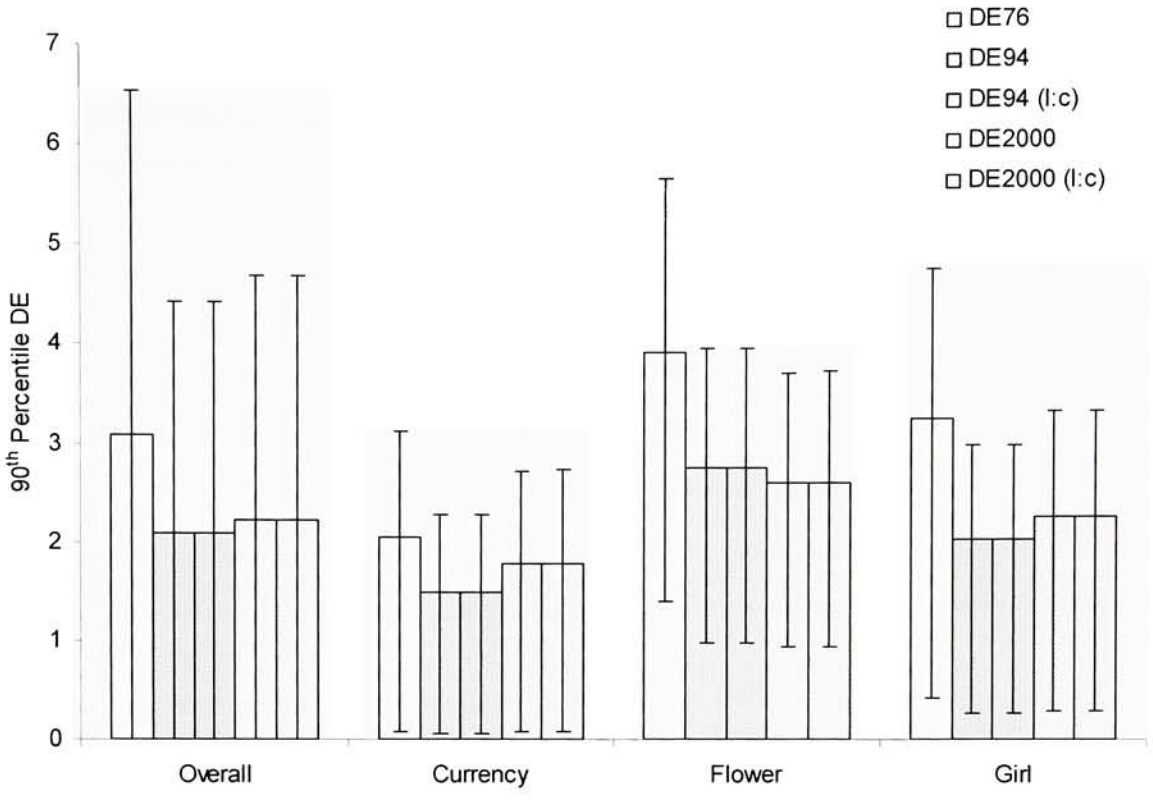

(b)

7.4.4. Overall Results – IBM LCD

The color difference versus percentile plots are seen to have similar progression to the Sony and SGI displays within a scale change. Given these similarities, it is unclear as to the overall value of this data collected at the suggestion of the CIE [2000]. Perhaps with more examples a clearer picture of their relation will become clear.

7.5. Fujix® Pictrography™ 3000 Printer

Pixel-wise colorimetric results for the Fujix Pictrography prints are show below. Results from both the average ΔE and 90th percentile ΔE summery statistics are show for comparison. In cases were the 95% error bars extend beyond the range of the graph, a text description of the value(s) will follow.

*7.5.1. Colorimetric Results for Sigmoidal Compression in L**

Figure 7.5-1 – Lightness Thresholds– Fujix Print

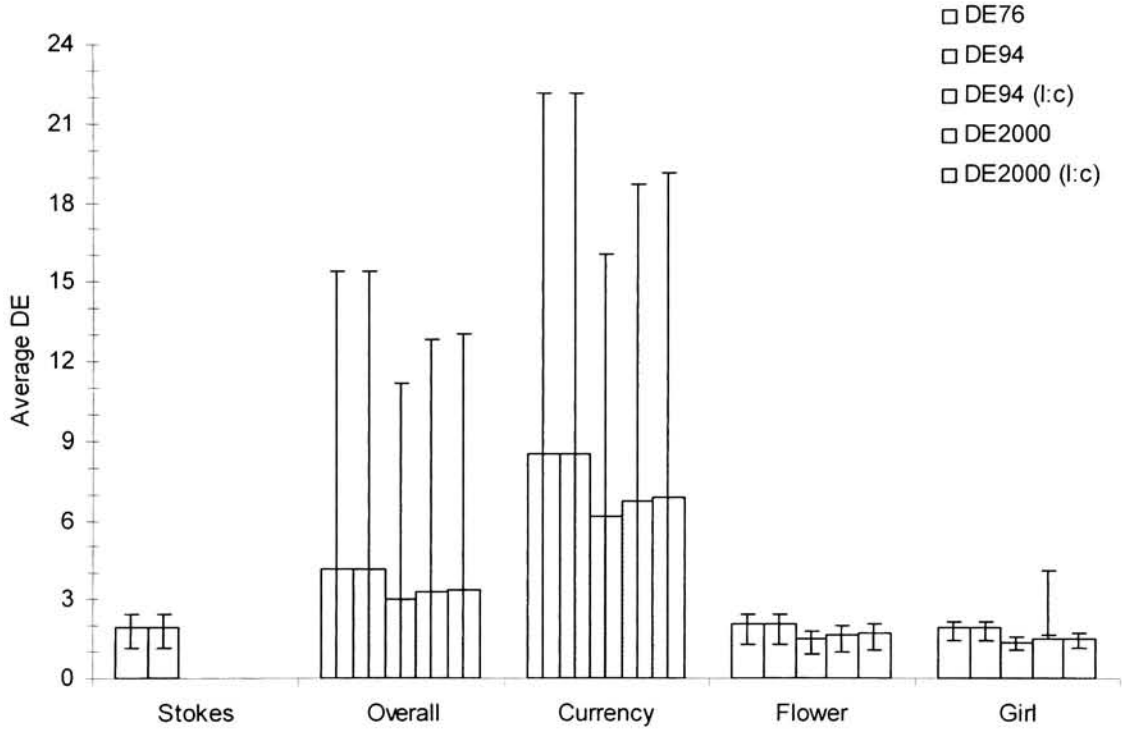

(a)

The fiducial limits on the Girl, ΔE_{2000} bar (and in several other graphs below) do not contain the mean response level. Thus the upper and lower bound markers are seen on top of the column representing the mean. Since only one side of each transform was used†, there was no data for SAS to properly estimate the confidence limits when the mean was very close to either end point of the range tested.

† For lightness and chroma only the compressive side ($k < 1$) was used. For hue, only positive rotations were studied since Stokes found the thresholds to be relatively symmetrical.

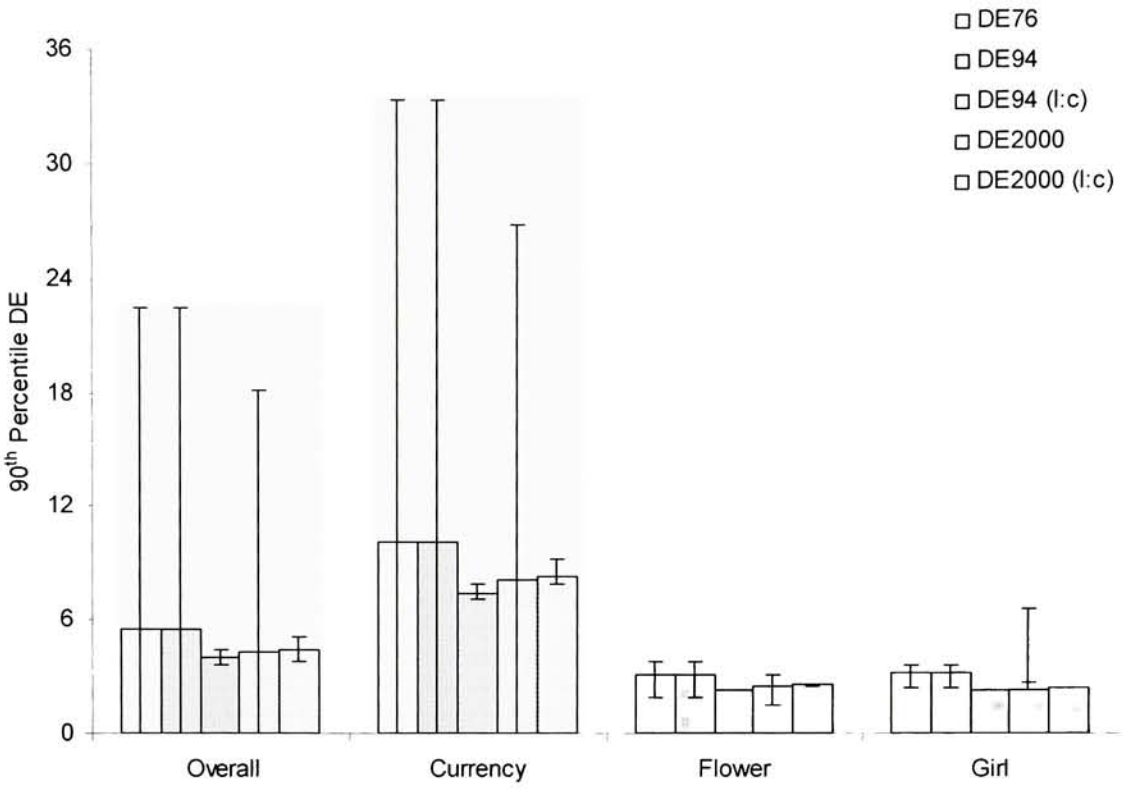
DE76
DE94
DE94 (l:c)
DE2000
DE2000 (l:c)
90th Percentile DE
36
30
24
18
12
6
0
Overall
Currency
Flower
Girl

(b)

Figure 7.5-2 – Chroma Thresholds– Fujix Print

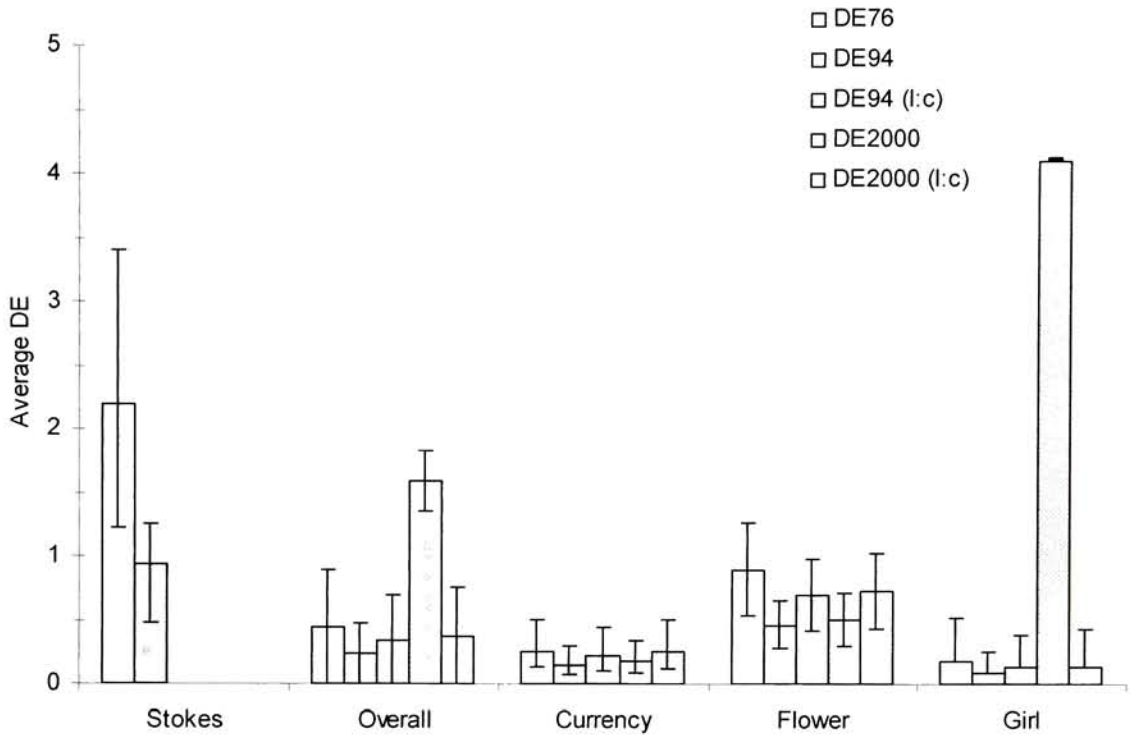

(a)

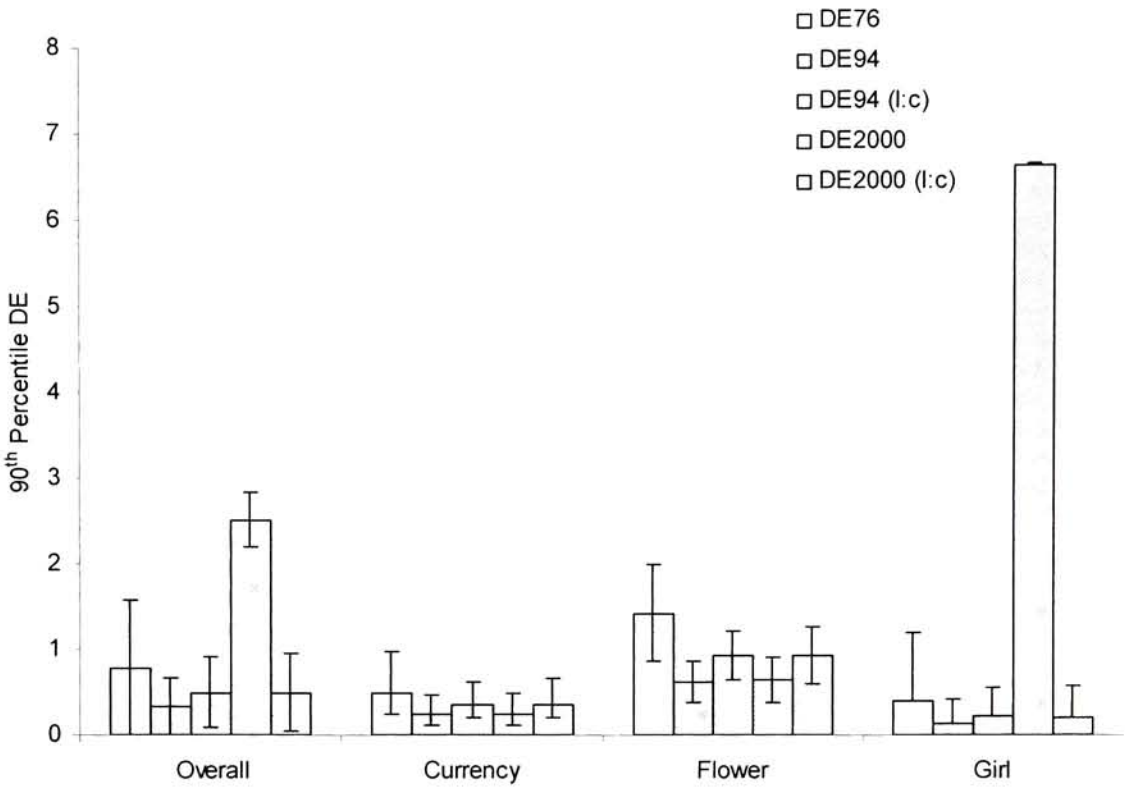

(b)

It is interesting to note that the results from the ΔE_{2000} formula are in direct contrast with those of ΔE^*_{ab} and ΔE_{94} as well as the parametric results presented in chapter 6.4.3.

Figure 7.5-3 – Hue Thresholds– Fujix Print

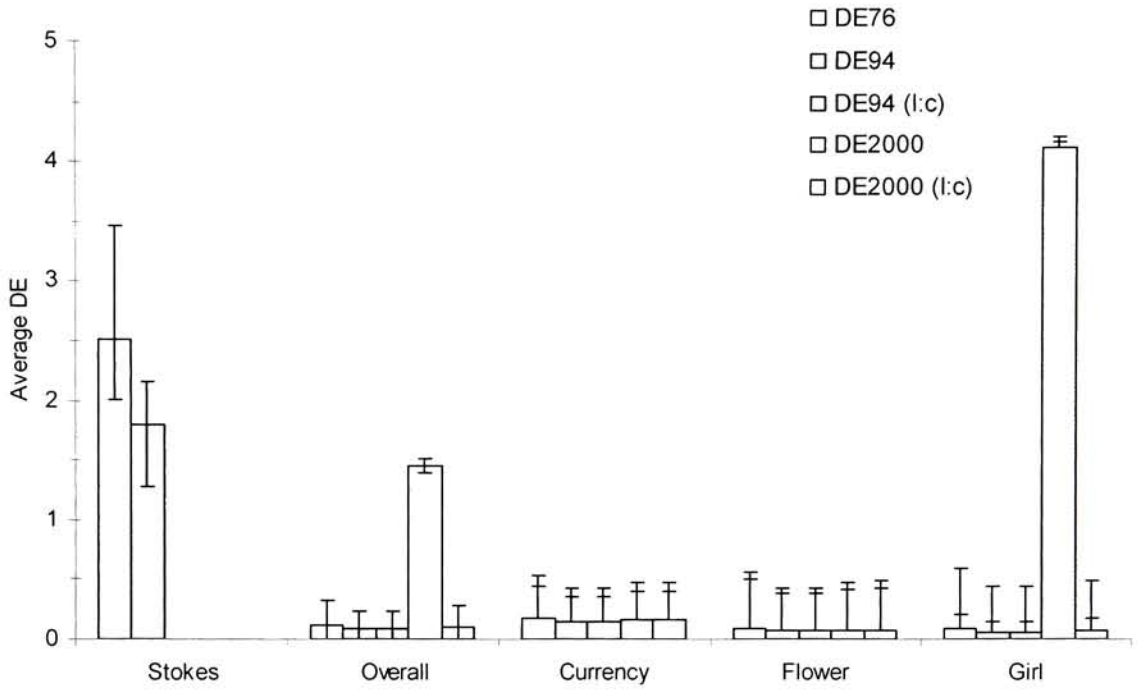

(a)

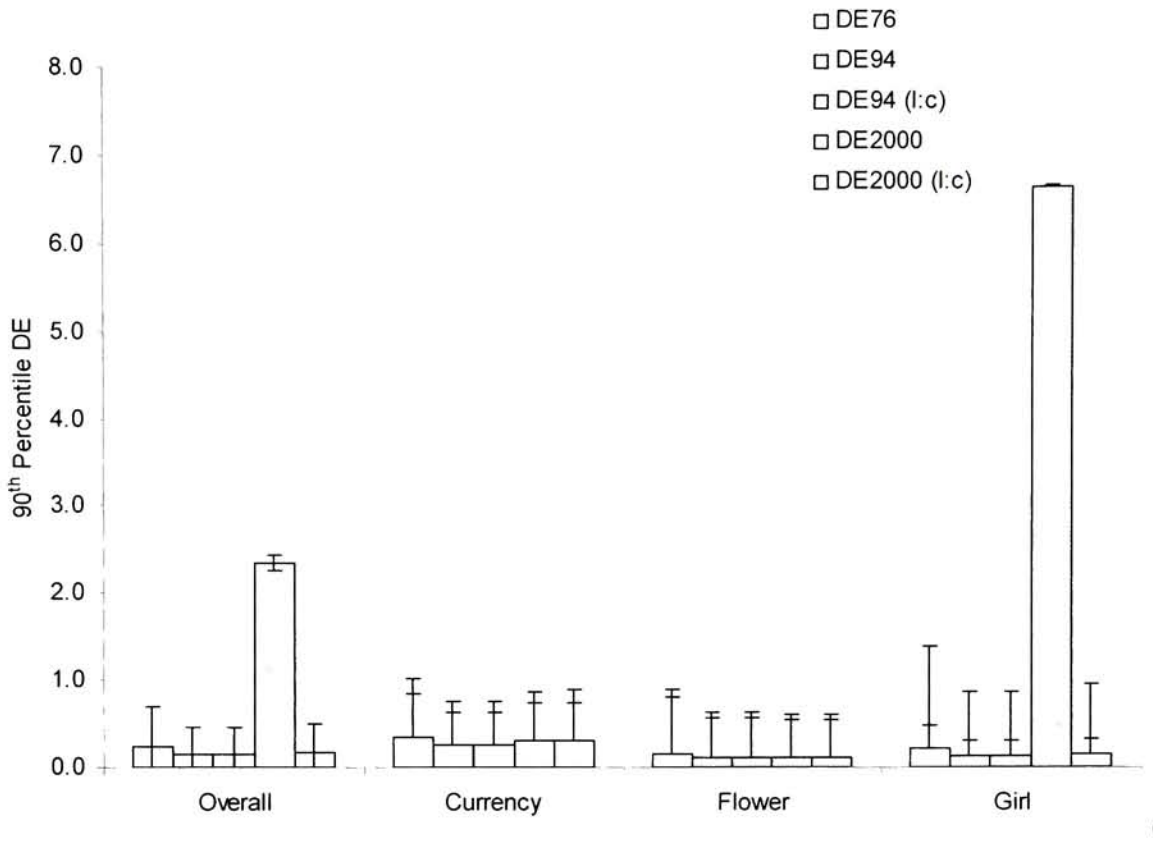

(b)

7.5.4. Overall Remarks – Fujix Prints

The discrepancy in Chroma and Hue results for the Girl image on this display are quite surprising. Given the difficulty of the observer task however, the results are of questionable reliability.

7.6. Summary Comparison of ΔE Thresholds

The graphs and tables in the following three sub sections present the overall results for each display in each dimension in terms of ΔE^*_{ab}, ΔE_{94} and ΔE_{2000} for both the average and 90th percentile differences. The overall results of Stokes [1991] are included for reference for the average difference results. Note that Stokes used the MCSL color difference formula which was the direct predecessor of the ΔE_{94} formula.

The data tables are interpreted as was shown in chapter 6.5. The boldface numbers represent the threshold for the display in that row for the equation in that column. The plain type numbers to the right of the threshold are the upper and lower 95% fiducials. For example, the estimated Average ΔE_{2000} for the IBM LCD in Table 7.6-1 (a) is 1.37 with fiducials of [1.14, 1.48]. An asterisk indicates a local of fit at α=0.05.

*7.6.1. Overall Colorimetric Results for Sigmoidal Compression in L**

Table 7.6-1 – Lightness Compression

Average ΔE	ΔE^*_{ab}		ΔE_{94}		ΔE_{2000}	
Stokes CRT	**1.94**	2.44 1.14	**1.94**	2.44 1.14	N/A	
Sony CRT	**1.96**	2.92 1.00	**1.96**	2.92 1.00	**1.53**	2.29 0.78
SGI LCD	**1.99**	2.99 0.98	**1.99**	2.99 0.98	**1.55**	2.34 0.76
IBM LCD	**1.73**	2.88 0.57	**1.73**	2.88 0.57	**1.36**	2.26 0.46
Fujix Print	**4.18**	15.44 -7.09	**4.18**	15.44 -7.09	**3.30**	12.89 -6.30

(a)

90th Percentile	ΔE^*_{ab}		ΔE_{94}		ΔE_{2000}	
Sony CRT	**2.71**	3.89 1.52	**2.71**	3.89 1.52	**2.12**	3.30 0.94
SGI LCD	**2.72**	3.98 1.45	**2.72**	3.98 1.45	**2.13**	3.40 0.87
IBM LCD	**2.45**	4.25 0.64	**2.45**	4.25 0.64	**1.93**	3.73 0.12
Fujix Print	**5.15**	22.43 -11.42	**5.15**	22.43 -11.42	**4.36**	21.28 -12.57

(b)

Figure 7.6-1 – Overall ΔE Thresholds for Lightness Compression

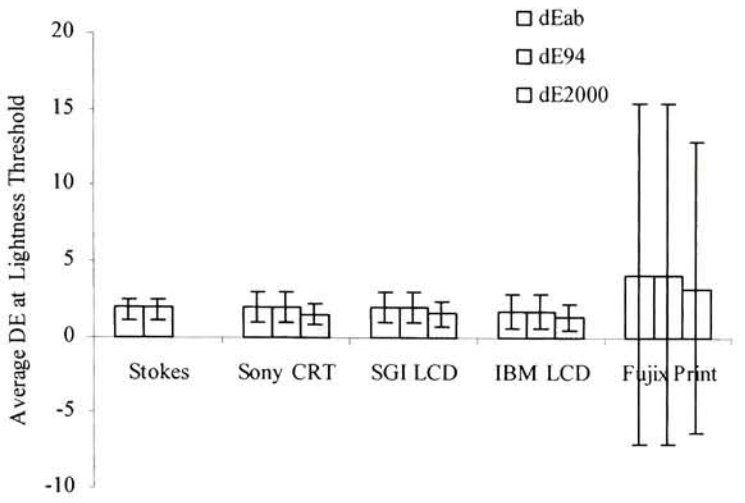

(a)

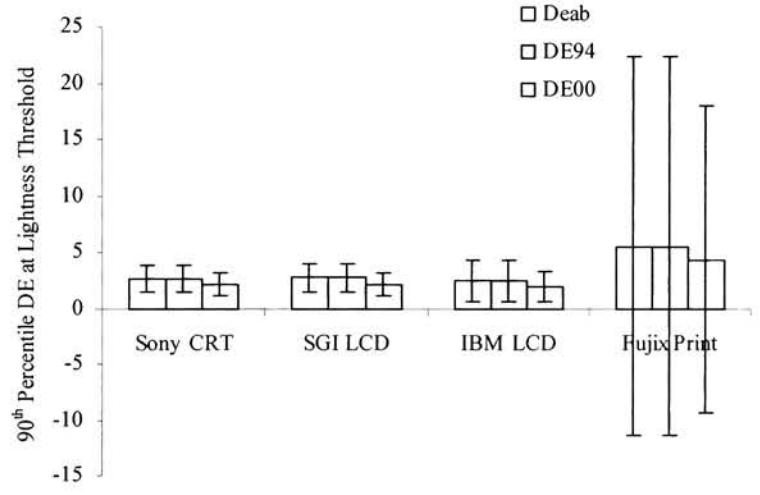

(b)

For lightness compression, the three monitors are in overall close agreement with each other and with the findings of Stokes [1991]. The Fujix prints had a slightly higher threshold, which is due in part to the lower contrast ratio of the prints versus the self-luminous displays. The ΔE^*_{ab} and ΔE_{94} thresholds are identical since $k_L=1.0$, and the images varied only in L^*.

Table 7.6-2 –Chroma Reduction

Average ΔE	ΔE^*_{ab}		ΔE_{94}		ΔE_{2000}	
Stokes CRT	**2.19**	3.41 1.23	**0.94**	1.26 0.48	N/A	
Sony CRT	**1.59**	2.41 0.76	**0.85**	1.28 0.42	**0.97**	1.47 0.47
SGI LCD	**1.48**	2.25 0.70	**0.78**	1.20 0.37	**0.88**	1.37 0.40
IBM LCD	**1.60**	2.74 0.45	**0.84**	1.45 0.23	**0.95**	1.67 0.24
Fujix Print	**0.44**	0.89 -0.01	**0.23**	0.47 0.00	**1.60**	1.84 1.35

(a)

90th Percentile	ΔE^*_{ab}		ΔE_{94}		ΔE_{2000}	
Sony CRT	**2.92**	4.62 1.22	**1.25**	2.95 -0.45	**1.33**	3.03 -0.38
SGI LCD	**2.69**	4.19 1.18	**1.14**	2.65 -0.37	**1.20**	2.71 -0.31
IBM LCD	**2.96**	5.23 0.70	**1.24**	3.50 -1.03	**1.30**	3.57 -0.97
Fujix Print	**0.77**	1.57 -0.02	**0.33**	1.13 -0.46	**2.52**	3.32 1.72

(b)

Figure 7.6-2 – Overall ΔE's Thresholds for Liner Chroma Reduction

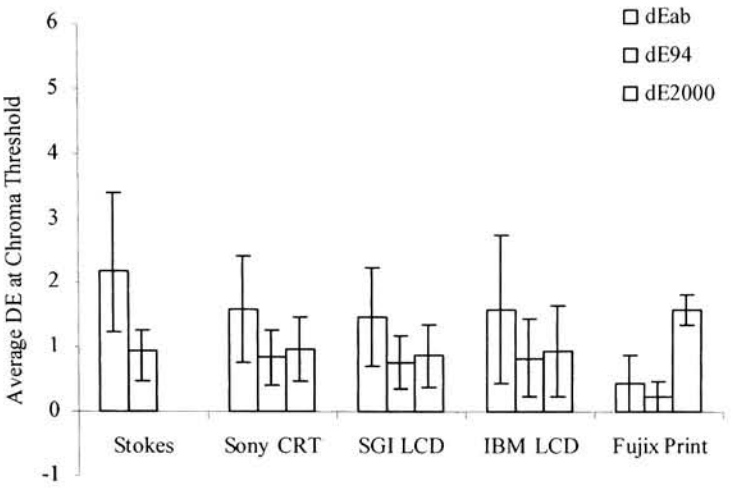

(a)

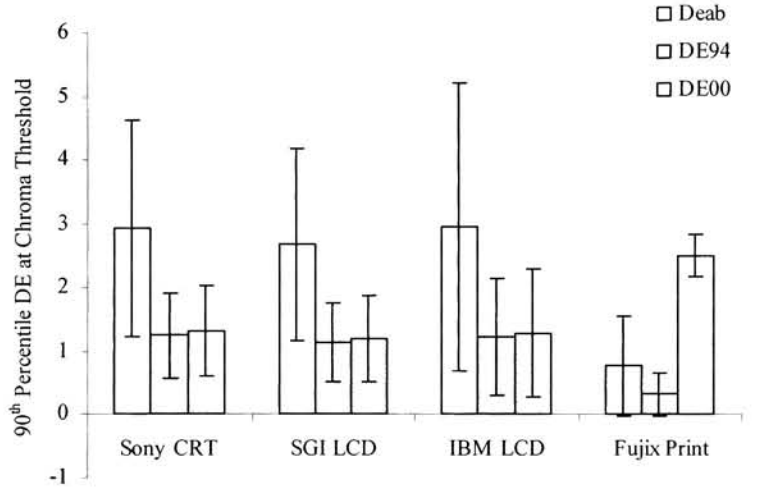

(b)

The chroma thresholds for the three monitors are in overall agreement with one another. The choice of color difference formula has a larger impact in chroma than in lightness. The Fujix prints had a very tight tolerance to changes in chroma, which is due in part to the high luminance levels at which the prints were viewed versus the other displays.

7.6.3. Overall Colorimetric Results for Additive Rotations in h_{ab}

Table 7.6-3– Hue Rotation

Average ΔE	ΔE^*_{ab}		ΔE_{94}		ΔE_{2000}	
Stokes CRT	**2.52**	3.47 2.01	**1.80**	2.16 1.28	N/A	
Sony CRT	**1.72**	2.65 0.80	**1.31**	2.01 0.61	**1.46**	2.22 0.69
SGI LCD	**1.17**	2.17 0.18	**0.89**	1.64 0.14	**0.99**	1.81 0.17
IBM LCD	**1.66**	3.51 -0.19	**1.25**	2.65 -0.15	**1.39**	2.92 -0.15
Fujix Print	**0.12**	0.33 -0.08	**0.09**	0.24 -0.06	**1.46**	1.51 1.41

(a)

90th Percentile	ΔE^*_{ab}		ΔE_{94}		ΔE_{2000}	
Sony CRT	**3.24**	4.99 1.50	**2.22**	3.96 0.48	**2.39**	4.13 0.64
SGI LCD	**2.12**	3.95 0.29	**1.47**	3.30 -0.36	**1.55**	3.39 -0.28
IBM LCD	**3.08**	6.53 -0.37	**2.10**	5.55 -1.35	**2.22**	5.67 -1.23
Fujix Print	**0.23**	0.70 -0.23	**0.16**	0.63 -0.30	**2.36**	2.82 1.89

(b)

Figure 7.6-3 – Overall ΔE Thresholds for Additive Hue Rotation

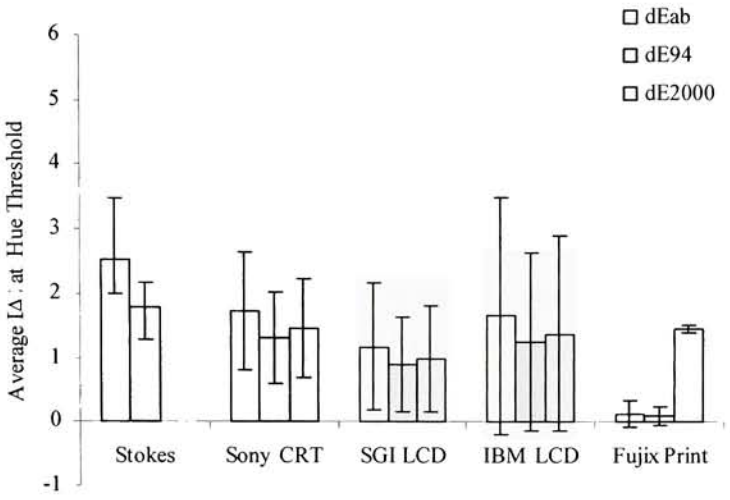

(a)

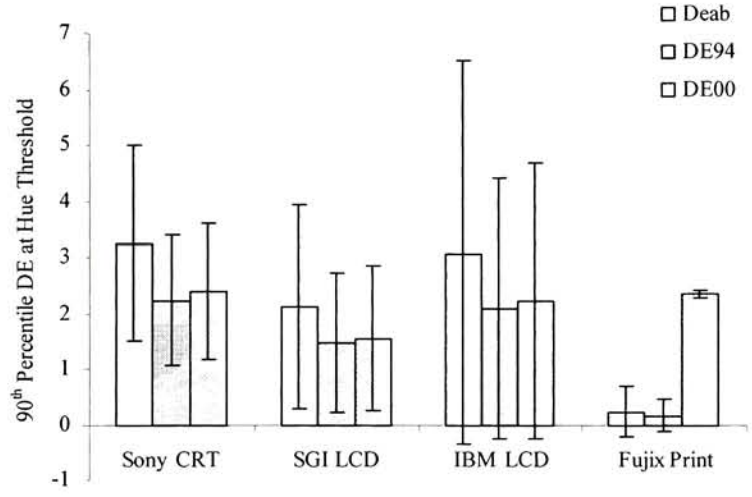

(b)

The Sony CRT used in this experiment had slightly lower threshold than a similar model used by Stokes [1991] indicating that the newer model has been improved, perhaps in luminance and contrast.. The lack of fit for the SGI, IBM and Fujix displays makes for wide error bars and difficult interpretation of their results. The results from the Fujix prints again could be attributed in part to the high luminance levels in which they were viewed.

For the Fujix prints the error bars do not contain the mean value. This is an artifact of the unconstrained probit model used and the circular nature of hue rotations.

7.6.4. Optimization Parameters

As discussed in chapter 5.3, one of the key features of both the ΔE_{94} and the proposed ΔE_{2000} formula apart from their overall better default performance, is there ability to adapt to non-standard conditions using parametric correction factors k_L, k_C and k_H. Under the reference conditions described in CIE 116-1995 [CIE 1995] these terms are set to 1.0 and do not affect the total color-difference. However, when experimental conditions differ their values can be adjusted to account for the changes. In practice, the k_H value is typically set to 1.0 while the k_L and k_C values are adjusted to fit experimentally determined perceptual differences, ΔV. In some industries the k values are set by common agreement. For example, within the textile industry it is common practice to set factors $k_L = 2.0$ though the experimental conditions leading to this correction are not yet well understood [CIE 1995].

For purposes of this experiment, the k-values were set by dividing the average lightness and chroma differences by the hue differences. This set k_H to 1.0 and set the total difference for each dimension to be equal to the difference in the hue dimension. This procedure was designed to equalize the average ΔE's for the three conditions. Similar results would be obtained using the 90th percentile difference as well.

Examining these k values is instructive in that it allows one to compare the relative weighting of the various terms to the total difference. The tables below tabulate these values for both the ΔE_{94} and ΔE_{2000} formulas.

Table 7.6-4 ΔE_{94} l:c Optimization Parameters

		k.=1	Optimized k's	l:c ratio
	L	1.96	1.49	
Sony CRT	C	0.85	0.65	2.3
	h	1.31	1.00	
	L	1.99	2.22	
SGI LCD	C	0.78	0.88	2.5
	h	0.89	1.00	
	L	1.73	1.38	
IBM LCD	C	0.84	0.67	2.1
	h	1.25	1.00	
	L	4.18	44.8	
Fujix Print	C	0.23	2.5	17.8
	h	0.09	1.00	

The average l:c ratio, excluding the Fujix Prints, is 2.3 for the ΔE_{94} formula. This indicates that the lightness component was nearly 2.5 times more sensitive than the chroma term. This is consistent with the findings in the textile industry as described above. Data from the Fujix prints are too noise for this procedure to work and was therefore ignored.

The effect of this optimization can be seen by re-examining the graphs in sections 7.2 – 7.5. Comparing the results for the overall image along all three dimensions, the l:c optimized results are much more consistent.

Table 7.6-5 ΔE_{2000} l:c Optimization Parameters

		$k_{\bullet}=1$	Optimized k's	l:c ratio
Sony CRT	L	1.53	1.05	1.6
	C	0.97	0.66	
	h	1.46	1.00	
SGI LCD	L	1.55	1.56	1.8
	C	0.88	0.89	
	h	0.99	1.00	
IBM LCD	L	1.36	0.98	1.4
	C	0.95	0.69	
	h	1.39	1.00	
Fujix Print	L	3.30	2.26	2.1
	C	1.60	1.09	
	h	1.46	1.00	

The average l:c ratio, excluding the Fujix Prints, is 1.6 for the ΔE_{2000} formula. From this result, it would appear that the addition of the systematic terms for lightness have helped balance the formula more. It will be interesting to see if the textile industry will still need a parametric correction factor once this formula is fully introduced. Again, the Fujix data was ignored due to unreliable data.

Due to the interaction term, the results of this method of optimizing the l:c parameters was much less successful than for ΔE_{94}. To be done correctly the values would have to be chosen so as to correlate to some visual difference scale using a method similar to Berns [1996].

7.7. Colorimetric Thresholds Versus Parameters

To further examine the possibility of trends between various display parameters and the resulting tolerances in images, the following sets of graphs were created. Each figure shows data for one of the three color difference equations used versus White Point Luminance, Contrast Ration or Resolution. Each figure contains three sub-graphs, one for each of the three transforms used. Data is presented for the 90th percentile summary statistic only. The trends for the average ΔE are similar.

Figure 7.7-1 –ΔE^*_{ab} Thresholds versus White Point Luminance

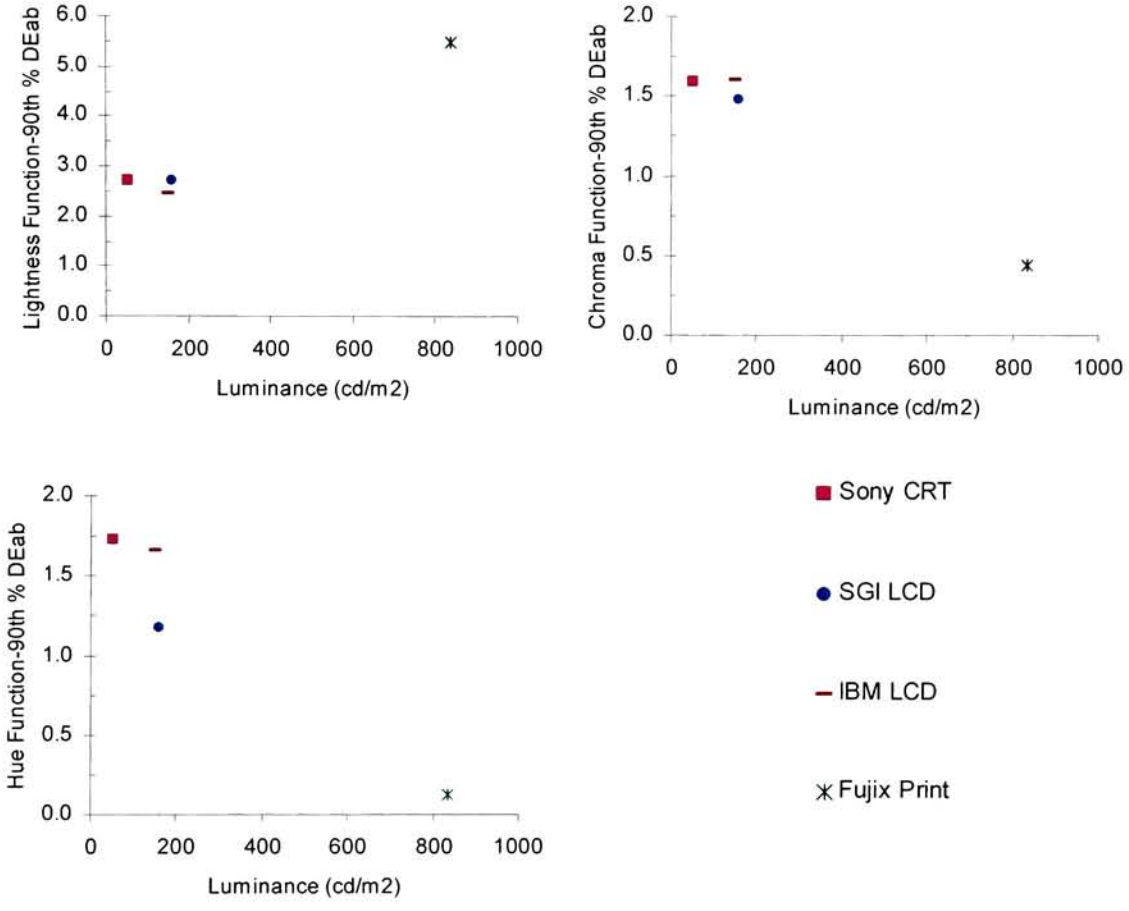

With regard to luminance, the detection thresholds determined using the three monitors were quite similar to one another for the lightness and chroma functions. The observers sensitivity to changes in the Fujix prints was lower (higher ΔE's) than on the monitors for the sigmoidal lightness compression function, and higher than those on the monitors for the linear chroma reduction. For the additive offset in hue, the change detection threshold was seen to decrease as luminance levels increased.

Figure 7.7-2 –ΔE_{94} Thresholds versus White Point Luminance

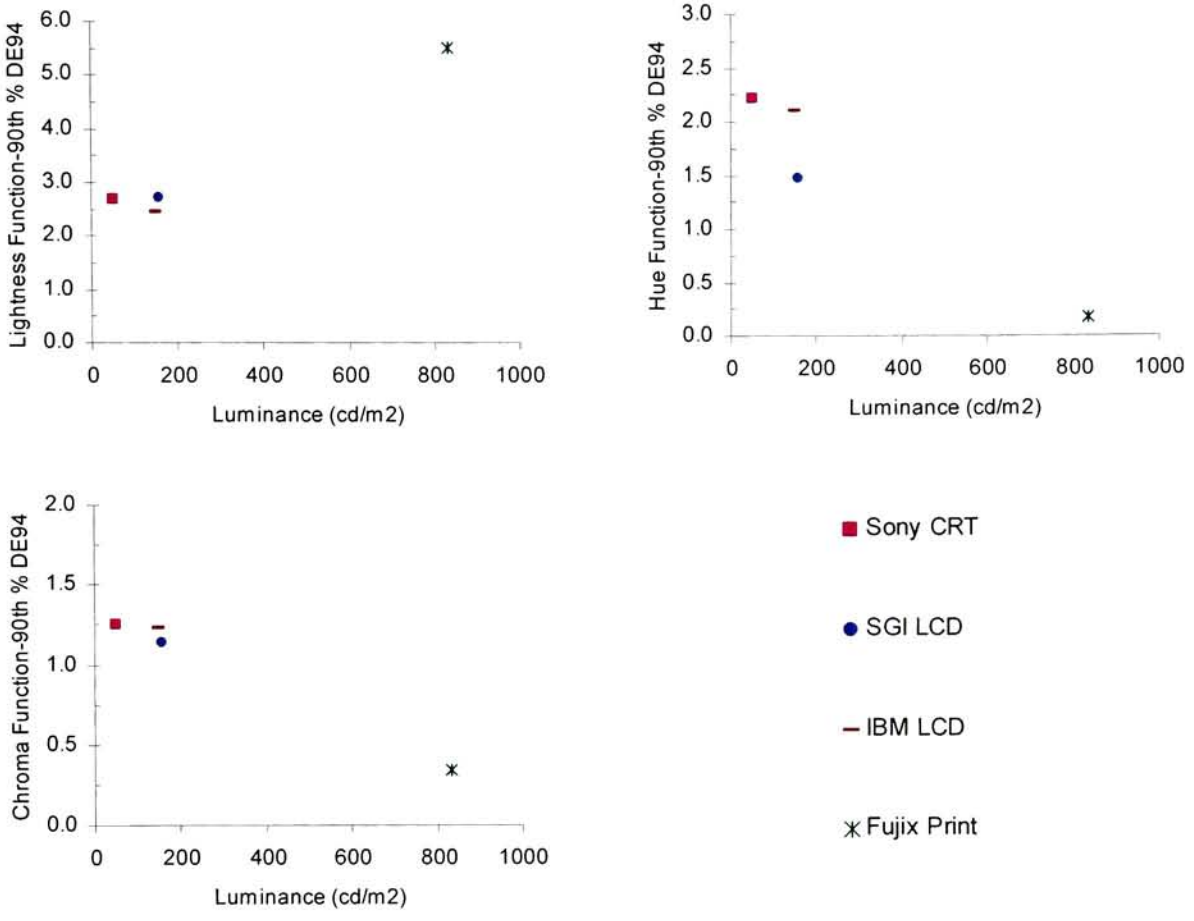

Figure 7.7-3 –ΔE_{2000} Thresholds versus White Point Luminance

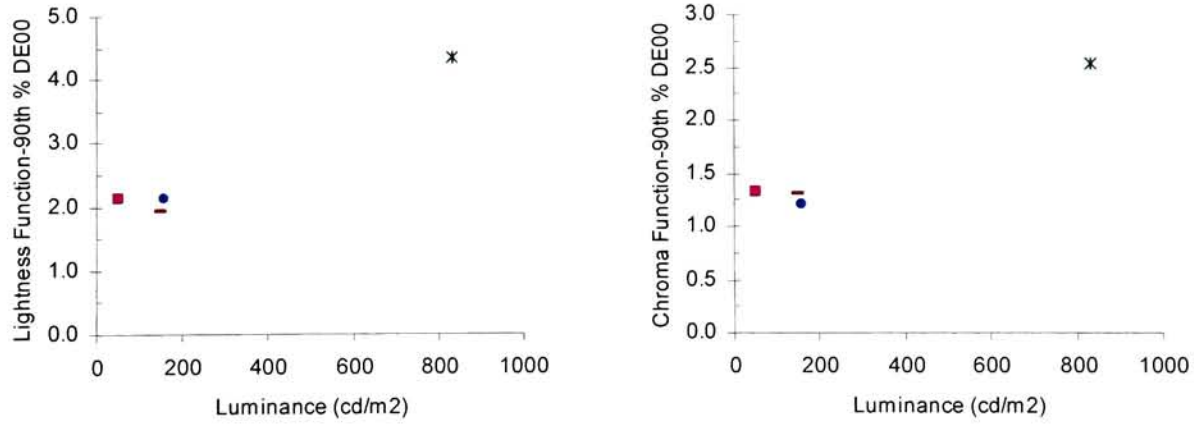

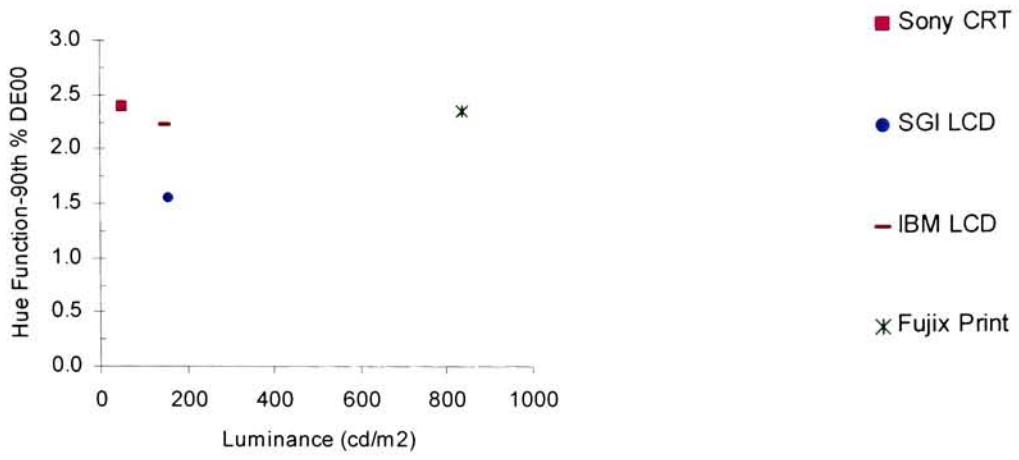

As expected, the trends seen using ΔE^*_{ab} are repeated in the ΔE_{94} and ΔE_{2000} measures. The clearest trend appears to be with the additive hue offset alteration.

Figure 7.7-4 –ΔE^*_{ab} Thresholds versus Contrast Ratio

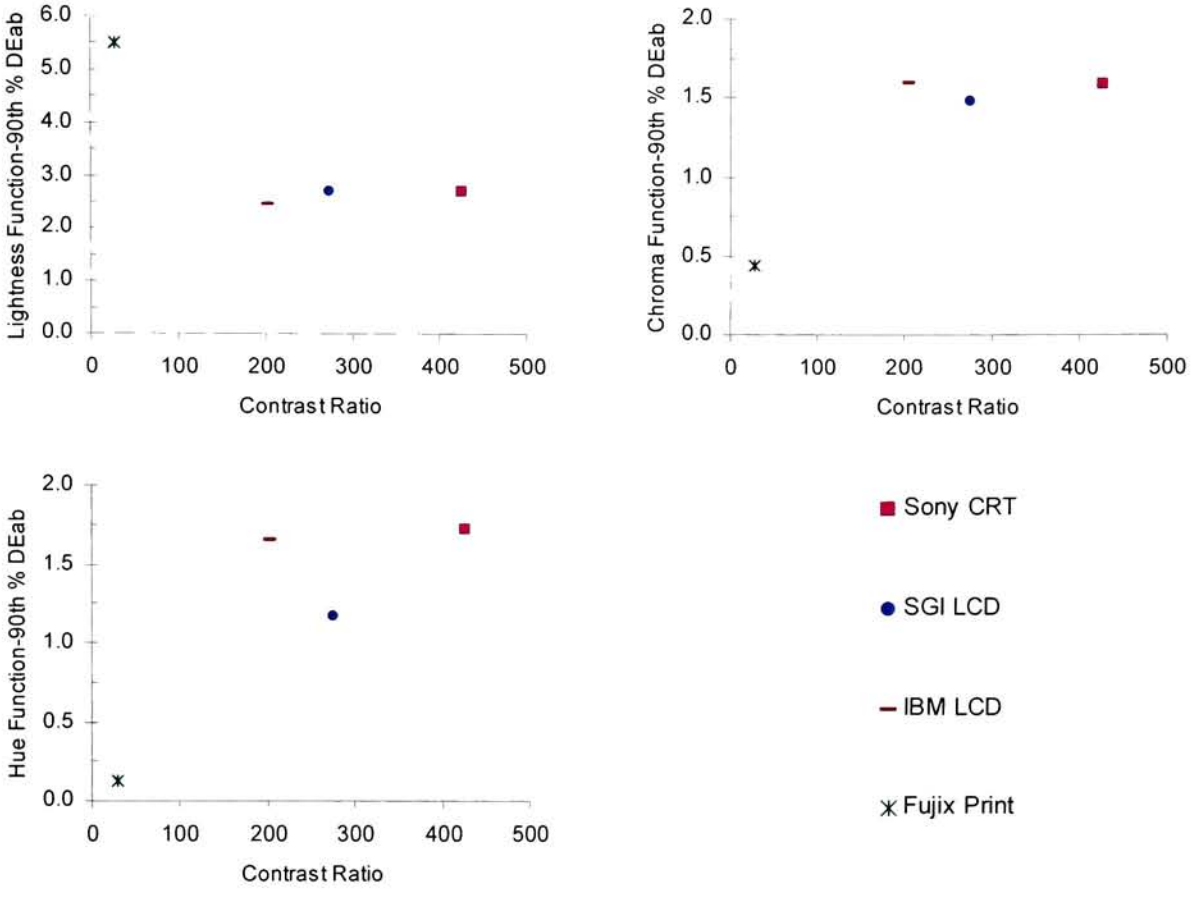

Figure 7.7-5 –ΔE_{94} Thresholds versus Contrast Ratio

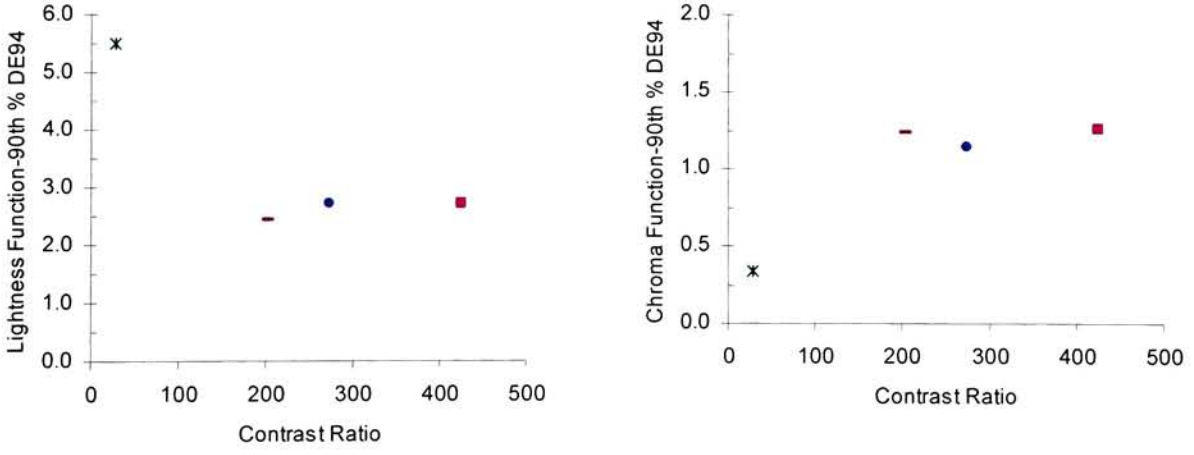

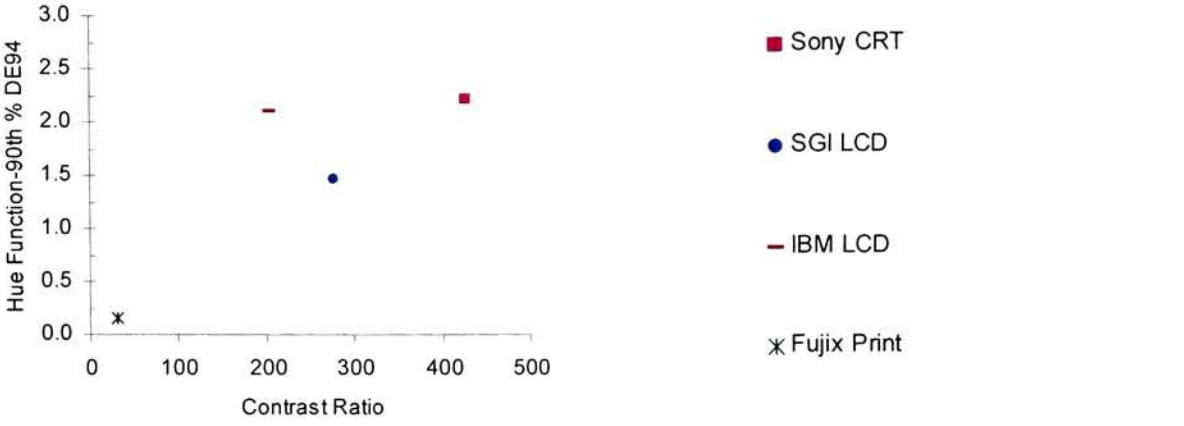

Figure 7.7-6 –ΔE_{2000} Thresholds versus Contrast Ratio

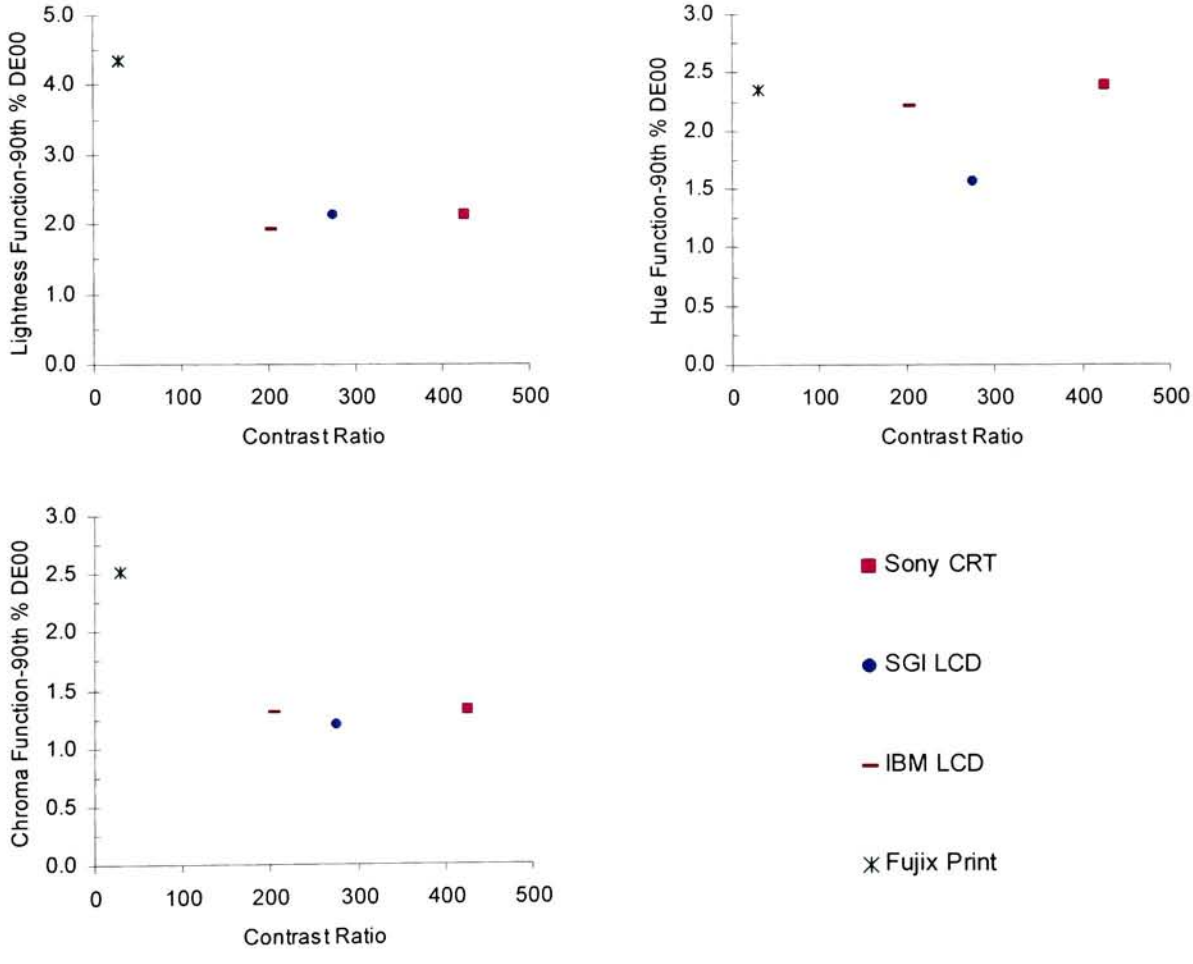

Again, the thresholds determined on the three monitors were all about equal with one another. Thresholds determined using the Fujix print were generally higher than those from the monitors for the lightness function and lower for the chroma and hue functions. These trends were similar for all three ΔE functions.

Figure 7.7-7 – ΔE^*_{ab} Thresholds versus Addressable Resolution

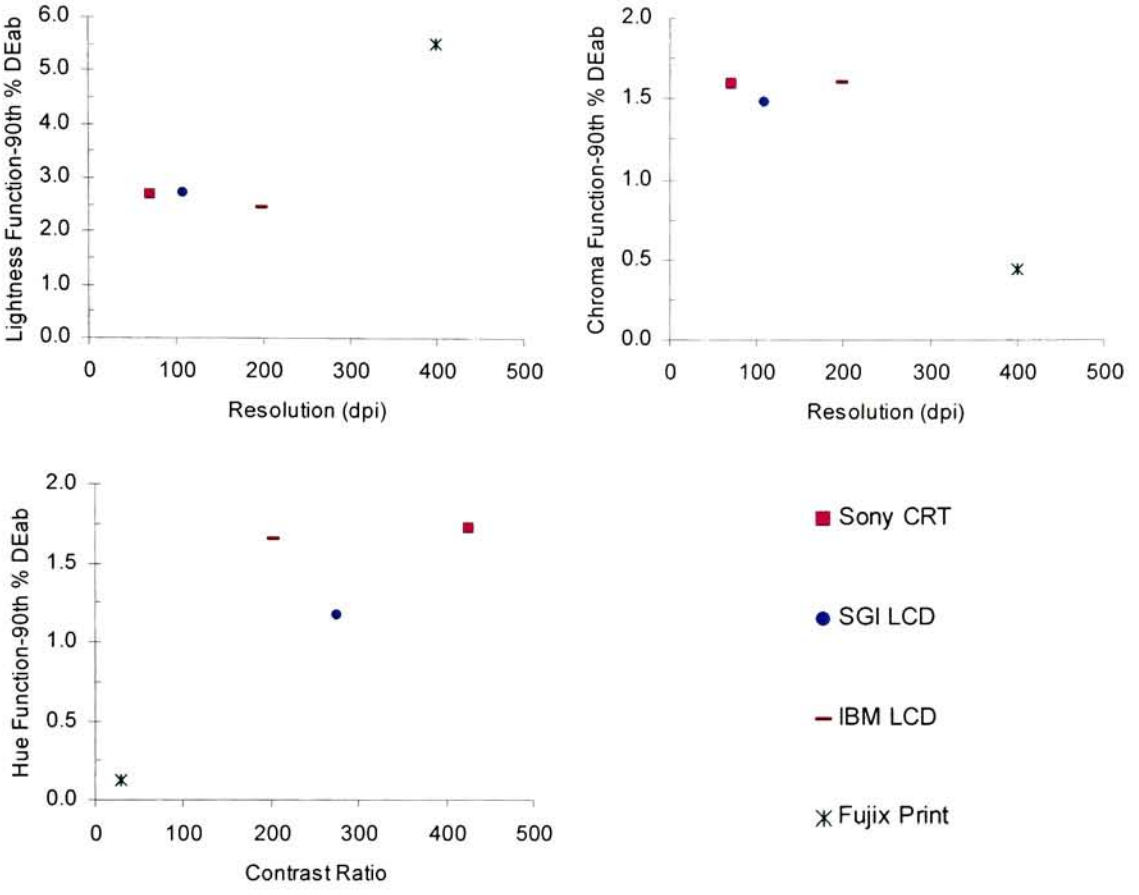

Figure 7.7-8 – ΔE_{94} Thresholds versus Addressable Resolution

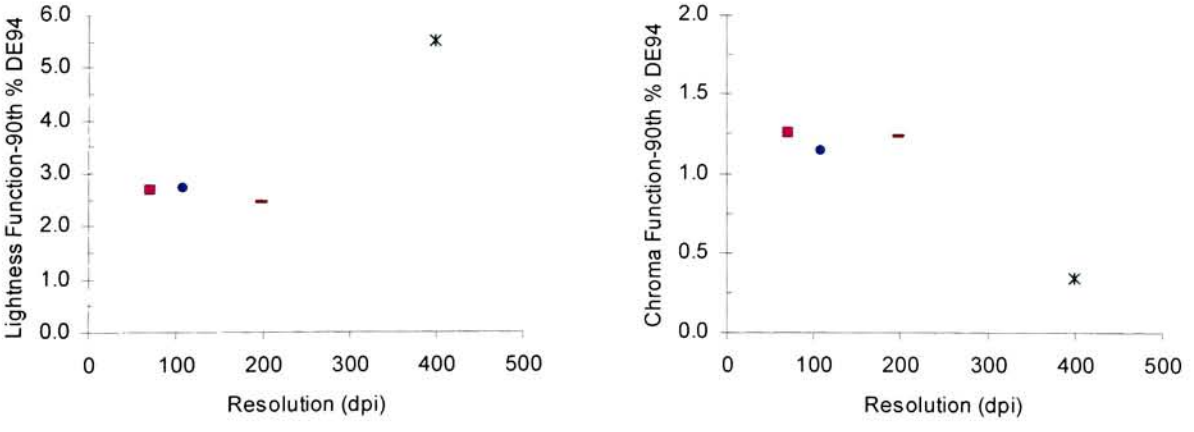

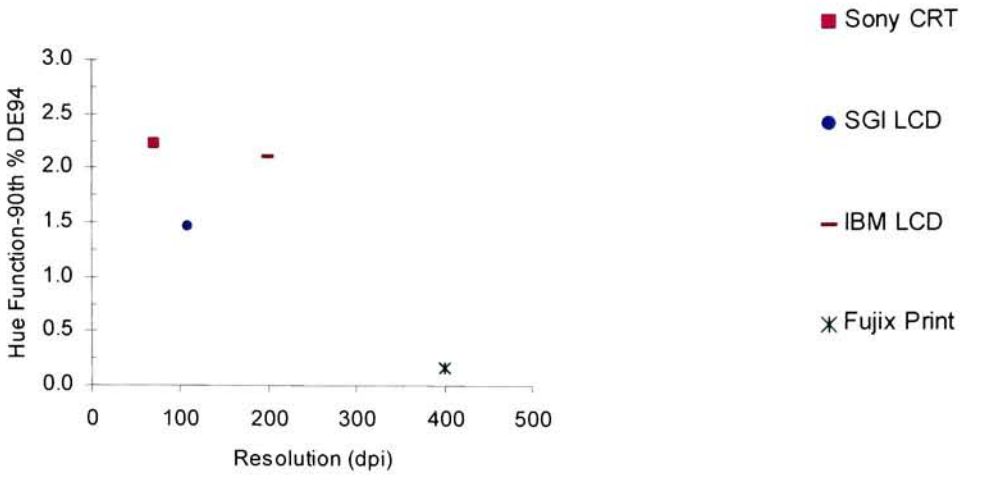

Figure 7.7-9 – ΔE_{2000} Thresholds versus Addressable Resolution

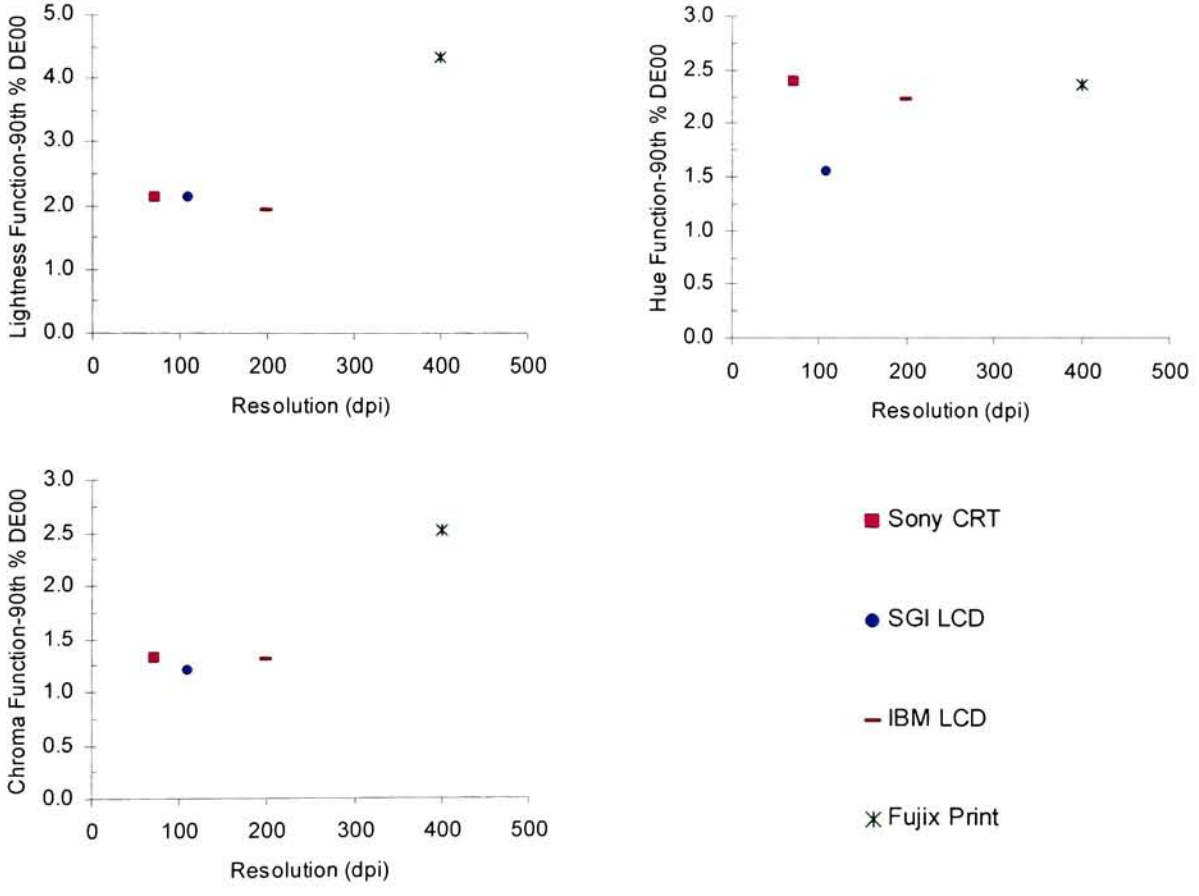

As with the previous two abscissas there were no clear trends other than the threshold determined using the Fujix prints are generally different than for the three monitors.

8 Colorimetric Threshold Results – SCIELAB Pre-Filtering

Whereas the pixel-by-pixel differencing performed in Chapter 7 has intuitive appeal, it dose not attempt to account for the potentially complex interactions between neighboring pixels in an image. To address this point, Zhang and Wandell's S-CIELAB filters [Zhang 1996] were applied to the test images prior to computing the pixel-wise average color difference.

8.1. Analysis Process

The amount of filtering applied by S-CIELAB is determined by the spatial parameters of the viewing geometry. Of particular interest is the number of samples (pixels) per degree of visual angle (SPD) for the observer. This is a function of both the spatial addressability of the display and the viewing distance and is computed as shown in Equation 8.1-1. The table below lists the SPD for the four displays used in this experiment.

Equation 8.1-1 Samples Per Degree of Visual Angle Calculation

$$spd = round\left(\frac{DPI}{\tan_{deg}^{-1}\left(1/View\right)}\right)$$

Where

spd = Samples per degree
DPI = Dots per Inch of display device
View = Viewing distance in inches
$\tan^{-1}_{deg}$ = Arctangent expressed in degrees

Table 8.1-1 Spatial Sampling of Displays Used

Display	DPI	Viewing Distance	SPD Visual Angle
Sony GDM-F500 CRT	72	21"	26
SGI 1600SW LCD	110	21"	40
IBM Roentgen LCD	200	21"	73
Fujix Pictrography 3000	400	18"	126

Since the transforms applied to the test images were global color changes, they should have had little to no effect on the spatial properties of the images. As such, S-CIELAB filtering is hypothesized to have little effect on the relative results of the images. To test this concept, the images from the Sony CRT, having the lowest sampling, and the IBM LCD, having high sampling, will be examined. The filtering in S-CIELAB increases in a strictly monotonic fashion with sampling rates. Thus, if no effect is observed for low and high frequencies in this sample set, then S-CIELAB can be assumed to have no effect on the results at intermediate sampling rates. The data from the Fujix prints were not used in this comparison since the data were collected under much different conditions and experimental design which would confound the comparison to the Sony data.

To apply the S-CIELAB to the images, the appropriate filters were computed based on the appropriate SPD figures shown above and then convolved with the threshold images described in chapter 6. The pixel-by-pixel color differences for the three individual images (Girl, Flower and Currency) were then computed as described in chapter 7. Results are presented in terms of ΔE^*_{ab}, ΔE_{94} and ΔE_{2000} using the 90th percentile summary statistic.

8.2. Sony GDM-F500 CRT

In this section, the S-CIELAB filtered results for the Sony CRT are presented. Both the results of the filtering and their correlation to the results with out filtering are presented.

8.2.1. Colorimetric Results with S-CIELAB filtering

The following three graphs compare to Figures 7.2-1 b, 7.2-3 b and 7.2.5 b of chapter 7 except that the S-CIELAB filters have been applied prior to computing the pixel-wise differences. Results are show for only the un-optimized color-difference formulas.

Figure 8.2-1 Lightness Thresholds–SONY CRT

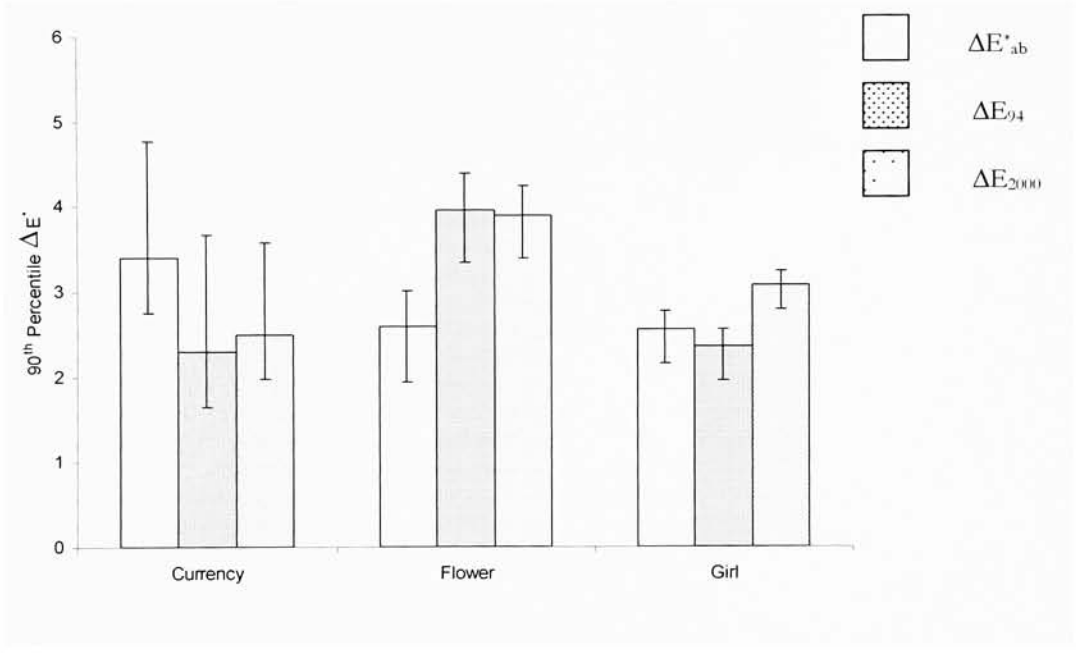

Figure 8.2-2 Chroma Thresholds–SONY CRT

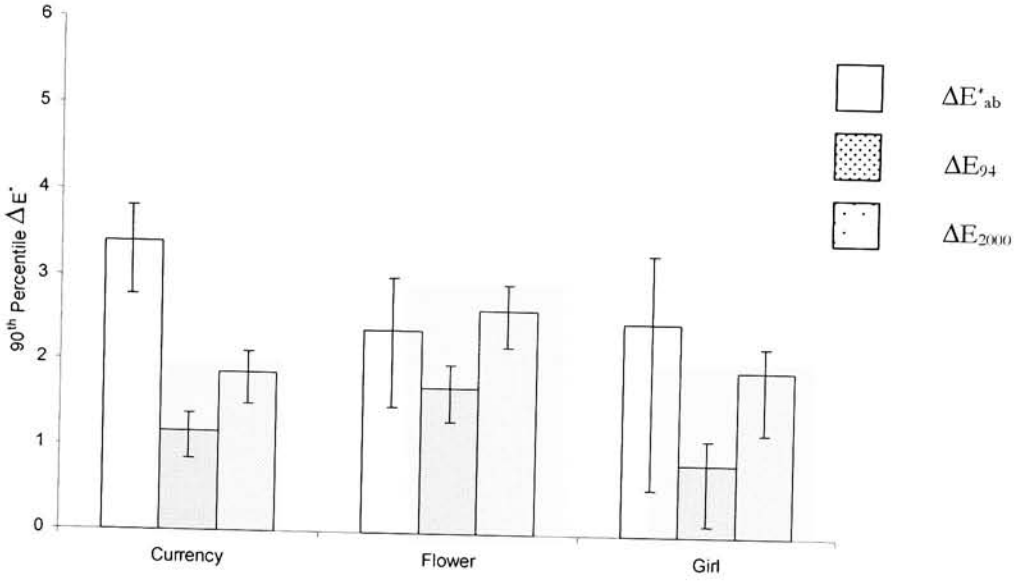

Figure 8.2-3 Hue Thresholds–SONY CRT

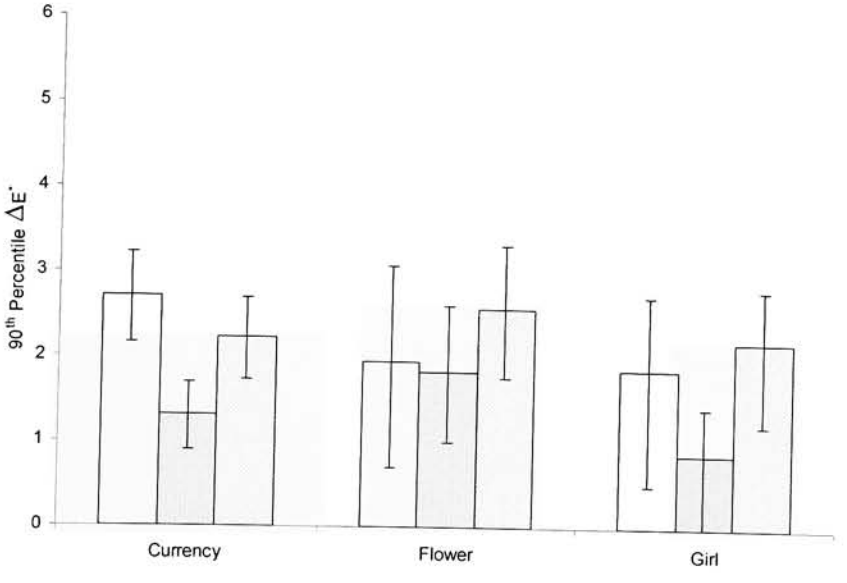

8.2.2. Correlations with un-filtered results

In this section, the correlation between results with and with out S-CIELAB pre-filtering are explored. Correlations are shown for all three color-difference formulas. Each plot contains the values from all three transforms, all three images, as well as the mean, upper and lower estimated thresholds for a total of 27 data points. For completeness, both the average and 90th percentile summery statistics correlations are shown.

Figure 8.2-4 Correlations for ΔE^*_{ab}

Average

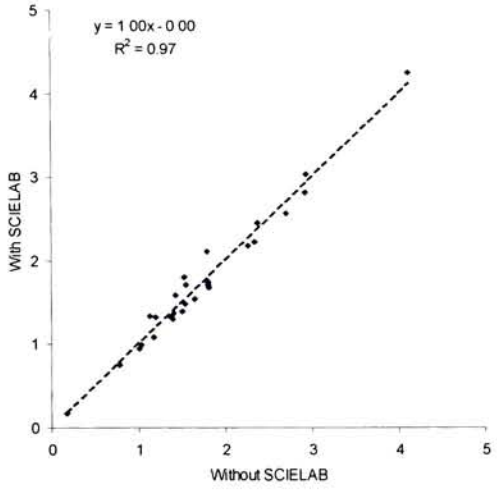

90th Percentile

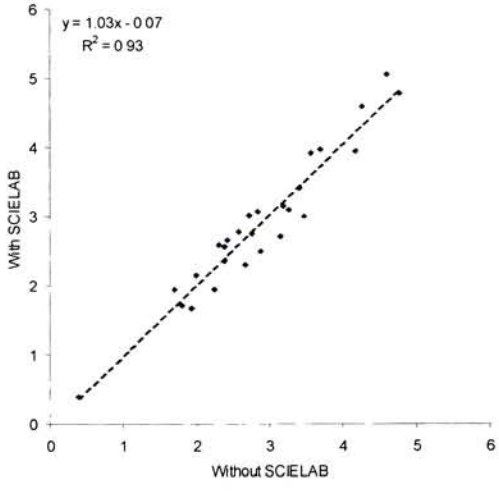

Figure 8.2-5 Correlations for ΔE_{94}

Average

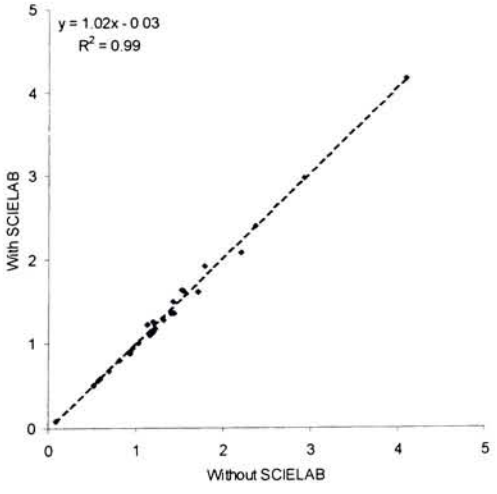

90th Percentile

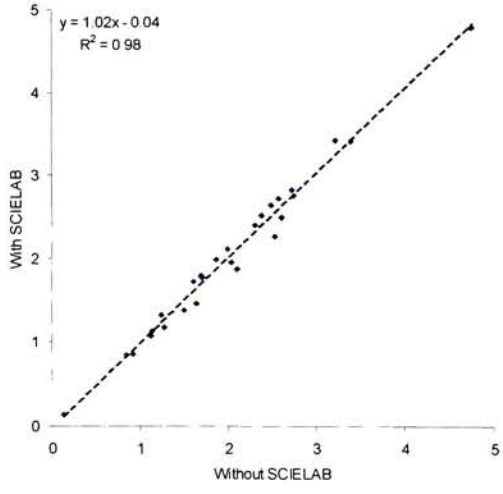

Figure 8.2-6 Correlations for ΔE_{2000}

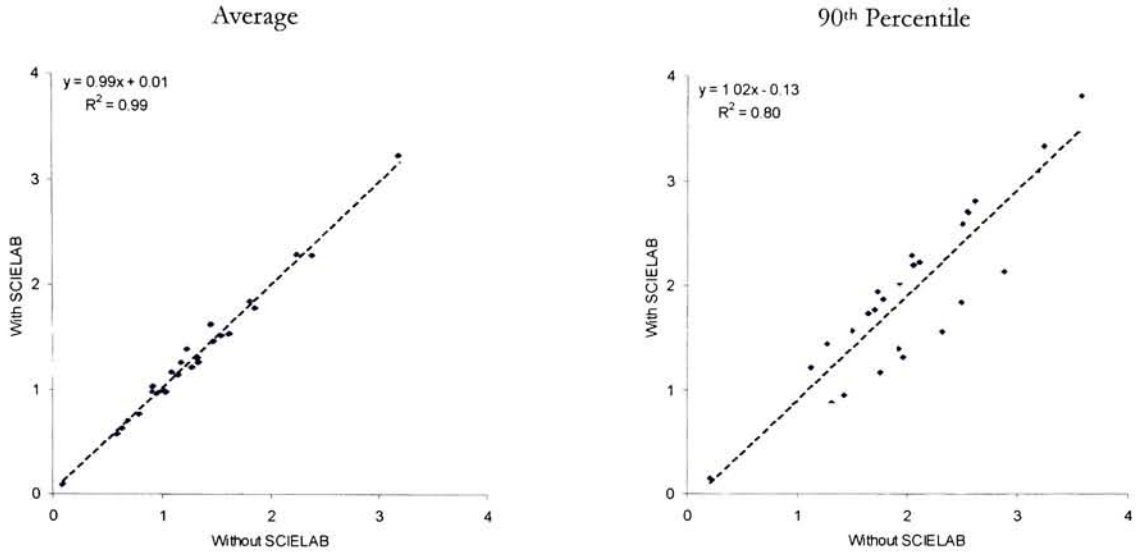

As shown in the above figures, the S-CIELAB filtering had little to no effect of the results. The high R^2 values indicate a strong linear correlation between the two data sets which implies that the relative results between each are preserved. Furthermore, the linear fits are very close to slope 1 which implies that the absolute results have not changed between the two methods either.

8.3. IBM Roentgen LCD prototype

In this section, the S-CIELAB filtered results for the IBM LCD are presented in the same form as the previous section.

8.3.1. Colorimetric Results with S-CIELAB filtering

Figure 8.3-1 Lightness Thresholds–IBM LCD

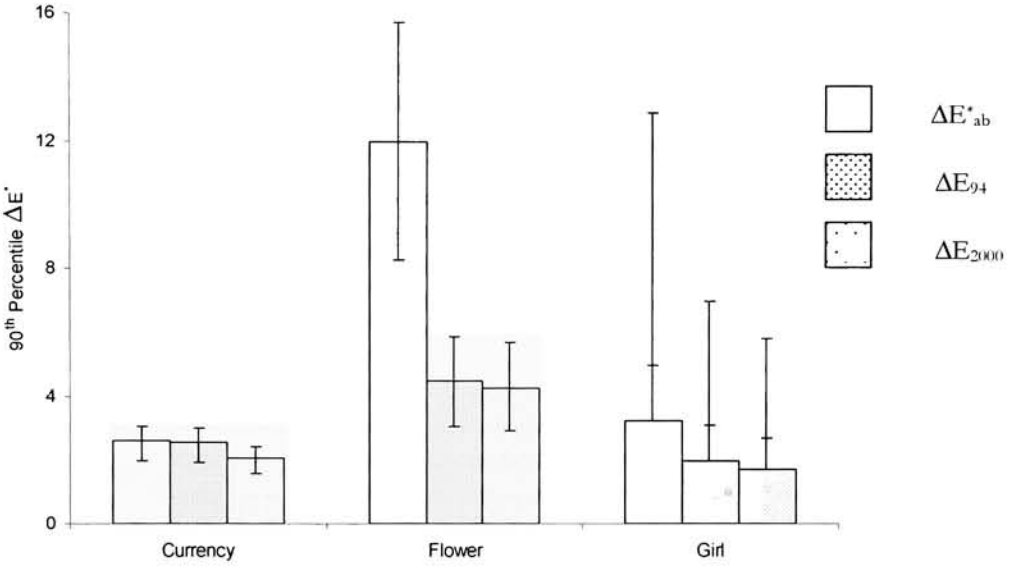

Figure 8.3-2 Chroma Thresholds–IBM LCD

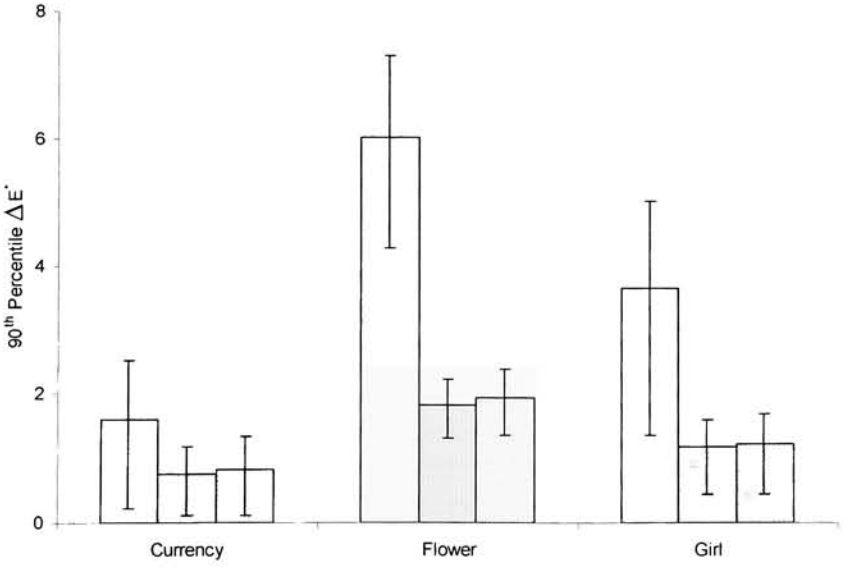

Figure 8.3-3 Hue Thresholds–IBM LCD

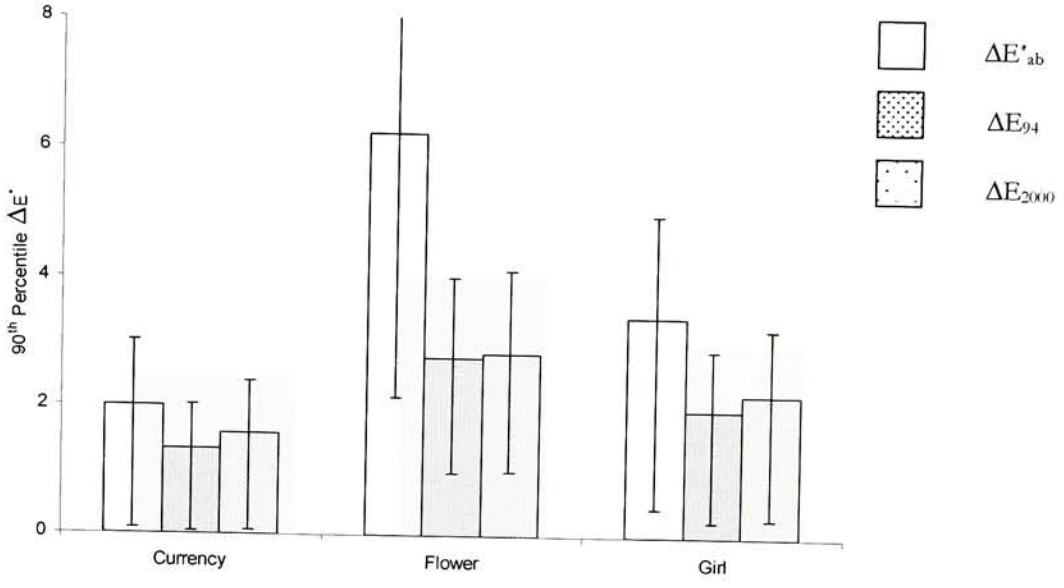

8.3.2. Correlations with un-filtered results

Figure 8.3-4 ΔE^*_{ab}

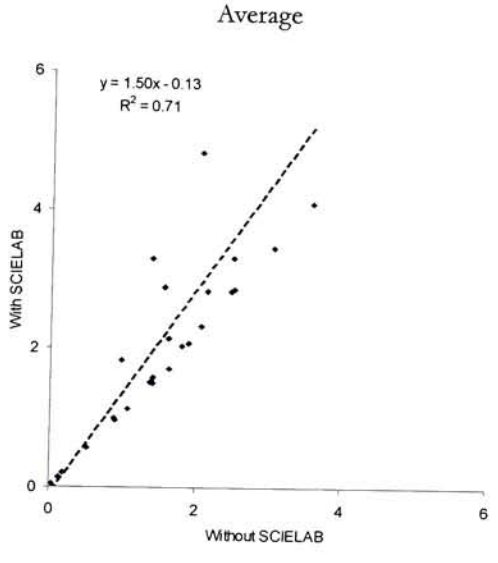

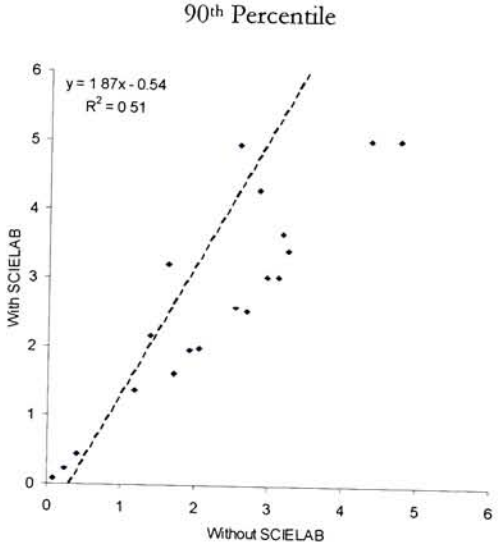

Figure 8.3-5 ΔE_{94}

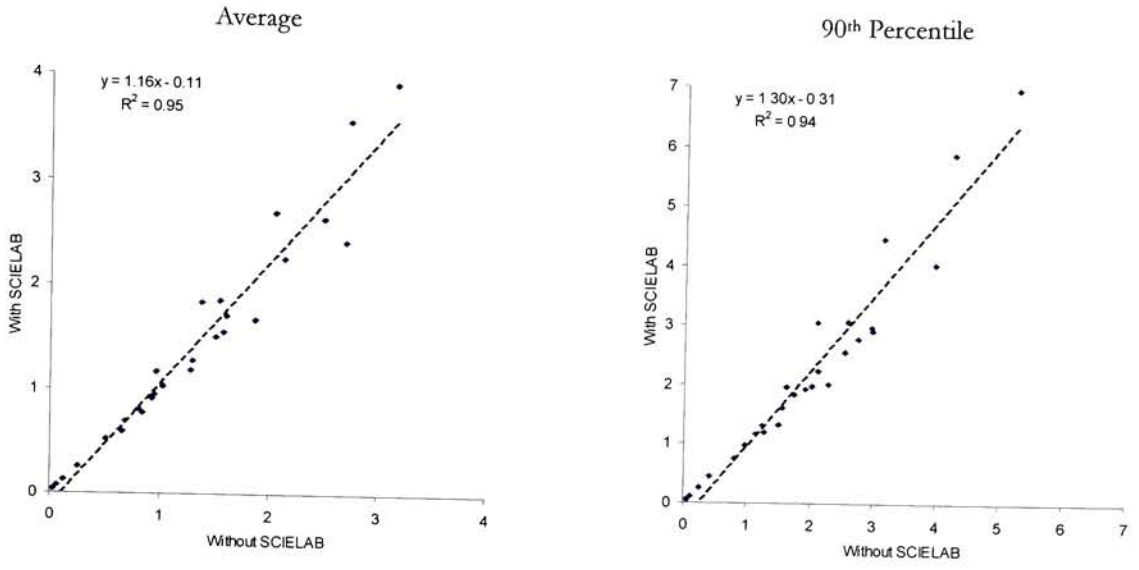

Figure 8.3-6 ΔE_{2000}

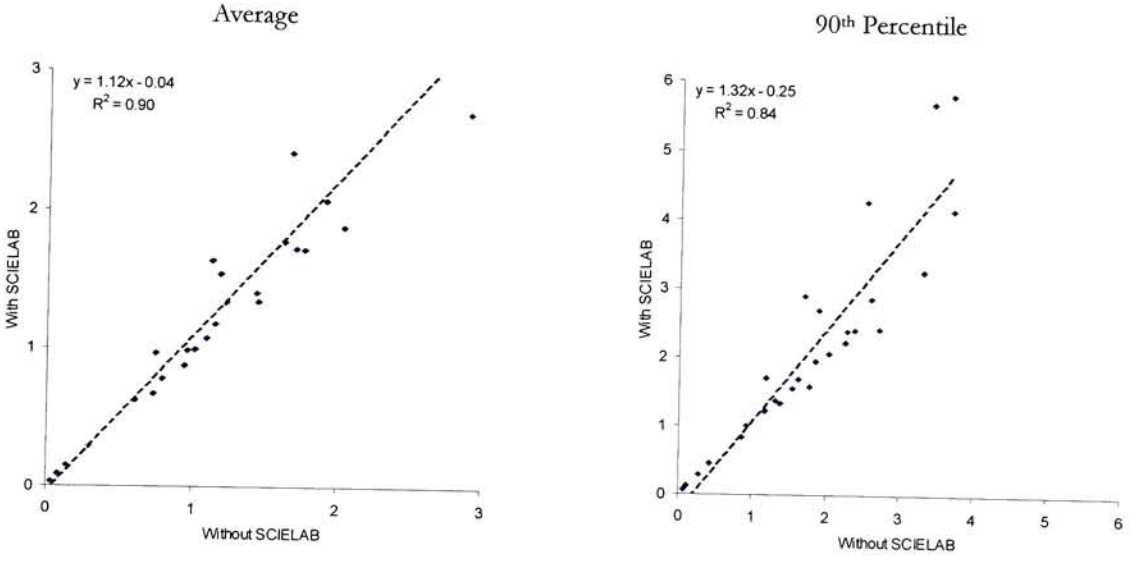

As with the Sony Display, the overall correlations (R^2) between the two methods are reasonable. The non-zero mean slopes seen for the CIE76 color difference formula, especially in the 90th percentile statistic indicate that the filtering may have had some effect for those images. To test the statistical significance of the non-zero slopes, 95% confidence intervals were calculated.

Table 8.3-1 95% Confidence Intervals on the Slope –Average ΔE's

	Lower	Upper
ΔE^*_{ab}	1.10	1.87
ΔE_{94}	1.04	1.28
ΔE_{2000}	0.97	1.28

Table 8.3-2 95% Confidence Intervals on the Slope –90th Percentile ΔE's

	Lower	Upper
ΔE^*_{ab}	1.11	2.63
ΔE_{94}	1.13	1.40
ΔE_{2000}	1.08	1.55

The lower bounds of these intervals are much closer to 1.0 than the mean value reported in the figures above. More data would lead to a better estimate of the mean and correspondingly tighter intervals. Given the width of these intervals and that they do not absolutely included slopes of 1.0 indicates that the filtering may still have had some effect on the data.

Given that the S-CIELAB is a blurring function which attempts to "throw-away" invisible information, it is strange that the slopes would be greater than 1.0 indicating that removal of this information made the differences greater. To preserve the equality of ΔE's for zero spatial frequency, some implementations of S-CIELAB actually boost the differences for middle spatial frequencies.

To determine the behavior of the S-CIELAB code implemented in this thesis the following experiment was conducted. First, a 288x432 pixel uniform images was created. A uniform ΔE^*_{ab} difference of 8.7 was then added to create a second image representing a reproduction of the original. The S-CIELAB code was then used to process these two uniform images at varying sampling frequencies from 5 to 125 samples per degree of visual angle subtended. Both images were processed by the S-CIELAB filters for the given SPD and the mean ΔE^*_{ab} computed. The S-CIELAB values were then subtracted from the conventional ΔE^*_{ab}'s and plotted in the figure below.

Figure 8.3-7 Difference between ΔE^*_{ab} with and without S-CIELAB

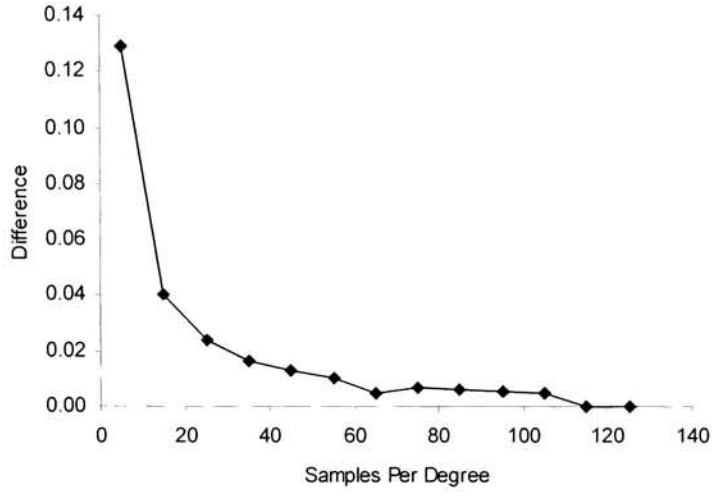

As can be seen, the differences were not zero even for a uniform sample. This difference may act as a low level noise added to the system which may have moved the slope away from 1.0. Further analysis of this observation is beyond the scope of this project.

9 Conclusions and Recommendations

This thesis has continued the exploration of colorimetric tolerances of digital images begun by Stokes [1991] and expanded it to included multiple display technologies including CRT, LCD and print. The results of this study are in agreement with those of Stokes [1991] and Uroz [1999] indicating that there may be some fundamental properties that can be measured to form an image color difference metric. This body of work will be combined with other related studies by CIE committee TC8-02 "Colour Differences Evaluation in Images" Visit the CIE Division 8 website (www.colour.org) for further information.

9.1. Conclusions

The major findings of this research are summarized below along with commentary regarding their significance. Where appropriate, relevant chapter numbers are listed in parenthesis for further details.

9.1.1. LCD Characterization

The process for characterizing LCD panels described by Fairchild [1998] was employed. Using a combination of 3 1D Shaper-LUTs derived from measuring primary ramps and a 3x3 mixing matrix, good models of LCD performance can be created.

Using LUTs to linearize the user controls is preferred to the GOG model used on CRT's since the latter is based on the physical properties of CRT's and therefore not applicable to LCD technology. Remember, care must be taken during measurements that the device not contact the surface of the panel or the cell gap structure of the panel will be disturbed. (Chapter 4)

9.1.2. LCD Performance vs. CRT

In general it was shown that LCD's can perform as well as or better than CRT's for the type of visual psychophysics used in this research. Both the parametric and colorimetric thresholds calculated for the CRT's and LCD's were of similar magnitude and compared favorably to the earlier results of Stokes [1991]. (Chapters 6.5 and 7.6)

LCD's have several advantages over conventional CRT's which can be of great benefit. For example, LCD's are not strongly affected by external magnetic fields and can be used in and near MRI devices where CRT's require specially designed shielding. Furthermore, LCD's exhibit minimal spatial dependencies which would allow researchers to, for example, change the background of a displayed image without having to re-compute it's displayed colorimetry. As this technology matures, especially to higher resolutions, LCD's may become the display of choice for visual psychophysics.

9.1.3. Threshold vs. Physical Parameters

As part of this research, the relationship between physical parameters of the display (white-point luminance, Contrast Ration and addressable resolution) and the measured thresholds were examined. Given the limited sampling of the parameters in question, only the strongest trends would have been observed. Examining the results in both the parameter and colorimetric space, no such trends were evident. (Chapters 6.6 and 7.7)

9.1.4. Affects of S-CIELAB

S-CIELAB has been used with success in various fields as an extension of CIELAB to account for the affects of spatial sampling in digital images. The affects of applying S-CIELAB filtering on both high and low frequency sampled images were examined and found to have little to no affect in this instance. This is primarily due to the fact that only global color changes were applied to the images which would have no affect on it's spatial properties.

In the case of the IBM display some affect of S-CIELAB filtering was noticed primarily with the CIE76 color difference metric using the 90th percentile summary statistic. Given the good fits to the CIE94 and CIE2000 equations, it is unclear as to the reason for this discrepancy. Further study is recommended.

9.2. Recommendations

As with any large project. There are many areas which are uncovered along the way that simply can not be addressed at the time, leaving open areas for further research. The sub sections below list several important areas of exploration that were only cursorily examined along the course of this project.

9.2.5. Verify Rank Confusion Scaling

Given the limited time scope of this project, there was insufficient time to perform extensive verification of the psychophysical method used for scaling the hardcopy output. Given the noisy nature of the results obtained, more research is recommended. This could be achieved by performing an experiment using both this method and the more conventional "same/different" ranking as used by Uroz [1999]. (Chapter 5.2.2)

9.2.6. Improve LCD Characterization Methods

The anomalous "super-additivity' seen on the IBM prototype display has not been fully explained and is an open issue for exploration. The display used was a "proof-of concept" prototype and therefore was not as refined as a commercial unit such as the SGI 1600SW and Apple Studio Display [Fairchild 1998] would be.

It is suspected that the answer may lie in part in the proper accounting of the black state. This prototype unit had a very poor black state (a factor of 10 larger than the SGI) and therefore may have required more attention to it's particular properties. Research by Cazes et. Al.[1999] found by the author after the prototype was returned to IBM may be useful in this area. In this research they accounted for the black state of each pixel in a triad separately and in combinations. That is, the black state of Red only is different that the black state with Red and Green both on.

9.2.7. Designed Experiment for Trends

This research was primarily an observational study in that the physical parameters of each display were not controlled by the researcher. An experiment exploring these relationships further would be of benefit both in creating an image-color-difference metric but also in defining the impact of these parameters on the image quality of the display.

A simple design might include using a high resolution display such as IBM's Roentgen displaying images at various spatial addressability levels (achieved by pixel replication or re-positioning of the display), Luminance and Contrast Ratios (combinations of filters and digital data processing). Carefully designed, such an experiment could uncover trends between these parameters and the displays ability to render color.

9.3. Future Prospects

As was mentioned in the beginning of this paper, CIE TC8-02 is developing a recommendation for a color difference evaluation in images. The details of this work are to be included in the data set being complied by this group. Once sufficient data has been collected various metrics will be developed and tested against this and new data underdevelopment. Researchers are encouraged to contribute their findings to this effort.

10 References and Bibliography

A

John H. Aldrich, Forrest D. Nelson, Linear Probability, Logit, and Probit Models, Sage University Paper series on Quantitative Applications in the Social Sciences, #07-45, Sage Publication, Beverly Hills, 1985.

D. H. Alman, R. S. Berns, W. A. Larsen, Performance Testing for Color-Difference Metrics Using a Color Tolerance Data set, *Color Res. and Appl.*, **14**, 139–151 (1989).

ANSI, PH2.30, Graphic Arts and Photography - Color Printing, Transparencies, and Photomechanical Reproductions - Viewing Conditions, ANSI (1989).

ASTM, E1499-92, Standard Guide to the Selection, Evaluation, and Training of Observers, ASTM (1992).

ASTM, E1808-96, Standard Guide for Designing and Conducting Visual Experiments, ASTM (1996).

B

Raja Balasubramanian, Optimization of the spectral Neugebauer Model for Pinter Characterization, *JEI*, **8**, 156–166 (1999).

L. Jiménez del Barco, J. A. Díaz, et. al., Consideration of the Calibration of Color Displays Assuming Constant Channel Chromaticity. *Color Res. and Appl.*, **20**, 377–387 (1995).

C. J. Bartleson, Influence of Observer Adaptation on the Acceptance of Color Prints, *Pho. Sci. Eng.*, **2**, 32–39 (1958).

C. J. Bartleson, Some Observations on the Reproduction of Flesh Colors, *Pho. Sci. Eng.*, **3**, 114–117 (1959).

C. J. Bartleson, C. P. Bray, On the Preferred Reproduction of Flesh, Blue-Sky, and Green-Grass Colors, *Pho. Sci. Eng.*, **6**, 19–25 (1962).

C. James Bartleson, Franc Grum, *Optical Radiation Measurements Volume 5: Visual Measurements*, Academic Press, Orlando, 1984.

Roy S. Berns, Color Tolerance Feasibility Study Comparing CRT-Generated Stimuli with an Acrylic-Lacquer Coating, *Color Res. and Appl.*, **16**, 232–242 (1991a).

Roy S. Berns, Methods for characterizing CRT Displays, *Displays*, **16**, 173-182 (1996).

Roy S. Berns, Deriving Instrumental Tolerances from Pass-Fail and Colorimetric Data, *CR&A*, **21**, 459 (1996).

Roy S. Berns, Personal Communication (2000).

Roy S. Berns, Mark E. Gorzynski, Neutral Reproduction of Soft-Copy and Hard-Copy Displays, AIC interim meeting, Sydney, June 1991b.

R. S. Berns, D. H. Alman, L. Reniff, Visual Determination of Supra-Threshold Color-Difference Tolerances Using Probit Analysis, Paper Presented at the ISCC Conference on Color Discrimination Psychophysics, Williamsburg, Virginia, November 28–31 (1989).

R. S. Berns, D. H. Alman, L. Reniff, G. D. Snyder, M. R. Balonon-Rosen, Visual Determination of Supra-Threshold Color-Difference Tolerances Using Probit Analysis, *Color Res. and Appl.*, **16**, 297–316 (1991c).

Roy S. Berns, Ricardo J. Motta, Mark E. Gorzynski, CRT Colorimetry. Part I: Theory and Practice, *Color Res. and Appl.*, **18**, 299–314 (1993a).

Roy S. Berns, Ricardo J. Motta, Mark E. Gorzynski, CRT Colorimetry. Part II: Metrology, *Color Res. and Appl.*, **18**, 315–325 (1993b).

Fred W. Billmeyer Jr., Paula J. Alessi, Assessment of Color-Measuring Instruments, , *Color Res. and Appl.*, **6**, 195-202 (1981).

F. J. Bingley, Colorimetry in Color Television, *Proc. I.R.E.*, 839–851 (1953).

F. J. Bingley, Colorimetry in Color Television— Part II, *Proc. I.R.E.*, 48–51 (1954a).

F. J. Bingley, Colorimetry in Color Television— Part III, *Proc. I.R.E.*, 51–57 (1954b).

R. D. Bock, L. V. Jones, *The Measurement and Prediction of Judgment and Choice*, Holden-Day Inc. San Francisco, CA, 1968.

David H. Brainard, Calibration of a Computer Controlled Color Monitor, *Color Res. and Appl.*, **14**, 23–34 (1989).

Karen M. Braun, Mark D. Fairchild, Paula J. Alessi, Viewing Techniques for Cross-Media Image Comparisons, *Color Res. and Appl.*, **21**, 6–17 (1996).

E.J. Breneman, A Color Chart for Use in Evaluating Quality of Color Reproduction, *Pho. Sci. Eng.*, **1**, 74–78 (1957).

Michael H. Brill, Gunilla Derefeldt, Comparison of Reference-White Standards for Video Display Units, *Color Res. and Appl.*, **16**, 26–30 (1991).

C

Albert Cazes, Gordon Braudaway, et. al., Color calibration of liquid crystal displays, *Proc. SPIE*, **3636**, 154–161 (1999).

CIE, Methods of Characterizing Illuminance Meters and Luminance Meters, CIE *Publ. 69*-1987, Central Bureau of the CIE, Paris (1987).

CIE, *Method of Measuring And Specifying Colour Rendering Properties of Light Sources*, 2nd ed., *CIE Publ. 13.2*, Central Bureau of the CIE, Paris (1974).

CIE, *Colorimetry*, Second Edition (Official Recommendations of the International Commission on Illumination), *CIE Publ. 15.2*, Central Bureau of the CIE, Vienna (1986).

CIE, *Industrial Colour-Difference Evaluation*, CIE Technical. Report 116 Vienna (1995).

CIE, The CIE 1997 Interim Color Appearance Model (Simple Version), CIECAM97s, TC1-34, April 1998.

CIE Methods to Derive Colour Differences For Images, TC 8-02 DRAFT report version 0.4, October 2000.

F.J.J. Clarke, R. McDonald, and B. Rigg, Modification to the JPC 79 Colour-Difference Formula, *J. Soc. Dyers Col.*, **100**, 128–132 (1984).

James N. Cook, Pamela A. Sample, Robert N. Weinreb, Solution to Spatial Inhomogeneity on Video Monitors, *Color Res. and Appl.*, **18**, 334–340 (1991).

G. P. Corey, M. J. Clayton, K. N. Cupery, Scene Dependence of Image Quality, *Phot. Sci. Eng.*, **27**, 9–13 (1983).

William B. Cowan, Nelson Rowell, On the Gun Independence and Phosphor Constancy of Colour Video Monitors, *Color Res. and Appl.*, **11**, S34–S38 (1986).

D

Norman R. Draper, Harry Smith, *Applied Regression Analysis 3rd Ed.*, Wiley, NY, 1998.

E

F. Ebner, M.D. Fairchild, Finding Constant Hue Surfaces in Color Space, *Proc. SPIE Color Imaging: Device Independent Color, Color Hardcopy and Graphic Arts III*, **330-16**, 107-117 (1998).

Peter G. Engeldrum, *Psychometric Scaling: A Toolkit for Imaging Systems Development*, IMCOTEK Press, MA, 2000.

Dan Evanicky, *Silicon Graphics 1600SW™ Flat Panel Monitor*, SGI white paper, www.sgi.com/flatpanel/pdf/lcdisplays.pdf, 1999.

F

S. P. Farnand, The Effect of Image Content on Color Difference Perceptibility, *Proc. Of the 4th IS&T/SID Color Imaging Conference 1996* (1996).

Mark D. Fairchild, Formulation and Testing of an Incomplete-Chromatic-Adaptation Model, *Color Res. and Appl.*, **16**, 243–250 (1991).

Mark D. Fairchild, Chromatic Adaptation to Image Displays, TAGA 2, 803–824 (1992).

Mark D. Fairchild, Considering the Surround in Device-Independent Color Imaging, *Color Res. and Appl.*, **20**, 352–363 (1995).

Mark D. Fairchild, The ZLAB color appearance model for practical image reproduction applications, *Proceedings of the CIE Expert Symposium '97 on Color Standards for Image Technology*, CIE Pub. X014, 89–94 (1998a).

Mark. D. Fairchild, *Color Appearance Models*, Addison-Wesley, MA, 1998b.

Mark D. Fairchild, A Victory for Equivalent Background –On Average, *Proceedings of the IS&T/SID 7th Color Imaging Conference*, 87–92 (1999).

Mark D. Fairchild, personal communication (2000).

Mark D. Fairchild, Garrett M. Johnson, Color-Appearance Reproduction: Visual Data and Predictive Modeling, *Color Res. and Appl.*, **24**, 121–131 (1999).

Mark D. Fairchild, David R. Wyble, *Colorimetric Characterization of the Apple Studio Display (Flat Panel LCD)*, Munsell Color Science Laboratory Technical Report, July 1998.

Mark. D. Fairchild, Roy S. Berns, Audrey A. Lester, Accurate Color Reproduction of CRT-Displayed Images as Projected 35-mm Slides, *JEI*, **5** 87–96 (1996).

D. J. Finney, *Probit Analysis*, 3rd ed., Cambridge U. Press, Cambridge, 1971.

J. D. Foley et al., *Computer Graphics: Principles and Practice*, 2nd ed, Addison-Wesley, MA, 1990.

G

George A. Gescheider, *Psychophysics: Method, Theory, and Application*, 2nd Ed. Lawrence Erlbaum Associates, Hilllsdale, 1985.

Jason E. Gibson, Mark D. Fairchild, *Colorimetric Characterization of Three Computer Displays (LCD and CRT)*, Munsell Color Science Laboratory Technical Report, January 2000.

J. Glasser, Principles of Display Measurement and Calibration, Chapter 14 in Display Systems: Design and Applications, L.W. MacDonald and A. C. Lowe, Eds., John Wiley & Sons, Chichester (1997).

H

Roy Hall, Illumination and Color In Computer Generated Imagery, Springer-Verlag, NY, 1989.

Sharron Henley, Personal Communication (1999).

David W. Hosmer, Stanley Lemeshow, Applied Logistic Regression, Wiley, NY, 1989.

Tung-Chang Hseue, Yu-Chuan Shen, et. al., Cross-Media Performance Evaluation of Color Models for Unequal luminance Levels and Dim Surround, Color Res. and Appl., **23**, 169–177 (1998).

P. Hung, R.S. Berns, Determination of Constant Hue Loci for a CRT Gamut and Their Predictions Using Color Appearance Spaces, *CR&A*, **20**, 285-295 (1995).

R.W. G. Hunt, I.T. Pitt, L. M. Winter, The Preferred Reproduction of Blue Sky, Green Grass, and Caucasian Skin in Colour Photography, J. Pho. Sci., **22**, 144–149 (1974).

R.W.G. Hunt, A Model of Colour Vision for Predicting Colour Appearance in Various Viewing Conditions, Color Res. and Appl., **12**, 297–314 (1987).

R.W.G. Hunt, Revised Colour-Appearance Model for Related and Unrelated Colours, Color Res. and Appl., **16**, 146–165 (1991).

R.W.G. Hunt, An Improved Predictor of Colorfulness in a Model of Color Vision, Color Res. and Appl., **19**, 23–26 (1994).

Dr. R.W.G. Hunt, The Reproduction of Colour, 5th ed., Fountain Press, England, 1995.

I

ISO 12640:1997, Graphic technology – Prepress digital data exchange – CMYK standard colour image data (CMYK/SCID), 1997a.

ISO 3664: Viewing Conditions for Graphic Technology and Photography, Working Draft of 1997-03-03, 1997b.

J

Garret M. Johnson, Mark D. Fairchild, Full-Spectral Color Calculations in Realistic Image Synthesis, *IEEE Computer Graphics and Applications*, **19-4**, 47–53 (1999).

L. A. Jones, Photographic Reproduction of Tone, *J. Opt. Soc. Am*, **5**, 232–258 (1921).

L. A. Jones, H. R. Condit, The Brightness Scale of Exterior Scenes and the Computation of Correct Photographic Exposure, *J. Opt. Soc. Am*, **31**, 651–678 (1941).

K

Yasuhiro Kawabata, Spatial Integration Properties in Vision with Chromatic Stimuli, *Color Res. and Appl.*, **18**, 390–398 (1993).

Eiji Kimura, Effects of Luminance Level on the Saturation Function: Sensitivities Based on Saturation Discrimination, *Color Res. and Appl.*, **16**, 289–296 (1991).

L

T. F. Liao, *Interpreting Probability Models: Logit, Probit, and other Generalized Linear Models*, Sage University Paper series on Quantitative Applications in the Social Sciences, #07-101, Sage Publication, Beverly Hills, 1994.

LMT, Application Note AN2-1187, San Diego, CA (1984).

LMT, Luminance Meters Series L1000 Manual, LMT Lichtmesstechnik GmbH Berlin (1991).

Mei-Chun Lo, M. Ronnier Luo, Peter A. Rhodes, Evaluating Colour Models' Performance Between Monitor and Print Images, *Color Res. and Appl.*, **21**, 277–291 (1996).

M. Ronnier Luo, B. Rigg, Chromaticity-Discrimination Ellipses for Surface Colours, *Color Res. and Appl.*, **11**, 25–42 (1986).

M. Ronnier Luo, X. W. Gao, S. A. R. Scrivener, Quantifying Colour Appearance. Part V. Simultaneous Contrast, *Color Res. and Appl.*, **20**, 18–28 (1995).

M. J. Luque, p. Capilla, et. al., Brightness Induction in a Chromatic Center-Achromatic Surround Configuration, *Color Res. and Appl.*, **22**, 288–239 (1997).

M

Lindsay MacDonald, Using Color Effectively in Computer Graphics, *IEEE Computer Graphics and Applications*, **19-4**, 20–35 (1999).

C.S. McCamy, H. Marcus, J.D. Davidson, A color-Rendition Chart, *Journal of Appl. Photographic Eng.*, **2**, 95–99 (1976).

John J. McCann, Color Theory and Color Imaging Systems: Past, Present and Future, *JIST*, **42**, 70–78 (1998).

R. McDonald, Industrial Pass/Fail Color Matching, Part III - Development of Pass/Fail Formula for Use with Instrumental Measurement of Colour Difference, *J. Soc. Dyers Col.*, **96**, 486–495 (1980).

R. McDonald, Acceptability and Perceptibility Decisions Using the CMC Color Difference Formula, *Tex. Chem. Col.* **20**, No. 6, 31–37 (1988).

N

Yoshinobu Nayatani, Hiroaki Sobagaki, et. al., Illuminance Dependency of Equivalent Lightness on Chromatic Object Colors, *Color Res. and Appl.*, **18**, 123–128 (1993a).

Yoshinobu Nayatani, Hiroaki Sobagaki, et. al., Illuminance Dependency of L/Y (Lightness/Luminance-Factor)-Ratio Effect, *Color Res. and Appl.*, **18**, 171–177 (1993b).

H.E.J. Neugebauer, Die theoretischen grundlagen des mehrfarbendrucks, *Zeitscrift fur wissenschaftliche Photographie Photophysik und Photochemie* **36**, 76–89 (1937) [Reprinted in Proc. SPIE **1184**: Neugebauer Memorial Seminar on Color Reproduction, 194-202 (1989).]

NTSC, Panel 12, The NTSC Color Television Standards, *Proc. I.R.E.*, 46-48 (1954).

O

Peyma Oskoui, Elizabeth Pirrotta, "Influence of Background Characteristics on Adapted White Pints of CRTs", *Proc. Of the IS&T/SID 1998 Color Imaging Conference*, 22–26 (1998).

P

Sumanta N. Pattanaik, James A. Ferwerda, Mark D. Fairchild, Donald P. Greenberg, "A Multiscale Model of Adaptation and Spatial Vision for Realistic Image Display", *Proc. Of SIGGRAPH 1998*, 287–298 (1998).

Joaquín Pérez-Carpinell, Rosa Baldoví, M. Dolores de Fez, José Castro, Color Memory Matching: Time Effect and Other Factors, *CR&A*, **23**, 234–247 (1998).

Joaquín Pérez-Carpinell, M. Dolores de Fez, Rosa Baldoví, J.C. Soriano, Familiar Objects and Memory Color, *CR&A*, **23**, 416–427 (1998b).

M.R. Pointer, Measuring Colour Reproduction, *J. Photographic Sciences*, **34**, 81-90 (1986).

David L. Post, Christopher S. Calhoun, Further Evaluation of Methods for Producing Desired Colors on CRT Monitors, *Color Res. and Appl.*, **25**, 90–104 (2000).

D. Pregibon, Logistic Regression Diagnostics, *Annals of Stat.*, **9**, 705–724 (1981).

Q

R

Lisa Reniff, Visual Determination of Color Differences using Probit Analysis: Phase II Master's Thesis, Rochester Institute of Technology (1989).

S

SAS Institute Inc., *SAS/STAT® User's Guide, Version 6, 4th Ed., Volume 1*, Cary, NC: SAS Institute Inc., 1989a.

SAS Institute Inc., *SAS/STAT® User's Guide, Version 6, 4th Ed., Volume 2*, Cary, NC: SAS Institute Inc., 1989b.

K. Schleupen, et al., High-Information-Content Color 16.3" Desktop-AMLCD with 15.7 Million a-Si:H TFTs, *Proc. Int. Display Res. Conf.*, 187 (1998).

Louis D. Sliverstein, Thomas G. Fiske, Colorimetric and Photometric Modeling of Liquid Crystal Displays, *Proc. Of the IS&T/SID Color Imaging Conference*, 150–156 (1993).

Peep F. M. Stalmeier, Charles M. M. de Weert, On the Conditions Affecting the Contribution of Color to Brightness Perception, *Color Res. and Appl.*, **19**, 192–201 (1994).

S. Stamm, An Investigation of Color Tolerance, *Proc. Tech. Assoc. Graphic Arts*, 156–173 (1981).

Mike Stokes, Colorimetric Tolerances of Digital Images, MS thesis, Rochester Institute of Technology, NY, 1991.

M.D. Stokes, M.D. Fairchild, and R.S. Berns, Precision requirements for Digital Color Reproduction, ACM Transactions on Graphics, 11, 406–422 (1992).

T

Paul M. Tannenbaum, The Colorimetry of Color Displays: 1950 to the Present, Extended Abstract, *Color Res. and Appl.*, **11**, S27–S28 (1986).

Jimmy M. Troost, Charles M. M. de Weert, Techniques for Simulating Object Color under Changing Illuminant Conditions of Electronic Displays, *Color Res. and Appl.*, **17**, 316–327 (1992).

A. Tremeau, et. al., A Local Color Correlation Measure for Color Image Comparison, *Proc. Of the IS&T/SID 1995 Color Imaging Conference*, 119–122 (1995).

U

Joan Uroz, Colour Difference Perceptibility for Large-Size Printed Images, MSc Thesis, University of Derby, Derby, (1999).

V

J. A. Stephen Viggiano, "Modeling the color of multi-colored half-tones", *Proc. TAGA* 1990, 44–62, (1990).

W

Brian A. Wandell and E. J. Chichilnisky, Color Appearance in Images: Measurements and Musings, *Proc. Of the IS&T/SID 2nd Color Imaging Conference*, 1–4 (1994)

Heino Widdel, David L. Post Ed., *Color in Electronic Displays*, Plenum Press, NY 1992.

K. Witt, G Döring, Parametric Variations in a Threshold Colour-Difference Ellipsoid for Green Painted Samples, *Color Res. and Appl.*, **8**, 153–163 (1983).

K. Witt, Three-dimensional Threshold for Colour-Difference Perceptibility in Painted Samples: Variability of Observers in Four CIE Colour Regions, *Color Res. and Appl.*, **12**, 128–134 (1987).

Steven L. Wright, Robert W. Nywening, et. al., "Image Quality Issues for High Resolution TFTLCDs", *Proc. Of the IS&T/SID 1998 Color Imaging Conference*, 100–105 (1998).

David R. Wyble, Roy S. Berns, A Critical Review of Spectral Models Applied to Binary Color Printing, *Color Res. and Appl.*, **25**, 4–19 (2000).

X

Y

J.A.C. Yule and W. J. Nielsen, The Penetration of Light into Paper and its Effects on Halftone Reproductions, *TAGA Proceedings*, **3**, 65–76 (1951).

Z

X. Zhang, B. A. Wandell, A Spatial Extension of CIELAB for Digital Color Image Reproduction, *Proc. IS&T/SID fourth Color Imaging Conference* (1996).

A Parametric Threshold Analysis

Listed below is the raw output from the SAS code (see Appendix C) used to analyze the raw psychophysical data and determine the threshold values. All data is corrected for a natural chance level of 50%.

The following abbreviations are used in the analysis:

Curr – Currency Image
Flow – Flower Image
Girl – Painted Girl Image

ls – Lightness Compression
cm – Chroma Reduction
hr – Hue rotation

A.1. Sony GDM-F500 CRT Display

DISPLAY=SNY IMAGE=Curr Transform=cm

Probit Procedure
Class Level Information

Class	Levels	Values
CORRECT	2	Yes No

Number of observations used 263

Probit Procedure

Data Set =WORK.RAW
Dependent Variable=CORRECT

Weighted Frequency Counts for the Ordered Response Categories

Level	Count
Yes	201
No	62

Log Likelihood for NORMAL -128.4832177

Goodness-of-Fit Tests

Statistic	Value	DF	Prob>Chi-Sq
Pearson Chi-Square	8.5823	7	0.2840
L.R. Chi-Square	9.4551	7	0.2216

Response Levels: 2 Number of Covariate Values: 9

NOTE: Since the chi-square is small (p > 0.1000), fiducial limits will be calculated using a t value of 1.96.

Probit Procedure

Variable	DF	Estimate	Std Err	ChiSquare	Pr>Chi	Label/Value
INTERCPT	1	11.8600415	2.591013	20.95238	0.0001	Intercept
AMT	1	-13.350819	2.974642	20.14403	0.0001	Amount

C=0.5000

Probit Model in Terms of Tolerance Distribution

MU	SIGMA
0.888338	0.074902

Estimated Covariance Matrix for Tolerance Parameters

	MU	SIGMA
MU	0.000152	0.000070110
SIGMA	0.000070110	0.000279

Probit Procedure
Probit Analysis on AMT

Probability	AMT	95 Percent Fiducial Limits	
		Lower	Upper
0.01	1.06259	1.00088	1.21530
0.02	1.04217	0.98633	1.17939
0.03	1.02921	0.97705	1.15666
0.04	1.01947	0.97004	1.13958
0.05	1.01154	0.96432	1.12571
0.06	1.00479	0.95943	1.11393
0.07	0.99888	0.95513	1.10361
0.08	0.99358	0.95127	1.09438
0.09	0.98876	0.94774	1.08600
0.10	0.98433	0.94449	1.07830
0.15	0.96597	0.93085	1.04656
0.20	0.95138	0.91979	1.02156
0.25	0.93886	0.91007	1.00034
0.30	0.92762	0.90107	0.98157
0.35	0.91720	0.89240	0.96448
0.40	0.90731	0.88378	0.94868
0.45	0.89775	0.87494	0.93388
0.50	0.88834	0.86559	0.91998
0.55	0.87893	0.85542	0.90688
0.60	0.86936	0.84411	0.89455
0.65	0.85948	0.83133	0.88291
0.70	0.84906	0.81672	0.87177
0.75	0.83782	0.79989	0.86082
0.80	0.82530	0.78018	0.84959
0.85	0.81071	0.75634	0.83738
0.90	0.79235	0.72550	0.82284
0.91	0.78791	0.71796	0.81942
0.92	0.78310	0.70974	0.81574
0.93	0.77780	0.70066	0.81172
0.94	0.77188	0.69049	0.80728
0.95	0.76514	0.67885	0.80224
0.96	0.75721	0.66513	0.79637
0.97	0.74746	0.64820	0.78922
0.98	0.73451	0.62563	0.77978
0.99	0.71409	0.58991	0.76503

NOTE: The above quantiles and fiducial limits refer to effects due to the independent variable and do not include any effect due to the natural threshold.

DISPLAY=SNY IMAGE=Curr Transform=hr

Probit Procedure
Class Level Information

Class	Levels	Values
CORRECT	2	Yes No

Number of observations used 286

Probit Procedure

Data Set =WORK.RAW
Dependent Variable=CORRECT

Weighted Frequency Counts for the Ordered Response Categories

Level	Count
Yes	209
No	77

Log Likelihood for NORMAL -146.5060584

Goodness-of-Fit Tests

Statistic	Value	DF	Prob>Chi-Sq
Pearson Chi-Square	11.2478	10	0.3385
L.R. Chi-Square	11.2972	10	0.3348

Response Levels: 2 Number of Covariate Values: 12

NOTE: Since the chi-square is small (p > 0.1000), fiducial limits will be calculated using a t value of 1.96.

Probit Procedure

Variable	DF	Estimate	Std Err	ChiSquare	Pr>Chi	Label/Value
INTERCPT	1	-1.6319763	0.39771	16.83815	0.0001	Intercept
AMT	1	0.23861577	0.049288	23.43822	0.0001	Amount

C=0.5000

Probit Model in Terms of Tolerance Distribution

MU	SIGMA
6.839348	4.190838

Estimated Covariance Matrix for Tolerance Parameters

	MU	SIGMA
MU	0.453331	-0.100781
SIGMA	-0.100781	0.749337

Probit Procedure
Probit Analysis on AMT

Probability	AMT	95 Percent Fiducial Limits	
		Lower	Upper
0.01	-2.9100	-10.1238	0.2604
0.02	-1.7676	-8.2278	1.0972
0.03	-1.0428	-7.0280	1.6311
0.04	-0.4975	-6.1273	2.0348
0.05	-0.0540	-5.3963	2.3647
0.06	0.3235	-4.7753	2.6467
0.07	0.6545	-4.2319	2.8951
0.08	0.9509	-3.7463	3.1185
0.09	1.2205	-3.3055	3.3225
0.10	1.4686	-2.9007	3.5111
0.15	2.4958	-1.2350	4.3027
0.20	3.3123	0.0723	4.9484
0.25	4.0127	1.1765	5.5196
0.30	4.6417	2.1489	6.0519
0.35	5.2245	3.0274	6.5676
0.40	5.7776	3.8342	7.0838
0.45	6.3127	4.5826	7.6153
0.50	6.8393	5.2814	8.1763
0.55	7.3660	5.9371	8.7803
0.60	7.9011	6.5569	9.4405
0.65	8.4542	7.1504	10.1701
0.70	9.0370	7.7305	10.9842
0.75	9.6660	8.3148	11.9045
0.80	10.3664	8.9276	12.9672
0.85	11.1829	9.6064	14.2413
0.90	12.2101	10.4251	15.8799
0.91	12.4582	10.6186	16.2799
0.92	12.7278	10.8274	16.7158
0.93	13.0241	11.0554	17.1968
0.94	13.3552	11.3084	17.7356
0.95	13.7327	11.5950	18.3520
0.96	14.1762	11.9295	19.0784
0.97	14.7214	12.3379	19.9743
0.98	15.4463	12.8771	21.1690
0.99	16.5887	13.7199	23.0589

NOTE: The above quantiles and fiducial limits refer to effects due to the independent variable and do not include any effect due to the natural threshold.

```
DISPLAY=SNY IMAGE=Curr Transform=ls

 Probit Procedure
 Class Level Information

 Class     Levels    Values

 CORRECT        2    Yes No

 Number of observations used   308


 Probit Procedure

 Data Set           =WORK.RAW
 Dependent Variable=CORRECT

 Weighted Frequency Counts for the Ordered Response Categories

 Level      Count
 Yes        208
  No        100


 Log Likelihood for NORMAL -186.6603989


                Goodness-of-Fit Tests

 Statistic                   Value      DF   Prob>Chi-Sq
 ------------------         --------    --   -----------
 Pearson Chi-Square           7.7563     9        0.5589
 L.R.    Chi-Square           7.8719     9        0.5471

 Response Levels:   2  Number of Covariate Values:   11


 NOTE: Since the chi-square is small (p > 0.1000), fiducial
       limits will be calculated using a t value of  1.96.

 Probit Procedure

 Variable  DF   Estimate  Std Err ChiSquare  Pr>Chi Label/Value

 INTERCPT   1 7.05925794 2.057341   11.7735  0.0006 Intercept
 AMT        1 -8.5274721 2.414273  12.47578  0.0004 Amount

 C=0.5000


 Probit Model in Terms of Tolerance Distribution

           MU         SIGMA
     0.827825      0.117268


 Estimated Covariance Matrix for Tolerance Parameters

                              MU             SIGMA

           MU           0.000339         -0.000208
        SIGMA          -0.000208          0.001102
```

Probit Procedure
Probit Analysis on AMT

Probability	AMT	95 Percent Fiducial Limits	
		Lower	Upper
0.01	1.10063	1.00708	1.41724
0.02	1.06866	0.98594	1.34600
0.03	1.04838	0.97243	1.30090
0.04	1.03312	0.96221	1.26703
0.05	1.02071	0.95384	1.23954
0.06	1.01015	0.94667	1.21618
0.07	1.00089	0.94034	1.19574
0.08	0.99260	0.93464	1.17747
0.09	0.98505	0.92942	1.16089
0.10	0.97811	0.92459	1.14567
0.15	0.94937	0.90407	1.08312
0.20	0.92652	0.88689	1.03427
0.25	0.90692	0.87105	0.99348
0.30	0.88932	0.85528	0.95839
0.35	0.87301	0.83850	0.92803
0.40	0.85753	0.81969	0.90212
0.45	0.84256	0.79807	0.88047
0.50	0.82783	0.77351	0.86244
0.55	0.81309	0.74632	0.84704
0.60	0.79812	0.71682	0.83327
0.65	0.78264	0.68504	0.82033
0.70	0.76633	0.65064	0.80760
0.75	0.74873	0.61285	0.79452
0.80	0.72913	0.57026	0.78048
0.85	0.70628	0.52016	0.76456
0.90	0.67754	0.45669	0.74496
0.91	0.67060	0.44131	0.74028
0.92	0.66306	0.42459	0.73520
0.93	0.65476	0.40618	0.72965
0.94	0.64550	0.38560	0.72346
0.95	0.63494	0.36210	0.71643
0.96	0.62253	0.33447	0.70819
0.97	0.60727	0.30047	0.69810
0.98	0.58699	0.25522	0.68474
0.99	0.55502	0.18381	0.66377

NOTE: The above quantiles and fiducial limits refer to effects due to the independent variable and do not include any effect due to the natural threshold.

DISPLAY=SNY IMAGE=Flow Transform=cm

Probit Procedure
Class Level Information

Class	Levels	Values
CORRECT	2	Yes No

Number of observations used 263

Probit Procedure

Data Set =WORK.RAW
Dependent Variable=CORRECT

Weighted Frequency Counts for the Ordered Response Categories

Level	Count
Yes	192
No	71

Log Likelihood for NORMAL -138.6849085

Goodness-of-Fit Tests

Statistic	Value	DF	Prob>Chi-Sq
Pearson Chi-Square	6.6238	7	0.4691
L.R. Chi-Square	6.5703	7	0.4749

Response Levels: 2 Number of Covariate Values: 9

NOTE: Since the chi-square is small (p > 0.1000), fiducial limits will be calculated using a t value of 1.96.

Probit Procedure

Variable	DF	Estimate	Std Err	ChiSquare	Pr>Chi	Label/Value
INTERCPT	1	10.9012745	2.309648	22.27731	0.0001	Intercept
AMT	1	-12.478418	2.667077	21.89011	0.0001	Amount

C=0.5000

Probit Model in Terms of Tolerance Distribution

MU	SIGMA
0.87361	0.080138

Estimated Covariance Matrix for Tolerance Parameters

	MU	SIGMA
MU	0.000159	0.000035086
SIGMA	0.000035086	0.000293

Probit Procedure
Probit Analysis on AMT

Probability	AMT	95 Percent Fiducial Limits	
		Lower	Upper
0.01	1.06004	0.99861	1.20491
0.02	1.03819	0.98279	1.16774
0.03	1.02433	0.97269	1.14422
0.04	1.01391	0.96506	1.12656
0.05	1.00543	0.95882	1.11222
0.06	0.99821	0.95349	1.10004
0.07	0.99188	0.94880	1.08938
0.08	0.98621	0.94458	1.07986
0.09	0.98106	0.94072	1.07121
0.10	0.97631	0.93716	1.06327
0.15	0.95667	0.92219	1.03058
0.20	0.94106	0.90999	1.00492
0.25	0.92766	0.89918	0.98324
0.30	0.91563	0.88909	0.96415
0.35	0.90449	0.87928	0.94692
0.40	0.89391	0.86942	0.93113
0.45	0.88368	0.85921	0.91652
0.50	0.87361	0.84836	0.90294
0.55	0.86354	0.83658	0.89029
0.60	0.85331	0.82362	0.87843
0.65	0.84273	0.80925	0.86715
0.70	0.83159	0.79317	0.85619
0.75	0.81956	0.77500	0.84519
0.80	0.80616	0.75403	0.83367
0.85	0.79055	0.72893	0.82090
0.90	0.77091	0.69669	0.80549
0.91	0.76616	0.68882	0.80185
0.92	0.76101	0.68025	0.79791
0.93	0.75534	0.67081	0.79361
0.94	0.74901	0.66022	0.78884
0.95	0.74179	0.64812	0.78344
0.96	0.73331	0.63385	0.77713
0.97	0.72289	0.61627	0.76942
0.98	0.70903	0.59283	0.75924
0.99	0.68718	0.55576	0.74332

NOTE: The above quantiles and fiducial limits refer to effects due to the independent variable and do not include any effect due to the natural threshold.

DISPLAY=SNY IMAGE=Flow Transform=hr

Probit Procedure
Class Level Information

Class	Levels	Values
CORRECT	2	Yes No

Number of observations used = 299

Probit Procedure

Data Set =WORK.RAW
Dependent Variable=CORRECT

Weighted Frequency Counts for the Ordered Response Categories

Level	Count
Yes	217
No	82

Log Likelihood for NORMAL -165.3322241

Goodness-of-Fit Tests

Statistic	Value	DF	Prob>Chi-Sq
Pearson Chi-Square	9.2438	10	0.5091
L.R. Chi-Square	8.7526	10	0.5557

Response Levels: 2 Number of Covariate Values: 12

NOTE: Since the chi-square is small (p > 0.1000), fiducial limits will be calculated using a t value of 1.96.

Probit Procedure

Variable	DF	Estimate	Std Err	ChiSquare	Pr>Chi	Label/Value
INTERCPT	1	-1.0420604	0.298041	12.22455	0.0005	Intercept
AMT	1	0.14493932	0.035212	16.94345	0.0001	Amount

C=0.5000

Probit Model in Terms of Tolerance Distribution

MU	SIGMA
7.189632	6.899439

Estimated Covariance Matrix for Tolerance Parameters

	MU	SIGMA
MU	0.958365	-0.105220
SIGMA	-0.105220	2.809479

Probit Procedure
Probit Analysis on AMT

Probability	AMT	95 Percent Fiducial Limits	
		Lower	Upper
0.01	-8.8609	-23.9188	-3.3668
0.02	-6.9801	-20.3580	-2.0631
0.03	-5.7868	-18.1030	-1.2318
0.04	-4.8891	-16.4094	-0.6036
0.05	-4.1589	-15.0339	-0.0906
0.06	-3.5374	-13.8649	0.3480
0.07	-2.9925	-12.8416	0.7340
0.08	-2.5046	-11.9267	1.0812
0.09	-2.0608	-11.0961	1.3982
0.10	-1.6524	-10.3327	1.6913
0.15	0.0388	-7.1891	2.9218
0.20	1.3829	-4.7186	3.9278
0.25	2.5360	-2.6312	4.8228
0.30	3.5716	-0.7961	5.6660
0.35	4.5311	0.8532	6.4986
0.40	5.4417	2.3498	7.3570
0.45	6.3226	3.7075	8.2778
0.50	7.1896	4.9305	9.2972
0.55	8.0566	6.0255	10.4446
0.60	8.9376	7.0115	11.7372
0.65	9.8481	7.9202	13.1836
0.70	10.8077	8.7892	14.7964
0.75	11.8432	9.6583	16.6057
0.80	12.9963	10.5717	18.6746
0.85	14.3404	11.5912	21.1316
0.90	16.0316	12.8319	24.2650
0.91	16.4401	13.1268	25.0266
0.92	16.8838	13.4455	25.8555
0.93	17.3718	13.7943	26.7687
0.94	17.9167	14.1820	27.7904
0.95	18.5382	14.6221	28.9578
0.96	19.2684	15.1368	30.3317
0.97	20.1661	15.7665	32.0237
0.98	21.3593	16.5996	34.2770
0.99	23.2401	17.9053	37.8358

NOTE: The above quantiles and fiducial limits refer to effects due to the independent variable and do not include any effect due to the natural threshold.

DISPLAY=SNY IMAGE=Flow Transform=ls

Probit Procedure
Class Level Information

Class	Levels	Values
CORRECT	2	Yes No

Number of observations used = 296

Probit Procedure

Data Set =WORK.RAW
Dependent Variable=CORRECT

Weighted Frequency Counts for the Ordered Response Categories

Level	Count
Yes	230
No	66

Log Likelihood for NORMAL -137.9914696

Goodness-of-Fit Tests

Statistic	Value	DF	Prob>Chi-Sq
Pearson Chi-Square	10.7274	9	0.2949
L.R. Chi-Square	11.3215	9	0.2543

Response Levels: 2 Number of Covariate Values: 11

NOTE: Since the chi-square is small (p > 0.1000), fiducial limits will be calculated using a t value of 1.96.

Probit Procedure

Variable	DF	Estimate	Std Err	ChiSquare	Pr>Chi	Label/Value
INTERCPT	1	14.1217689	2.942619	23.03086	0.0001	Intercept
AMT	1	-16.018445	3.415235	21.99882	0.0001	Amount

C=0.5000

Probit Model in Terms of Tolerance Distribution

MU	SIGMA
0.881594	0.062428

Estimated Covariance Matrix for Tolerance Parameters

	MU	SIGMA
MU	0.000103	0.000059715
SIGMA	0.000059715	0.000177

Probit Procedure
Probit Analysis on AMT

Probability	AMT	95 Percent Fiducial Limits	
		Lower	Upper
0.01	1.02682	0.97555	1.14846
0.02	1.00981	0.96329	1.11947
0.03	0.99901	0.95549	1.10111
0.04	0.99089	0.94960	1.08732
0.05	0.98428	0.94479	1.07612
0.06	0.97866	0.94069	1.06660
0.07	0.97372	0.93708	1.05826
0.08	0.96931	0.93384	1.05080
0.09	0.96529	0.93089	1.04402
0.10	0.96160	0.92816	1.03779
0.15	0.94630	0.91677	1.01211
0.20	0.93413	0.90757	0.99184
0.25	0.92370	0.89951	0.97461
0.30	0.91433	0.89211	0.95931
0.35	0.90565	0.88504	0.94534
0.40	0.89741	0.87808	0.93233
0.45	0.88944	0.87103	0.92008
0.50	0.88159	0.86366	0.90843
0.55	0.87375	0.85575	0.89733
0.60	0.86578	0.84702	0.88675
0.65	0.85754	0.83716	0.87665
0.70	0.84886	0.82583	0.86694
0.75	0.83949	0.81264	0.85742
0.80	0.82905	0.79705	0.84772
0.85	0.81689	0.77805	0.83725
0.90	0.80159	0.75336	0.82487
0.91	0.79789	0.74730	0.82197
0.92	0.79388	0.74069	0.81885
0.93	0.78946	0.73340	0.81545
0.94	0.78453	0.72522	0.81168
0.95	0.77891	0.71585	0.80742
0.96	0.77230	0.70481	0.80246
0.97	0.76418	0.69118	0.79640
0.98	0.75338	0.67299	0.78843
0.99	0.73636	0.64420	0.77598

NOTE: The above quantiles and fiducial limits refer to effects due to the independent variable and do not include any effect due to the natural threshold.

DISPLAY=SNY IMAGE=Girl Transform=cm

Probit Procedure
Class Level Information

Class	Levels	Values
CORRECT	2	Yes No

Number of observations used 276

Probit Procedure

Data Set =WORK.RAW
Dependent Variable=CORRECT

Weighted Frequency Counts for the Ordered Response Categories

Level	Count
Yes	237
No	39

Log Likelihood for NORMAL -95.85272322

Goodness-of-Fit Tests

Statistic	Value	DF	Prob>Chi-Sq
Pearson Chi-Square	4.6841	9	0.8609
L.R. Chi-Square	5.1299	9	0.8228

Response Levels: 2 Number of Covariate Values: 11

NOTE: Since the chi-square is small (p > 0.1000), fiducial limits will be calculated using a t value of 1.96.

Probit Procedure

Variable	DF	Estimate	Std Err	ChiSquare	Pr>Chi	Label/Value
INTERCPT	1	13.2886101	2.93402	20.51317	0.0001	Intercept
AMT	1	-14.101987	3.249999	18.82757	0.0001	Amount

C=0.5000

Probit Model in Terms of Tolerance Distribution

MU	SIGMA
0.942322	0.070912

Estimated Covariance Matrix for Tolerance Parameters

	MU	SIGMA
MU	0.000203	0.000153
SIGMA	0.000153	0.000267

Probit Procedure
Probit Analysis on AMT

Probability	AMT	95 Percent Fiducial Limits	
		Lower	Upper
0.01	1.10729	1.04094	1.27910
0.02	1.08796	1.02739	1.24408
0.03	1.07569	1.01876	1.22189
0.04	1.06647	1.01226	1.20521
0.05	1.05896	1.00695	1.19166
0.06	1.05257	1.00243	1.18013
0.07	1.04697	0.99845	1.17004
0.08	1.04196	0.99488	1.16100
0.09	1.03740	0.99163	1.15279
0.10	1.03320	0.98864	1.14524
0.15	1.01582	0.97614	1.11406
0.20	1.00200	0.96610	1.08939
0.25	0.99015	0.95737	1.06834
0.30	0.97951	0.94940	1.04956
0.35	0.96965	0.94188	1.03231
0.40	0.96029	0.93457	1.01611
0.45	0.95123	0.92727	1.00065
0.50	0.94232	0.91980	0.98573
0.55	0.93341	0.91193	0.97121
0.60	0.92436	0.90337	0.95702
0.65	0.91500	0.89373	0.94314
0.70	0.90514	0.88246	0.92964
0.75	0.89449	0.86883	0.91652
0.80	0.88264	0.85194	0.90363
0.85	0.86883	0.83046	0.89039
0.90	0.85144	0.80169	0.87550
0.91	0.84725	0.79455	0.87209
0.92	0.84269	0.78673	0.86845
0.93	0.83767	0.77807	0.86451
0.94	0.83207	0.76833	0.86017
0.95	0.82568	0.75716	0.85529
0.96	0.81818	0.74395	0.84964
0.97	0.80895	0.72762	0.84279
0.98	0.79669	0.70580	0.83380
0.99	0.77736	0.67120	0.81982

NOTE: The above quantiles and fiducial limits refer to effects due to the independent variable and do not include any effect due to the natural threshold.

DISPLAY=SNY IMAGE=Girl Transform=hr

Probit Procedure
Class Level Information

Class	Levels	Values
CORRECT	2	Yes No

Number of observations used 286

Probit Procedure

Data Set =WORK.RAW
Dependent Variable=CORRECT

Weighted Frequency Counts for the Ordered Response Categories

Level	Count
Yes	231
No	55

Log Likelihood for NORMAL -123.1521647

Goodness-of-Fit Tests

Statistic	Value	DF	Prob>Chi-Sq
Pearson Chi-Square	7.9843	9	0.5357
L.R. Chi-Square	8.1493	9	0.5192

Response Levels: 2 Number of Covariate Values: 11

NOTE: Since the chi-square is small (p > 0.1000), fiducial limits will be calculated using a t value of 1.96.

Probit Procedure

Variable	DF	Estimate	Std Err	ChiSquare	Pr>Chi	Label/Value
INTERCPT	1	-1.0797016	0.364186	8.789443	0.0030	Intercept
AMT	1	0.22793188	0.05228	19.00834	0.0001	Amount

C=0.5000

Probit Model in Terms of Tolerance Distribution

MU	SIGMA
4.736949	4.387276

Estimated Covariance Matrix for Tolerance Parameters

	MU	SIGMA
MU	0.557352	-0.377464
SIGMA	-0.377464	1.012618

Probit Procedure
Probit Analysis on AMT

Probability	AMT	95 Percent Fiducial Limits	
		Lower	Upper
0.01	-5.4694	-15.2894	-1.6482
0.02	-4.2734	-13.1329	-0.8069
0.03	-3.5146	-11.7667	-0.2711
0.04	-2.9438	-10.7402	0.1332
0.05	-2.4795	-9.9061	0.4630
0.06	-2.0843	-9.1970	0.7445
0.07	-1.7378	-8.5759	0.9919
0.08	-1.4275	-8.0203	1.2141
0.09	-1.1453	-7.5156	1.4167
0.10	-0.8856	-7.0516	1.6037
0.15	0.1898	-5.1365	2.3842
0.20	1.0445	-3.6242	3.0142
0.25	1.7778	-2.3368	3.5648
0.30	2.4363	-1.1921	4.0707
0.35	3.0464	-0.1449	4.5530
0.40	3.6254	0.8317	5.0276
0.45	4.1856	1.7545	5.5090
0.50	4.7369	2.6330	6.0124
0.55	5.2883	3.4712	6.5561
0.60	5.8485	4.2690	7.1625
0.65	6.4275	5.0247	7.8581
0.70	7.0376	5.7411	8.6712
0.75	7.6961	6.4307	9.6321
0.80	8.4294	7.1203	10.7805
0.85	9.2841	7.8542	12.1889
0.90	10.3595	8.7137	14.0250
0.91	10.6192	8.9144	14.4755
0.92	10.9014	9.1301	14.9670
0.93	11.2117	9.3649	15.5099
0.94	11.5582	9.6247	16.1187
0.95	11.9534	9.9183	16.8157
0.96	12.4177	10.2601	17.6378
0.97	12.9885	10.6766	18.6520
0.98	13.7473	11.2253	20.0053
0.99	14.9433	12.0817	22.1467

NOTE: The above quantiles and fiducial limits refer to effects due to the independent variable and do not include any effect due to the natural threshold.

DISPLAY=SNY IMAGE=Girl Transform=ls

Probit Procedure
Class Level Information

Class	Levels	Values
CORRECT	2	Yes No

Number of observations used 295

Probit Procedure

Data Set =WORK.RAW
Dependent Variable=CORRECT

Weighted Frequency Counts for the Ordered Response Categories

Level	Count
Yes	221
No	74

Log Likelihood for NORMAL -143.1599878

Goodness-of-Fit Tests

Statistic	Value	DF	Prob>Chi-Sq
Pearson Chi-Square	10.2038	8	0.2510
L.R. Chi-Square	8.1624	8	0.4178

Response Levels: 2 Number of Covariate Values: 10

NOTE: Since the chi-square is small (p > 0.1000), fiducial limits will be calculated using a t value of 1.96.

Probit Procedure

Variable	DF	Estimate	Std Err	ChiSquare	Pr>Chi	Label/Value
INTERCPT	1	15.647884	3.018231	26.87858	0.0001	Intercept
AMT	1	-17.940044	3.518063	26.00398	0.0001	Amount

C=0.5000

Probit Model in Terms of Tolerance Distribution

MU	SIGMA
0.872232	0.055741

Estimated Covariance Matrix for Tolerance Parameters

	MU	SIGMA
MU	0.000081104	0.000033010
SIGMA	0.000033010	0.000119

Probit Procedure
Probit Analysis on AMT

Probability	AMT	95 Percent Fiducial Limits	
		Lower	Upper
0.01	1.00191	0.95919	1.09491
0.02	0.98671	0.94794	1.07050
0.03	0.97707	0.94077	1.05505
0.04	0.96982	0.93536	1.04345
0.05	0.96392	0.93094	1.03402
0.06	0.95890	0.92716	1.02602
0.07	0.95449	0.92384	1.01901
0.08	0.95055	0.92085	1.01274
0.09	0.94697	0.91813	1.00705
0.10	0.94367	0.91561	1.00182
0.15	0.93000	0.90509	0.98028
0.20	0.91915	0.89657	0.96333
0.25	0.90983	0.88909	0.94894
0.30	0.90146	0.88219	0.93621
0.35	0.89371	0.87559	0.92462
0.40	0.88635	0.86907	0.91387
0.45	0.87924	0.86247	0.90377
0.50	0.87223	0.85560	0.89421
0.55	0.86523	0.84828	0.88509
0.60	0.85811	0.84031	0.87635
0.65	0.85075	0.83148	0.86792
0.70	0.84300	0.82154	0.85967
0.75	0.83464	0.81018	0.85140
0.80	0.82532	0.79691	0.84280
0.85	0.81446	0.78085	0.83338
0.90	0.80080	0.76005	0.82212
0.91	0.79750	0.75495	0.81947
0.92	0.79391	0.74939	0.81662
0.93	0.78997	0.74326	0.81350
0.94	0.78557	0.73637	0.81006
0.95	0.78055	0.72849	0.80616
0.96	0.77465	0.71919	0.80161
0.97	0.76739	0.70772	0.79607
0.98	0.75775	0.69240	0.78876
0.99	0.74256	0.66816	0.77734

NOTE: The above quantiles and fiducial limits refer to effects due to the independent variable and do not include any effect due to the natural threshold.

A.2. SGI® 1600SW™ LCD Panel

```
DISPLAY=SGI IMAGE=Curr Transform=cm

 Probit Procedure
 Class Level Information

 Class     Levels    Values

 CORRECT        2    Yes No

 Number of observations used   271


 Probit Procedure

 Data Set          =WORK.RAW
 Dependent Variable=CORRECT

 Weighted Frequency Counts for the Ordered Response Categories

 Level      Count
 Yes          222
  No           49


 Log Likelihood for NORMAL -115.9977567


                Goodness-of-Fit Tests

 Statistic                  Value      DF   Prob>Chi-Sq
 ------------------        --------    --   -----------
 Pearson Chi-Square          1.4858     8        0.9929
 L.R.    Chi-Square          1.6959     8        0.9890

 Response Levels:   2  Number of Covariate Values:   10


 NOTE: Since the chi-square is small (p > 0.1000), fiducial
       limits will be calculated using a t value of  1.96.

 Probit Procedure

 Variable  DF   Estimate  Std Err ChiSquare  Pr>Chi Label/Value

 INTERCPT   1 9.98955082 2.239614  19.89507  0.0001 Intercept
 AMT        1 -10.776847 2.516634  18.33764  0.0001 Amount

 C=0.5000


 Probit Model in Terms of Tolerance Distribution

           MU         SIGMA
     0.926946      0.092792


 Estimated Covariance Matrix for Tolerance Parameters

                              MU             SIGMA

           MU           0.000253          0.000196
        SIGMA           0.000196          0.000470
```

Probit Procedure
Probit Analysis on AMT

Probability	AMT	95 Percent Fiducial Limits	
		Lower	Upper
0.01	1.14281	1.06006	1.36054
0.02	1.11752	1.04240	1.31419
0.03	1.10147	1.03117	1.28483
0.04	1.08939	1.02269	1.26276
0.05	1.07957	1.01578	1.24482
0.06	1.07122	1.00988	1.22957
0.07	1.06389	1.00470	1.21621
0.08	1.05732	1.00005	1.20426
0.09	1.05136	0.99581	1.19340
0.10	1.04586	0.99190	1.18341
0.15	1.02312	0.97559	1.14218
0.20	1.00504	0.96245	1.10958
0.25	0.98953	0.95100	1.08180
0.30	0.97561	0.94051	1.05705
0.35	0.96270	0.93054	1.03437
0.40	0.95045	0.92078	1.01315
0.45	0.93861	0.91092	0.99303
0.50	0.92695	0.90067	0.97378
0.55	0.91529	0.88963	0.95532
0.60	0.90344	0.87731	0.93766
0.65	0.89119	0.86310	0.92089
0.70	0.87829	0.84626	0.90508
0.75	0.86436	0.82608	0.89002
0.80	0.84885	0.80169	0.87518
0.85	0.83077	0.77156	0.85957
0.90	0.80803	0.73216	0.84142
0.91	0.80253	0.72249	0.83720
0.92	0.79657	0.71192	0.83266
0.93	0.79000	0.70026	0.82773
0.94	0.78268	0.68718	0.82227
0.95	0.77432	0.67220	0.81610
0.96	0.76450	0.65453	0.80892
0.97	0.75242	0.63274	0.80017
0.98	0.73638	0.60366	0.78865
0.99	0.71108	0.55764	0.77066

NOTE: The above quantiles and fiducial limits refer to effects due to the independent variable and do not include any effect due to the natural threshold.

DISPLAY=SGI IMAGE=Curr Transform=hr

Probit Procedure
Class Level Information

Class	Levels	Values
CORRECT	2	Yes No

Number of observations used = 256

Probit Procedure

Data Set =WORK.RAW
Dependent Variable=CORRECT

Weighted Frequency Counts for the Ordered Response Categories

Level	Count
Yes	209
No	47

Log Likelihood for NORMAL -105.159552

Goodness-of-Fit Tests

Statistic	Value	DF	Prob>Chi-Sq
Pearson Chi-Square	5.1968	7	0.6360
L.R. Chi-Square	4.9263	7	0.6690

Response Levels: 2 Number of Covariate Values: 9

NOTE: Since the chi-square is small (p > 0.1000), fiducial limits will be calculated using a t value of 1.96.

Probit Procedure

Variable	DF	Estimate	Std Err	ChiSquare	Pr>Chi	Label/Value
INTERCPT	1	-0.935891	0.311408	9.032148	0.0027	Intercept
AMT	1	0.21180291	0.043646	23.54886	0.0001	Amount

C=0.5000

Probit Model in Terms of Tolerance Distribution

MU	SIGMA
4.418688	4.721371

Estimated Covariance Matrix for Tolerance Parameters

	MU	SIGMA
MU	0.646035	-0.366788
SIGMA	-0.366788	0.946600

Probit Procedure
Probit Analysis on AMT

Probability	AMT	95 Percent Fiducial Limits	
		Lower	Upper
0.01	-6.5649	-15.4308	-2.6943
0.02	-5.2778	-13.2916	-1.7577
0.03	-4.4612	-11.9366	-1.1611
0.04	-3.8469	-10.9189	-0.7108
0.05	-3.3473	-10.0921	-0.3434
0.06	-2.9220	-9.3893	-0.0297
0.07	-2.5491	-8.7739	0.2460
0.08	-2.2152	-8.2236	0.4937
0.09	-1.9115	-7.7237	0.7195
0.10	-1.6320	-7.2641	0.9279
0.15	-0.4747	-5.3686	1.7982
0.20	0.4451	-3.8732	2.5009
0.25	1.2342	-2.6014	3.1149
0.30	1.9428	-1.4715	3.6786
0.35	2.5994	-0.4386	4.2150
0.40	3.2225	0.5243	4.7412
0.45	3.8254	1.4347	5.2716
0.50	4.4187	2.3034	5.8207
0.55	5.0120	3.1373	6.4048
0.60	5.6148	3.9401	7.0427
0.65	6.2379	4.7150	7.7569
0.70	6.8946	5.4680	8.5732
0.75	7.6032	6.2118	9.5229
0.80	8.3923	6.9707	10.6499
0.85	9.3121	7.7880	12.0306
0.90	10.4694	8.7498	13.8346
0.91	10.7489	8.9745	14.2780
0.92	11.0526	9.2160	14.7622
0.93	11.3864	9.4789	15.2972
0.94	11.7594	9.7697	15.8977
0.95	12.1847	10.0981	16.5857
0.96	12.6843	10.4803	17.3976
0.97	13.2986	10.9458	18.4002
0.98	14.1152	11.5586	19.7389
0.99	15.4022	12.5142	21.8592

NOTE: The above quantiles and fiducial limits refer to effects due to the independent variable and do not include any effect due to the natural threshold.

```
DISPLAY=SGI IMAGE=Curr Transform=ls

 Probit Procedure
 Class Level Information

 Class     Levels    Values

 CORRECT        2    Yes No

 Number of observations used   273


 Probit Procedure

 Data Set          =WORK.RAW
 Dependent Variable=CORRECT

 Weighted Frequency Counts for the Ordered Response Categories

 Level      Count
 Yes          175
  No           98


 Log Likelihood for NORMAL -170.9876201


                Goodness-of-Fit Tests

 Statistic                  Value      DF   Prob>Chi-Sq
 ------------------        --------    --   -----------
 Pearson Chi-Square          5.2326     7        0.6316
 L.R.    Chi-Square          5.2863     7        0.6251

 Response Levels:   2  Number of Covariate Values:    9


 NOTE: Since the chi-square is small (p > 0.1000), fiducial
       limits will be calculated using a t value of  1.96.

 Probit Procedure

 Variable  DF   Estimate  Std Err ChiSquare  Pr>Chi Label/Value

 INTERCPT   1 9.07989604 2.794117  10.56021  0.0012 Intercept
 AMT        1  -11.22408  3.34641  11.24975  0.0008 Amount

 C=0.5000


 Probit Model in Terms of Tolerance Distribution

           MU         SIGMA
     0.808966      0.089094


 Estimated Covariance Matrix for Tolerance Parameters

                             MU             SIGMA

          MU           0.000292         -0.000193
       SIGMA          -0.000193          0.000706
```

Probit Procedure
Probit Analysis on AMT

Probability	AMT	95 Percent Fiducial Limits	
		Lower	Upper
0.01	1.01623	0.94453	1.27760
0.02	0.99194	0.92857	1.21980
0.03	0.97653	0.91834	1.18323
0.04	0.96494	0.91057	1.15579
0.05	0.95551	0.90420	1.13353
0.06	0.94749	0.89872	1.11464
0.07	0.94045	0.89387	1.09812
0.08	0.93415	0.88948	1.08337
0.09	0.92842	0.88545	1.06999
0.10	0.92314	0.88170	1.05772
0.15	0.90131	0.86560	1.00749
0.20	0.88395	0.85177	0.96861
0.25	0.86906	0.83858	0.93657
0.30	0.85569	0.82497	0.90957
0.35	0.84330	0.81006	0.88685
0.40	0.83154	0.79320	0.86800
0.45	0.82016	0.77417	0.85248
0.50	0.80897	0.75315	0.83950
0.55	0.79777	0.73041	0.82824
0.60	0.78639	0.70608	0.81801
0.65	0.77464	0.68008	0.80830
0.70	0.76224	0.65205	0.79870
0.75	0.74887	0.62131	0.78883
0.80	0.73398	0.58669	0.77822
0.85	0.71663	0.54599	0.76621
0.90	0.69479	0.49443	0.75144
0.91	0.68951	0.48193	0.74792
0.92	0.68378	0.46834	0.74411
0.93	0.67748	0.45338	0.73993
0.94	0.67044	0.43666	0.73528
0.95	0.66242	0.41757	0.73000
0.96	0.65299	0.39511	0.72381
0.97	0.64140	0.36748	0.71624
0.98	0.62599	0.33070	0.70622
0.99	0.60170	0.27265	0.69051

NOTE: The above quantiles and fiducial limits refer to effects due to the independent variable and do not include any effect due to the natural threshold.

DISPLAY=SGI IMAGE=Flow Transform=cm

Probit Procedure
Class Level Information

Class	Levels	Values
CORRECT	2	Yes No

Number of observations used = 271

Probit Procedure

Data Set =WORK.RAW
Dependent Variable=CORRECT

Weighted Frequency Counts for the Ordered Response Categories

Level	Count
Yes	189
No	82

Log Likelihood for NORMAL -147.2337669

Goodness-of-Fit Tests

Statistic	Value	DF	Prob>Chi-Sq
Pearson Chi-Square	11.6580	8	0.1671
L.R. Chi-Square	10.1299	8	0.2560

Response Levels: 2 Number of Covariate Values: 10

NOTE: Since the chi-square is small (p > 0.1000), fiducial limits will be calculated using a t value of 1.96.

Probit Procedure

Variable	DF	Estimate	Std Err	ChiSquare	Pr>Chi	Label/Value
INTERCPT	1	15.6295728	3.528931	19.61588	0.0001	Intercept
AMT	1	-18.157745	4.151772	19.12744	0.0001	Amount

C=0.5000

Probit Model in Terms of Tolerance Distribution

MU	SIGMA
0.860766	0.055073

Estimated Covariance Matrix for Tolerance Parameters

	MU	SIGMA
MU	0.000109	0.000034331
SIGMA	0.000034331	0.000159

Probit Procedure
Probit Analysis on AMT

Probability	AMT	95 Percent Fiducial Limits	
		Lower	Upper
0.01	0.98888	0.94251	1.10565
0.02	0.97387	0.93179	1.07880
0.03	0.96435	0.92495	1.06180
0.04	0.95718	0.91978	1.04904
0.05	0.95135	0.91554	1.03869
0.06	0.94639	0.91193	1.02989
0.07	0.94204	0.90874	1.02219
0.08	0.93815	0.90587	1.01531
0.09	0.93461	0.90325	1.00907
0.10	0.93134	0.90083	1.00333
0.15	0.91785	0.89065	0.97973
0.20	0.90712	0.88234	0.96119
0.25	0.89791	0.87498	0.94551
0.30	0.88965	0.86812	0.93168
0.35	0.88199	0.86147	0.91916
0.40	0.87472	0.85482	0.90762
0.45	0.86769	0.84797	0.89688
0.50	0.86077	0.84072	0.88681
0.55	0.85385	0.83287	0.87734
0.60	0.84681	0.82422	0.86839
0.65	0.83955	0.81455	0.85987
0.70	0.83189	0.80361	0.85164
0.75	0.82362	0.79108	0.84348
0.80	0.81442	0.77645	0.83507
0.85	0.80369	0.75876	0.82592
0.90	0.79019	0.73584	0.81505
0.91	0.78693	0.73023	0.81250
0.92	0.78338	0.72411	0.80976
0.93	0.77949	0.71735	0.80677
0.94	0.77514	0.70977	0.80346
0.95	0.77018	0.70109	0.79973
0.96	0.76435	0.69085	0.79538
0.97	0.75719	0.67822	0.79008
0.98	0.74766	0.66135	0.78311
0.99	0.73265	0.63465	0.77224

NOTE: The above quantiles and fiducial limits refer to effects due to the independent variable and do not include any effect due to the natural threshold.

DISPLAY=SGI IMAGE=Flow Transform=hr

Probit Procedure
Class Level Information

Class	Levels	Values
CORRECT	2	Yes No

Number of observations used = 256

Probit Procedure

Data Set =WORK.RAW
Dependent Variable=CORRECT

Weighted Frequency Counts for the Ordered Response Categories

Level	Count
Yes	197
No	59

Log Likelihood for NORMAL -128.7791525

Goodness-of-Fit Tests

Statistic	Value	DF	Prob>Chi-Sq
Pearson Chi-Square	4.6904	7	0.6977
L.R. Chi-Square	5.0162	7	0.6580

Response Levels: 2 Number of Covariate Values: 9

NOTE: Since the chi-square is small (p > 0.1000), fiducial limits will be calculated using a t value of 1.96.

Probit Procedure

Variable	DF	Estimate	Std Err	ChiSquare	Pr>Chi	Label/Value
INTERCPT	1	-0.8830484	0.311531	8.034649	0.0046	Intercept
AMT	1	0.14813492	0.037566	15.54945	0.0001	Amount

C=0.5000

Probit Model in Terms of Tolerance Distribution

MU	SIGMA
5.961109	6.750603

Estimated Covariance Matrix for Tolerance Parameters

	MU	SIGMA
MU	1.078040	-0.599842
SIGMA	-0.599842	2.930691

Probit Procedure
Probit Analysis on AMT

Probability	AMT	95 Percent Fiducial Limits	
		Lower	Upper
0.01	-9.7431	-26.8426	-3.8563
0.02	-7.9029	-23.2090	-2.6018
0.03	-6.7354	-20.9069	-1.8025
0.04	-5.8571	-19.1773	-1.1992
0.05	-5.1426	-17.7721	-0.7067
0.06	-4.5346	-16.5774	-0.2862
0.07	-4.0014	-15.5310	0.0837
0.08	-3.5240	-14.5952	0.4160
0.09	-3.0898	-13.7451	0.7192
0.10	-2.6901	-12.9636	0.9992
0.15	-1.0354	-9.7397	2.1706
0.20	0.2797	-7.1968	3.1210
0.25	1.4079	-5.0365	3.9576
0.30	2.4211	-3.1219	4.7343
0.35	3.3600	-1.3801	5.4863
0.40	4.2509	0.2297	6.2430
0.45	5.1128	1.7276	7.0346
0.50	5.9611	3.1191	7.8964
0.55	6.8094	4.3988	8.8700
0.60	7.6714	5.5608	9.9975
0.65	8.5623	6.6125	11.3123
0.70	9.5011	7.5818	12.8369
0.75	10.5143	8.5124	14.5975
0.80	11.6426	9.4575	16.6493
0.85	12.9577	10.4858	19.1143
0.90	14.6124	11.7153	22.2800
0.91	15.0120	12.0053	23.0516
0.92	15.4462	12.3181	23.8921
0.93	15.9236	12.6596	24.8187
0.94	16.4568	13.0385	25.8560
0.95	17.0649	13.4679	27.0419
0.96	17.7793	13.9691	28.4384
0.97	18.6576	14.5814	30.1590
0.98	19.8252	15.3902	32.4516
0.99	21.6654	16.6557	36.0741

NOTE: The above quantiles and fiducial limits refer to effects due to the independent variable and do not include any effect due to the natural threshold.

DISPLAY=SGI IMAGE=Flow Transform=ls

Probit Procedure
Class Level Information

Class	Levels	Values
CORRECT	2	Yes No

Number of observations used = 273

Probit Procedure

Data Set =WORK.RAW
Dependent Variable=CORRECT

Weighted Frequency Counts for the Ordered Response Categories

Level	Count
Yes	227
No	46

Log Likelihood for NORMAL -106.589387

Goodness-of-Fit Tests

Statistic	Value	DF	Prob>Chi-Sq
Pearson Chi-Square	5.8260	7	0.5602
L.R. Chi-Square	5.7047	7	0.5746

Response Levels: 2 Number of Covariate Values: 9

NOTE: Since the chi-square is small (p > 0.1000), fiducial limits will be calculated using a t value of 1.96.

Probit Procedure

Variable	DF	Estimate	Std Err	ChiSquare	Pr>Chi	Label/Value
INTERCPT	1	13.3625774	2.656732	25.29793	0.0001	Intercept
AMT	1	-14.771192	3.047777	23.48902	0.0001	Amount

C=0.5000

Probit Model in Terms of Tolerance Distribution

MU	SIGMA
0.904638	0.067699

Estimated Covariance Matrix for Tolerance Parameters

	MU	SIGMA
MU	0.000146	0.000098672
SIGMA	0.000098672	0.000195

Probit Procedure
Probit Analysis on AMT

Probability	AMT	95 Percent Fiducial Limits	
		Lower	Upper
0.01	1.06213	1.00457	1.19466
0.02	1.04368	0.99119	1.16392
0.03	1.03197	0.98267	1.14444
0.04	1.02316	0.97625	1.12980
0.05	1.01599	0.97101	1.11791
0.06	1.00989	0.96654	1.10780
0.07	1.00455	0.96261	1.09894
0.08	0.99976	0.95908	1.09102
0.09	0.99541	0.95587	1.08382
0.10	0.99140	0.95291	1.07721
0.15	0.97480	0.94055	1.04988
0.20	0.96161	0.93061	1.02829
0.25	0.95030	0.92196	1.00988
0.30	0.94014	0.91406	0.99349
0.35	0.93072	0.90659	0.97845
0.40	0.92179	0.89932	0.96436
0.45	0.91314	0.89205	0.95095
0.50	0.90464	0.88460	0.93806
0.55	0.89613	0.87677	0.92556
0.60	0.88749	0.86827	0.91338
0.65	0.87855	0.85879	0.90150
0.70	0.86914	0.84790	0.88988
0.75	0.85898	0.83504	0.87844
0.80	0.84766	0.81952	0.86690
0.85	0.83447	0.80020	0.85469
0.90	0.81788	0.77466	0.84055
0.91	0.81387	0.76836	0.83727
0.92	0.80952	0.76146	0.83376
0.93	0.80473	0.75383	0.82995
0.94	0.79938	0.74525	0.82574
0.95	0.79328	0.73542	0.82099
0.96	0.78612	0.72380	0.81547
0.97	0.77731	0.70945	0.80877
0.98	0.76560	0.69026	0.79995
0.99	0.74715	0.65987	0.78623

NOTE: The above quantiles and fiducial limits refer to effects due to the independent variable and do not include any effect due to the natural threshold.

DISPLAY=SGI IMAGE=Girl Transform=cm

Probit Procedure
Class Level Information

Class	Levels	Values
CORRECT	2	Yes No

Number of observations used = 271

Probit Procedure

Data Set =WORK.RAW
Dependent Variable=CORRECT

Weighted Frequency Counts for the Ordered Response Categories

Level	Count
Yes	235
No	36

Log Likelihood for NORMAL -81.83719749

Goodness-of-Fit Tests

Statistic	Value	DF	Prob>Chi-Sq
Pearson Chi-Square	8.8537	8	0.3548
L.R. Chi-Square	9.6199	8	0.2927

Response Levels: 2 Number of Covariate Values: 10

NOTE: Since the chi-square is small (p > 0.1000), fiducial limits will be calculated using a t value of 1.96.

Probit Procedure

Variable	DF	Estimate	Std Err	ChiSquare	Pr>Chi	Label/Value
INTERCPT	1	18.9766909	3.841222	24.40631	0.0001	Intercept
AMT	1	-20.15034	4.193435	23.09006	0.0001	Amount

C=0.5000

Probit Model in Terms of Tolerance Distribution

MU	SIGMA
0.941755	0.049627

Estimated Covariance Matrix for Tolerance Parameters

	MU	SIGMA
MU	0.000102	0.000057256
SIGMA	0.000057256	0.000107

Probit Procedure
Probit Analysis on AMT

Probability	AMT	95 Percent Fiducial Limits	
		Lower	Upper
0.01	1.05720	1.01373	1.15739
0.02	1.04368	1.00389	1.13478
0.03	1.03509	0.99762	1.12046
0.04	1.02864	0.99288	1.10970
0.05	1.02338	0.98902	1.10096
0.06	1.01891	0.98573	1.09353
0.07	1.01499	0.98283	1.08703
0.08	1.01148	0.98022	1.08121
0.09	1.00829	0.97785	1.07593
0.10	1.00535	0.97566	1.07107
0.15	0.99319	0.96652	1.05103
0.20	0.98352	0.95914	1.03521
0.25	0.97523	0.95271	1.02174
0.30	0.96778	0.94682	1.00976
0.35	0.96088	0.94124	0.99878
0.40	0.95433	0.93580	0.98851
0.45	0.94799	0.93037	0.97874
0.50	0.94176	0.92480	0.96935
0.55	0.93552	0.91895	0.96023
0.60	0.92918	0.91266	0.95132
0.65	0.92263	0.90570	0.94257
0.70	0.91573	0.89779	0.93392
0.75	0.90828	0.88855	0.92529
0.80	0.89999	0.87745	0.91649
0.85	0.89032	0.86361	0.90713
0.90	0.87816	0.84522	0.89634
0.91	0.87522	0.84066	0.89385
0.92	0.87203	0.83566	0.89119
0.93	0.86852	0.83013	0.88830
0.94	0.86460	0.82390	0.88513
0.95	0.86013	0.81674	0.88156
0.96	0.85487	0.80828	0.87742
0.97	0.84842	0.79780	0.87241
0.98	0.83983	0.78378	0.86583
0.99	0.82631	0.76152	0.85564

NOTE: The above quantiles and fiducial limits refer to effects due to the independent variable and do not include any effect due to the natural threshold.

DISPLAY=SGI IMAGE=Girl Transform=hr

Probit Procedure
Class Level Information

Class	Levels	Values
CORRECT	2	Yes No

Number of observations used = 256

Probit Procedure

Data Set =WORK.RAW
Dependent Variable=CORRECT

Weighted Frequency Counts for the Ordered Response Categories

Level	Count
Yes	229
No	27

Log Likelihood for NORMAL -68.06970268

Goodness-of-Fit Tests

Statistic	Value	DF	Prob>Chi-Sq
Pearson Chi-Square	9.8969	7	0.1945
L.R. Chi-Square	9.6485	7	0.2094

Response Levels: 2 Number of Covariate Values: 9

NOTE: Since the chi-square is small (p > 0.1000), fiducial limits will be calculated using a t value of 1.96.

Probit Procedure

Variable	DF	Estimate	Std Err	ChiSquare	Pr>Chi	Label/Value
INTERCPT	1	-0.6024611	0.323082	3.477213	0.0622	Intercept
AMT	1	0.27524622	0.060587	20.63909	0.0001	Amount

C=0.5000

Probit Model in Terms of Tolerance Distribution

MU	SIGMA
2.188808	3.633111

Estimated Covariance Matrix for Tolerance Parameters

	MU	SIGMA
MU	0.639785	-0.419846
SIGMA	-0.419846	0.639539

Probit Procedure
Probit Analysis on AMT

Probability	AMT	95 Percent Fiducial Limits	
		Lower	Upper
0.01	-6.2631	-14.6339	-2.8491
0.02	-5.2727	-12.9064	-2.1428
0.03	-4.6443	-11.8119	-1.6931
0.04	-4.1716	-10.9895	-1.3539
0.05	-3.7871	-10.3213	-1.0773
0.06	-3.4599	-9.7531	-0.8413
0.07	-3.1729	-9.2554	-0.6338
0.08	-2.9160	-8.8101	-0.4477
0.09	-2.6823	-8.4056	-0.2780
0.10	-2.4672	-8.0336	-0.1215
0.15	-1.5767	-6.4974	0.5308
0.20	-0.8689	-5.2828	1.0555
0.25	-0.2617	-4.2468	1.5116
0.30	0.2836	-3.3227	1.9275
0.35	0.7889	-2.4735	2.3201
0.40	1.2684	-1.6760	2.7008
0.45	1.7323	-0.9146	3.0794
0.50	2.1888	-0.1780	3.4647
0.55	2.6453	0.5418	3.8668
0.60	3.1092	1.2506	4.2980
0.65	3.5887	1.9522	4.7747
0.70	4.0940	2.6487	5.3198
0.75	4.6393	3.3427	5.9658
0.80	5.2465	4.0416	6.7590
0.85	5.9543	4.7685	7.7714
0.90	6.8448	5.5843	9.1441
0.91	7.0599	5.7695	9.4874
0.92	7.2936	5.9669	9.8643
0.93	7.5505	6.1798	10.2828
0.94	7.8375	6.4132	10.7545
0.95	8.1647	6.6746	11.2973
0.96	8.5492	6.9765	11.9403
0.97	9.0219	7.3413	12.7371
0.98	9.6503	7.8179	13.8047
0.99	10.6407	8.5552	15.5012

NOTE: The above quantiles and fiducial limits refer to effects due to the independent variable and do not include any effect due to the natural threshold.

DISPLAY=SGI IMAGE=Girl Transform=ls

Probit Procedure
Class Level Information

Class	Levels	Values
CORRECT	2	Yes No

Number of observations used 273

Probit Procedure

Data Set =WORK.RAW
Dependent Variable=CORRECT

Weighted Frequency Counts for the Ordered Response Categories

Level	Count
Yes	205
No	68

Log Likelihood for NORMAL -132.3191278

Goodness-of-Fit Tests

Statistic	Value	DF	Prob>Chi-Sq
Pearson Chi-Square	6.5592	7	0.4762
L.R. Chi-Square	6.6719	7	0.4638

Response Levels: 2 Number of Covariate Values: 9

NOTE: Since the chi-square is small (p > 0.1000), fiducial limits will be calculated using a t value of 1.96.

Probit Procedure

Variable	DF	Estimate	Std Err	ChiSquare	Pr>Chi	Label/Value
INTERCPT	1	15.6442764	3.175428	24.27205	0.0001	Intercept
AMT	1	-18.015344	3.72258	23.42054	0.0001	Amount

C=0.5000

Probit Model in Terms of Tolerance Distribution

MU	SIGMA
0.868386	0.055508

Estimated Covariance Matrix for Tolerance Parameters

	MU	SIGMA
MU	0.000086500	0.000038866
SIGMA	0.000038866	0.000132

Probit Procedure
Probit Analysis on AMT

Probability	AMT	95 Percent Fiducial Limits	
		Lower	Upper
0.01	0.99752	0.95316	1.09898
0.02	0.98239	0.94213	1.07382
0.03	0.97279	0.93509	1.05789
0.04	0.96556	0.92978	1.04592
0.05	0.95969	0.92544	1.03620
0.06	0.95469	0.92173	1.02795
0.07	0.95030	0.91847	1.02072
0.08	0.94638	0.91554	1.01426
0.09	0.94281	0.91287	1.00839
0.10	0.93952	0.91040	1.00299
0.15	0.92592	0.90008	0.98077
0.20	0.91510	0.89171	0.96326
0.25	0.90583	0.88437	0.94841
0.30	0.89749	0.87760	0.93525
0.35	0.88977	0.87111	0.92326
0.40	0.88245	0.86471	0.91214
0.45	0.87536	0.85820	0.90170
0.50	0.86839	0.85141	0.89180
0.55	0.86141	0.84414	0.88238
0.60	0.85432	0.83618	0.87338
0.65	0.84700	0.82729	0.86474
0.70	0.83928	0.81722	0.85635
0.75	0.83095	0.80564	0.84800
0.80	0.82167	0.79205	0.83940
0.85	0.81086	0.77555	0.83002
0.90	0.79725	0.75414	0.81888
0.91	0.79396	0.74889	0.81627
0.92	0.79039	0.74316	0.81345
0.93	0.78647	0.73684	0.81039
0.94	0.78208	0.72975	0.80699
0.95	0.77708	0.72162	0.80315
0.96	0.77121	0.71204	0.79867
0.97	0.76399	0.70022	0.79322
0.98	0.75439	0.68444	0.78604
0.99	0.73925	0.65945	0.77482

NOTE: The above quantiles and fiducial limits refer to effects due to the independent variable and do not include any effect due to the natural threshold.

A.3. IBM Roentgen LCD Prototype

DISPLAY=IBM IMAGE=Curr Transform=cm

Probit Procedure
Class Level Information

Class	Levels	Values
CORRECT	2	Yes No

Number of observations used = 296

Probit Procedure

Data Set =WORK.RAW
Dependent Variable=CORRECT

Weighted Frequency Counts for the Ordered Response Categories

Level	Count
Yes	243
No	53

Log Likelihood for NORMAL -131.8036551

Goodness-of-Fit Tests

Statistic	Value	DF	Prob>Chi-Sq
Pearson Chi-Square	3.2649	6	0.7749
L.R. Chi-Square	3.3577	6	0.7628

Response Levels: 2 Number of Covariate Values: 8

NOTE: Since the chi-square is small (p > 0.1000), fiducial limits will be calculated using a t value of 1.96.

Probit Procedure

Variable	DF	Estimate	Std Err	ChiSquare	Pr>Chi	Label/Value
INTERCPT	1	6.55914894	1.711341	14.69	0.0001	Intercept
AMT	1	-7.0866459	1.965692	12.99723	0.0003	Amount

C=0.5000

Probit Model in Terms of Tolerance Distribution

MU	SIGMA
0.925565	0.14111

Estimated Covariance Matrix for Tolerance Parameters

	MU	SIGMA
MU	0.000572	0.000623
SIGMA	0.000623	0.001532

Probit Procedure
Probit Analysis on AMT

Probability	AMT	95 Percent Fiducial Limits	
		Lower	Upper
0.01	1.25384	1.11512	1.71616
0.02	1.21537	1.08988	1.63218
0.03	1.19096	1.07383	1.57894
0.04	1.17260	1.06173	1.53892
0.05	1.15767	1.05187	1.50638
0.06	1.14496	1.04346	1.47870
0.07	1.13381	1.03607	1.45444
0.08	1.12383	1.02945	1.43273
0.09	1.11476	1.02341	1.41300
0.10	1.10641	1.01784	1.39485
0.15	1.07182	0.99467	1.31982
0.20	1.04433	0.97604	1.26039
0.25	1.02074	0.95985	1.20963
0.30	0.99956	0.94505	1.16429
0.35	0.97994	0.93103	1.12260
0.40	0.96131	0.91729	1.08346
0.45	0.94330	0.90340	1.04620
0.50	0.92556	0.88880	1.01045
0.55	0.90783	0.87273	0.97618
0.60	0.88981	0.85395	0.94380
0.65	0.87119	0.83065	0.91423
0.70	0.85157	0.80092	0.88824
0.75	0.83039	0.76359	0.86544
0.80	0.80680	0.71789	0.84418
0.85	0.77931	0.66170	0.82231
0.90	0.74472	0.58886	0.79695
0.91	0.73637	0.57107	0.79103
0.92	0.72729	0.55167	0.78465
0.93	0.71732	0.53028	0.77771
0.94	0.70617	0.50633	0.77002
0.95	0.69346	0.47895	0.76131
0.96	0.67852	0.44670	0.75116
0.97	0.66016	0.40696	0.73877
0.98	0.63576	0.35403	0.72242
0.99	0.59729	0.27040	0.69683

NOTE: The above quantiles and fiducial limits refer to effects due to the independent variable and do not include any effect due to the natural threshold.

DISPLAY=IBM IMAGE=Curr Transform=hr

Probit Procedure
Class Level Information

Class	Levels	Values
CORRECT	2	Yes No

Number of observations used 296

Probit Procedure

Data Set =WORK.RAW
Dependent Variable=CORRECT

Weighted Frequency Counts for the Ordered Response Categories

Level	Count
Yes	236
No	60

Log Likelihood for NORMAL -142.1535399

Goodness-of-Fit Tests

Statistic	Value	DF	Prob>Chi-Sq
Pearson Chi-Square	8.3679	6	0.2124
L.R. Chi-Square	8.8221	6	0.1838

Response Levels: 2 Number of Covariate Values: 8

NOTE: Since the chi-square is small (p > 0.1000), fiducial limits will be calculated using a t value of 1.96.

Probit Procedure

Variable	DF	Estimate	Std Err	ChiSquare	Pr>Chi	Label/Value
INTERCPT	1	-0.47384	0.247212	3.673885	0.0553	Intercept
AMT	1	0.09883627	0.027447	12.96671	0.0003	Amount

C=0.5000

Probit Model in Terms of Tolerance Distribution

MU	SIGMA
4.794191	10.11774

Estimated Covariance Matrix for Tolerance Parameters

	MU	SIGMA
MU	2.309101	-2.294510
SIGMA	-2.294510	7.894732

Probit Procedure
Probit Analysis on AMT

Probability	AMT	95 Percent Fiducial Limits	
		Lower	Upper
0.01	-18.743	-50.587	-9.193
0.02	-15.985	-44.560	-7.382
0.03	-14.235	-40.739	-6.230
0.04	-12.919	-37.867	-5.361
0.05	-11.848	-35.532	-4.653
0.06	-10.937	-33.546	-4.049
0.07	-10.137	-31.805	-3.518
0.08	-9.422	-30.248	-3.041
0.09	-8.771	-28.833	-2.607
0.10	-8.172	-27.531	-2.207
0.15	-5.692	-22.153	-0.537
0.20	-3.721	-17.897	0.809
0.25	-2.030	-14.266	1.983
0.30	-0.512	-11.029	3.063
0.35	0.896	-8.062	4.095
0.40	2.231	-5.291	5.118
0.45	3.523	-2.675	6.174
0.50	4.794	-0.204	7.316
0.55	6.066	2.102	8.623
0.60	7.357	4.190	10.207
0.65	8.693	6.012	12.180
0.70	10.100	7.587	14.604
0.75	11.619	9.012	17.495
0.80	13.309	10.407	20.906
0.85	15.281	11.898	25.017
0.90	17.761	13.669	30.294
0.91	18.360	14.086	31.579
0.92	19.010	14.537	32.978
0.93	19.726	15.028	34.520
0.94	20.525	15.574	36.245
0.95	21.436	16.192	38.217
0.96	22.507	16.915	40.538
0.97	23.824	17.798	43.396
0.98	25.573	18.965	47.202
0.99	28.332	20.793	53.212

NOTE: The above quantiles and fiducial limits refer to effects due to the independent variable and do not include any effect due to the natural threshold.

DISPLAY=IBM IMAGE=Curr Transform=ls

Probit Procedure
Class Level Information

Class	Levels	Values
CORRECT	2	Yes No

Number of observations used 333

Probit Procedure

Data Set =WORK.RAW
Dependent Variable=CORRECT

Weighted Frequency Counts for the Ordered Response Categories

Level	Count
Yes	256
No	77

Log Likelihood for NORMAL -159.1950179

Goodness-of-Fit Tests

Statistic	Value	DF	Prob>Chi-Sq
Pearson Chi-Square	4.8110	7	0.6830
L.R. Chi-Square	4.8456	7	0.6788

Response Levels: 2 Number of Covariate Values: 9

NOTE: Since the chi-square is small (p > 0.1000), fiducial limits will be calculated using a t value of 1.96.

Probit Procedure

Variable	DF	Estimate	Std Err	ChiSquare	Pr>Chi	Label/Value
INTERCPT	1	12.0889226	2.221837	29.60403	0.0001	Intercept
AMT	1	-13.876733	2.607609	28.31975	0.0001	Amount

C=0.5000

Probit Model in Terms of Tolerance Distribution

MU	SIGMA
0.871165	0.072063

Estimated Covariance Matrix for Tolerance Parameters

	MU	SIGMA
MU	0.000108	0.000052539
SIGMA	0.000052539	0.000183

Probit Procedure
Probit Analysis on AMT

Probability	AMT	95 Percent Fiducial Limits	
		Lower	Upper
0.01	1.03881	0.98560	1.15112
0.02	1.01916	0.97096	1.12030
0.03	1.00670	0.96164	1.10079
0.04	0.99732	0.95460	1.08613
0.05	0.98970	0.94886	1.07422
0.06	0.98321	0.94396	1.06410
0.07	0.97751	0.93965	1.05524
0.08	0.97242	0.93578	1.04732
0.09	0.96778	0.93226	1.04012
0.10	0.96352	0.92900	1.03350
0.15	0.94585	0.91541	1.00623
0.20	0.93181	0.90443	0.98472
0.25	0.91977	0.89483	0.96645
0.30	0.90895	0.88600	0.95025
0.35	0.89893	0.87759	0.93547
0.40	0.88942	0.86932	0.92173
0.45	0.88022	0.86097	0.90880
0.50	0.87116	0.85229	0.89652
0.55	0.86211	0.84304	0.88481
0.60	0.85291	0.83296	0.87360
0.65	0.84340	0.82176	0.86280
0.70	0.83337	0.80912	0.85225
0.75	0.82256	0.79464	0.84170
0.80	0.81052	0.77774	0.83074
0.85	0.79648	0.75730	0.81869
0.90	0.77881	0.73088	0.80424
0.91	0.77455	0.72442	0.80083
0.92	0.76991	0.71737	0.79715
0.93	0.76481	0.70959	0.79314
0.94	0.75912	0.70087	0.78869
0.95	0.75263	0.69088	0.78365
0.96	0.74501	0.67912	0.77777
0.97	0.73563	0.66460	0.77059
0.98	0.72317	0.64524	0.76112
0.99	0.70352	0.61461	0.74629

NOTE: The above quantiles and fiducial limits refer to effects due to the independent variable and do not include any effect due to the natural threshold.

DISPLAY=IBM IMAGE=Flow Transform=cm

Probit Procedure
Class Level Information

Class	Levels	Values
CORRECT	2	Yes No

Number of observations used = 296

Probit Procedure

Data Set =WORK.RAW
Dependent Variable=CORRECT

Weighted Frequency Counts for the Ordered Response Categories

Level	Count
Yes	220
No	76

Log Likelihood for NORMAL -159.0230664

Goodness-of-Fit Tests

Statistic	Value	DF	Prob>Chi-Sq
Pearson Chi-Square	2.5651	6	0.8611
L.R. Chi-Square	2.5420	6	0.8637

Response Levels: 2 Number of Covariate Values: 8

NOTE: Since the chi-square is small (p > 0.1000), fiducial limits will be calculated using a t value of 1.96.

Probit Procedure

Variable	DF	Estimate	Std Err	ChiSquare	Pr>Chi	Label/Value
INTERCPT	1	7.95035728	2.033282	15.28897	0.0001	Intercept
AMT	1	-9.2138581	2.391637	14.842	0.0001	Amount

C=0.5000

Probit Model in Terms of Tolerance Distribution

MU	SIGMA
0.86287	0.108532

Estimated Covariance Matrix for Tolerance Parameters

	MU	SIGMA
MU	0.000245	0.000108
SIGMA	0.000108	0.000794

Probit Procedure
Probit Analysis on AMT

Probability	AMT	95 Percent Fiducial Limits	
		Lower	Upper
0.01	1.11535	1.02202	1.39532
0.02	1.08577	1.00202	1.33548
0.03	1.06700	0.98927	1.29758
0.04	1.05288	0.97965	1.26909
0.05	1.04139	0.97179	1.24595
0.06	1.03161	0.96509	1.22628
0.07	1.02304	0.95918	1.20905
0.08	1.01536	0.95388	1.19364
0.09	1.00838	0.94904	1.17964
0.10	1.00196	0.94457	1.16677
0.15	0.97536	0.92586	1.11370
0.20	0.95421	0.91065	1.07186
0.25	0.93607	0.89722	1.03634
0.30	0.91978	0.88468	1.00492
0.35	0.90469	0.87245	0.97642
0.40	0.89037	0.85999	0.95023
0.45	0.87651	0.84673	0.92610
0.50	0.86287	0.83198	0.90404
0.55	0.84923	0.81502	0.88420
0.60	0.83537	0.79524	0.86659
0.65	0.82105	0.77232	0.85085
0.70	0.80596	0.74611	0.83633
0.75	0.78967	0.71626	0.82223
0.80	0.77153	0.68182	0.80771
0.85	0.75038	0.64075	0.79174
0.90	0.72378	0.58824	0.77246
0.91	0.71735	0.57547	0.76789
0.92	0.71037	0.56157	0.76296
0.93	0.70270	0.54625	0.75756
0.94	0.69413	0.52910	0.75157
0.95	0.68435	0.50952	0.74478
0.96	0.67286	0.48646	0.73684
0.97	0.65874	0.45807	0.72713
0.98	0.63997	0.42025	0.71429
0.99	0.61039	0.36053	0.69418

NOTE: The above quantiles and fiducial limits refer to effects due to the independent variable and do not include any effect due to the natural threshold.

DISPLAY=IBM IMAGE=Flow Transform=hr

Probit Procedure
Class Level Information

Class	Levels	Values
CORRECT	2	Yes No

Number of observations used 296

Probit Procedure

Data Set =WORK.RAW
Dependent Variable=CORRECT

Weighted Frequency Counts for the Ordered Response Categories

Level	Count
Yes	217
No	79

Log Likelihood for NORMAL -155.963749

Goodness-of-Fit Tests

Statistic	Value	DF	Prob>Chi-Sq
Pearson Chi-Square	11.7220	6	0.0685
L.R. Chi-Square	12.4207	6	0.0532

Response Levels: 2 Number of Covariate Values: 8

WARNING: All variances and covariances have been multiplied by the heterogeneity factor H= 1.9537. Please check to be sure that the large chi-square (p < 0.0685) is not caused by systematic departure from the model. A t value of 2.4469 will be used in computing fiducial limits.

Probit Procedure

Variable	DF	Estimate	Std Err	ChiSquare	Pr>Chi	Label/Value
INTERCPT	1	-1.3395218	0.470687	8.099071	0.0044	Intercept
AMT	1	0.16886126	0.048623	12.06101	0.0005	Amount

C=0.5000

Probit Model in Terms of Tolerance Distribution

MU	SIGMA
7.932677	5.922021

Estimated Covariance Matrix for Tolerance Parameters

	MU	SIGMA
MU	1.504847	-0.390973
SIGMA	-0.390973	2.907745

Probit Procedure
Probit Analysis on AMT

Probability	AMT	95 Percent Fiducial Limits	
		Lower	Upper
0.01	-5.8440	-41.0188	0.5987
0.02	-4.2297	-35.6053	1.5968
0.03	-3.2054	-32.1775	2.2368
0.04	-2.4349	-29.6034	2.7229
0.05	-1.8082	-27.5131	3.1217
0.06	-1.2747	-25.7368	3.4640
0.07	-0.8070	-24.1818	3.7667
0.08	-0.3882	-22.7918	4.0401
0.09	-0.0073	-21.5298	4.2908
0.10	0.3433	-20.3701	4.5236
0.15	1.7949	-15.5949	5.5135
0.20	2.9486	-11.8424	6.3429
0.25	3.9383	-8.6706	7.1021
0.30	4.8272	-5.8799	7.8415
0.35	5.6508	-3.3682	8.6010
0.40	6.4323	-1.0845	9.4212
0.45	7.1885	0.9889	10.3510
0.50	7.9327	2.8456	11.4499
0.55	8.6768	4.4695	12.7815
0.60	9.4330	5.8565	14.3976
0.65	10.2146	7.0328	16.3253
0.70	11.0382	8.0510	18.5783
0.75	11.9270	8.9732	21.1862
0.80	12.9168	9.8619	24.2284
0.85	14.0705	10.7850	27.8872
0.90	15.5221	11.8455	32.5919
0.91	15.8727	12.0905	33.7394
0.92	16.2535	12.3529	34.9897
0.93	16.6723	12.6376	36.3683
0.94	17.1401	12.9513	37.9123
0.95	17.6735	13.3045	39.6777
0.96	18.3003	13.7141	41.7573
0.97	19.0708	14.2112	44.3203
0.98	20.0950	14.8630	47.7364
0.99	21.7094	15.8747	53.1363

NOTE: The above quantiles and fiducial limits refer to effects due to the independent variable and do not include any effect due to the natural threshold.

DISPLAY=IBM IMAGE=Flow Transform=ls

Probit Procedure
Class Level Information

Class	Levels	Values
CORRECT	2	Yes No

Number of observations used 333

Probit Procedure

Data Set =WORK.RAW
Dependent Variable=CORRECT

Weighted Frequency Counts for the Ordered Response Categories

Level	Count
Yes	243
No	90

Log Likelihood for NORMAL -189.1796042

Goodness-of-Fit Tests

Statistic	Value	DF	Prob>Chi-Sq
Pearson Chi-Square	4.0115	7	0.7785
L.R. Chi-Square	4.0763	7	0.7709

Response Levels: 2 Number of Covariate Values: 9

NOTE: Since the chi-square is small (p > 0.1000), fiducial limits will be calculated using a t value of 1.96.

Probit Procedure

Variable	DF	Estimate	Std Err	ChiSquare	Pr>Chi	Label/Value
INTERCPT	1	5.58907318	1.857928	9.049445	0.0026	Intercept
AMT	1	-6.6313152	2.194197	9.133731	0.0025	Amount

C=0.5000

Probit Model in Terms of Tolerance Distribution

MU	SIGMA
0.84283	0.1508

Estimated Covariance Matrix for Tolerance Parameters

	MU	SIGMA
MU	0.000368	-0.000031892
SIGMA	-0.000031892	0.002490

Probit Procedure
Probit Analysis on AMT

Probability	AMT	95 Percent Fiducial Limits	
		Lower	Upper
0.01	1.19364	1.05329	1.84051
0.02	1.15253	1.02794	1.72396
0.03	1.12645	1.01180	1.65007
0.04	1.10683	0.99961	1.59453
0.05	1.09087	0.98967	1.54939
0.06	1.07729	0.98117	1.51099
0.07	1.06538	0.97370	1.47735
0.08	1.05471	0.96699	1.44725
0.09	1.04502	0.96087	1.41990
0.10	1.03609	0.95521	1.39474
0.15	0.99912	0.93149	1.29087
0.20	0.96975	0.91212	1.20882
0.25	0.94454	0.89487	1.13908
0.30	0.92191	0.87845	1.07738
0.35	0.90094	0.86178	1.02165
0.40	0.88103	0.84345	0.97128
0.45	0.86178	0.82123	0.92704
0.50	0.84283	0.79202	0.89084
0.55	0.82388	0.75411	0.86334
0.60	0.80463	0.70875	0.84223
0.65	0.78472	0.65776	0.82452
0.70	0.76375	0.60170	0.80818
0.75	0.74112	0.53981	0.79196
0.80	0.71591	0.46995	0.77482
0.85	0.68654	0.38783	0.75553
0.90	0.64957	0.28390	0.73187
0.91	0.64064	0.25873	0.72622
0.92	0.63095	0.23137	0.72010
0.93	0.62028	0.20126	0.71339
0.94	0.60837	0.16761	0.70593
0.95	0.59479	0.12921	0.69745
0.96	0.57883	0.08406	0.68751
0.97	0.55921	0.02851	0.67533
0.98	0.53313	-0.04539	0.65920
0.99	0.49202	-0.16194	0.63386

NOTE: The above quantiles and fiducial limits refer to effects due to the independent variable and do not include any effect due to the natural threshold.

```
DISPLAY=IBM IMAGE=Girl Transform=cm

 Probit Procedure
 Class Level Information

 Class    Levels    Values

 CORRECT       2    Yes No

 Number of observations used = 296


 Probit Procedure

 Data Set          =WORK.RAW
 Dependent Variable=CORRECT

 Weighted Frequency Counts for the Ordered Response Categories

 Level     Count
 Yes       246
  No        50


 Log Likelihood for NORMAL -121.1251998


                Goodness-of-Fit Tests

 Statistic                  Value      DF   Prob>Chi-Sq
 ------------------        --------    --   -----------
 Pearson Chi-Square          7.4406     6        0.2820
 L.R.    Chi-Square          7.1660     6        0.3058

 Response Levels:   2  Number of Covariate Values:    8


 NOTE: Since the chi-square is small (p > 0.1000), fiducial
       limits will be calculated using a t value of  1.96.

 Probit Procedure

 Variable  DF   Estimate  Std Err ChiSquare  Pr>Chi Label/Value

 INTERCPT   1 9.14614725 1.882271  23.61086  0.0001 Intercept
 AMT        1  -9.929133 2.147497  21.37754  0.0001 Amount

 C=0.5000


 Probit Model in Terms of Tolerance Distribution

           MU         SIGMA
     0.921143      0.100714


 Estimated Covariance Matrix for Tolerance Parameters

                             MU             SIGMA

          MU           0.000281          0.000221
       SIGMA           0.000221          0.000474
```

Probit Procedure
Probit Analysis on AMT

Probability	AMT	95 Percent Fiducial Limits	
		Lower	Upper
0.01	1.15544	1.06889	1.36516
0.02	1.12798	1.04931	1.31780
0.03	1.11056	1.03685	1.28779
0.04	1.09746	1.02745	1.26524
0.05	1.08680	1.01979	1.24691
0.06	1.07773	1.01326	1.23133
0.07	1.06977	1.00752	1.21767
0.08	1.06265	1.00237	1.20545
0.09	1.05618	0.99768	1.19435
0.10	1.05021	0.99335	1.18414
0.15	1.02553	0.97532	1.14198
0.20	1.00591	0.96083	1.10864
0.25	0.98907	0.94822	1.08020
0.30	0.97396	0.93672	1.05486
0.35	0.95995	0.92583	1.03159
0.40	0.94666	0.91523	1.00979
0.45	0.93380	0.90461	0.98905
0.50	0.92114	0.89368	0.96913
0.55	0.90849	0.88207	0.94988
0.60	0.89563	0.86933	0.93126
0.65	0.88234	0.85486	0.91333
0.70	0.86833	0.83791	0.89612
0.75	0.85321	0.81766	0.87952
0.80	0.83638	0.79312	0.86302
0.85	0.81676	0.76265	0.84565
0.90	0.79207	0.72264	0.82547
0.91	0.78611	0.71280	0.82078
0.92	0.77963	0.70204	0.81574
0.93	0.77251	0.69016	0.81025
0.94	0.76456	0.67683	0.80419
0.95	0.75548	0.66157	0.79734
0.96	0.74482	0.64355	0.78936
0.97	0.73172	0.62132	0.77965
0.98	0.71430	0.59164	0.76686
0.99	0.68685	0.54467	0.74689

NOTE: The above quantiles and fiducial limits refer to effects due to the independent variable and do not include any effect due to the natural threshold.

DISPLAY=IBM IMAGE=Girl Transform=hr

Probit Procedure
Class Level Information

Class	Levels	Values
CORRECT	2	Yes No

Number of observations used 296

Probit Procedure

Data Set =WORK.RAW
Dependent Variable=CORRECT

Weighted Frequency Counts for the Ordered Response Categories

Level	Count
Yes	243
No	53

Log Likelihood for NORMAL -115.3007536

Goodness-of-Fit Tests

Statistic	Value	DF	Prob>Chi-Sq
Pearson Chi-Square	10.6710	6	0.0991
L.R. Chi-Square	7.9709	6	0.2402

Response Levels: 2 Number of Covariate Values: 8

WARNING: All variances and covariances have been multiplied by the heterogeneity factor H= 1.7785. Please check to be sure that the large chi-square (p < 0.0991) is not caused by systematic departure from the model. A t value of 2.4469 will be used in computing fiducial limits.

Probit Procedure

Variable	DF	Estimate	Std Err	ChiSquare	Pr>Chi	Label/Value
INTERCPT	1	-1.0127339	0.387375	6.834828	0.0089	Intercept
AMT	1	0.21397404	0.050964	17.62758	0.0001	Amount

C=0.5000

Probit Model in Terms of Tolerance Distribution

MU	SIGMA
4.732976	4.673464

Estimated Covariance Matrix for Tolerance Parameters

	MU	SIGMA
MU	1.004643	-0.494724
SIGMA	-0.494724	1.239039

Probit Procedure
Probit Analysis on AMT

Probability	AMT	95 Percent Fiducial Limits	
		Lower	Upper
0.01	-6.1391	-24.2546	-1.1279
0.02	-4.8651	-21.2354	-0.2885
0.03	-4.0568	-19.3239	0.2481
0.04	-3.4488	-17.8885	0.6543
0.05	-2.9542	-16.7229	0.9867
0.06	-2.5332	-15.7323	1.2712
0.07	-2.1641	-14.8652	1.5220
0.08	-1.8336	-14.0899	1.7478
0.09	-1.5330	-13.3859	1.9542
0.10	-1.2563	-12.7389	2.1452
0.15	-0.1108	-10.0726	2.9485
0.20	0.7997	-7.9726	3.6060
0.25	1.5808	-6.1903	4.1893
0.30	2.2822	-4.6109	4.7344
0.35	2.9322	-3.1719	5.2641
0.40	3.5490	-1.8362	5.7965
0.45	4.1457	-0.5812	6.3488
0.50	4.7330	0.6061	6.9402
0.55	5.3202	1.7313	7.5937
0.60	5.9170	2.7948	8.3375
0.65	6.5338	3.7944	9.2060
0.70	7.1837	4.7305	10.2385
0.75	7.8852	5.6130	11.4805
0.80	8.6663	6.4666	12.9926
0.85	9.5767	7.3368	14.8800
0.90	10.7223	8.3087	17.3776
0.91	10.9989	8.5295	17.9948
0.92	11.2995	8.7647	18.6700
0.93	11.6300	9.0184	19.4173
0.94	11.9992	9.2965	20.2571
0.95	12.4201	9.6080	21.2207
0.96	12.9147	9.9675	22.3593
0.97	13.5228	10.4014	23.7670
0.98	14.3311	10.9674	25.6491
0.99	15.6051	11.8412	28.6339

NOTE: The above quantiles and fiducial limits refer to effects due to the independent variable and do not include any effect due to the natural threshold.

DISPLAY=IBM IMAGE=Girl Transform=ls

Probit Procedure
Class Level Information

Class	Levels	Values
CORRECT	2	Yes No

Number of observations used 333

Probit Procedure

Data Set =WORK.RAW
Dependent Variable=CORRECT

Weighted Frequency Counts for the Ordered Response Categories

Level	Count
Yes	270
No	63

Log Likelihood for NORMAL -154.6747783

Goodness-of-Fit Tests

Statistic	Value	DF	Prob>Chi-Sq
Pearson Chi-Square	12.1155	7	0.0968
L.R. Chi-Square	15.0185	7	0.0358

Response Levels: 2 Number of Covariate Values: 9

WARNING: All variances and covariances have been multiplied by the heterogeneity factor H= 1.7308. Please check to be sure that the large chi-square (p < 0.0968) is not caused by systematic departure from the model. A t value of 2.3646 will be used in computing fiducial limits.

Probit Procedure

Variable	DF	Estimate	Std Err	ChiSquare	Pr>Chi	Label/Value
INTERCPT	1	6.22777509	2.191146	8.078359	0.0045	Intercept
AMT	1	-6.849515	2.548868	7.221461	0.0072	Amount

C=0.5000

Probit Model in Terms of Tolerance Distribution

MU	SIGMA
0.909229	0.145996

Estimated Covariance Matrix for Tolerance Parameters

	MU	SIGMA
MU	0.000882	0.001046
SIGMA	0.001046	0.002952

Probit Procedure
Probit Analysis on AMT

Probability	AMT	95 Percent Fiducial Limits	
		Lower	Upper
0.01	1.24887	1.06153	4.12138
0.02	1.20907	1.03989	3.79036
0.03	1.18382	1.02611	3.58040
0.04	1.16482	1.01570	3.42249
0.05	1.14937	1.00720	3.29407
0.06	1.13622	0.99994	3.18480
0.07	1.12469	0.99356	3.08900
0.08	1.11436	0.98783	3.00325
0.09	1.10497	0.98259	2.92527
0.10	1.09633	0.97776	2.85352
0.15	1.06054	0.95754	2.55663
0.20	1.03210	0.94113	2.32102
0.25	1.00770	0.92667	2.11926
0.30	0.98579	0.91323	1.93854
0.35	0.96548	0.90015	1.77169
0.40	0.94622	0.88683	1.61428
0.45	0.92757	0.87248	1.46343
0.50	0.90923	0.85572	1.31764
0.55	0.89088	0.83331	1.17747
0.60	0.87224	0.79640	1.04920
0.65	0.85297	0.72347	0.95140
0.70	0.83267	0.59898	0.89597
0.75	0.81076	0.43617	0.86461
0.80	0.78636	0.24292	0.84164
0.85	0.75791	0.01201	0.82052
0.90	0.72213	-0.28194	0.79737
0.91	0.71348	-0.35323	0.79207
0.92	0.70409	-0.43077	0.78641
0.93	0.69377	-0.51611	0.78026
0.94	0.68224	-0.61152	0.77349
0.95	0.66909	-0.72042	0.76586
0.96	0.65364	-0.84848	0.75699
0.97	0.63464	-1.00602	0.74622
0.98	0.60939	-1.21560	0.73205
0.99	0.56959	-1.54619	0.70999

NOTE: The above quantiles and fiducial limits refer to effects due to the independent variable and do not include any effect due to the natural threshold.

A.4. FJX® Pictrography™ 3000 Printer

```
Display=FJX IMAGE=Curr XFORM=CM

 Probit Procedure
 Class Level Information

 Class     Levels    Values

 CORRECT        2    Yes No

 Number of observations used   1260


 Probit Procedure

 Data Set          =WORK.RAW
 Dependent Variable=CORRECT

 Weighted Frequency Counts for the Ordered Response Categories

 Level      Count
 Yes         1134
  No          126


 Log Likelihood for NORMAL -352.6031758


                Goodness-of-Fit Tests

 Statistic                  Value      DF   Prob>Chi-Sq
 ------------------        --------    --   -----------
 Pearson Chi-Square         21.9954    16        0.1433
 L.R.    Chi-Square         18.9331    16        0.2721

 Response Levels:   2  Number of Covariate Values:   18


 NOTE: Since the chi-square is small (p > 0.1000), fiducial
       limits will be calculated using a t value of  1.96.

 Probit Procedure

 Variable  DF   Estimate  Std Err ChiSquare  Pr>Chi Label/Value

 INTERCPT   1 -0.3251587 0.141917  5.249583  0.0220 Intercept
 AMT        1  15.105396 1.764839  73.25785  0.0001 Amount

 C=0.5000


 Probit Model in Terms of Tolerance Distribution

           MU          SIGMA
     0.021526       0.066202


 Estimated Covariance Matrix for Tolerance Parameters

                             MU             SIGMA

          MU        0.000053470      -0.000043782
       SIGMA       -0.000043782       0.000059825
```

Probit Procedure
Probit Analysis on AMT

Probability	AMT	95 Percent Fiducial Limits	
		Lower	Upper
0.01	-0.132482	-0.193494	-0.093878
0.02	-0.114435	-0.170171	-0.079110
0.03	-0.102985	-0.155383	-0.069731
0.04	-0.094372	-0.144264	-0.062671
0.05	-0.087366	-0.135223	-0.056923
0.06	-0.081402	-0.127532	-0.052028
0.07	-0.076174	-0.120791	-0.047733
0.08	-0.071492	-0.114757	-0.043885
0.09	-0.067234	-0.109272	-0.040383
0.10	-0.063315	-0.104225	-0.037158
0.15	-0.047087	-0.083352	-0.023780
0.20	-0.034191	-0.066799	-0.013112
0.25	-0.023126	-0.052633	-0.003925
0.30	-0.013190	-0.039947	0.004362
0.35	-0.003983	-0.028233	0.012082
0.40	0.004754	-0.017167	0.019456
0.45	0.013207	-0.006520	0.026651
0.50	0.021526	0.003879	0.033810
0.55	0.029845	0.014173	0.041075
0.60	0.038298	0.024483	0.048606
0.65	0.047035	0.034920	0.056610
0.70	0.056242	0.045588	0.065376
0.75	0.066178	0.056602	0.075334
0.80	0.077243	0.068160	0.087129
0.85	0.090139	0.080738	0.101773
0.90	0.106367	0.095566	0.121196
0.91	0.110286	0.099034	0.125999
0.92	0.114544	0.102767	0.131254
0.93	0.119226	0.106834	0.137069
0.94	0.124454	0.111338	0.143601
0.95	0.130418	0.116435	0.151090
0.96	0.137424	0.122380	0.159934
0.97	0.146037	0.129637	0.170857
0.98	0.157487	0.139219	0.185442
0.99	0.175534	0.154216	0.208535

NOTE: The above quantiles and fiducial limits refer to effects due to the independent variable and do not include any effect due to the natural threshold.

DISPLAY=FJX IMAGE=Curr XFORM=HR

Probit Procedure
Class Level Information

Class	Levels	Values
CORRECT	2	Yes No

Number of observations used 1260

Probit Procedure

Data Set =WORK.RAW
Dependent Variable=CORRECT

Weighted Frequency Counts for the Ordered Response Categories

Level	Count
Yes	1178
No	82

Log Likelihood for NORMAL -242.26446

Goodness-of-Fit Tests

Statistic	Value	DF	Prob>Chi-Sq
Pearson Chi-Square	78.0611	21	0.0000
L.R. Chi-Square	38.3826	21	0.0116

Response Levels: 2 Number of Covariate Values: 23

WARNING: All variances and covariances have been multiplied by the heterogeneity factor H= 3.7172. Please check to be sure that the large chi-square (p < 0.0001) is not caused by systematic departure from the model. A t value of 2.0796 will be used in computing fiducial limits.

Probit Procedure

Variable	DF	Estimate	Std Err	ChiSquare	Pr>Chi	Label/Value
INTERCPT	1	-0.2383963	0.312678	0.581305	0.4458	Intercept
AMT	1	0.31742491	0.076949	17.01673	0.0001	Amount

C=0.5000

Probit Model in Terms of Tolerance Distribution

MU	SIGMA
0.751032	3.150351

Estimated Covariance Matrix for Tolerance Parameters

	MU	SIGMA
MU	0.692358	-0.513455
SIGMA	-0.513455	0.583233

Probit Procedure
Probit Analysis on AMT

Probability	AMT	95 Percent Fiducial Limits	
		Lower	Upper
0.01	-6.5778	-16.9496	-3.0906
0.02	-5.7190	-15.2269	-2.5104
0.03	-5.1741	-14.1349	-2.1413
0.04	-4.7642	-13.3140	-1.8632
0.05	-4.4308	-12.6467	-1.6365
0.06	-4.1471	-12.0790	-1.4432
0.07	-3.8982	-11.5815	-1.2734
0.08	-3.6754	-11.1364	-1.1212
0.09	-3.4728	-10.7317	-0.9825
0.10	-3.2863	-10.3594	-0.8546
0.15	-2.5141	-8.8205	-0.3229
0.20	-1.9004	-7.6009	0.1032
0.25	-1.3738	-6.5579	0.4720
0.30	-0.9010	-5.6247	0.8068
0.35	-0.4629	-4.7638	1.1207
0.40	-0.0471	-3.9513	1.4231
0.45	0.3552	-3.1707	1.7211
0.50	0.7510	-2.4093	2.0213
0.55	1.1469	-1.6572	2.3308
0.60	1.5492	-0.9061	2.6582
0.65	1.9649	-0.1491	3.0161
0.70	2.4031	0.6181	3.4238
0.75	2.8759	1.3957	3.9142
0.80	3.4024	2.1775	4.5442
0.85	4.0162	2.9573	5.4101
0.90	4.7884	3.7619	6.6762
0.91	4.9749	3.9346	7.0036
0.92	5.1775	4.1154	7.3661
0.93	5.4003	4.3071	7.7718
0.94	5.6491	4.5141	8.2320
0.95	5.9329	4.7427	8.7644
0.96	6.2663	5.0033	9.3978
0.97	6.6762	5.3146	10.1856
0.98	7.2211	5.7173	11.2440
0.99	8.0798	6.3345	12.9296

NOTE: The above quantiles and fiducial limits refer to effects due to the independent variable and do not include any effect due to the natural threshold.

```
DISPLAY=FJX IMAGE=Curr XFORM=LS

 Probit Procedure
 Class Level Information

 Class    Levels    Values

 CORRECT       2    Yes No

 Number of observations used   1260


 Probit Procedure

 Data Set          =WORK.RAW
 Dependent Variable=CORRECT

 Weighted Frequency Counts for the Ordered Response Categories

 Level     Count
 Yes       725
  No       535


 Log Likelihood for NORMAL -857.3229233


                Goodness-of-Fit Tests

 Statistic                  Value      DF   Prob>Chi-Sq
 ------------------        --------    --   -----------
 Pearson Chi-Square         13.0410    15        0.5991
 L.R.    Chi-Square         13.0232    15        0.6005

 Response Levels:   2  Number of Covariate Values:   17


 NOTE: Since the chi-square is small (p > 0.1000), fiducial
       limits will be calculated using a t value of  1.96.

 Probit Procedure

 Variable  DF   Estimate  Std Err ChiSquare  Pr>Chi Label/Value

 INTERCPT   1 -1.3299529   0.2205  36.37922  0.0001 Intercept
 AMT        1 3.10884987 1.644589  3.573425  0.0587 Amount

 C=0.5000


 Probit Model in Terms of Tolerance Distribution

           MU         SIGMA
     0.427796      0.321662


 Estimated Covariance Matrix for Tolerance Parameters

                             MU             SIGMA

          MU           0.029063          0.028289
       SIGMA           0.028289          0.028954
```

Probit Procedure
Probit Analysis on AMT

Probability	AMT 95 Percent Fiducial Limits	
	Lower	Upper
0.01	-0.32050	
0.02	-0.23282	
0.03	-0.17718	
0.04	-0.13533	
0.05	-0.10129	
0.06	-0.07232	
0.07	-0.04691	
0.08	-0.02416	
0.09	-0.00347	
0.10	0.01557	
0.15	0.09441	
0.20	0.15708	
0.25	0.21084	
0.30	0.25912	
0.35	0.30385	
0.40	0.34630	
0.45	0.38738	
0.50	0.42780	
0.55	0.46822	
0.60	0.50929	
0.65	0.55174	
0.70	0.59648	
0.75	0.64475	
0.80	0.69851	
0.85	0.76118	
0.90	0.84002	
0.91	0.85907	
0.92	0.87975	
0.93	0.90250	
0.94	0.92791	
0.95	0.95688	
0.96	0.99093	
0.97	1.03278	
0.98	1.08841	
0.99	1.17609	

NOTE: The above quantiles and fiducial limits refer to effects due to the independent variable and do not include any effect due to the natural threshold.

DISPALY=FJX IMAGE=Flow XFORM=CM

Probit Procedure
Class Level Information

Class	Levels	Values
CORRECT	2	Yes No

Number of observations used = 1260

Probit Procedure

Data Set =WORK.RAW
Dependent Variable=CORRECT

Weighted Frequency Counts for the Ordered Response Categories

Level	Count
Yes	1029
No	231

Log Likelihood for NORMAL -571.0470027

Goodness-of-Fit Tests

Statistic	Value	DF	Prob>Chi-Sq
Pearson Chi-Square	19.4341	16	0.2468
L.R. Chi-Square	18.5162	16	0.2945

Response Levels: 2 Number of Covariate Values: 18

NOTE: Since the chi-square is small (p > 0.1000), fiducial limits will be calculated using a t value of 1.96.

Probit Procedure

Variable	DF	Estimate	Std Err	ChiSquare	Pr>Chi	Label/Value
INTERCPT	1	-0.3788129	0.11935	10.07398	0.0015	Intercept
AMT	1	7.87573503	1.08112	53.06822	0.0001	Amount

C=0.5000

Probit Model in Terms of Tolerance Distribution

MU	SIGMA
0.048099	0.126972

Estimated Covariance Matrix for Tolerance Parameters

	MU	SIGMA
MU	0.000101	-0.000112
SIGMA	-0.000112	0.000304

Probit Procedure
Probit Analysis on AMT

Probability	AMT	95 Percent Fiducial Limits	
		Lower	Upper
0.01	-0.24728	-0.37447	-0.17350
0.02	-0.21267	-0.32726	-0.14609
0.03	-0.19071	-0.29732	-0.12868
0.04	-0.17419	-0.27481	-0.11557
0.05	-0.16075	-0.25650	-0.10490
0.06	-0.14931	-0.24093	-0.09581
0.07	-0.13929	-0.22728	-0.08784
0.08	-0.13031	-0.21507	-0.08069
0.09	-0.12214	-0.20396	-0.07419
0.10	-0.11462	-0.19375	-0.06820
0.15	-0.08350	-0.15151	-0.04333
0.20	-0.05876	-0.11802	-0.02348
0.25	-0.03754	-0.08939	-0.00636
0.30	-0.01849	-0.06380	0.00913
0.35	-0.00083	-0.04022	0.02363
0.40	0.01593	-0.01803	0.03757
0.45	0.03214	0.00317	0.05133
0.50	0.04810	0.02365	0.06525
0.55	0.06405	0.04352	0.07978
0.60	0.08027	0.06280	0.09546
0.65	0.09702	0.08141	0.11297
0.70	0.11468	0.09944	0.13301
0.75	0.13374	0.11739	0.15616
0.80	0.15496	0.13615	0.18316
0.85	0.17970	0.15709	0.21554
0.90	0.21082	0.18272	0.25701
0.91	0.21834	0.18884	0.26710
0.92	0.22650	0.19547	0.27809
0.93	0.23548	0.20273	0.29018
0.94	0.24551	0.21081	0.30372
0.95	0.25695	0.22001	0.31918
0.96	0.27039	0.23079	0.33738
0.97	0.28691	0.24400	0.35978
0.98	0.30887	0.26153	0.38961
0.99	0.34348	0.28907	0.43670

NOTE: The above quantiles and fiducial limits refer to effects due to the independent variable and do not include any effect due to the natural threshold.

DISPLAY=FJX IMAGE=Flow XFORM=HR

Probit Procedure
Class Level Information

Class	Levels	Values
CORRECT	2	Yes No

Number of observations used = 1260

Probit Procedure

Data Set =WORK.RAW
Dependent Variable=CORRECT

Weighted Frequency Counts for the Ordered Response Categories

Level	Count
Yes	1114
No	146

Log Likelihood for NORMAL -418.8461743

Goodness-of-Fit Tests

Statistic	Value	DF	Prob>Chi-Sq
Pearson Chi-Square	19.3204	21	0.5646
L.R. Chi-Square	17.6946	21	0.6682

Response Levels: 2 Number of Covariate Values: 23

NOTE: Since the chi-square is small (p > 0.1000), fiducial limits will be calculated using a t value of 1.96.

Probit Procedure

Variable	DF	Estimate	Std Err	ChiSquare	Pr>Chi	Label/Value
INTERCPT	1	-0.0430939	0.119898	0.129183	0.7193	Intercept
AMT	1	0.14112065	0.019166	54.21509	0.0001	Amount

C=0.5000

Probit Model in Terms of Tolerance Distribution

MU	SIGMA
0.305369	7.086135

Estimated Covariance Matrix for Tolerance Parameters

	MU	SIGMA
MU	0.663824	-0.653246
SIGMA	-0.653246	0.926187

Probit Procedure
Probit Analysis on AMT

Probability	AMT	95 Percent Fiducial Limits	
		Lower	Upper
0.01	-16.1794	-24.0403	-11.5953
0.02	-14.2478	-21.4145	-10.0631
0.03	-13.0222	-19.7492	-9.0902
0.04	-12.1002	-18.4969	-8.3580
0.05	-11.3503	-17.4787	-7.7620
0.06	-10.7120	-16.6122	-7.2545
0.07	-10.1523	-15.8527	-6.8092
0.08	-9.6512	-15.1729	-6.4104
0.09	-9.1954	-14.5547	-6.0475
0.10	-8.7759	-13.9859	-5.7132
0.15	-7.0389	-11.6329	-4.3274
0.20	-5.6585	-9.7659	-3.2230
0.25	-4.4742	-8.1670	-2.2726
0.30	-3.4106	-6.7345	-1.4158
0.35	-2.4251	-5.4107	-0.6182
0.40	-1.4899	-4.1591	0.1432
0.45	-0.5851	-2.9539	0.8856
0.50	0.3054	-1.7758	1.6242
0.55	1.1958	-0.6089	2.3740
0.60	2.1006	0.5596	3.1531
0.65	3.0358	1.7396	3.9861
0.70	4.0213	2.9364	4.9108
0.75	5.0849	4.1498	5.9867
0.80	6.2692	5.3857	7.3001
0.85	7.6497	6.6922	8.9651
0.90	9.3866	8.2120	11.1840
0.91	9.8061	8.5672	11.7319
0.92	10.2619	8.9495	12.3306
0.93	10.7630	9.3666	12.9922
0.94	11.3227	9.8289	13.7346
0.95	11.9610	10.3527	14.5849
0.96	12.7110	10.9643	15.5875
0.97	13.6329	11.7119	16.8244
0.98	14.8585	12.7004	18.4740
0.99	16.7902	14.2501	21.0823

NOTE: The above quantiles and fiducial limits refer to effects due to the independent variable and do not include any effect due to the natural threshold.

```
DISPLAY IMAGE=Flow XFORM=LS

 Probit Procedure
 Class Level Information

 Class    Levels    Values

 CORRECT       2    Yes No

 Number of observations used   1260


 Probit Procedure

 Data Set          =WORK.RAW
 Dependent Variable=CORRECT

 Weighted Frequency Counts for the Ordered Response Categories

 Level     Count
 Yes       870
  No       390


 Log Likelihood for NORMAL -770.2046567


                Goodness-of-Fit Tests

 Statistic                  Value      DF   Prob>Chi-Sq
 ------------------        --------    --   -----------
 Pearson Chi-Square         13.4669    15        0.5663
 L.R.    Chi-Square         14.0711    15        0.5201

 Response Levels:   2  Number of Covariate Values:   17


 NOTE: Since the chi-square is small (p > 0.1000), fiducial
       limits will be calculated using a t value of  1.96.

 Probit Procedure

 Variable  DF   Estimate  Std Err ChiSquare  Pr>Chi Label/Value

 INTERCPT   1 -0.7638002 0.137172  31.00461  0.0001 Intercept
 AMT        1 4.88322672   1.1187    19.054  0.0001 Amount

 C=0.5000


 Probit Model in Terms of Tolerance Distribution

           MU          SIGMA
     0.156413       0.204783


 Estimated Covariance Matrix for Tolerance Parameters

                             MU             SIGMA

          MU           0.000336          0.000544
       SIGMA           0.000544          0.002201
```

Probit Procedure
Probit Analysis on AMT

Probability	AMT	95 Percent Fiducial Limits	
		Lower	Upper
0.01	-0.31998	-0.66897	-0.18603
0.02	-0.26416	-0.56796	-0.14720
0.03	-0.22874	-0.50392	-0.12252
0.04	-0.20210	-0.45578	-0.10391
0.05	-0.18042	-0.41665	-0.08875
0.06	-0.16198	-0.38337	-0.07582
0.07	-0.14580	-0.35422	-0.06445
0.08	-0.13132	-0.32814	-0.05426
0.09	-0.11815	-0.30444	-0.04496
0.10	-0.10603	-0.28264	-0.03638
0.15	-0.05583	-0.19273	-0.00056
0.20	-0.01594	-0.12189	0.02854
0.25	0.01829	-0.06205	0.05444
0.30	0.04902	-0.00992	0.07930
0.35	0.07751	0.03538	0.10535
0.40	0.10453	0.07305	0.13539
0.45	0.13068	0.10280	0.17113
0.50	0.15641	0.12698	0.21141
0.55	0.18215	0.14837	0.25450
0.60	0.20829	0.16864	0.29972
0.65	0.23532	0.18879	0.34727
0.70	0.26380	0.20953	0.39789
0.75	0.29454	0.23157	0.45284
0.80	0.32876	0.25585	0.51429
0.85	0.36866	0.28395	0.58613
0.90	0.41885	0.31910	0.67672
0.91	0.43098	0.32757	0.69863
0.92	0.44415	0.33676	0.72243
0.93	0.45863	0.34686	0.74861
0.94	0.47480	0.35812	0.77786
0.95	0.49325	0.37096	0.81123
0.96	0.51492	0.38604	0.85045
0.97	0.54157	0.40455	0.89868
0.98	0.57699	0.42914	0.96282
0.99	0.63281	0.46786	1.06394

NOTE: The above quantiles and fiducial limits refer to effects due to the independent variable and do not include any effect due to the natural threshold.

DISPALY=FJX IMAGE=Girl XFORM=CM

Probit Procedure
Class Level Information

Class	Levels	Values
CORRECT	2	Yes No

Number of observations used 1260

Probit Procedure

Data Set =WORK.RAW
Dependent Variable=CORRECT

Weighted Frequency Counts for the Ordered Response Categories

Level	Count
Yes	1179
No	81

Log Likelihood for NORMAL -252.4716484

Goodness-of-Fit Tests

Statistic	Value	DF	Prob>Chi-Sq
Pearson Chi-Square	7.9546	16	0.9502
L.R. Chi-Square	8.7250	16	0.9243

Response Levels: 2 Number of Covariate Values: 18

NOTE: Since the chi-square is small (p > 0.1000), fiducial limits will be calculated using a t value of 1.96.

Probit Procedure

Variable	DF	Estimate	Std Err	ChiSquare	Pr>Chi	Label/Value
INTERCPT	1	-0.1195121	0.164945	0.52498	0.4687	Intercept
AMT	1	17.7114307	2.445699	52.44467	0.0001	Amount

C=0.5000

Probit Model in Terms of Tolerance Distribution

MU	SIGMA
0.006748	0.056461

Estimated Covariance Matrix for Tolerance Parameters

	MU	SIGMA
MU	0.000072299	-0.000056744
SIGMA	-0.000056744	0.000060784

Probit Procedure
Probit Analysis on AMT

Probability	AMT	95 Percent Fiducial Limits	
		Lower	Upper
0.01	-0.124600	-0.193639	-0.084656
0.02	-0.109208	-0.172603	-0.072476
0.03	-0.099443	-0.159263	-0.064742
0.04	-0.092097	-0.149232	-0.058920
0.05	-0.086122	-0.141075	-0.054182
0.06	-0.081036	-0.134134	-0.050146
0.07	-0.076576	-0.128051	-0.046606
0.08	-0.072584	-0.122606	-0.043434
0.09	-0.068952	-0.117655	-0.040548
0.10	-0.065610	-0.113100	-0.037890
0.15	-0.051770	-0.094254	-0.026868
0.20	-0.040771	-0.079301	-0.018085
0.25	-0.031334	-0.066495	-0.010526
0.30	-0.022860	-0.055018	-0.003715
0.35	-0.015008	-0.044410	0.002623
0.40	-0.007556	-0.034373	0.008667
0.45	-0.000347	-0.024699	0.014551
0.50	0.006748	-0.015224	0.020388
0.55	0.013843	-0.005811	0.026286
0.60	0.021052	0.003667	0.032366
0.65	0.028503	0.013336	0.038778
0.70	0.036356	0.023322	0.045738
0.75	0.044830	0.033756	0.053592
0.80	0.054266	0.044778	0.062934
0.85	0.065266	0.056615	0.074835
0.90	0.079105	0.070026	0.091291
0.91	0.082448	0.073076	0.095454
0.92	0.086079	0.076327	0.100040
0.93	0.090072	0.079840	0.105143
0.94	0.094531	0.083701	0.110907
0.95	0.099617	0.088038	0.117546
0.96	0.105593	0.093063	0.125415
0.97	0.112939	0.099164	0.135168
0.98	0.122704	0.107177	0.148229
0.99	0.138095	0.119662	0.168959

NOTE: The above quantiles and fiducial limits refer to effects due to the independent variable and do not include any effect due to the natural threshold.

DISPLAY=FJX IMAGE=Girl XFORM=HR

Probit Procedure
Class Level Information

Class	Levels	Values
CORRECT	2	Yes No

Number of observations used 1260

Probit Procedure

Data Set =WORK.RAW
Dependent Variable=CORRECT

Weighted Frequency Counts for the Ordered Response Categories

Level	Count
Yes	1202
No	58

Log Likelihood for NORMAL -193.1049141

Goodness-of-Fit Tests

Statistic	Value	DF	Prob>Chi-Sq
Pearson Chi-Square	21.9365	21	0.4032
L.R. Chi-Square	17.1229	21	0.7036

Response Levels: 2 Number of Covariate Values: 23

NOTE: Since the chi-square is small (p > 0.1000), fiducial limits will be calculated using a t value of 1.96.

Probit Procedure

Variable	DF	Estimate	Std Err	ChiSquare	Pr>Chi	Label/Value
INTERCPT	1	0.08702177	0.173306	0.252133	0.6156	Intercept
AMT	1	0.29303599	0.044675	43.02474	0.0001	Amount

C=0.5000

Probit Model in Terms of Tolerance Distribution

MU	SIGMA
-0.29697	3.41255

Estimated Covariance Matrix for Tolerance Parameters

	MU	SIGMA
MU	0.398396	-0.291161
SIGMA	-0.291161	0.270670

Probit Procedure
Probit Analysis on AMT

Probability	AMT	95 Percent Fiducial Limits	
		Lower	Upper
0.01	-8.2357	-13.2301	-5.5179
0.02	-7.3055	-11.9074	-4.7976
0.03	-6.7153	-11.0686	-4.3403
0.04	-6.2713	-10.4378	-3.9960
0.05	-5.9101	-9.9249	-3.7158
0.06	-5.6027	-9.4885	-3.4771
0.07	-5.3332	-9.1059	-3.2678
0.08	-5.0918	-8.7635	-3.0802
0.09	-4.8724	-8.4521	-2.9096
0.10	-4.6703	-8.1656	-2.7524
0.15	-3.8338	-6.9802	-2.1008
0.20	-3.1690	-6.0395	-1.5816
0.25	-2.5987	-5.2336	-1.1350
0.30	-2.0865	-4.5111	-0.7326
0.35	-1.6119	-3.8430	-0.3584
0.40	-1.1615	-3.2105	-0.0019
0.45	-0.7258	-2.6004	0.3449
0.50	-0.2970	-2.0023	0.6885
0.55	0.1319	-1.4070	1.0350
0.60	0.5676	-0.8063	1.3912
0.65	1.0180	-0.1912	1.7652
0.70	1.4926	0.4477	2.1686
0.75	2.0048	1.1214	2.6196
0.80	2.5751	1.8425	3.1511
0.85	3.2399	2.6257	3.8279
0.90	4.0764	3.5030	4.7875
0.91	4.2784	3.6982	5.0360
0.92	4.4979	3.9043	5.3119
0.93	4.7392	4.1247	5.6215
0.94	5.0088	4.3646	5.9735
0.95	5.3162	4.6317	6.3815
0.96	5.6773	4.9385	6.8678
0.97	6.1213	5.3081	7.4733
0.98	6.7116	5.7903	8.2872
0.99	7.6418	6.5370	9.5835

NOTE: The above quantiles and fiducial limits refer to effects due to the independent variable and do not include any effect due to the natural threshold.

DISPLAY=PJX IMAGE=Girl XFORM=LS

Probit Procedure
Class Level Information

Class	Levels	Values
CORRECT	2	Yes No

Number of observations used 1260

Probit Procedure

Data Set =WORK.RAW
Dependent Variable=CORRECT

Weighted Frequency Counts for the Ordered Response Categories

Level	Count
Yes	833
No	427

Log Likelihood for NORMAL -792.7671724

Goodness-of-Fit Tests

Statistic	Value	DF	Prob>Chi-Sq
Pearson Chi-Square	9.4711	15	0.8516
L.R. Chi-Square	9.3769	15	0.8570

Response Levels: 2 Number of Covariate Values: 17

NOTE: Since the chi-square is small (p > 0.1000), fiducial limits will be calculated using a t value of 1.96.

Probit Procedure

Variable	DF	Estimate	Std Err	ChiSquare	Pr>Chi	Label/Value
INTERCPT	1	-1.0863992	0.160112	46.03942	0.0001	Intercept
AMT	1	6.48177617	1.232195	27.67127	0.0001	Amount

C=0.5000

Probit Model in Terms of Tolerance Distribution

MU	SIGMA
0.167608	0.154279

Estimated Covariance Matrix for Tolerance Parameters

	MU	SIGMA
MU	0.000241	0.000297
SIGMA	0.000297	0.000860

Probit Procedure
Probit Analysis on AMT

Probability	AMT	95 Percent Fiducial Limits	
		Lower	Upper
0.01	-0.19130	-0.37510	-0.10603
0.02	-0.14924	-0.30843	-0.07503
0.03	-0.12256	-0.26619	-0.05530
0.04	-0.10249	-0.23446	-0.04041
0.05	-0.08616	-0.20869	-0.02826
0.06	-0.07226	-0.18679	-0.01789
0.07	-0.06007	-0.16761	-0.00876
0.08	-0.04916	-0.15047	-0.00056
0.09	-0.03924	-0.13492	0.00692
0.10	-0.03011	-0.12062	0.01384
0.15	0.00771	-0.06185	0.04289
0.20	0.03776	-0.01596	0.06680
0.25	0.06355	0.02223	0.08850
0.30	0.08670	0.05472	0.10978
0.35	0.10816	0.08222	0.13212
0.40	0.12852	0.10526	0.15637
0.45	0.14822	0.12487	0.18250
0.50	0.16761	0.14233	0.21006
0.55	0.18700	0.15866	0.23876
0.60	0.20669	0.17455	0.26863
0.65	0.22705	0.19051	0.29995
0.70	0.24851	0.20701	0.33328
0.75	0.27167	0.22458	0.36949
0.80	0.29745	0.24395	0.41000
0.85	0.32751	0.26636	0.45739
0.90	0.36532	0.29439	0.51719
0.91	0.37446	0.30114	0.53165
0.92	0.38438	0.30847	0.54737
0.93	0.39529	0.31651	0.56466
0.94	0.40748	0.32549	0.58398
0.95	0.42137	0.33573	0.60602
0.96	0.43770	0.34774	0.63193
0.97	0.45777	0.36249	0.66380
0.98	0.48446	0.38207	0.70619
0.99	0.52651	0.41290	0.77302

NOTE: The above quantiles and fiducial limits refer to effects due to the independent variable and do not include any effect due to the natural threshold.

B Analysis Programs

The sections below contain listing of code used in analyzing the data for this thesis. The display code is rather large and is included only on the CD (see Appendix C)f.

B.1. SAS Probit Analysis Code

B.1.a. For Sony, SGI and IBM displays

```
Option Ls=64 Pagesize=10000 nocenter;

/* Set up some formats to make the output easier to read */
Proc Format;
  Value yn 1='Yes' 0='No';
RUN;

/* Read in the Raw data as produced by my IDL code */
Data Raw;
  Infile Data;
  Input Initials $ Age Gender $ Exp Display $ Image $ Xform $ AmtH Correct ImgTime TotTimeS;

  TotTime = TotTimeS/60.0;
  Amt = AmtH/100.0;

  label Exp    'Experienced'
        Xform = 'Transform'
        Amt    'Amount'
        ImgTime    'Time on Image (Sec)'
        TotTime    'Total Time (Min)';

  format Exp yn.;
  format Correct yn.;
  drop TotTimeS;
  drop AmtH;
RUN;

/* I need to sort the data by xform so that I can process it by Xform */
Proc Sort;
  By Display Image Xform;
RUN;

/* Run the Probit Analysis on it */
Proc Probit c=0.5 order=Freq;
  class Correct;
  model Correct   Amt /D=Normal Lackfit Inversecl;
  By Display Image Xform;
RUN;
```

B.1.b. For Fujix Pictrography Prints

```
Option Ls=64 Pagesize=10000 nocenter;

/* Set up some formats to make the output easier to read */
Proc Format;
  Value yn 1='Yes' 0='No'.
RUN;

/* Read in the Raw data as produced by my IDL code */
Data Raw;
  Infile Fjx_Data;
  Input Image $ XForm $ Amt Correct;
  label Amt = 'Amount';
  format Correct yn.;
RUN;

/* I need to sort the data by Image so that I can process it by Image*/
Proc Sort;
 By Display Image Xform;
RUN;

/* Run the Probit Analysis IMAGEWISE*/
Proc Probit c=0.5 order=Freq;
  class Correct;
  model Correct = Amt /D=Normal Lackfit Inversecl;
  By Display Image Xform;
RUN;
```

B.2. IDL Code for Colorimetric Difference Analysis

The following code assumes a directory structure with contents as follows:

B.2.a. Code for Creating Images at Threshold Levels

```
;; MakeThresholdImages (1.0)
;;
;; purpose   read in an original LCh text file, manipulate it by the threshold parameter
;;     (either image specific,or overall) and save off the manipulated LCh file.

pro MakeThresholdImages

  Display   'SGI'
  resolution = 110L

  base_path = '/md2/jeg7324/Thesis/' + Display
  image_path = base_path + '/LCh_images/'
  threshold_path   base_path + '/Psych/'

  n_pixels   (4L*resolution) * (6L * resolution)
  percentiles   dblarr(14)

  imageFile_suffix = ['_LCh_Curr','_LCh_Flow','_LCh_Girl']
  manipulations = ['ls','cm','hr']
  thresh_word   ['M','L','U']

  thresholds = load_data(3,12,threshold_path + 'thresholds.txt')  ;; assume the cols are: M, L,
U and the rows are:LS,CM,HR

;Read in each image one at a time, and do the 9 manipulations on it
  for img=0,2 do BEGIN

    filename   image_path + Display + imageFile_suffix[img] + '.txt'
    LCh_orig   load_data(3,n_pixels,filename)

    for manip=0,2 do BEGIN
      xform   manipulations[manip]
      for lev =0,2 do BEGIN
        thresh   thresholds[lev,manip+(img*3.0)]
        out_file   Image_path + Display + imageFile_suffix[img] + '_' + manipulations[manip] +
thresh_word[lev] + '.txt'
        OpenW, output_lun, out_file, width=600, /get_lun

        ; Manipulated Image
        LCh_manip   process(LCh_orig, xform, thresh)

        printf, output_lun, LCh_manip
        free_lun, output_lun
      endfor ;threshold
    endfor ; manipulation
  endfor ;image

end
```

B.2.b. Code for Performing Pixel-wise differences

```
;; pixelwise_diff (1.0)
;;
;; purpose   read in an original LCh text file, the various manipulated versions of it
;;           and compute the pixel by pixel DE's, their average, std, and quartiles.

pro pixelwise_diff
start_time   systime(1)
  Display   'SNY'    ; 'SNY','SGI','IBM','FJX'
  resolution = 72L   ; '72L','110L','200L','400L'
  deType = 'ab'      ; 'ab','94','94lc','2000', '2000lc'
KL   9999D           ; Fill in as appropriate for given display and deType
KC   9999D           ; Fill in as appropriate for given display and deType
KH = 1.0D
  base_path   '/md2/jeg7324/Thesis/' + Display
  image_path   base_path + '/LCh_images/'
  threshold_path   base_path + '/Psych/'

  n_pixels = (4L*resolution) * (6L * resolution)
  percentiles = dblarr(14)

  imageFile_suffix = ['_LCh_Curr','_LCh_Flow','_LCh_Girl']
  manipulations = ['ls','cm','hr']
  thresh_letter = ['M','L','U']
  thresh_word   ['__Mean__','__Lower__'.'__Upper__']

;Read in each original image and compare it to the nine manipulated ones

  for img=0,2 do BEGIN

  , Original Image
   orig_file   image_path + Display + imageFile_suffix[img] + '.txt'
   LCh_orig   load_data(3,n_pixels,orig_file)
   LabCh_orig = dblarr(5,n_pixels)
   LabCh_orig[0:2,*]   lch2lab(LCh_orig)
   LabCh_orig[3:4,*]   LCh_orig[1:2,*]

delvarx,LCh_orig,orig_file


   out_file   threshold_path + Display + 'Cstats_' + deType+ '_'+
strmid(imageFile_suffix[img],5) + '.txt'
      OpenW, output_lun, out_file, width=600, /get_lun
delvarx,out_file
   for manip=0,2 do BEGIN
help, /memory
     xform   manipulations[manip]
     printf, output_lun, ' '
     printf, output_lun, '---' + xform + '---'

     for lev =0,2 do BEGIN

       printf, output_lun, ' '
       printf, output_lun, thresh_word[lev]

     , Manipulated Image

       manip_file = image_path + Display + imageFile_suffix[img] + '_' + xform +
thresh_letter[lev] + '.txt'
       LCh_manip = load_data(3,n_pixels,manip_file)
       LabCh_manip = dblarr(5,n_pixels)
       LabCh_manip[0:2,*] = lch2lab(LCh_manip)
       LabCh_manip[3:4,*] = LCh_manip[1:2,*]

delvarx,LCh_manip,manip_file
```

```
  ; Now, we do all sorts of stats on it to see what we can find
      Case deType OF
  '94':    de = de_94(LabCh_orig, LabCh_manip)
  '94lc':    de    de_94(LabCh_orig, LabCh_manip, KL=KL, KC=KC, KH=KH)
  'ab':    de = de_ab(LabCh_orig, LabCh_manip)
  '2000': de    de_2000(LabCh_orig, LabCh_manip)
      '2000lc': de    de_2000(LabCh_orig, LabCh_manip, KL=KL, KC=KC, KH=KH)
      endCase

     printf, output_lun, '_Moments_'
       printf, output_lun, moment(de)
       printf, output_lun, '_Moments of dL, da, db, dC, dh_'

; process the remaining de stuff and get rid of it
minDE    min(DE)
maxDE    max(DE)
deciles    percentile(de,[10,20,30,40,50,60,70,80,90]/100.0D)
quartiles    percentile(de,[25,50,75]/100.0D)

delvarx, de


      deltas    LabCh_orig    LabCh_manip
help, /memory
delvarx,Labch_manip

     , Compute the Moments
       printf, output_lun, moment(deltas[0,*]) ;L
       printf, output_lun, moment(deltas[1,*]) ;a
       printf, output_lun, moment(deltas[2,*]) ;b
       printf, output_lun, moment(deltas[3,*]) ;C
       printf, output_lun, moment(deltas[4,*]) ;h

     ; Compute Correlations
       printf, output_lun, '_Correlations (LabCh)_'
       printf, output_lun, Correlate(deltas)

delvarx,deltas

       printf, output_lun, '_Min and Max_'
       printf, output_lun, string(minde) + ' ' + string(maxde)

       printf, output_lun, 'deciles'
       printf, output_lun, deciles

       printf, output_lun, 'quartiles'
       printf, output_lun,  quartiles

     endfor ;Level
     printf, output_lun, '-------------------'
    endfor , manipulation
    free_lun, output_lun
  endfor ;image

print, 'That took (min):'
print, (systime(1)-start_time)/60.0
end
```

Transform an Image by Given Amount

```
function process, original, xform, amount

  manipulated = original  ; just to set them to be the same size
  Case xform of
     'ls': manipulated[0,*] = 100.0D*(sigmoidal((temporary(original[0,*]))/100.0D, Amount,
0.50))
     'cm': manipulated[1,*] = temporary(original[1,*]) * Amount
     'hr': manipulated[2,*] = temporary(original[2,*]) + Amount
    ENDCASE

  return, manipulated
end
```

Compute ΔE_{ab}

```
;; DEab (1.1)
;; Function   input 2 (3 by m) Lab arrays and compute delta Eab from them
;;
;; Input    Lab_Original     3 by n array of the standard Lab values
;;        Lab_Reproduction     3 by 1 array of sample Lab values
;;
;; Output   1 by n array of Delta Eab values
;;
;; Dependencies   none
;;  delta_Eab=  de_ab(Lab_Original, Lab_Reproduction)

function de_ab, Lab_Original, Lab_Reproduction

   delta_L   Lab_Original[0,*]-Lab_Reproduction[0,*]
   delta_a   Lab_Original[1,*]-Lab_Reproduction[1,*]
   delta_b   Lab_Original[2,*]-Lab_Reproduction[2,*]

   delta_e   sqrt( (delta_L^2.0D) + (delta_a^2.0D) + (delta_b^2.0D) )
   return, delta_e
end
```

Compute ΔE_{94}

```
;; DE94 (1.1)
;; Function   input 2 (5{4} by m) LabCh arrays and compute delta E94 from them
;;
;; Input    LabCh_Original      . 4+ by m array of the standard LabC{h} values
;;          LabCh_Reproduction     4+ by m array of sample LabC{h} values
;;        KL, KC, KH          · OPTIONAL weighting factors for the various terms, DEFALUT   1.0
;;
;; Output   1 by m array of dEab values
;;
;; Dependencies   dEab
;;  delta_E94=  de_94(LabCh_Original, LabCh_Reproduction, KL   kl, KC = kc, KH   kh)

function de_94, LabCh_Original, LabCh_Reproduction, KL = kl, KC   kc, KH = kh

 delta_L   LabCh_Original[0,*]-LabCh_Reproduction[0,*]
 delta_a = LabCh_Original[1,*]-LabCh_Reproduction[1,*]
    delta_b   LabCh_Original[2,*]-LabCh_Reproduction[2,*]
    delta_C   LabCh_Original[3,*]-LabCh_Reproduction[3,*]
 delta_Eab   de_ab(LabCh_Original, LabCh_Reproduction)

; Before we calculate Delta_H, we need to check to see if it's value is > 0
 e   size(LabCh_Original)
 delta_H = dblarr(1,e[2])

 Terms   (delta_Eab^2.0D)   (delta_L^2.0D)   (delta_C^2.0D)
 not_zero = WHERE( Terms GT 0.0D, count)
    if count NE 0 then delta_H(not_zero)   sqrt( Terms(not_zero) )
 is_zero   WHERE( Terms LE 0.0D, count)
 if count NE 0 then delta_H(is_zero)   0.0D

; define the Systamatic defects of CIELAB space with the S terms
 Sl - 1.0D
 Sc = 1.0D + 0.045D*LabCh_Original[3,*]
 Sh = 1.0D + 0.015D*LabCh_Original[3,*]

; Default conditions are KL = KC   KH   1.0

 if NOT (keyword_set(KL)) then KL   1.0D
 if NOT (keyword_set(KC)) then KC   1.0D
 if NOT (keyword_set(KH)) then KH   1.0D

 L_term = Delta_L/(KL*Sl)
 C_term = Delta_C/(KC*Sc)
 H_term = Delta_H/(KH*Sh)

 delta_e94   sqrt( (L_term^2.0D) + (C_term^2.0D) + (H_term^2.0D) )

 return, delta_e94

end
```

```
;; DE_2000 (1.0)
;; By: Jason Gibson
;;
;; Purpose -- To compute DeltaE2000 between two input LabCh vectors
;;
;; Initial Code based on an article submitted to CR&A in early 2000,
;;    based on work of Luo et. al.'s work on.
;; Revised Coded based on committe report current as of CIC8 (Nov 2000)
;;  CIE TC1-45, this will likely replace DEab and DE94 as the recommended color difference
formula
;;
;; Variables:
;;  LabChOrig -- The LabCh values of the original sample(s)
;;  LabChRepo -- The LabCh values of the manipulated sample(s)
;; KL, KC, KH -- optional parameters used for parametric corrections
;;
;;
;; Functions Called: NONE
;;
;;
;; Revision History
;; 4/20/2000 -- Initial code written, unable to match example data.
;;         Ex may be bad, ie. Lbar1=Lbar2 yet SH1!=SH2; also RC's are both -ve yet 2*sqrt(X)>=0!
;; 1/2/2001 -- Updated the formula to more recent version (CIC8),
;;             Basically a change in T formula & L'=L*, b'=b*, it checks with 10 examples

function de_2000, LabChOrig, LabChRepo, KL=kl, KC=kc, KH=kh


; ***********************************
; Compute a', C', and h' -- Modified version of a,C, & h to correct for distortions in CIELAB
; ***********************************
 ; Compute Cbar(mean of C's) & G(a modifying factor for a* based on Cbar)
  Cbar   (LabChOrig[3,*] + LabChRepo[3,*])/2
  G = 0.5 * [1   sqrt( (Cbar^7) / [ (Cbar^7) + (25.0D^7.0D) ] ) ]

 ;a'C'h' for the original
  apO   (1+G)*LabChOrig[1,*]                    , (1+G)a*
  CpO   sqrt(apO^2 + LabChOrig[2,*]^2)          ; sqrt(a'^2 + b*^2)
  hpO   atan( LabChOrig[2,*], apO )  * !RADEG   ; h'_deg
    ind - WHERE(hpO LT 0, count)                ; correct for +- PI
    if count GT 0 then BEGIN
       hpO[ind] = temporary(hpO[ind]) + 360     , add 360 deg
    endif

 ;a'C'h' for the Reporduction
  apR   (1+G)*LabChRepo[1,*]                  ; (1+G)a*
  CpR   sqrt(apR^2 + LabChRepo[2,*]^2)        ; sqrt(a'^2 + b*^2)
  hpR   atan( LabChRepo[2,*], apR )  * !RADEG ; h'_deg
    ind   WHERE(hpR LT 0, count)              , correct for +- PI
    if count GT 0 then BEGIN
       hpR[ind] = temporary(hpR[ind]) + 360   ; add 360 deg
    endif


; ***********************************
; Calculate deltaL*, deltaC', deltaH'
; ***********************************
 dL   LabChRepo[0,*]   LabChOrig[0,*]
 dCp = CpR   CpO
 dlhP = hpR   hpO
 dHp = 2 * sqrt(CpR * CpO) * sin((!DTOR*dlhP)/2)
```

```
; ***********************************
; Calculate the systematic terms SL, SC, SH
; ***********************************
  ; Calculate some intermediate terms
    Lsbar    (LabChOrig[0,*] + LabChRepo[0,*])/2.0D
    Cpbar    (CpO + CpR)/2.0D
    hPbar    (hpO+hpR)/2.0D

    T    1- 0.17*cos(!DTOR*(hpbar-30)) + 0.24*cos(!DTOR*(2*hpbar)) + 0.32*cos(!DTOR*(3*hpbar+6))
   0.20*cos( !DTOR*(4*hpbar-63) )
    RC    2*sqrt( (Cpbar^7)/[ (Cpbar^7) + (25.0D^7.0D) ] )
    DeltaTheta    30*exp( -1.0D* [(hpbar-275)/25]^2 )
    RT    -1*sin(!DTOR*(2*DeltaTheta))*RC

; Actually compute the SL,SH, SC terms
  SL = 1 + [0.015*(Lsbar -50)^2]/sqrt(20+[Lsbar-50]^2)
  SC = 1 + 0.045*Cpbar
  SH = 1 + 0.015*Cpbar*T


; ***********************************
; Determine the Parametric terms KL, KC, KH
; ***********************************
  , Default conditions are KL = KC    KH    1.0

    if NOT (keyword_set(KL)) then KL = 1.0D
    if NOT (keyword_set(KC)) then KC = 1.0D
    if NOT (keyword_set(KH)) then KH = 1.0D


; ***********************************
; Compute DE2000
; ***********************************
  ; Compute Intermediate Terms
    Lterm = dL/(KL * SL)
    Cterm    dCp / (KC * SC)
    Hterm    dHp / (KH * SH)
    CHterm =(dCp*dHp) / (SC*SH)

  , Actually do the computation
    de2000 = sqrt( Lterm^2 + Cterm^2 + Hterm^2 + RT*CHterm )

  return, de2000
end
```

Calculate the d^{th} percentile of sample

```
;; percentile
;;  compute the dth percentiles of a sample based on the method given in
;; Statistical Inference by George Casella, and Roger L. Berger , Dubbury press 1990 pg230

function percentile, data, d


  n   N_elements(data)
  Q   lonarr(N_elements(d))

  sorted   data(sort(data))
  q_if_pLEhalf   round(n*d)
  q_if_pGThalf   (n+1)-round(n*(1-d))

  ind   where(d LE 0.5, count)
  if count GT 0 then BEGIN
   Q[ind] = q_if_pLEhalf[ind]
  endif

  ind   where(d GT 0.5, count)
  if count GT 0 then BEGIN
   Q[ind] = q_if_pGThalf[ind]
  endif

  return, sorted(Q-1)
end
```

Convert Lab to LCh

```
;; lab2lch (1.1)
;; Function   take input (3,m) Lab values and compute CIE L*, C*, and h_deg
;;
;; Input    Lab_array   (3,n) array of sample L*, a*, b* values
;;
;; Output   (3,n) array of L*, C*, h_deg values
;;
;; Dependencies   none
;;  Lch_values = lab2lch(lab_array)
;; lab2lch (1.0)
;; Function   input a (3,m) Lab array {rectangular} and output a (3,m) LCh array {polar}
;;
;; Input - Lab_array  : a (3,m) array of CIELab rectangular coordinates
;; Output- LCh_array which is (3,m) in degree polar coordinates
;;
;; Dependencies   none
;; LCh_array = lab2lch(Lab_array)

Function lab2lch , Lab_array

   LCh_array = Lab_array  ; Set the size of the output array to be the same as the input one

   LCh_array[1,*]   sqrt( (Lab_array[1,*]^2.0D) + (Lab_array[2,*]^2.0D) )            ;; C*
   LCh_array[2,*]   atan( Lab_array[2,*], Lab_array[1,*] ) * (180.0D/(asin(1.0D)*2.0D)) ;; h_deg
     ind   WHERE(LCh_array[2,*] LT 0, count)                                  ;; correct for +- PI
     if count GT 0 then BEGIN
       LCh_array[2,ind] = temporary(LCh_array[2,ind]) + 360.0D                ;; add 360 deg
     endif

Return, LCh_array
end
```

Sigmoidal Transform

```
;; Sigmoidal (1.0)
;; Function   input a [1,m] array and apply a sigmoidal transform to it...
;;
;; Input     In          1 by n array of data to apply the transform to
;;           constant      The exponential parameter on the sigmoid
;;          threshold      Where the function will switch
;;
;; Output      [1,m] array of data transformed by the sigmoid
;;
;; Dependencies    none
;;  Xformed_data     sigmoidal(in, constant, threshold)

function sigmoidal, In, Constant, Threshold

  Out = In ; This sets the size of the output array w/o the need for size which fails if m=1

  ind = where(In LT Threshold, count)
  if count GT 0 then BEGIN
   Out[0,ind]    ( (In[0,ind]*2.0D)^Constant ) / 2.0D
  endif

   ind   where(In GE Threshold, count)
   if count GT 0 then BEGIN
    Out[0,ind]    ((((In[0,ind]*2.0D)-1.0D)^(1.0D/Constant))+1.0D)/2.0D
  endif

 return, out
end
```

Delete Variable from Memory (Obtained from unknown source)

```
;+
; NAME:
; DELVARX
; PURPOSE:
;  Delete variables for memory management (can call from routines)
; EXPLANATION:
; Like intrinsic DELVAR function, but can be used from any calling level
;
, CALLING SEQUENCE:
,  DELVARX,  a [,b,c,d,e,f,g,h,i,j]
,
; INPUTS:
; p0, p1...p9   variables to delete
;
; RESTRICTIONS:
; Can't use recursively due to EXECUTE function
;
; METHOD:
; Uses EXECUTE and TEMPORARY function
;
; REVISION HISTORY:
; Copied from the Solar library, written by slf, 25-Feb-1993
; Added to Astronomy Library,  September 1995
; Converted to IDL V5.0   W. Landsman   September 1997
;-

PRO delvarx, p0,p1,p2,p3,p4,p5,p6,p7,p8,p9
   FOR i   0, N_PARAMS()-1 DO BEGIN ; for each parameter
      param = STRCOMPRESS("p" + STRING(i),/remove)
;  only delete if defined on inpu (avoids error message)
      exestat   execute("defined=n_elements(" + param + ")" )
      IF defined GT 0 THEN BEGIN
         exestat   execute(param + "=0")
         exestat = execute("dvar=temporary(" + param + ")" )
      ENDIF
   ENDFOR
   RETURN
END
```

C Description of CD Contents

The CD (ISO 9660 Level 2 Mode 1 Joliet) associated with this work contains the complete text of this document as well as many other files of interest. This section will explain the layout of the CD as well as brief descriptions of the files within.

At the top level of the CD is four main directories:

Analysis – Containing raw and processed data from the psychophysical experiments conducted.

Code – Containing useful pieces of code written during the course of the experiment in both IDL, MATLAB, and SAS.

Images – Containing the CIELCh values of the image pixels displayed to the observer on each display.

Thesis – Containing a PDF 5.0 version of this document in both word and PDF formats.

A full listing of the CD contents is given in Table C1 at the end of this chapter.

C.1. Analysis

In this section the Excel workbooks used by the author to analyze the data are included. Comments are sparse but the files should be relatively self explanatory. The data in the Raw directories contain the actual data collected during the experiment and are parsed as follows:

Each row represents a single observation

The 11 columns contain:

1-4	Observer Initials, Age, Gender, and Experienced observer (1 – yes, 0-no)
5-8	Display, Image, Transform, Level of transform * 100 with leading 0's
9	1 if correctly detected, 0 if not
10, 11	Time for image in seconds, Total Observation Time in seconds

C.2. Code

This section contains various programs written during the course of this thesis that may be useful to others both in conducting their own experiments, or in interpreting the current results. All files can be viewed using a simple text editor.

C.3. Images

The LCh values of the images show to the observer are included in this section. The files are raw text files for portability. The columns are L^*, C^* and h_{ab}. The pixel order is top left to bottom right. The images sizes are listed in section 5.1.1. All images are 4x6" at the appropriate display resolution. Files are self extracting compressed using WinZip 8.0 from www.winzip.com.

C.4. Thesis

The full text of this document as a PDF.

Table C1—Recursive Listing of CD Contents

```
Analysis/
Code/
Images/
Thesis/

  ./Analysis:
  RawData/
  Comparison.xls
  FJX_Results.xls
  IBM_Results.xls
  IBM_SCIELAB_Results.xls
  SGI_Results.xls
  SNY_Results.xls
  SNY_SCIELAB_Results.xls

    ./Analysis/RawData:
    FJX/
    IBM/
    SGI/
    SNY/

      ./Analysis/RawData/FJX:
      FJX Experiment Data.xls
      fjx_lis.txt
      fjx_log.txt

      ./Analysis/RawData/IBM:
      01_fhi_sbt_eom_drw.txt
      02_mdf_qxs_hxk_sdb.txt
      03_lat_srf_sah_gmj.txt
      04_xxj_mrr_jag_kag.txt
      05_jab_jsl_sjp_axa.txt
      06_edm_jhk_sxg_jsb.txt
      07_blp_rxd_dxk_ksl.txt
      08_drp_jbp_jwk_jeg.txt
      09_mrg_bln_jass_pas_slw.txt
      ibm_lis.txt
      ibm_log.txt

      ./Analysis/RawData/SGI:
      01_LAT_SXQ_MXZ.txt
      02_JEG_MDF_GMJ.txt
      03_BLN_DRW_MRR.txt
      04_PAF_JHK_JAB.txt
      05_JWK_SXQ_XXJ.txt
      06_EDM_JSL_DPD.txt
      07_SBT_JAG_SRF.txt
      08_CMD_PAS_FHI.txt
      09_HXK_EOM_SAH.txt
      10_AXA_SJP_LaT.txt
      11_SPG_TFP.txt
      SGI_Results.xls
      sgi_lis.txt
      sgi_log.txt

      ./Analysis/RawData/SNY:
      01_jeg_exm_sbt_mdf.txt
      02_mrr_bln_edm_kag.txt
      03_sah_pas.txt
      04_jsa_lar_xxj_sxq.txt
      05_gmj_qxs_hxk_lat.txt
      06_sjp_fhi.txt
      07_axa_srf_cmd_mcz.txt
      08_jsl_paf_drw_jab.txt
      09_mlg_chd_sxg_nxt.txt
      10_nxt_dcw_dxk.txt
      sny_lis.txt
      sny_log.txt

  ./Code:
  IDL/
  MATLAB/
  SAS/
```

```
    ./Code/IDL:
    MakeThresholdImages.pro
    de_94.pro
    de_ab.pro
    delvarx.pro
    lab2lch.pro
    percentile.pro
    pixelwise_diff.pro
    process.pro
    sigmoidal.pro

    ./Code/MATLAB:
    SCIELAB/

    ./Code/MATLAB/SCIELAB:
    CommentedExample.m
    Example.m
    README
    RUN_ME.m
    SmithPokornyCones.mat
    UseScielab.m
    changeColorSpace.m
    cmatrix.m
    dac2rgb.m
    deltaE94.m
    deltaLab.m
    displayGamma.mat
    displaySPD.mat
    gauss.m
    gauss2.m
    getPlanes.m
    hats.mat
    hats.tiff
    hatsCompressed.mat
    hatsCompressed.tiff
    lab2xyz.m
    pad4conv.m
    resize.m
    rgb2dac.m
    scielab.m
    separableConv.m
    separableFilters.m
    sumGauss.m
    visualAngle.m
    xyz2lab.m

    ./Code/SAS:
    print.sas
    display.sas

  ./Images
  fjx.exe:
    FJX_LCh_Curr.txt
    FJX_LCh_Flow.txt
    FJX_LCh_Girl.txt

  ibm.exe:
    IBM_LCh_Curr.txt
    IBM_LCh_Flow.txt
    IBM_LCh_Girl.txt

  sgi.exe:
    SGI_LCh_Curr.txt
    SGI_LCh_Flow.txt
    SGI_LCh_Girl.txt

  sny.exe:
    SNY_LCh_Curr.txt
    SNY_LCh_Flow.txt
    SNY_LCh_Girl.txt

./Thesis
ColorTolofDisplay.pdf
```